17

PNL-2500 PT1
UC-48

Pacific Northwest Laboratory
Annual Report for 1977
to the DOE Assistant Secretary
for Environment

February 1978

Part 1

Biomedical Sciences

Prepared for the
U.S. Department of Energy
under Contract EY-76-C-06-1830

Battelle
Pacific Northwest Laboratories

PNL-2500 PT1

PACIFIC NORTHWEST LABORATORY
operated by
BATTELLE
for the
UNITED STATES DEPARTMENT OF ENERGY
Under Contract EY-76-C-06-1830

Printed in the United States of America
Available from
National Technical Information Service
United States Department of Commerce
5285 Port Royal Road
Springfield, Virginia 22151

Price: Printed Copy $ _____*; Microfiche $3.00

*Pages	NTIS Selling Price
001-025	$4.50
026-050	$5.00
051-075	$5.50
076-100	$6.00
101-125	$6.50
126-150	$7.00
151-175	$7.75
176-200	$8.50
201-225	$8.75
226-250	$9.00
251-275	$10.00
276-300	$10.25

PNL-2500 PT1
UC-48

Pacific Northwest Laboratory Annual Report for 1977 to the DOE Assistant Secretary for Environment

Part 1 Biomedical Sciences

by
W. R. Wiley and Staff Members
of Pacific Northwest Laboratory

February 1978

Battelle
Pacific Northwest Laboratories
Richland, Washington 99352

PREFACE

The 1977 Annual Report from Pacific Northwest Laboratory (PNL) to the DOE Assistant Secretary for Environment introduces a new cover. The earth-green color used on past annual reports has been replaced by the "environmental colors," blue and green. The cover's abstract design is not intended to represent anything specific, but we would not be unhappy if it suggests something environmental or biological to the reader. The blue and green color pattern on the cover is different for each part of this report to help distinguish the five parts.

The five parts of the Report are oriented to particular segments of our program. Parts 1-4 report research performed for the DOE Office of Biomedical and Environmental Research. Part 5 reports progress on all other research performed for the Assistant Secretary for Environment, including the Office of Environmental Control Technology, Office of Technology Impact, and Office of Operational and Environmental Safety.

Each part consists of project reports authored by scientists from several PNL research departments, reflecting the interdisciplinary nature of the research effort. Parts 1-4 are organized primarily by energy technology, although it is recognized that much of the research performed at PNL is applicable to more than one energy technology.

The parts of the 1977 Annual Report are:

Part 1: Biomedical Sciences		
	Program Manager - W. R. Wiley	R. C. Thompson, Report Coordinator D. L. Felton, Editor
Part 2: Ecological Sciences		
	Program Manager - B. E. Vaughan	B. E. Vaughan, Report Coordinator J. L. Helbling, Editor
Part 3: Atmospheric Sciences		
	Program Manager - C. L. Simpson	R. L. Drake, Report Coordinator C. M. Gilchrist, Editor
Part 4: Physical Sciences		
	Program Manager - J. M. Nielsen	J. M. Nielsen, Report Coordinator G. M. Garnant/L. Carson, Editors

Part 5: Control Technology, Overview, Health, Safety, and Policy Analysis

Program Managers - N. E. Carter
D. B. Cearlock
J. C. Fox
D. L. Hessel
H. V. Larson
S. Marks

W. J. Bair, Report Coordinator
R. W. Baalman, Editor

Activities of the scientists whose work is described in this Annual Report are broader in scope than the articles indicate. Knowledge and experience obtained by PNL staff in carrying out research in the Environment, Health, and Safety Research program have contributed to many other DOE interests. These include assistance in the preparation of several Environmental Development Plans for the Assistant Secretary for Environment, preparation of environmental statements for which the Laboratory is responsible, key membership in several national and international organizations, and numerous responses to the media on research projects of public interest

W. J. Bair, Manager
S. Marks, Associate Manager
Environment, Health, and Safety Research Program

Previous Reports in this Series:

Annual Report for

1951	W-25021, HW-25709
1952	HW-27814, HW-28636
1953	HW-30437, HW-30464
1954	HW-30306, HW-33128, HW-35905, HW-35917
1955	HW-39558, HW-41315, HW-41500
1956	HW-47500
1957	HW-53500
1958	HW-59500
1959	HW-63824, HW-65500
1960	HW-69500, HW-70050
1961	HW-72500, HW-73337
1962	HW-76000, HW-77609
1963	HW-80500, HW-81746
1964	BNWL-122
1965	BNWL-280, BNWL-235, Vol. 1-4, BNWL-361
1966	BNWL-480, Vol. 1, BNWL-481, Vol. 2, Pt 1-4
1967	BNWL-714, Vol. 1, BNWL-715, Vol. 2, Pt 1-4
1968	BNWL-1050, Vol. 1, Pt. 1-2, BNWL-1051, Vol. 2, Pt. 1-3
1969	BNWL-1306, Vol. 1, Pt. 1-2, BNWL-1307, Vol. 2, Pt. 1-3
1970	BNWL-1550, Vol. 1, Pt. 1-2, BNWL-1551, Vol. 2, Pt. 1-2
1971	BNWL-1650, Vol. 1, Pt. 1-2, BNWL-1651, Vol. 2, Pt. 1-2
1972	BNWL-1750, Vol. 1, Pt. 1-2, BNWL-1751, Vol. 2, Pt. 1-2
1973	BNWL-1850, Pt. 1-4
1974	BNWL-1950, Pt. 1-4
1975	BNWL-2000, Pt. 1-4
1976	BNWL-2100, Pt. 1-5

FOREWORD

This volume describes progress on biomedical and health effects research conducted at PNL in 1977. The contents of the volume are a reflection of our continuing emphasis on the evaluation of risk to man from existing and/or developing energy-re1ated technologies. The emphasis of the PNL program is consistent with the DOE goal of increasing and diversifying national energy resources without increasing risks to human health.

Most of the studies described in this report relate to process-specific activities for four major energy technologies: nuclear fuel cycle; fossil fuel cycle (oil, gas, and coal processing, mining, and utilization); shale oil processing; and fusion (biomagnetic effects). The report is organized under these technologies. In addition, research reports are included on the application of nuclear energy to biomedical problems.

Technically, the energy-related projects presented here all center around a common research format involving multitiered toxicologic evaluation of potentially hazardous by-products, fugitive gases and effluents from process-specific energy activities. The shale oil projects, for example, are illustrative of the multitiered toxicologic concept. By-products and fugitive effluents are examined by an inexpensive niicrobial mutagenesis assay. The results of these investigations are used to set priorities for materials to be used in the more expensive animal carcinogenicity and teratogenicity test systems. The initial acute animal studies, in turn, are used to identify the need for examining noncarcinogenic effects, such as damage to respiratory, neurologic, and immunologic systems.

The validity of applying results from animal experimentation to man is firmly based on empirical observations. However, as indicated in reports on animal life-span studies associated with nuclear fuel cycles, some progress is being made in obtaining data which will provide a more quantitative basis for the extrapolation of animal data to man.

Major progress was made in gastrointestinal studies involving the quantitative absorption of actinides from the adult and juvenile gut in various animal species.

The biomedical and health effects program at PNL is an interdisciplinary effort requiring scientific contributions from practically all research departments at PNL. The personnel in the Biology Department, the principal contributors to the volume, are listed on page 8.5. Requests for reprints from the list of publications and presentations for 1977 on pages 7.1 to 7.7 will be honored, except as noted.

CONTENTS

1.0 Coal

1.0 COAL

Studies in the area of coal energy technology encompass research relevant to occupational hazards, efforts dealing with potential effects of combustion products, and basic studies analyzing processes and pathologies that may be operationally affected upon exposure to aerosols generated by combustion or coal/synthetic fuel processing.

Toxicologic studies deal with the potential hazard to miners of elements found in mine atmospheres, and with effects of inhaled heavy metals that may be present in fly ash. More basic studies consider the effect of the anemic state upon the translocation of heavy metals that may be released by coal combustion/processing, pharmacologic analyses of effects of aerosolized sulfuric acid and potential blockers of such effects. In addition, analysis of a basic lung process (phagocytosis of inhaled particulates) is being pursued.

COAL

• Inhalation Hazard to Coal Miners

Acceleration in coal mining activities to satisfy present and future energy needs is linked with potentially severe health hazards. Coal workers pneumoconiosis (CWP) is a chronic debilitating disease associated with present coal mine dusts. Additional inhalation hazards may be associated with future extensive use of diesel engines in coal mines.

The objectives of this project are to study the development of pneumonconiosis and its progression to massive pulmonary fibrosis and/or emphysema in experimental animals, to clarify the mechanisms of induction of these diseases and the levels of specific mine air contaminants that are necessary to induce them.

BIOLOGICAL EFFECTS OF CHRONIC INHALATION OF COAL MINE DUST AND/OR DIESEL ENGINE EXHAUST IN RODENTS

Investigators:

B. O. Stuart, R. F. Palmer, R. E. Filipy

Technical Assistance:

K. Mapstead, D. Teats

Rats are being exposed daily, to inhaled high-CWP bituminous coal mine dust (6 mg/m^3 and 14 mg/m^3), separately or combined with unscrubbed exhaust from a diesel engine operated under load-rpni cycling. These studies are designed to determine whether there will be increased risk of long-term pulmonary disease from the proposed use of diesel engines in coal mining operation.

The goal of this research is to determine the biological behavior and effects of inhaled coal mine air contaminants, with particular emphasis on developing pathology related to the chronic respiratory disease known in man as "coal workers' pneumoconiosis" (CWP). This study will show whether or not there is likely to be an increased risk of chronic respiratory disease (including pneumoconiosis, fibrosis, bronchitis, and emphysema) from the proposed use of diesel engines in coal mines.

We have developed, tested and placed in operation a conipletely automated diesel engine exhaust exposure system for use with either efficient or inefficient engine operation, incorporating cycling through periods of high/low rpm and programmed engine load. It is during periods of acceleration and deceleration that the highest quantities of carcinogenic polycyclic aromatic hydrocarbons are produced in an inefficient engine (factors of 100X more than for well-tuned diesel

engines). This system is integrated with the chronic, whole-body rodent coal dust exposure system.

The pathogenesis of pneumoconiosis and progressive fibrosis is being investigated initially in male, specific-pathogen-free (SPF) rats. The experimental protocol is described in Table 1.1. Chamber concentrations for aerosol particulates by weight are given in Table 1.2. Chemical analyses for specific gas-aerosol constituents (inorganic and organic composition, particle size spectra, aerosol behavior) are carried out to correlate daily exposures with the developing pathology observed in animals sacrificed at 4-month intervals during the course of the exposure. All animals are weighed weekly, and quarterly hematological sampling is used to assess general health status and specific blood cell response of the animals. Carboxyhemoblogin levels in rats exposed to diesel engine exhaust are given in Table 1.3.

TABLE 1.1. Experimental Protocol

Group[a]	Exposure Regimen[b]
1	High CWP bituminous coal at 6 mg/m³
2	Inefficient diesel engine exhaust (50 ppm CO, 10 mg/m³ soot)
3	High CWP bituminous coal at 6 mg/m³ plus inefficient diesel engine exhaust at 10 mg/m³ soot = 16 mg/m³ total particulate
4	High CWP bituminous coal at 16 mg/m³ total particulate
5	Controls (identical exposure times and handling, with chamber air only)

[a] 48 male SPF rats per group; groups of 6 are sacrificed periodically to observe progression of possible chronic pulmonary disease

[b] Six hours/day; 5 days/week.

Chamber parameters being measured are:

1. CO (continuous monitoring)
2. Respirable and total coal or soot mass concentrations
3. Aerosol particle size distributions
4. NO, NO_2 and SO_2 in diesel exhaust chambers
5. Temperature and humidity in all chambers
6. Inorganic and organic analysis of aerosolized coal dusts and soot particulates

TABLE 1.2. Average Coal Dust and/or Exhaust Particulate Weights as mg/m³ (Mean ± SD) During the First 8 Mo of Daily Exposure(a)

Chamber 1	Coal dust	6.5 ± 2.2
Chamber 2	Diesel exhaust only	8.3 ± 1.9
Chamber 3	Diesel exhaust + coal dust	14.8 ± 3.8[b]
Chamber 4	Coal dust	15.3 ± 5.3

[a] The NO levels in Chambers 1 and 2 have ranged between 8 and 12 ppm; NO_2 levels between 1.5 and 0.5 ppm

[b] Total particulate

TABLE 1.3. Carboxyhemoglobin Levels in Rats Exposed to Diesel Exhaust (% COHb ± SD)

Group	Exposure	4 mo of Daily Exposure	8 mo of Daily Exposure
2	Diesel exhaust	7.14 ± 0.31	6.00 ± 0.32
3	Diesel exhaust + coal dust	7.53 ± 0.42	7.25 ± 0.63
5	Control	3.43 ± 0.21	2.90 ± 0.17

Histopathological examination of the lungs of six rats per group after 4 mo of daily exposures showed aggregations of particulate-bearing macrophages, with very slight emphysema and focal epithelial hyperplasia associated with the particulate accumulations. After 8 mo of daily exposures there were more extensive foci of accumulations of soot or coal dust particulates, with more advanced vesicular emphysema, beginning interstitial fibrosis (Figure 1.1), and proliferation of bronchiolar epithelium (Figure 1.2). These changes were most pronounced in Groups 2 and 3. Group 4 rats showed focal inflammation, with slightly more diffuse lung discoloration (Figure 1.3). Group 1 rats also showed focal reaction to accumulated coal dust, but to a lesser degree than Group 4 rats (Figure 1.4). Daily exposures are continuing in these studies of coal mine inhalation hazards.

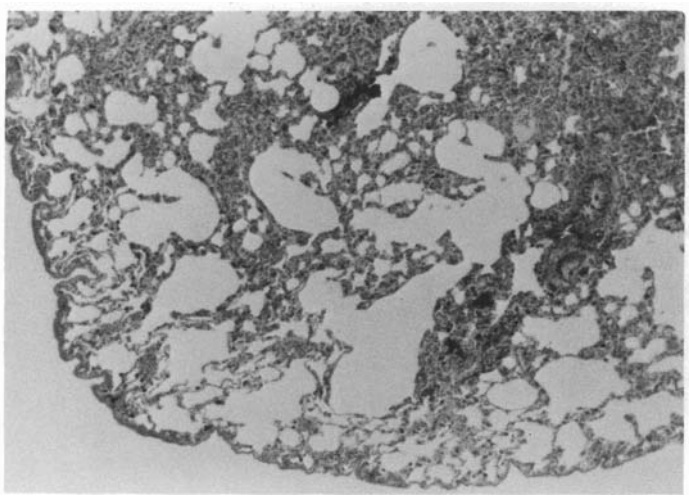

FIGURE 1.1. Focal Emphysema and Fibrosis in Lungs of a Rat that Received 8 Mo of Daily Exposure to Diesel Engine Exhaust (H&E 64X)

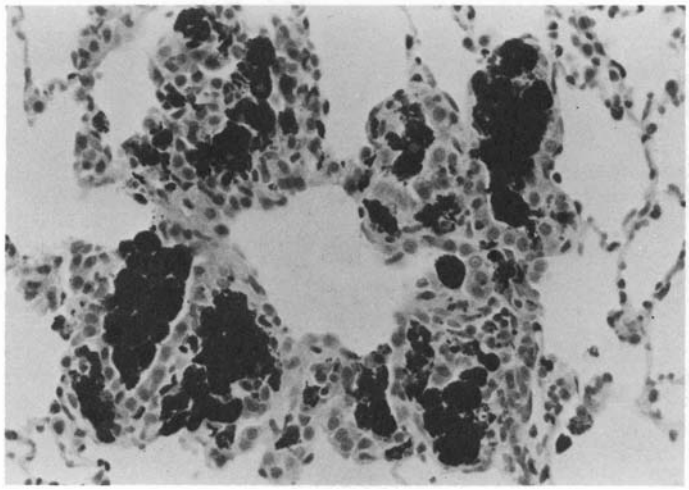

FIGURE 1.2. Bronchiolar Epithelial Proliferation and Inflammatory Reaction to Inhaled Particles in Lung of a Rat that Received 8 Mo of Daily Exposure to Coal Min Dust and Diesel Engine Exhaust (H&E 320X)

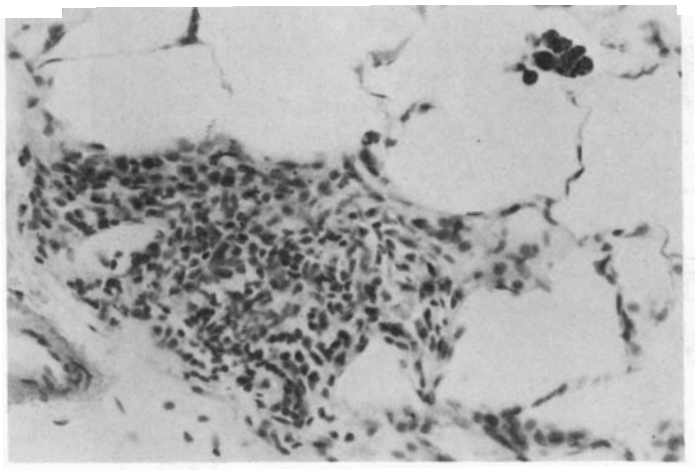

FIGURE 13. Focal Inflammation of Alveolar Epithelium in Lungs of a Rat that Received 8 Mo of Daily Exposures to Aerosols of 5 mg/m³ on Coal Mine Dust (H&E 320X)

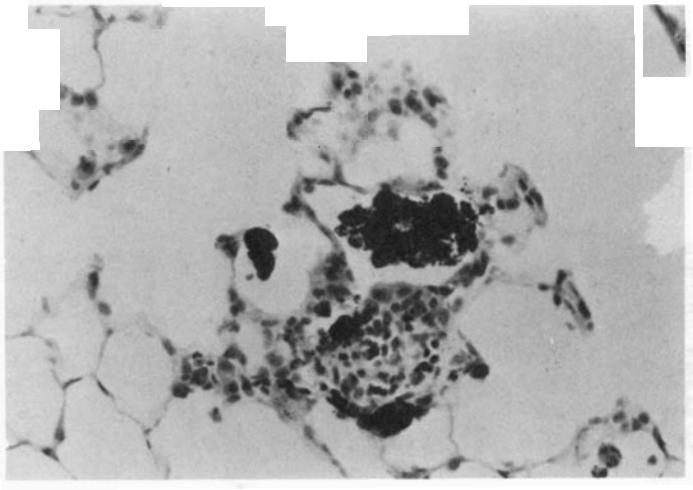

FIGURE 14. Inflammatory Reaction to Pigment in Lungs of a Rat that Received 8 Mo of Daily Exposures to Aerosols of 6 mg/m³ of Coal Mine Dust (H&E 320X)

• Lung Toxicity of Sulfure Pollutants

Sensitive humans develop respiratory and cardiovascular difficulty during episodes of high sulfur pollution due to the inhalation and subsequent effects of atmospheric sulfur compounds. This project will determine (using animal models) whether inhibiting bronchoconstriction caused by exposure to sulfur pollutants will protect sensitive animals from complications associated with pollutant exposure. If protection is found using animal models, a means of protecting sensitive humans may be suggested.

PULMONARY DISEASE MODELS IN THE GUINEA PIG: ASTHMA, BRONCHITIS AND EMPHYSEMA

Investigators:

S. M. Loscutoff and G. M. Zwicker

Technical Assistance:

A. J. Clary and B. W. Killand

Guinea pigs were developed as animal models for asthma and emphysema by sensitization to horseradish peroxidase and intratracheal instillation of elastase. These models will be used in future studies to determine methods for protecting sensitive animals from sulfuric acid aerosol exposures.

Humans with lung diseases are known to be more sensitive to high levels of sulfur pollutants than "normal" individuals. The purpose of these experiments was to develop guinea pigs as models for asthma, bronchitis and emphysema, with characteristics similar to those of the human diseases. Means of protecting these sensitized animals from exposures to sulfur pollutants can then be evaluated. The guinea pig was chosen because of its greater sensitivity to sulfur pollutants, compared with other experimental animals.

Exposure regimens for producing the various disease conditions are shown in Table 1.4. The extent of the disease produced was evaluated by both physiologic and histopathologic criteria.

Experimental asthma was induced by sensitizing guinea pigs to horseradish peroxidase (HRP) 1 mg/ml saline, administered intraperitoneally. Sensitivity was evaluated 2, 3 and 4 wk postinjection by exposing the animals to aerosolized HRP (1 mg/ml saline), using a Lovelace nebulizer. Results of these experiments are shown in Table 1.5. Tidal volume decreased during HRP aerosol exposure at each time postinjection.

The physiologic and histopathologic effects of elastase exposure are shown in Table 1.6. The five control animals killed 2 wk postexposure had no histologic or physiologic indications of emphysema. Two of the animals dosed with 10 units elastase/ 100 g body weight died approximately 112-hour postinstillation and had vascular damage and alveolar

hemorrhage. In the three animals killed 2 wk postinstillation, severity of lesions ranged from moderate focal (++) to panlobular (+++) emphysema. This degree of emphysema was associated with an increased mean linear alveolar intercept, and dynamic pulmonary compliance and decrease in pulmonary flow resistance, compared with controls. These results indicate that guinea pigs can be used as animal models of asthma and emphysema.

TABLE 1.4. Exposure Regimen for Producing Lung Diseases in Guinea Pigs

	Asthma		Emphysema		Bronchitis	
	Control	Exposed	Control	Exposed	Control	Exposed
No. of Animals	5	10	5	12	5	18
Material	Saline	HRP[a]	Saline	Elastase	Air	SO_2
Dose	1 ml	1 mg HRP/ ml Saline	0.5 ml/ 100 g	5-10 Units/100 g in 0.5 ml Saline	—	100 ppm 300 ppm 500 ppm
Route	Intraperitoneal		Intratracheal Instillation		Inhalation	
Exposure Frequency	0, 2 wk,[b] 3 wk[c]		0	0	3 hr/day, 2 day/wk for 6 wk	

[a] Horseradish peroxidase
[b] 1 mg HRP/ml saline; aerosolized for 20-min exposure
[c] 1 mg HRP/ml saline; aerosolized for 10-min exposure

TABLE 1.5. Tidal Volume in Sensitized Guinea Pigs Before, During and After Exposure to Aerosolized Horseradish Peroxidase

	During Exposure				
Time Postsensitization	Pre-Exposure	+5 min	+10 min	+20 min	5 min Postexposure
2 wk TV $\bar{X}$	1.90	1.66	1.59	1.39	1.55
SE	0.18	0.23	0.20	0.13	0.15
3 wk TV $\bar{X}$	1.80	1.56	1.43	—	1.51
SE	0.25	0.26	0.21	—	0.23
4 wk TV $\bar{X}$	2.44	1.81	1.83	—	2.00
SE	0.27	0.17	0.17	—	0.28

TABLE 1.6. Physiologic and Histopathologic Effects of Elastase Exposure in Guinea Pigs

		Elastase, 100 mg	
	Control N = 5	5 Units	10 Units
Died/Killed Time Postexposure	K 2 wk	K 2 wk	D 1/2 hr
Emphysema	—	++ to +++	—
Vascular Damage	—	—	++
MLAI[a] $\bar{X}$	12.78	5.85	—
SD	2.71	2.60	
Pulmonary Resistance (cm H_2O/ml/sec) $\bar{X}$	0.62	0.43	
SD	0.23	0.04	
Dynamic Pulmonary Compliance (ml/cm/H_2O) $\bar{X}$	0.59	0.77	
SD	0.25	0.06	

[a] Mean Linear Alveolar Intercept

INHIBITION OF BRONCHOCONSTRICTION CAUSED BY EXPOSURE OF GUINEA PIGS TO SULFURIC ACID AEROSOLS

Investigator:
Susan M. Loscutoff
Technical Assistance:
B. W. Killand

The degree of bronchoconstriction in guinea pigs exposed to sulfuric acid aerosols was assessed from measurements of pulmonary resistance and dynamic pulmonary compliance during exposure. Pretreatment of animals with the antihistamine, chlorpheniramine, prevented bronchoconstriction usually caused by sulfuric acid aerosol exposure. Parasympathetic blockade with atropine decreased but did not eliminate bronchoconstriction. Propanolol, a 8-adrenergic blocker, did not affect and may have potentiated the response to H_2SO_4.

Humans with lung disease are particularly sensitive to high sulfur pollution. The purpose of these experiments is to determine if animal models mimicking human lung diseases can be protected from harmful effects of sulfuric acid aerosol inhalation by inhibiting bronchoconstriction produced by these aerosols.

Pulmonary flow resistance and dynamic pulmonary compliance were measured in awake guinea pigs to assess the degree of bronchoconstriction. Methods for making these measurements were described in the 1976 Annual Report. Resistance and compliance were recorded on each guinea pig during a half-hour control period breathing room air, and during a 1-hr exposure period breathing H_2SO_4 aerosol. Aerosol mass concentration was approximately 20 mg/m^3 with a mass median aerodynamic diameter (MMAD) of less than 2 μm. Bronchoconstriction was inhibited by injecting pharmacologic blocking agents before exposure to acid according to the schedule and dosage shown in Table 1.7.

Results of pulmonary function measurements in controls and pharmacologically blocked animals are shown in Table 1.8, as percentage of control values measured during the 30-min period of room air breathing before acid exposures. These data indicate that exposure to 20 mg/m^3 sulfuric acid aerosols increases resistance to 3 times normal, and decreases compliance to one-third normal. The antihistamine, chlorpheniramine, prevents these changes in resistance and compliance, while parasympathetic blockade with atropine decreases but does not abolish the response. 8-adrenergic blockade with propranolol does not inhibit and may potentiate bronchoconstrictive effects of aerosol exposure. These results indicate that antihistamines are effective in preventing changes in pulmonary resistance and dynamic pulmonary compliance caused by sulfuric acid aerosol exposure in guinea pigs.

TABLE 1.7. Drug Protocol for Pharmacologic Blockade

Drug	Dose, mg/kg	Time Preinjection, min	Affected Endogenous Compound
Atropine	5	45	Acetylcholine
Propanolol	10	60	Catecholamines (5-receptors)
Chlorpheniramine	10	15	Histamine

TABLE 1.8. Pulmonary Resistance and Dynamic Compliance in Guinea Pigs Exposed to Sulfuric Acid Aerosols and Treated with Pharmacologic Blocking Agents[a]

Time Exposed to H_2SO_4 Aerosols, min	Pulmonary Resistance (% of control breathing room air)				Pulmonary Resistance (% of control breathing room air)			
	Control[b]	Chlorpheniramine	Atropine	Propanolol	Control[b]	Chlorpheniramine	Atropine	Propanolol
5	138	95	96	107	91	97	89	83
15	278	86	127	128	74	85	85	74
30	294	90	125	352	53	93	91	39
45	305	95	103	376	49	85	91	35
60	249	95	122	283	55	91	71	36

[a] Mean values for 10 animals per group
[b] H_2SO_4 Aerosol—Exposed, no pharmacologic blockage

Malnutrition and Metal Toxicity

Nutritional deficiencies are common in both industrialized and underdeveloped countries. Several heavy metal pollutants from energy conversion sources are known to be detrimental to to the hematopoietic and immune systems, and some are carcinogenic. However, there is a paucity of information concerning potential synergistic effects of nutritional deficiencies combined with heavy metal exposure. This project will examine the interactions of specific nutritional deficiencies and heavy metal exposures with particular emphasis on gastrointestinal absorption of the metals and subsequent effect on the hematopoietic and immune system.

EFFECTS OF IRON DEFICIENCY ON ABSORPTION OF NICKEL

Investigator:
H. A. Ragan
Technical Assistance:
E. T. Edmerson, S. L. English, M. C. Perkins and M. J. Pipes

Moderately anemic, iron-deficient rats absorbed ∿ 2.5 times as much ^{63}Ni, administered via gavage, as did those on a control diet.

Previous Annual Reports have described the absorption of various pollutant metals in iron-deficient animals. In brief, iron-deficient mice, but not rats, absorbed more plutonium than control animals. Enhanced absorption in iron-deficient rats was found for lead, cadmium, zinc, and mercury, but not arsenic. Control rats absorbed more vanadium than iron-deficient rats. The present study, on nickel, continues to evaluate effects of energy-related pollutant metals in iron-deficient animals.

Weanling rats were fed an iron-deficient or control diet until 63 days of age when they were gavaged with ∿ 20 μCi of ^{63}Ni citrate. Forty-eight hours after the gavage blood samples were obtained, rats were killed, skin and gastrointestinal tract removed, and organs and remaining carcass saved for radioanalyses.

At the time of necropsy the iron-deficient rats were moderately anemic with microcytic erythrocytes and reduced body iron stores (Table 1.9); there was no significant difference in mean body weight between the two groups.

Iron-deficient rats had significantly higher body burdens of ^{63}Ni than the control group (Table 1.10). As is common in absorption studies, there was considerable individual variation among animals in both groups, but a 2.5-fold difference in mean total body ^{63}Ni. Serum, liver and kidney retained the largest fractions of administered ^{63}Ni (Table 1.10). ^{63}Ni in other organs was usually below detection limits of the scintillation counter.

Since nickel is a known carcinogen, future studies will examine that aspect by chronic feeding of stable nickel to iron-deficient and control rats.

TABLE 1.9. Hematologic and Body-Iron Status of Iron-Deficient Control Rats (Mean ± SD; n=10/group)

	Iron-Deficient	Control	P<
Body weight (g)	349 ± 28	366 ± 28	NS
VPRC[a] (ml/100 ml)	31.0 ± 5.2	42.9 ± 0.8	0.01
MCV[b] (μ^3)	43.1 ± 2.1	56.9 ± 0.9	0.01
Serum iron (μg/dl)	73 ± 42	181 ± 46	0.01
TIBC[c] (μg/dl)	720 ± 112	463 ± 42	0.01
Spleen iron[d]	1.2 ± 1.0	3.0 ± 0.7	0.01
Marrow iron[d]	1.1 ± 0.3	2.5 ± 1.1	0.01

[a] Volume of packed red cells
[b] Mean corpuscular volume
[c] Total iron binding capacity
[d] Histochemical iron graded progressively from 0-4+

TABLE 1.10. Percent of Administered ^{63}Ni Dose Present 48 hr After Gavage (Mean + 1 SD; n=10/group)

	% Dose x 10^3		
	Iron-Deficient	Control	P<
Total body burden	161 ± 91	64 ± 47	0.02
Serum[a]	24.8 ± 26.5	4.1 ± 7.0	0.05
Liver	4.4 ± 1.8	1.0 ± 1.3	0.01
Kidney	23.3 ± 15.2	9.4 ± 5.7	0.02

[a] Based on estimated blood volume of 7.5%

HEMATOLOGIC EFFECTS OF CHRONIC LEAD AND CADMIUM INGESTION IN IRON-DEFICIENT RATS

Investigator:

H. A. Ragan

Technical Assistance:

M. J. Pipes, E. T. Edmerson, S. L. English, M. C. Perkins, K. H. Debban, and J. Sweeny

Neither lead nor cadmium markedly altered the hematologic effects of iron deficiency in male rats; in the slower-growing female rats, lead tended to exacerbate the hematologic effects of the iron-deficient diet.

Iron-deficient rats administered tracer amounts of radioactive lead and cadmium by gavage absorbed and retained more of these elements than did age-related control rats (Kagan, H. A., J Lab Clin Med 90: 700-706, 1977). It was therefore considered important to evaluate the chronic effects of these elements on the hematopoietic system in iron-deficient rats.

Male and female Wistar rats were fed either an iron-deficient (∿ 4 ppm iron) or control (∿ 150 ppm iron) diet for 30 days, starting at about 21 days of age. After this 30-day period, half of each group received 1100 ppm lead (as the citrate) for an additional 30 days (males) or 60 days (females). A concurrent study was performed with male rats only, using 50 ppm cadmium (as the chloride) in place of lead, for 60 days.

Results of the lead studies with male rats are shown in Table 1.11. There was a significant weight reduction in rats on the iron-deficient + lead diet. Though food consumption appeared comparable in all groups (∿ 25 g/day), more food appeared to be wasted by rats on lead-containing diets. The erythroid series was severely affected by both the iron-deficient and lead-containing diets, as indicated by effects on the volume of packed red cells (VPRC) and mean corpuscular volume (MCV). Reticulocyte concentrations in both groups on iron-deficient diets were increased over both control and control + lead diets. The resistance of red cells to osmotic lysis was increased in iron-deficient groups but was unaffected by addition of lead. Serum iron values were decreased in all iron-deficient groups. Histochemical staining for iron confirmed the presence of an iron deficit in rats on the iron-deficient diet. However, it appears that lead also stains in the Prussian blue reaction, causing a false-positive reaction when used for evaluation of tissue iron stores. Chemical analyses revealed a highly significant increase in lead concentrations in the iron-deficient + lead as compared to the control + lead group.

Effects in female rats, after 60 days, were similar, though less marked than in male rats (Table 1.12), even though the females were on the diet a longer time. The slower growth rate of females may have resulted in a less severe and slower-developing iron deficit. This interpretation is supported by the moderate decrease in VPRC, MCV, serum iron, and histochemical grading of spleen-iron in the iron-deficient diet group. Chemical analyses for tissue lead are not complete for the female groups.

In the cadmium study (Table 1.13) body weights were reduced in both groups fed cadmium. Cadmium is known to interfere with iron metabolism, and this is reflected by effects on VPRC, MCV, and reticulocyte concentrations. The interference of cadmium with iron utilization is also evident when serum iron values are compared. Histochemical iron stains and chemical analyses for tissue cadmium are not complete.

TABLE 1.11. Hematologic Effects of Iron-Deficient and Lead-Containing Diets Fed Male Rats for 30 Days (Mean ± SD)

	Control	Iron-Deficient	Control + Lead		Iron-Deficient + Lead	
				P< (a)		P< (b)
Weight, g	382 ± 24	328 ± 32	376 ± 44	NS	260 ± 44	0.001
VPRC,(c) ml/100 ml	42.5 ± 2.0	33.1 ± 8.0	38.3 ± 1.7	0.001	28.5 ± 4.2	0.001
MCV,(d) μ^3	55.4 ± 1.4	43.0 ± 2.9	50.7 ± 2.0	0.001	42.2 ± 2.4	0.001
Reticulocytes, x $10^3/mm^3$	176 ± 74	389 ± 194	211 ± 41	NS	413 ± 146	NS
MCF,(e) % Saline	0.42 ± 0.01	0.34± 0.03	0.41 ± 0.02	NS	0.34 f0.02	0.001
Marrow Cellularity, x 10^3	73.8 ± 20.4	72.2 ± 14.1	100.0 ± 15.8	0.01	94.1 ± 12.6	NS
Serum Iron, μg/dl	311 ± 115	77 ± 49	145 ± 13	0.01	171 ± 26	0.01
Histochemical Spleen Iron	1.8 ± 1.0	0.2 ± 0.4	4.0 ± 0	0.001	2.9 ± 1.6	0.05
Lead, μg/g						
Liver			4.30 ± 0.56	—	7.31 ± 1.64	P < 0.001
Femur			153 ± 56	—	479 ± 139	P < 0.001
Kidney			17.2 ± 4.3	—	180.3 ± 162.7	P < 0.01

(a) In relation to control group
(b) In relation to control + lead group
(c) Volume of packed red cells
(d) Mean corpuscular volume
(e) Mean corpuscular fragility

TABLE 1.12. Hematologic Effects of Iron-Deficient and Lead-Containing Diets Fed Female Rats for 60 Days (Mean ± SD)

	Control	Iron-Deficient	Control + Lead		Iron-Deficient + Lead	
				P< (a)		P< (b)
Weight, g	278 ± 16	265 ± 26	237f 28	0.01	213 ± 26	NS
VPRC,(c) ml/100 ml	43.3 ± 1.5	42.6 ± 4.2	39.6 ± 3.4	0.01	33.2 ± 2.9	0.001
MCV,(d) μ^3	56.2 ± 1.3	48.3 ± 5.3	49.2 ± 1.8	0.001	43.2 ± 2.0	0.001
Reticulocytes, x $10^3/mm^3$	97 ± 21	129 ± 58	151 ± 61	0.02	320 ± 140	0.01
MCF,(e) % Saline	0.46f0.01	0.40f0.04	0.44f0.01	NS	0.38f0.03	0.001
Marrow Cellularity, x 10^3	82.9 ± 5.1	68.8± 19.0	79.0± 10.8	NS	81.7 ± 7.3	NS
Serum Iron, μg/dl	270 ± 58	245 ± 88	304 ± 60	NS	266 ± 55	NS
Histochemical Spleen Iron	4.0 ± 0	1.1 ± 1.8	4.0 ± 0	NS	4.0 ± 0	NS

(a) In relation to control group
(b) In relation to control + lead group
(c) Volume of packed red cells
(d) Mean corpuscular volume
(e) Mean corpuscular fragility

TABLE 1.13. Hematologic Effects of Iron-Deficient and Cadmium-Containing Diets Fed Male Rats for 60 Days (Mean ± SD)

	Control	Iron-Deficient	Control + Cadmium	P < (a)	Iron-Deficient + Cadmium	P < (b)
Weight, g	452 ± 51	400 ± 36	310 ± 20	0.001	244 ± 25	0.001
VPRC,[c] ml/100 ml	43.8 ± 0.9	24.1 ± 8.7	41.4 ± 2.8	0.02	26.9 ± 4.4	0.001
MCV,[d] μ^3	55.8 ± 2.3	40.3 ± 4.6	50.7 ± 1.4	0.001	39.8 ± 1.5	0.001
Reticulocytes, x $10^3/mm^3$	175 ± 35	222 ± 81	129 ± 41	0.02	127 ± 49	NS
MCF,[e] % Saline	—	—	0.44 ± 0.02	—	0.39 ± 0.02	0.001
Marrow Cellularity, x 10^3	65.5 ± 11.8	76.6 ± 6.8	62.0 ± 7.7	NS	63.4 ± 7.5	NS
Serum Iron, $\mu g/dl$	148 ± 33	56 ± 24	392 ± 105	0.001	96 ± 46	0.001

(a) In relation to control group
(b) In relation to control + cadmium group
(c) Volume of packed red cells
(d) Mean corpuscular volume
(e) Mean corpuscular fragility

• Alveolar Clearance of Metal Oxides

Metal oxides produced during the combustion of fossil fuels constitute a potential hazard to man. The purpose of this project is to determine the role of pulmonary cells in influencing the fate of inhaled metal oxides and the acute and chronic toxicity of inhaled metal oxides in the lungs of rodents.

TOXICITY OF INHALED CADMIUM OXIDE

Investigators:
J. G. Hadley, C. L. Sanders,
A. Conklin, and R. R. Adee

Pretreatment of rats with WR2721 was found to protect partially against the edematogenic effects of inhaled cadmium oxide. Using transmission electron microscopy, disruption of Type I epithelial cells was shown to be the probable cause for the increased permeability of lung tissue following cadmium inhalation.

In a previous Annual Report (1976) we showed that inhalation of cadmium oxide (CdO) by rats produces a severe and frequently fatal pulmonary toxicity characterized by massive pulmonary edema. Additionally, it was found that pretreatment of rats with compound WR2721 (S-2-[3-aminopropylaminoethyl phosphorothioic acid hydrate]) offered partial protection against the acute toxicity of inhaled CdO.

To investigate further the effect of WR2721 pretreatment on CdO toxicity, 25 female Wistar SPF rats were injected intraperitoneally with 80 mg WR2721 and exposed (with 25 nontreated rats) to an aerosol of CdO for 50 min. Initial lung burden was 33.0 ± 12.7 μg/Cd. Groups of six animals were sacrificed at 3-hr intervals following exposure. Bronchopulmonary lavage was performed and the protein content of the lavaged fluid determined as an index of pulmonary edema.

Animals pretreated with WR2721 had a decreased rate of edema formation (as judged by lavage protein content) (Figure 1.5). Although the mechanism by which WR2721 decreases CdO-induced pulmonary edema is unknown, it does not appear to result from an increased clearance of CdO from the lung (Annual Report, 1976).

In an attempt to correlate the specific structural alterations in the lung resulting from CdO inhalation with the observed fluid translocation and resultant edema formation, 68 female rats were exposed to an aerosol of CdO. Groups of three animals were sacrificed at hourly intervals and lung tissue prepared for electron microscopy. The results indicate that inhaled CdO appears to initially disrupt Type I alveolar epithelium (Figures 1.6 to 1.9). This alteration is seen 14 hr postexposure (Figure 1.7) and begins as a "bubbling" of Type I epithelial cell

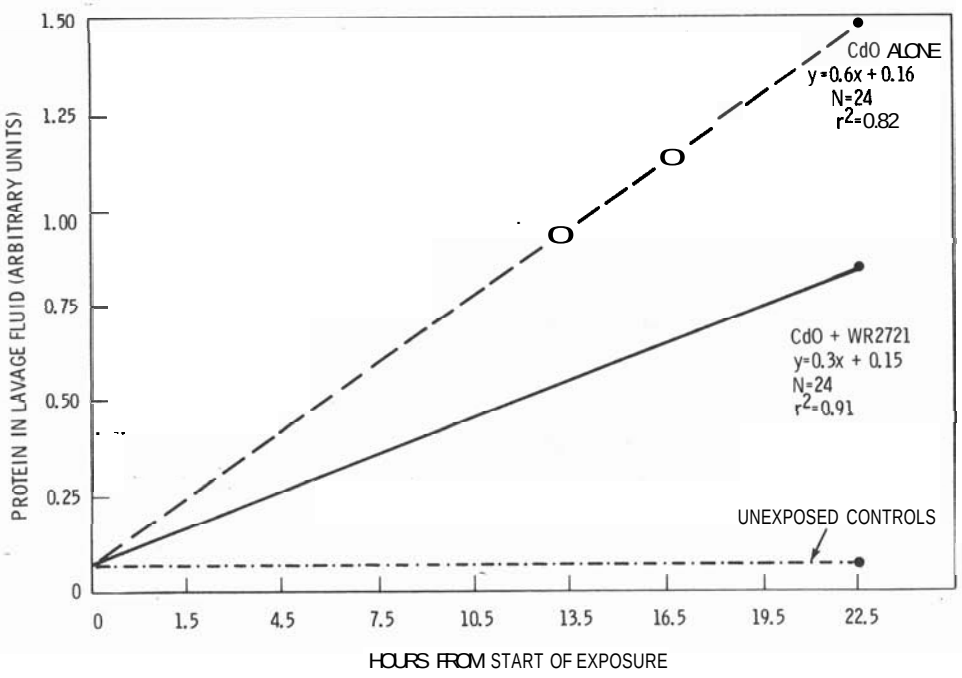

FIGURE 15. Influence of WR2721 Pretreatment on CdO-Induced Protein Accumulation. Lines are least squares analysis of data from three animals of each group, sacrificed at indicated time points.

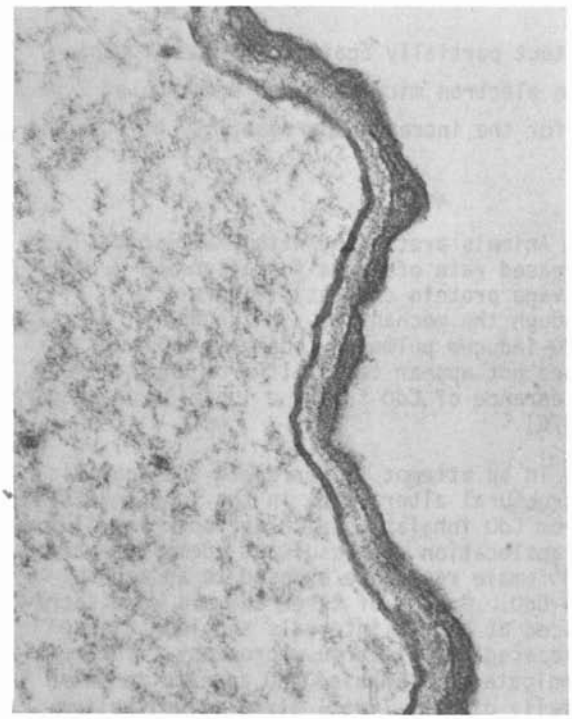

FIGURE 16. Normal Blood-Air Barrier, Showing (from right to left): Air Space, Type I Alveolar Epithelium, Basement Membrane and Interstitium, Endothelium, and Capillary Space (50,000X)

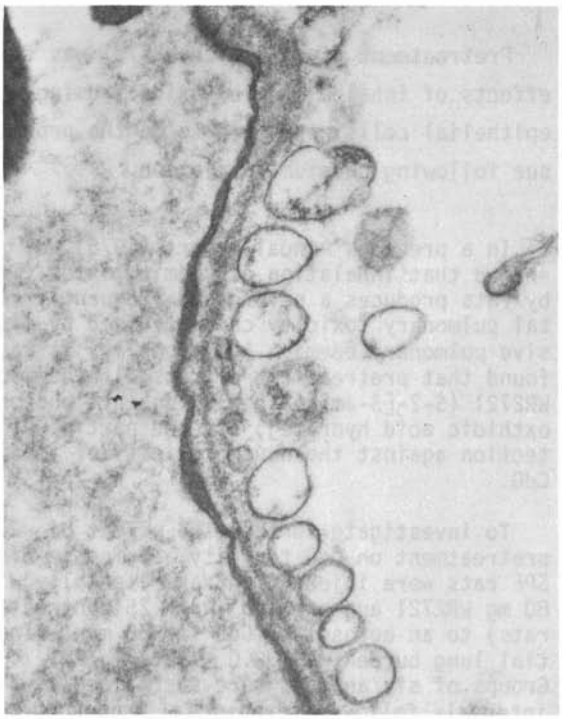

FIGURE 17. "Bubbling" of Type I Alveolar Epithelium, Exposing Basement Membrane; 14 hr After Inhalation of CdO (50,000X)

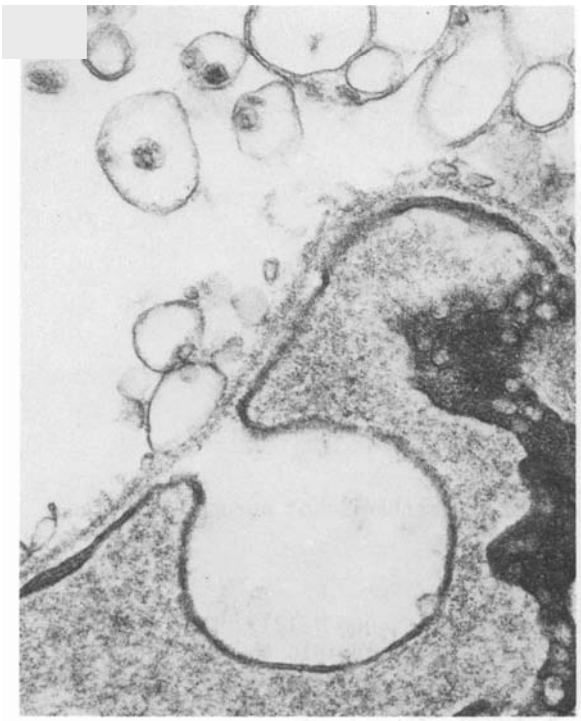

FIGURE 1.8. Near-Complete Loss of Type I Alveolar Epithelium Due to "Bubbling." Note deep invagination of capillary endothelium; at 21 hr after inhalation of CdO (50,000X).

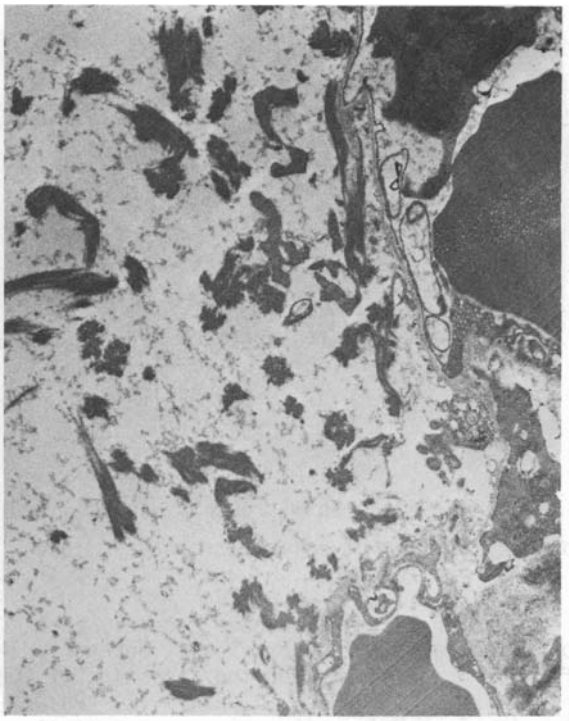

FIGURE 1.9. Complete Loss of Type I Alveolar Epithelium Associated with Accumulation of a Protein-Like and Elastin-Like Material in the Air Space at 22 hr After Inhalation of CdO (9600X)

membrane. At later time periods (Figures 1.8, 1.9), the damage progresses in severity and leads to complete loss of Type I alveolar epithelium. It is likely that the pulmonary edema observed in CdO-exposed animals is related to the increased permeability of the alveolar epithelium caused by disruption of Type I epithelial cells.

Experiments are in progress to investigate the chronic effects of CdO inhalation on pulmonary, cardiovascular, and reproductive systems.

A SCANNING ELECTRON MICROSCOPIC STUDY OF AGRAPOD-MEDIATED PHAGOCYTOSIS

Investigators:

J. G. Hadley, R. R. Adee, and J. Coleman

Scanning electron microscopy was utilized to elucidate the mechanism of agropod-mediated phagocytosis by alveolar macrophages.

Alveolar macrophages have recently been observed to utilize a previously unreported form of phagocytosis for the ingestion of foreign particles (Hadley, J. G., 1977. Ph.D. Thesis, Duke University, NC. This process involves the projection of large tubular extensions of macrophage membrane which ingest particles lying within a 50- to 60-μm radius about the macrophage cell body. Through the use of these tubular structures, which have been designated 'agrapods', the macrophage extends its effective phagocytic range 30- to 40-fold.

The basic morphology of agrapod-mediated phagocytosis has been studied by time-lapse microcinamatographic techniques in conjunction with light microscopic examinations.

A four-stage model of the process has been described and consists of 1) attachment, 2) elongation, 3) engulfment, and 4) withdrawal (Figure 1.10).

In an attempt to understand more fully the membrane events occurring during agropod formation, rabbit alveolar macrophages were cultured with yeast particles (Saccharomyces cerevisiae) as described in the reference cited above. Cover slips were fixed in glutaraldehyde, dehydrated, and critical point dried. Fixed cells were sputtered with gold and examined in a scanning electron microscope.

Figures 1.11 through 1.14 illustrate the appearance of alveolar macrophages at various stages of agrapod-mediated phagocytosis. During the elongation phase the agrapod maintains the surface irregularities characteristic of macrophages. The particles are attached to discrete processes at the tip of the growing agrapod (Figure 1.11). Invagination of the particle into the tip of the agrapods occurs by an infolding of the membrane attached to the particle (Figure 1.12). The particle is drawn completely into the agrapod and membrane closure occurs (Figure 1.13). As the agrapod containing the particle is withdrawn toward the cell body, the agrapod membrane loses its wrinkled appearance and becomes quite smooth (Figure 1.14).

Studies are in progress to ascertain the influence of cadmium and other heavy metals on agrapod-mediated phagocytosis by alveolar macrophages.

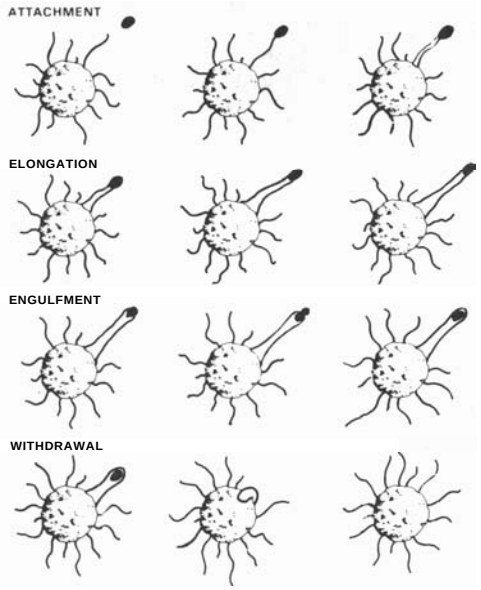

FIGURE 1.10. Schematic Representation of Agrapod-Mediated Phagocytosis. The attachment phase begins with contact of the small filipodia of the macrophage with the particle. Filipodia rapidly increase in diameter to approximate particle size. Elongation occurs at rates up to 15 μm/min. The engulfment phase occurs rapidly (≈1.0 min) and constitutes stage three. After engulfment the particle-containing macrophage withdraws into the cell body.

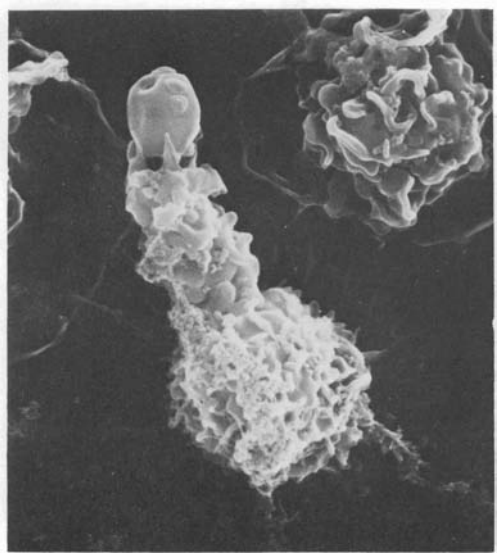

FIGURE 1.11. Alveolar Macrophage Utilizing Agrapod for Ingestion of Yeast Cell. Probably elongation phase. Note discrete attachment sites on yeast cell (2400X).

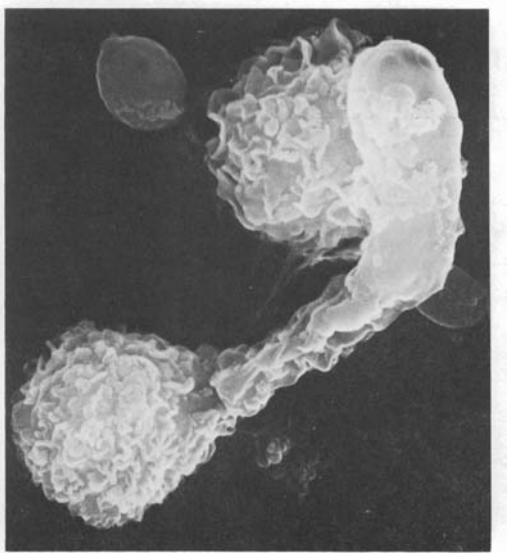

FIGURE 1.13. Alveolar Macrophage with Agrapod Containing a Fully Engulfed Yeast Cell, Representing the End of the Engulfment Phase (3200X)

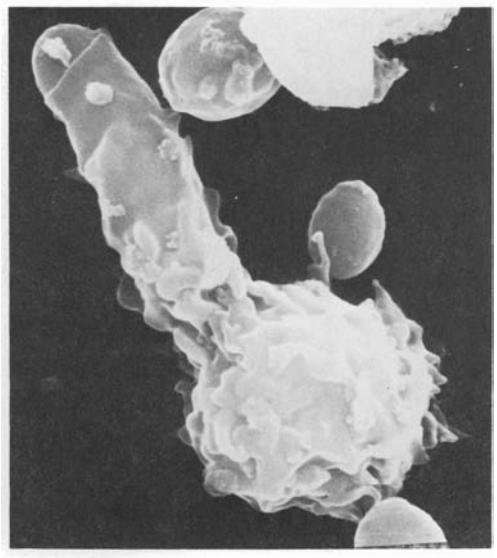

FIGURE 1.12. Yeast Cell Entering Agrapod, Apparently by Enfolding of the Agrapod Membrane (400X)

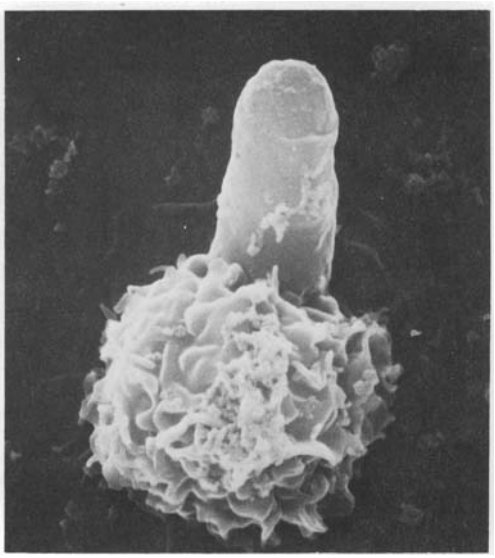

FIGURE 1.14. Withdrawal Phase of Agrapod-mediated Phagocytosis is Characterized by Loss of Surface Irregularities as Agrapod Containing a Yeast Cell is Withdrawn into the Macrophage Cell Body (4000X)

• Cross-Placental Transfer of Metals (EPA)

This project seeks to define the specific influences of factors affecting the cross-placental transfer of heavy metals and their distribution throughout the fetoplacental unit as a function of time after exposure. These data will define the tissues at risk and provide a quantitative estimate of dose. As such, they will provide a rational basis on which to interpret and interrelate the results of teratologic studies.

DISTRIBUTION OF INHALED LEAD NITRATE IN PREGNANT RATS

Investigators:

P. L. Hackett, J. O. Hess, M. R. Sikov, W. C. Cannon, E. F. Blanton, J. O. Herring, and A. C. Case

Technical Assistance:,

M. J. Conger, A. C. Crosby, L. F. Hensley and K. A. Poston

Lead distribution in maternal tissue and fetoplacental units was studied at various stages of gestation following inhalation exposure of rats to two levels of lead nitrate with ^{210}Pb tracer. Maternal deposition and distribution were dose-dependent. Lead nitrate was rapidly absorbed and transferred to major organ systems and to the fetoplacental unit where deposition depended on the stage of gestation.

Intravenous administration of lead nitrate to pregnant rats at specific gestation times has been shown to cause prenatal death and resorption, as well as characteristic developmental abnormalities. It was also found that the kinetics of lead distribution within the maternal and fetoplacental units were dose-dependent (Annual Report, 1976). Since the most probable route of exposure of the general population is by inhalation, studies were initiated to determine the distribution and cross-placental transfer of two levels of inhaled soluble lead nitrate in pregnant animals for comparison with our previous studies of intravenously administered lead nitrate.

Aerosols were generated from 0.2 N HNO_3 solutions containing freshly-separated ^{210}Pb (tracer exposure) or stable $Pb(NO_3)_2$ with ^{210}Pb (carrier exposure), employing a Lovelace nebulizer. Characteristics of these solutions and aerosols are shown in Table 1.14.

Thirty-six rats were exposed for 1 hr, nose-only, to each aerosol at 8, 9, 14, 15, or 19 days gestation (dg). Groups of six to twelve animals were killed immediately after exposure and at 1, 2, 5, 6, and 11 days. Radiolead activities were determined in maternal and fetal tissues and excreta by measuring the 47-KeV gamma emission of ^{210}Pb with a scintillation counter, after decay of biologically translocated ^{210}Bi.

TABLE 1.14. Characteristics of Generating Solutions and Aerosols for ^{210}Pb Inhalation Exposure of Rats

Generating Solution	Tracer Exposure	Carrier Exposure
μCi ^{210}Pb/ml	772	745
ng Pb/μCi	0.0167	28
Aerosol		
μCi ^{210}Pb/ℓ	1.81	1.34
ng Pb/ℓ	0.030	37.5
Mass Median Aerodynamic Diameter	1.85	2.45
Geometric Standard Deviation	2.30	2.33
Count Median Diameter	0.11	0.14

The average deposition value (total body burden plus excreta minus head and skin) for the tracer group amounted to 9.42 ± 0.29 μCi (0.157 ± 0.005 ng Pb), and a value of 8.16 ± 0.29 μCi (228 ± 8 ng Pb) was found in the carrier-exposed rats. Because of the small sample sizes in this initial study, no differences in distribution could be attributed to the period of gestation; all maternal values were therefore pooled.

The distribution of ^{210}Pb in animals sacrificed during the first 6 hr after exposure is shown in Figure 1.15. Fractions of the body burden in the gastrointestinal (GI) tract and lung appeared to bear a reciprocal relationship, since the GI tract values for the carrier group were 10% higher and the lung values were 10% lower than comparable tissues in the tracer group. A high percentage of the body burden was noted in the GI tract at the initial sampling period, reflecting particles cleared from the upper respiratory tract. Figure 1.16 demonstrates very rapid transit rate through the GI tract since most of the ^{210}Pb was in the jejunum and ileum by 0.5 to 3 hr after inhalation exposure and peak activity was in the cecum by 3 to 6 hr. At 24 hr, fecal values were equal to the original GI tract values.

The very high skeletal burdens in the initial samples (Figure 1.15) implied rapid absorption and deposition of the inhaled lead nitrate. Blood values were higher in tracer than in carrier animals and, within dose groups, were similar to hepatic and renal values.

The percentage of the maternal body burden transferred to the fetoplacental unit (FPU) at different stages of gestation is shown in Figure 1.17. FPU values for carrier-exposed rats tended to be lower than those

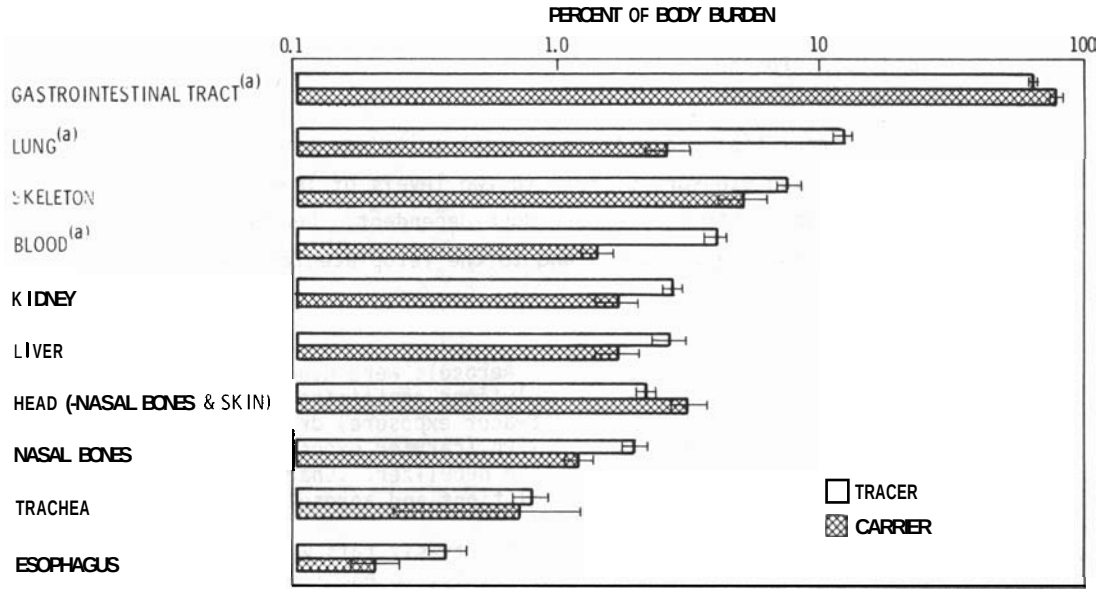

(a) TRACER AND CARRIER VALUES ARE SIGNIFICANTLY DIFFERENT ($P < 0.051$)

FIGURE 1.15. Distribution of ^{210}Pb in Female Rats Following Inhalation Exposure to Lead Nitrate

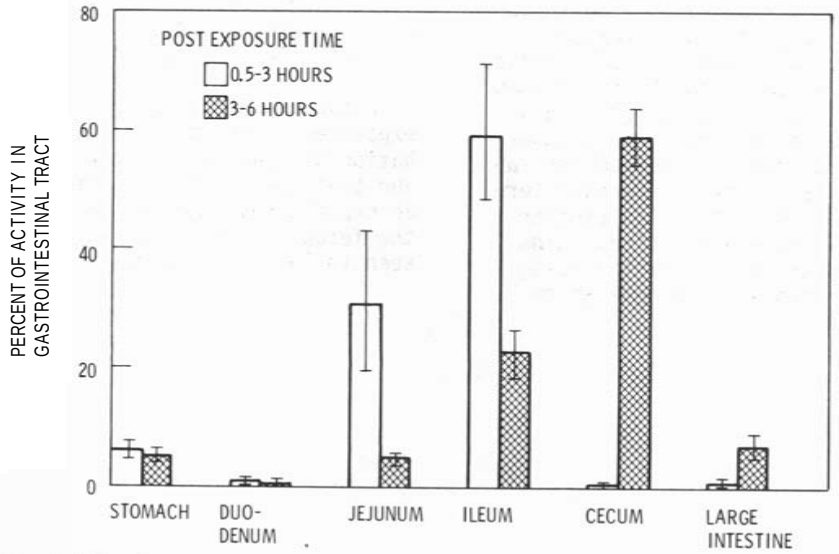

FIGURE 1.16. Percent Activity in Gastrointestinal Tract Segments Following Inhalation Exposure to $^{210}Pb(NO_3)_2$

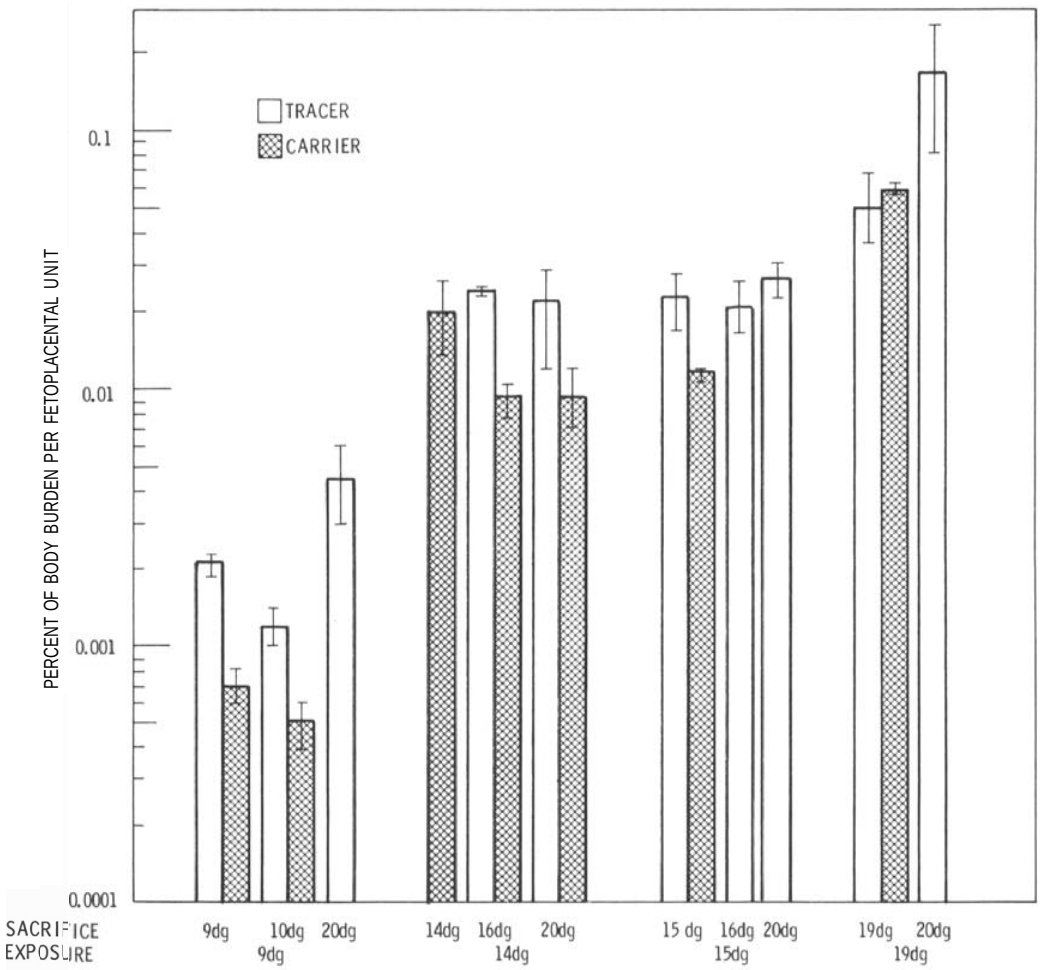

FIGURE 1.17. Percent of Maternal ^{210}Pb Body Burden per Fetoplacental Unit Following Inhalation Exposure on Different Days of Gestation (dg)

for tracer-exposed rats at earlier gestation periods and probably reflected maternal blood values. FPU values for animals exposed at 14 or 15 dg were equal and about 10 times higher than values for the 9-dg FPU. This relationship was similar to the results obtained in the intravenous study. Concentration (% dose/g) relationships between maternal blood and these FPUs were also similar following either intravenous or inhalation exposure. The higher values for the 19-dg FPUs on the day of exposure as well as on 1 day postexposure (Figure 1.17) demonstrated the influence of rapid skeletal growth and calcification on fetal lead uptake.

Data obtained from this initial inhalation exposure suggest that deposition and distribution of lead nitrate are dose-dependent, and that lead absorption is very rapid. Once absorption has occurred, metal deposition in the fetoplacental unit is similar to that seen following intravenous administration.

2.0 Conservation

CONSERVATION

- **Mutagenic Effects of Electric Fields (EPA)**

This project was initiated in FY 1976 to examine the possibility that electric fields induce changes in the genetic mechanism of cells. The project is initially directed toward evaluation of genetic changes induced by DC fields, then moves to a similar evaluation of effects from AC fields. Data for mutation frequencies are obtained in several bacterial strains and in the fruit fly, Drosophila.

MUTAGENIC EFFECTS OF STATIC ELECTRIC FIELDS

Investigator:
F. P. Hungate

Static DC fields are being evaluated for their ability to induce mutations in bacteria and Drosophila. Present data suggest that mutations are produced in the Ames TA-100 strain of Salmonella, Photobacterium fisheri (tetracycline resistance) and Drosophila (recessive sex-linked lethals). No increased mutation frequency was observed in the Ames TA-98 strain.

With the exception of special purpose studies, such as the Navy's Project Sanguine, little attention has been given to the possibility that electric fields might cause subtle changes in biological systems due to factors other than current flow. Literature on electric field effects generally indicates lack of effects, but in most studies, fields tested were similar in strength to those to which organisms (including humans) have been typically exposed.

Assuming that stronger electric fields might produce a relatively greater effect, we chose first to determine if mutational effects could be detected in fields approaching those in which corona would be expected, i.e., voltage approaching 10 kV/cm.

The exposure system utilized parallel copper plates separated by a ring of lucite, as described in the 1976 Annual Report. Sterile humidified air flows into the chamber during exposures minimizing buildup of possible secondary factors such as ozone. Voltage is supplied either by a high-voltage DC power supply or by a series stack of batteries. At field strengths used to date we have been unable to detect corona, either photographically or by monitoring current. Control subjects are maintained concomitantly under identical conditions except for the electric field. Air flow for exposed and control subjects is in parallel, from a common source.

Salmonella strains TA-98 and TA-100, developed by and obtained from Dr. Bruce Ames, are used as primary bacterial test systems. Since both strains require histidine for growth, mutants are identified as colonies able to grow in the absence of

histidine. In addition, we use the luminescent bacterium, Photobacterium fisheri, strain MAV, and evaluate the frequency of genetically undefined mutations permitting growth on a concentration of tetracycline (2.5 µg/ml) that prevents growth of nonmutant cells. Bacteria are usually exposed overnight (16-24 hr) at ambient temperature (20-24°C).

To avoid chain formation with resultant spark discharge, observed with adult flies, day-old Drosophila pupae were exposed to a 1850-V,cm^{-1} battery-driven field for 3 days. Flies were then tested by the Muller-5 technique for the presence of sex-linked recessive lethals.

Figures 2.1, 2.2, and 2.3 show data acquired from exposures of bacteria to fields. Mutation frequencies are shown as ratio of frequency in exposed cultures divided by that in control cultures simultaneously exposed, each representing 10 replicate plates. Points above 1 indicate a positive effect from the field; those below 1 indicate fewer mutations in exposed than in control cultures. Suitably transformed mutation counts for each strain of bacteria were analyzed by multiple regression to reduce the effect of differences in cell counts that also assumed a linear dose-effect relationship.

There was no consistent induction of mutation in strain TA-98 by the fields used (Figure 2.1). This observation was born out by analysis, which showed a nonsignificant ($a > 0.05$) linearly increasing relationship

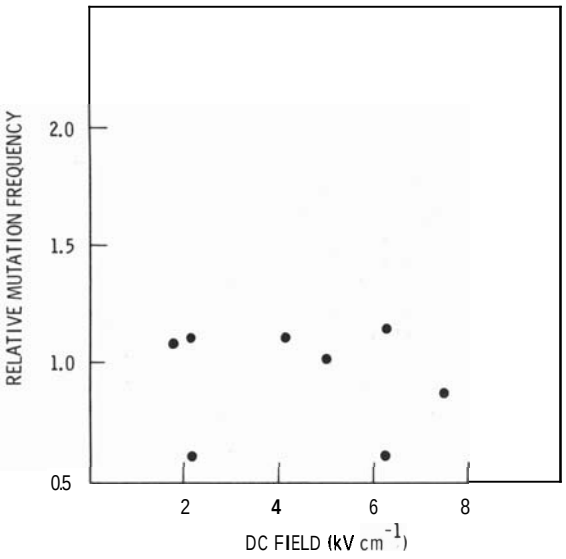

FIGURE 2.1. Relative Mutation Frequency of Salmonella TA-98 Exposed to Static DC Fields

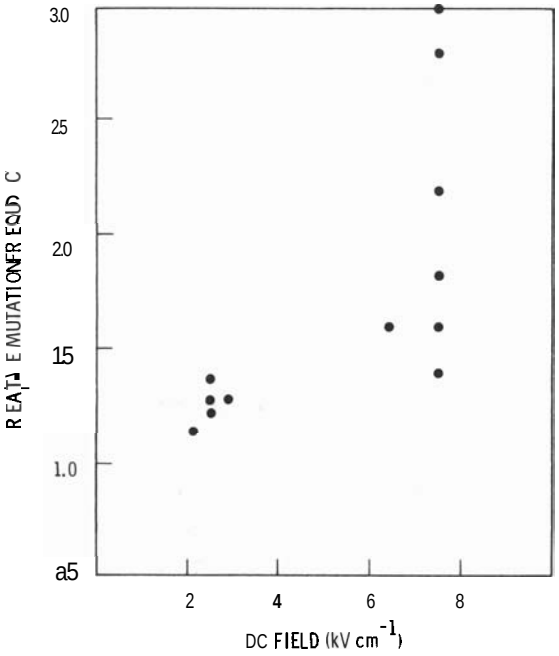

FIGURE 2.2. Relative Mutation Frequency of Salmonella TA-100 Exposed to Static DC Fields

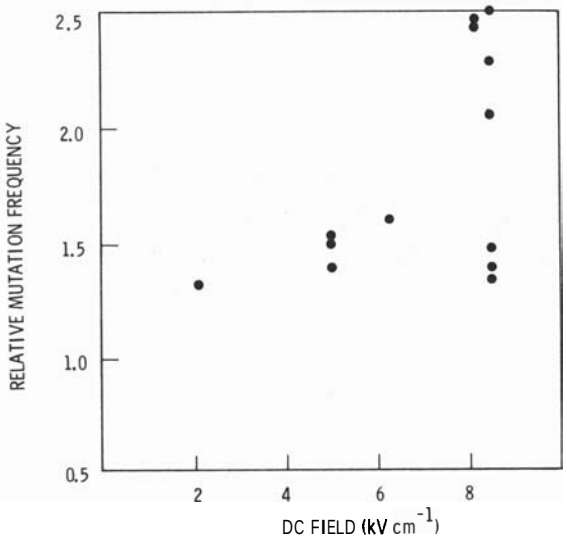

FIGURE 2.3. Relative Mutation Frequency (Exposed/Control) of Photobacterium fisheri Strain MAV, Mutation to Tetracycline Resistance

between field strength and mutation count. Strain TA-100, which mutates primarily by base exchange, showed a significant ($a < 0.01$) linearly increasing relationship between field strength and mutation count with 79% of the variability accounted for by the model (Figure 2.2). MAV data (Figure 2.3), produced a similar result, with 94% of the variability accounted for by the model. The

relationship between field strength and mutation count for TA-100 and MAV may or may not be linear. The paucity of data does not permit a valid assessment of the dose-effect relationship.

Table 2.1 shows the results of four experiments with Drosophila. When analyzed by Chi-square, the significance level (a) of a difference between exposed and control pupae lies between 0.1 and 0.2 for males, and between 0.8 and 0.9 for female groups. Clearly more data are needed to confirm that such fields produce mutations and to identify whether such effects are dependent on cell environment, i.e., whether the mutation increase is restricted to events in male flies or also occurs in both X chromosomes of females.

TABLE 2.1. Mutation Frequencies from 0.25-Hr Drosophila Pupae Exposed 3 Days in an 1850-V/cm DC Field

	Male		Female	
Expt.	Exposed	Control	Exposed	Control
1	3 / 901	1 / 495	1 / 517	0 / 525
2	11 / 2477	6[a] / 1897	4 / 2418	2 / 1125
3	3 / 1225	1 / 1188	0 / 3249	3 / 3119
4	5[a] / 1159	3 / 1435	4 / 2954	1 / 1786
Combined Data	22 / 5762 (0.38%)	11 / 5015 (0.22%)	9 / 9138 (0.098%)	6 / 6555 (0.092%)

[a] Two mutants from one parent of the P_1 generation


3.0
Fission

3.0 FISSION

Biomedical studies in the fission energy technology area are mostly concerned with the evaluation of long-term effects from low-level exposure to radioactive pollutants. These include studies in progress for many years in dogs that have inhaled various plutonium compounds. The inhalation toxicity of a wider variety of actinide compounds is being studied in rodents. Both dogs and rodents are employed in continuing studies of the effects of chronic exposure to simulated uranium mine atmospheres.

Recently instituted studies are concerned with specific reactor technology problems, such as the toxicity of sodium that might be accidentally released from an LMFBR (liquid metal fast breeder reactor), or the toxicity of mixed aerosols of plutonium and sodium. The toxicity of chronically inhaled krypton-85, released in small amounts from nuclear reactors, is also being studied. Because of recent interest in nonproliferative fuel cycles, special hazards that might be associated with reactors employing a thorium fuel cycle are being investigated.

More basic studies are concerned with the effects of age on the toxicity of incorporated radionuclides, and the effect of age, and other factors, on the gastrointestinal absorption of radionuclides. Viral and biochemical factors that may be involved in radiation carcinogenesis are also under study.

In the more strictly medical areas, procedures are being developed that may reduce the probability of radiation effects by hastening removal from the body of internally deposited radionuclides. In other studies, advantage is taken of radionuclides incorporated in a device designed to irradiate the blood, which may be a useful treatment for leukemia or for the prevention of tranplant rejectior

FISSION

• Aerosol and Analytical Technology

One objective of this program is to improve aerosol exposure techniques: the generation and characterization of inhalation atmospheres, relation of aerosol properties to respiratory deposition and clearance, and accuracy of aerosol exposure dose control. The other objective is to improve sample analysis and handling techniques, including improvement of sample management and quality control to reduce sample backlog and storage problems, improvement of the sensitivity of Pu analysis procedures, and development of new and less costly techniques for low-level assay of radioisotopes.

INITIAL DEPOSITION OF INHALED PuO_2 AEROSOLS IN PIGS

Investigators:

D. K. Craig, M. T. Karagianes, J. L. Beamer, W. C. Cannon, J. R. Decker, J. P. Herring, and R. L. Buschbom

Technical Assistance:

A. J. Clary, J. S. Barnett, and E. F. Blanton

Techniques developed for determining the deposition of aerosols as a function of particle size in dogs were applied to data obtained from the nose-only inhalation exposure of four pigs. The results indicate that despite the deposition of a considerable fraction of the inhaled activity in the exposure mask, deposition of aerosols in pigs is probably quite representative of that in humans.

As part of the study to determine the feasibility of using pigs for nose-only inhalation toxicology studies, the exposure system developed for beagles was modified to accommodate Hanford miniature swine. The concentration and volume of inhaled aerosol and the respiration parameters of four pigs were measured during their exposure to $^{239}PuO_2$ aerosols having AMADs of 2 to 3 μm and GSDs of 2.0 to 2.4. The expired aerosol was separated from that inspired and the aerodynamic size distribution of both were determined (Table 3.1). Total initial deposition in the pig and in the plumbing as a function of particle size was determined from these measurements. This calculation of the fractional deposition of aerosols in each of the eight size ranges of the cascade impactors was carried out as follows:

If f_i = fraction of activity SA_{IN} on the i th stage of the cascade impactor sampling inhaled air,

g_i = fraction of activity SA_{OUT} on the i th stage of the cascade impactor sampling exhaled air,

and t_i = fraction of aerosols in the i th stage size range that is "lost",

TABLE 3.1. Particle Size Distribution of Inhaled and Exhaled $^{239}PuO_2$ Aerosols

	Inhaled Aerosols			Exhaled Aerosols		
Pig No.	AMAD,[a] um	GSD[b]	SA_{in},[c] nCi	AMAD, μm	GSD	SA_{out}, nCi
1	2.96	2.44	5,157	1.04	1.99	847
2	3.18	2.24	18,128	1.25	1.79	2,979
3	2.02	1.95	6,967	1.34	1.89	1,182
4	1.79	2.04	8,140	1.12	1.76	2,069

[a]Activity Median Aerodynamic Diameter
[b]Geometric Standard Deviation
[c]Sum of ^{239}Pu activity on 8 stages of cascade impactors for a fixed sample volume

then $t_i = 1 - \frac{g_i}{f_i}\frac{SA_{OUT}}{SA_{IN}}$.

Since some of the inhaled and exhaled activity is deposited in the exposure system plumbing between the pig's nose and the respective samplers, these t_i values represent the total fractional deposition in the pig and the exposure system of aerosols in the i th size range. A crude correction can be made for the material deposited in the exposure system by multiplying the SA values by a factor based upon the measured activity in the plumbing in relation to these SAs. This procedure makes the simplifying assumption that such deposition does not modify the aerosol size distributions; obviously not correct, but the best we can do until a complete characterization of losses in the exposure system as a function of particle size can be carried out.

The initial body burden of each pig was obtained by adding the activity excreted in feces and urine to that left in the pig at sacrifice. This was from 5 to 10% of inhaled activity (Table 3.2). The aerosol concentration in the expired air was about one-fifth of that in the inspired air. However, a considerable fraction was deposited in the exposure masks, mostly in the narrow tubes that were inserted in the nostrils of the anesthetized pigs. Preferential deposition of the larger particles undoubtedly modified both the size distribution and the total quality of PuO_2 aerosol actually inhaled by each pig.

The last row of Table 3.2 gives Q_{LOST}, that portion of the calculated inhaled activity not accounted for after adding all the activity found in each pig and its excreta and exhaled air, plus that recovered from the exposure system, including the pig exposure mask. Besides material that resisted being washed from the Pu-contaminated system, most of this was probably snorted up by the pig and deposited on the walls of the metabolism cages in which they were housed.

More than 95% of particles greater than 4 μm were deposited in these tubes and in the respiratory tract of the pig, decreasing to about 15% in the range 0.6 to 1 μm and about 25% for 0.1-μm particles (Figure 3.1). These deposition fractions are quite similar to those that have been observed for dogs, and may also be compared with the ICRP Task Group curves for man.

TABLE 32. Distribution of ^{239}Pu in Pig Tissues and Excreta, Inhaled and Exhaled Air, and Deposited on Plumbing [a]

Item	Pig No. 1	2	3	4	Mean ± SD
Calculated Inhaled Activity = A_{in}	52,200	167,400	38,600	50,900	
Plumbing + Mask Deposition - % of A_{in}	32	33	37	40	35.5 ± 3.7
Corrected $A_{in} = Q_{in}$	35,600	113,100	24,500	30,700	
Final Body Burden = FBB	1,385	3,490	457	87	
Total Excreta = Σ Ex	469	3,173	2,064	2,784	
Initial Body Burden = FBB + Σ Ex = IBB	1,854	6,663	2,521	2,871	
IBB as % of Q_{in}	5.2	5.9	10.3	9.4	7.7 ± 2.5
First Week's Fecal Excreta - % of IBB	16.6	34.3	53.6	64.5	
Initial Lung Burden = IBB - 1st week's feces = ILB	1,546	4,378	1,171	1,019	
ILB as % of Q_{in}	4.3	3.9	4.8	3.3	4.1 ± 0.6
Activity Exhaled = Q_{out}	12,400	41,900	13,570	23,300	
A_{in} - (IBB + Plumbing + Q_{out}) = Q_{lost}	21,350	64,540	8,400	4,530	
Q_{lost} as % of A_{in}	40.9	38.6	21.8	8.9	27.5 ± 15.1

[a] All activity values given in nCi

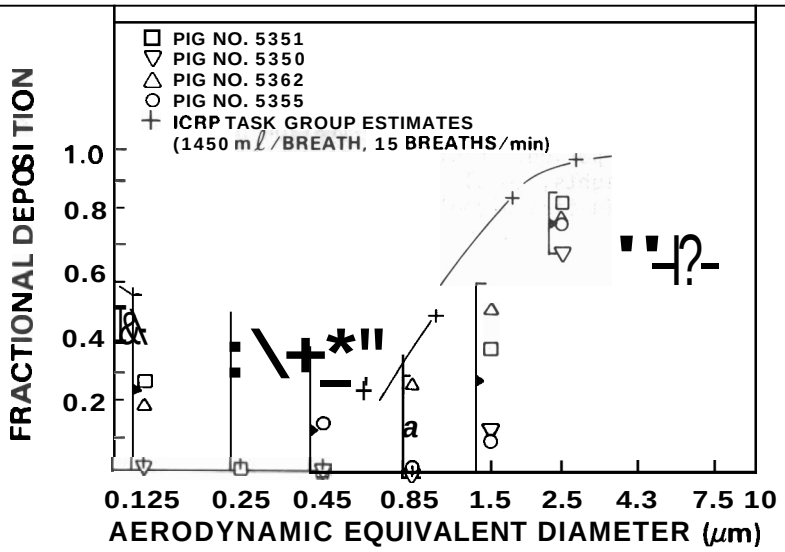

FIGURE 31. Total Initial Deposition as a Function of Aerosol Particle Size (corrected for deposition in plumbing)

DEPOSITION OF $^{239}Pu(NO_3)_4$ AEROSOLS IN BEAGLE DOGS

Investigators:

W. C. Cannon, J. P. Herring, G. E. Dagle

Technical Assistance:

E. F. Blanton and B. F. Garrity

Deposition characteristics of inhaled $^{239}Pu(NO_3)_4$ aerosols are being studied in beagle dogs. No significant correlations between percentage deposition and measured aerosol concentrations were observed.

Deposition of $^{239}Pu(NO_3)_4$ aerosols is being studied in beagle dogs exposed for the project "Inhaled Plutonium Nitrate in Dogs." The dogs were individually exposed, "nose only", to aerosols ranging in concentration from 1 nCi/ℓ to 600 nCi/ℓ to attain initial alveolar depositions varying from 2 nCi to 2000 μCi. To achieve the desired deposition, aerosol concentrations were varied by varying the specific activity of the generator solution (SSA). All animals in an exposure group inhaled the same amount of activity, as determined by the product of chamber aerosol concentration (measured just prior to exposure of each dog) and the inhaled volume (measured during exposure of each dog).

The thorax of the dogs was counted 14 days postexposure, and excreta were collected and analyzed over this period. From these data and animal body weights, total initial deposition (TID) and initial alveolar deposition (IAD) were estimated. These estimates, together with pertinent aerosol data, such as concentration and particle size, are shown in Table 3.3. There is a strong correlation between SSA and aerosol concentration, but TID and IAD percentages are not significantly correlated with SSA or aerosol concentration, and only slightly correlated with AMAD and GSD. This is due, in part, to the narrow ranges in both AMAD and GSD. Particle size is not correlated to SSA or aerosol concentration. Comparison of data from these exposures to data from previous exposures of rats to $^{239}Pu(NO_3)$, in which there were some exposures with higher SSAs, suggests that particle size is only affected if SSA is above 100 μCi/ml. These data show that varying the generator solution concentration has very little effect upon percentage deposition in dogs.

TABLE 3.3. Deposition of Inhaled $^{239}Pu(NO_3)_4$

Aerosol Data						Exposure Data			
	Concentration nCi/ℓ					TID as % Total Activity		IAD as % Total Activity	
SSA[a] μCi/ml	Mean	SD	AMAD[b] μm	GSD[c]	No. of Dogs	Mean	SD	Mean	SD
0.08	**0.38**	**0.09**	**0.51**	**5.8**	**3**	**24**	**12**	**21**	**10**
0.24	0.83	0.23	0.65	2.47	10	45	39	35	39
1.02	3.22	0.45	0.64	2.02	10	31	15	23	16
2.2	6.8	0.6	0.50	2.7	3	24	4	27	5
3.4	12.9	2.0	0.56	1.94	14	49	11	42	11
5.1	21.9	7	0.64	1.93	7	52	12	38	11
5.3	24.8	6.9	0.88	2.07	9	57	9	42	11
5.3	14.4	0.6	0.52	1.94	6	64	23	41	8
23.6	111	12	0.77	1.90	7	53	12	42	11
25.3	97.7	15.0	0.69	1.94	3	65	8	52	7
28.0	71.6	5.2	1.02	2.27	3	100	22	48	8
55	194	4	0.59	2.21	3	36	6	31	7
104.3	321.8	66.1	0.93	2.23	10	62	11	59	11
148.2	533.4	117.3	0.85	2.37	5	58	10	55	11

[a] Solution **Specific Activity**
[b] Activity **Median Aerodynamic Diameter**
[c] Geometric **Standard Deviation, assuming a Log Normal distribution**

CHARACTERIZATION OF A MONODISPERSED AEROSOL EXPOSURE SYSTEM FOR BEAGLE DOGS

Investigators:

W. C. Cannon, J. P. Herring, and D. K. Craig

Technical Assistance:

E. F. Blanton and B. F. Garrity

A monodispersed aerosol exposure system for dogs is described and data are presented on aerosol depositions in the exposure system which could affect the aerosol presented to the animals by reducing the concentration and changing the particle size distribution.

A May spinning top aerosol generator, located inside an aerosol chamber, generates a labeled, monodispersed aerosol of iron oxide particles into this chamber (Figure 3.2). This procedure eliminates the necessity for transporting the particles between a generator containment vessel and the aerosol chamber, which would be difficult because of the strong pumping action of the generator designed to sweep away unwanted satellite particles.

Aerosols used in this experiment were generated from a mixture of a hydrated iron colloid and a gold colloid labeled with ^{198}Au. The geometric standard deviations were, for the most part, close to 1.3, as determined from Mercer impactor data. Dogs inhaled these aerosols from the chamber for inhaled particle deposition studies. Particles which deposited in valves and plumbing of the exposure system were washed out and analyzed to measure exposure system losses as a function of particle size. Since the valves and plumbing of this system are similar to those in polydispersed aerosol exposure systems used at PNL, this characterization should help in predicting losses of polydispersed aerosols in those exposure systems.

In Table 3.4, depositions in the parts of the exposure system are expressed as percent of total activity drawn from the aerosol chamber. Total activity includes that collected on the nose or muzzle of the dog during exposure. The correlation coefficient is 0.98 between particle size and activity collected from the dog's nose. The correlation coefficient between aerosol particle size and alveolar deposition is 0.84; between particle size and total exhaled activity it is 0.72. It is clear from the data that depositions in the venturi, mask, valve, and exhalation system plumbing are not strongly particle-size-dependent.

We have not considered effects of dead space in the system. For example, dead space in the valve causes uninhaled aerosol to be expelled into the exhalation system, increasing the activity measured in these compartments.

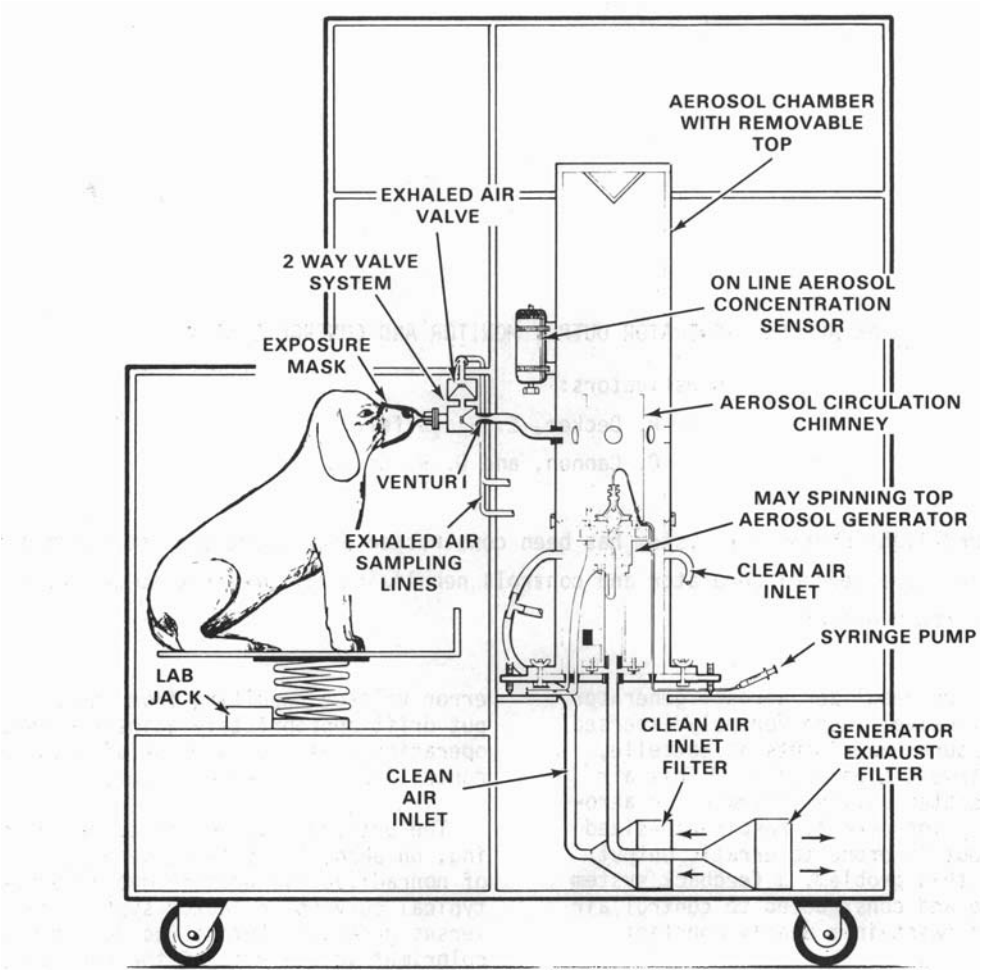

FIGURE 3.2. Monodispersed Aerosol Exposure System

TABLE 3.4. Effect of Particle Size on Exposure System Depositions (Percent of Total Activity)

AED	Venturi	Valve	Mask	Nose	Alveolar	Total Dog	Exhaled Plumbing	Total Exhaled Activity
1.5	2	0.4	1	8	58	76	1	21
1.65	2	1	1	8	50	74	1	23
1.90	2	1	9	16	37	72	0.4	17
2.65	9	1	3	20	11	63	1	24
3.35	11	1	8	25	6	70	2	10
4.5	5	1	3	40	11	79	3	12

AN AEROSOL GENERATOR OUTPUT MONITOR AND CONTROL SYSTEM

Investigators:
J. R. Decker, E. G. Kuffel,
W. C. Cannon, and D. K. Craig

A scattered-light photometer system has been constructed and tested that monitors output of a nebulizer-type aerosol generator and controls nebulizing air pressure to maintain a constant generator output.

The Lovelace nebulizer aerosol generator has been extensively used for polydispersed aerosol exposure experiments at Battelle, Pacific Northwest Laboratories. This air pressure-operated device generates an aerosol of nearly log normal, respirable-sized particles, but is prone to erratic output. To minimize this problem, a feedback system was designed and constructed to control air pressure and maintain a nearly constant output.

The block diagram of this photo-controlled aerosol generator is shown in Figure 3.3. The aerosol output monitor, positioned at the output of the generator, is a forward-scattering photosensor, consisting of an infrared light-emitting diode and a matched infrared photodetecting transistor. The output of the photosensor, which is linearly related to the droplet mass concentration, is fed to a multiplier circuit through a variable gain amplifier and damping circuit.

Droplet mass output can be held constant if multiplier output is constant, accomplished by comparing multiplier output with a manually set reference level. Comparison error voltage resulting from generator output drift appropriately adjusts generator operating pressure by means of a voltage-controlled pressure regulator.

The detector system was tested by collecting, on absolute filters, generator output of nonradioactive uranine dye aerosols. A typical curve of detector systems output versus generator output (as determined by colorimetric analysis of the dye) is shown in Figure 3.4. The feedback system was tested by manually changing generator nebulizer level with respect to reservoir fluid level in order to affect the efficiency of generation. The system then automatically increased or decreased the operating air pressure in attempt to maintain constant generator output. Figure 3.5 is a typical plot of generator output (colorimetrically determined from filter samples of uranine dye aerosols) versus operating pressure. In Figure 3.4 this is compared with the expected generator output without feedback.

This system is now being tested under animal exposure conditions.

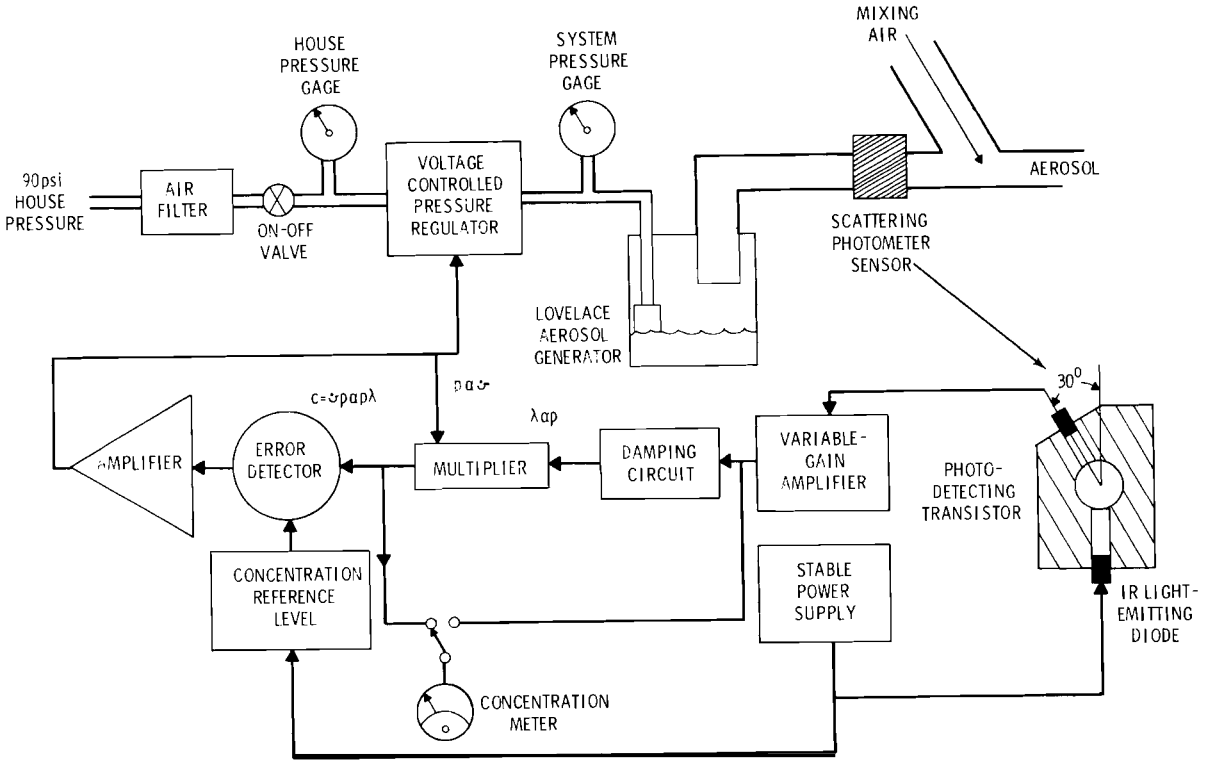

FIGURE 3.3. Block Diagram of Photo-Controlled Aerosol Generator (PHOCAG) Systems

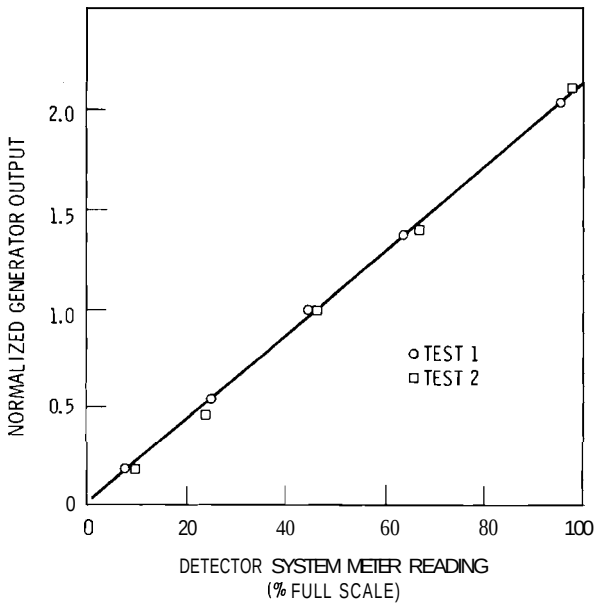

FIGURE 3.4. Generator Aerosol Output (Normalized at 20 PSI Generator Operating Pressure) Versus Detector System Output as Observed by the Meter

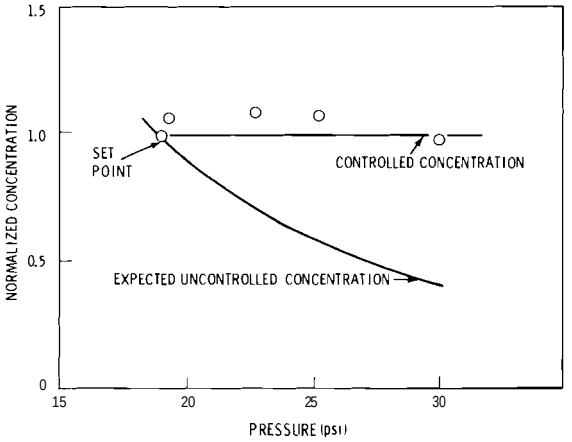

FIGURE 3.5. Normalized Generator Aerosol Output (Circles) Under Feedback Control and Expected Generator Output Without Feedback Control Versus Automatically Controlled Generator Operating Pressure

TRACE ANALYSIS OF ACTINIDES IN BIOLOGICAL SAMPLES

Investigators:

R. E. Schirmer and D. W. Phelps

Technical Assistance:

K. D. Wiemers and K. R. Hanson

Methods of improving procedures for the analysis of trace actinides in biological samples are being investigated, including use of freeze drying prior to ashing, separation of the actinides by high pressure liquid chromatography (HPLC), and separation and measurement of actinides by gas chromatography.

Preparation of biological materials for actinide analysis begins with oven drying and ashing of the samples. Freeze drying has been evaluated as an alternate to oven drying in an effort to increase the number of samples that can be processed through the ashing step. We found that freeze drying is slower than oven drying, but that freeze-dried samples ash twice as fast as oven-dried ones. Use of a freeze dryer would also free hood and oven space for ashing. The net effect of changing from oven to freeze drying would be to approximately double the capacity of our laboratory for carrying samples through the drying and ashing steps. Studies of spiked dog feces show no loss of uranium or plutoniuni in either drying process.

After ashing, the actinides are separated from other components of the ash using column chromatography. Horwitz and coworkers at Argonne National Laboratories have shown that separations of this type can be carried out in minutes, instead of hours, by using high pressure liquid chromatography. Since the eluting solvents are typically strong acids, a special chromatograph is required to do this work. During FY 1977 we completed construction of a suitable high pressure chromatograph (Figure 3.6) based on the Cheminert^{R} CMP-2VK metering pump and Cheminert^{R} valves. During FY 1978, methods will be developed for separating thorium, uranium, plutonium, and americium using this instrument and the potential of HPLC for increasing the capacity of our laboratory for routine actinide separations will be evaluated.

We have also begun work to develop gas chromatographic procedures for the analysis of trace levels of actinides. The procedure consists of complexing the metal ion with a fluorinated derivative of acetyl acetone and measuring the complex by gas chromatography (GLC) with an electron capture detector. The ligands used to date are listed in Table 3.5. In preliminary work we prepared $Cr(HFA)_3$, $Fe(HFA)_3$ and $Al(HFA)_3$ and found that 10^{-12} to 10^{-13} g of each of these metals can be quantitated by the GLC procedure. ThL_4 and UO_2L_2 complexes have also been prepared where L is TFA, HFA or FOD, and work is in progress to find suitable conditions for their chromatography. The actinide complexes are harder to chromatograph than the complexes of Cr, Fe and Al because they are less stable thermally. If sensitivities on the order of 10^{-12} g are achieved for the actinides, the GLC method will be more sensitive than the usual counting procedures for isotopes with half-lives greater than 10^3 yr. In addition to being fast, GLC offers the advantages of combining the separation and detection of the metal into a single step. During FY 1978 our efforts will be concentrated on finding the best combination of ligand and chromatographic conditions to maximize sensitivity and reproducibility in the analysis, and to extend the work to plutoniuni.

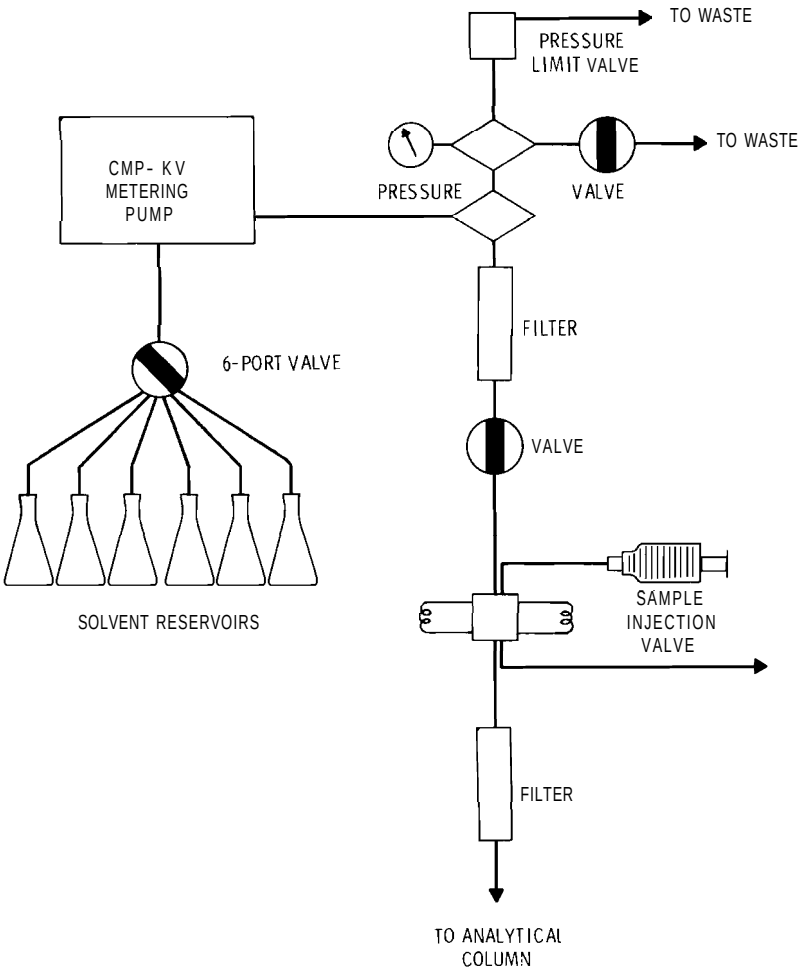

FIGURE 3.6. High-Pressure Liquid Chromatograph

TABLE 3.5. List of Ligands

TFA	**1,1,1-Trifluoro-2,4-pentanedione**
HFA	**1,1,1,5,5,5-Hexafluoro-2,4-pentanedione**
FOD	1,1,1,2,2,3,3-Heptafluoro-7,7-dimethyl-4,6-octanedione

• Inhaled Plutonium Oxide in Dogs

This project is concerned with: a) long-term experiments to determine the life-span dose-effect relationships of inhaled $^{239}PuO_2$ in beagles, b) long-term experiments to determine the life-span dose-effect relationship of inhaled $^{238}PuO_2$ in beagles, c) continuing studies on the late effects of inhaled $^{238}PuO_2$ in beagles, d) continuing studies on the late effects of single large $^{238}PuO_2$ microspheres in the lungs of beagles, e) continuing studies on the late effects of inhaled large $^{238}PuO_2$ microspheres in beagles, and f) shorter-term experiments in beagles to study the retention and translocation of transplutonium elements, such as $^{241}AmO_2$, and $^{244}CmO_2$ that are prominent components of nuclear fuels.

DOSE-EFFECT STUDIES WITH INHALED PLUTONIUM OXIDE IN BEAGLES

Investigators:

J. F. Park, A. C. Case, D. L. Catt, D. K. Craig, G. E. Dagle, R. M Madison, G. J. Powers, H. A. Ragan, S. E. Rowe, D. L. Stevens, J. R. Tadlock, C. R. Watson, E. L. Wierman, and G. M. Zwicker

Technical Assistance:

D. H. Akin, J. S. Barnett, E. F. Edmerson, E. A. Emory, S. L. English, V. T. Faubert, R. E. Flores, G. D. Irwin, S. L. Krum, B. G. Moore, S. L. Owzarski, M. C. Perkins, M. J. Pipes, L. R. Peters, and G. L. Webb

Beagle dogs given a single exposure to $^{239}PuO_2$ and $^{238}PuO_2$ aerosols are being observed for life-span dose-effect relationships. The ^{239}Pu body burden of the nine dogs that died of pulmonary fibrosis-induced respiratory insufficiency during the first 3 yr after exposure was 1 to 12 μCi. One of these dogs had a pulmonary tumor; nine additional dogs with body burdens of 0.6 to 1.8 μCi died due to pulmonary neoplasia 3 to 6 yr after exposure. Two of the dogs exposed to ^{238}Pu have died during the first 4 yr postexposure, due to bone and lung tumors, with body burdens at death of 10 μCi. Lymphocytopenia was the earliest observed effect after inhalation of $^{239}PuO_2$ or $^{238}PuO_2$, occurring 0.5 to 2 yr after deposition of $\geq$80 nCi plutonium in the lungs.

To determine the life-span dose-effect relationships of inhaled plutonium, 18-month-old beagle dogs were exposed to aerosols of $^{239}PuO_2$ (mean AMAD 2.3 μm, mean GSD 1.9), prepared by calcining the oxalate at 750°C for 2 hr; or to $^{238}PuO_2$ (mean AMAD 1.8 μm, mean GSD 1.9), prepared by calcining the oxalate at 700°C and subjecting the product to $H_2{}^{16}O$ steam in argon exchange at 800°C for 96 hr. This material, referred to as pure plutonium oxide, is used as fuel in space-nuclear power systems.

One hundred thirty dogs exposed to $^{239}PuO_2$ in 1973 and 1974 were selected for long-term studies; 22 will be sacrificed to obtain plutoniuni distribution and pathology data, and 108 were assigned to life-span dose-effect studies (Table 3.6). One hundred thirteen dogs exposed to $^{238}PuO_2$ in 1972 and 1973 were selected for life-span dose-effect studies (Table 3.7). Twenty-four additional dogs were exposed for periodic sacrifice. The appendix (following the entire Annual Report) shows the status of the dogs on these experiments.

During the first 6 yr following exposure to $^{239}PuO_2$, eight dogs in the highest-level dose group and ten dogs in Dose Level Group 5 were euthanized when death was imminent. Fourteen dogs were sacrificed for comparison of plutonium tissue distribution. Table 3.8 and Figure 3.7 show the primary causes of death and the distribution of ^{239}Pu in the tissues of these animals. One 80-month-old control dog was euthanized because of an oral tumor.

As survival time increased, the fraction of plutonium in the lung decreased to 40% of the final body burden by 5-6 yr postexposure. During the first postexposure year, plutonium was translocated primarily to the thoracic lymph nodes, with little plutonium translocated to other tissues. Plutonium content of the thoracic lymph nodes was about 30% of the final body burden 5-6 yr after exposure. Plutonium was also found in abdominal lymph nodes, principally the hepatic lymph nodes. The fraction of plutonium in liver increased, accounting for 15 to 29% of final body burden 4 to 6 yr after exposure. The organ distribution of plutonium in the periodically sacrificed dogs was generally similar to that of the high-dose-level dogs euthanized when death was imminent during the first 2 yr after exposure. The low-dose-level dog sacrificed during the 4th and 6th postexposure year had a much smaller fraction of the final body burden in the liver with a larger fraction retained in the lungs and thoracic lymph nodes.

The dogs euthanized because of respiratory insufficiency during the 3-yr postexposure period had increased respiration rates, hypercapnia and hypoxemia associated with lesions in the lungs. Intermittent anorexia and body weight loss accompanied the respiratory insufficiency. Histopathologic examination of the lungs showed radiation pneumonitis characterized by focal interstitial and subpleural fibrosis, increased numbers of alveolar macrophages, alveolar epithelial hyperplasia, and foci of squamous metaplasia. Autoradiographs

TABLE 3.6. Life-Span Dose Effect Studies with Inhaled $^{239}PuO_2$ in Beagles[a]

Dose Level Group	Number of Dogs		Initial Alveolar Deposition[b]	
	Male	Female	nCi[c]	nCi/g Lung[c]
0	10	10	0	0
1	10	10	3.5 ± 1.3	0.029 ± 0.11
2	10	10	22 ± 4	0.18 ± 0.04
3	10	10	79 ± 14	0.66 ± 0.13
4	10	10	300 ± 62	2.4 ± 0.4
5	10	10	1100 ± 170	9.3 ± 1.4
6	3	5	5800 ± 3300	50 ± 22
	63	65		

[a] Exposed in 1970 and 1971
[b] Estimated from external thorax counts at 14 and 30 days postexposure and estimated lung weights (0.011 x body weight)
[c] Mean ± 95% confidence intervals around the means

TABLE 3.7. Life-Span Dose-Effect Studies with Inhaled $^{238}PuO_2$ in Beagles[a]

Dose Level Group	Number of Dogs		Initial Alveolar Deposition[b]	
	Male	Female	nCi[c]	nCi/g Lung[c]
0	10	10	0	0
1	10	10	2.3 ± 0.8	0.016 ± 0.007
2	10	10	18 ± 3	0.15 ± 0.03
3	10	10	77 ± 11	0.56 ± 0.07
4	10	10	350 ± 81	2.6 ± 0.5
5	10	10	1300 ± 270	10 ± 1.9
6	7	6	5200 ± 1400	43 ± 12
	67	66		

[a] Exposed in 1973 and 1974
[b] Estimated from external thorax counts at 14 and 30 days post-exposure and estimated lung weights (0.11 x body weight)
[c] Mean ± 95% confidence intervals around the means

showed activity primarily composed of large stars, more numerous in areas of interstitial and subpleural fibrosis. Dog 804 M also had a pulmonary tumor classified as a bronchiolar-alveolar carcinoma.

The nine dogs euthanized 3 to 6 yr after exposure showed radiographic evidence of pulmonary neoplasia before respiratory insufficiency was observed. In seven of the dogs the lung tumors were classified as bronchiolar-alveolar carcinoma; in one dog as adenosquamous carcinoma; and in the other dog as epidermoid carcinoma. The epidermoid carcinoma metastasized to the skeleton; the bronchiolar-alveolar carcinomas metastasized to the thoracic lymph nodes in two dogs, and to several organs including the thoracic lymph nodes, mediastinum, kidney, skeleton, adrenal, aorta, and axillary, prescapular and hepatic lymph nodes in two other dogs. Two of the dogs had lesions of secondary hypertrophic osteoarthropathy. Sclerosing lymphadenitis was associated with the high concentration of plutonium in the thoracic and hepatic lymph nodes. There was also a generalized lymphoid atrophy which may be related to the debilitation in the dogs with respiratory insufficiency, or to lymphocytopenia. The liver of the dogs euthanized during the 4- to 6-yr postexposure period showed moderate diffuse centrilobular congestion. Liver cells in these areas contained fine granular yellow pigment resembling lipofuscin and were frequently vacuolated. Focal aggregation of vacuolated lipofuscin-containing cells in the sinusoids was associated with alpha stars on autoradiographs.

Lymphocytopenia developed after inhalation of $^{239}PuO_2$ in the dose level groups with mean initial alveolar depositions of 79 nCi and greater (Figure 3.8). Through 71 mo postexposure mean lymphocyte values were significantly lower ($P < 0.02 - 0.001$) than the control group. The reduction in lymphocytes was dose-related, both in time of appearance and magnitude. At mean alveolar depositions of 3.5 and 22 nCi, lymphocyte values were within ranges observed in control dogs. A reduction in total leukocytes was evident in the higher dose groups that were also lyniphocytopenic. This decrease, with the exception of the highest-level groups, was due to the reduction in lymphocytes, since no reduction was evident in neutrophils, eosinophils, or monocytes. No effects have been observed on red cell parameters following $^{239}PuO_2$ inhalation.

During the first 4 yr following exposure to $^{238}PuO_2$, three dogs in the highest-level dose group and one dog in dose level Group 5 were euthanized when death was imminent. Eighteen dogs were sacrificed for comparison of plutonium tissue distribution. Table 3.9 and Figure 3.7 show the causes of death and the distribution of ^{239}Pu in the tissues of these animals.

One dog (1025 M) was euthanized due to a fractured femur, however, there was radiographic evidence of a lung tumor for 2 mo prior to necropsy. The lung tumor was classified as a bronchiolar-alveolar carcinoma. Dog 1064 M was euthanized due to a bone tumor (osteosarcoma) in the pelvis. This dog also

TABLE 3.8. Tissue Distribution of Plutonium in Beagles after Inhalation of PuO_2

DOG NUMBER	TIME AFTER EXPOSURE, MONTHS	FINAL BODY BURDEN, µCi	PERCENT OF FINAL BODY BURDEN					CAUSE OF DEATH
			LUNGS	THORACIC LYMPH NODES[a]	ABDOMINAL LYMPH NODES[b]	LIVER	SKELETON	
478 M	0.25	0.29	98	0.15	0.017	0.24	0.08	SACRIFICE
435 F	0.25	3.8	99	0.10	0.006	0.00	0.03	SACRIFICE
816 M	0.50	0.40	99	0.12	0.010	0.00	0.03	SACRIFICE
918 M	1	0.074	99	0.82	0.014	0.11	0.08	SACRIFICE
920 F		0.011	94	0.47	0.029	0.08	0.61	SACRIFICE
913 M		4.8	98	1.1	0.002	0.03	0.05	SACRIFICE
702 F	5	1.7	94	5.7	0.0004	0.01	0.09	SACRIFICE
709 M	5	1.7	97	2.2	0.003	0.00	0.05	SACRIFICE
734 M	5	0.91	96	3.4	0.0002	0.01	0.05	SACRIFICE
739 F	5	1.5	95	4.7	0.03	0.001	0.00	SACRIFICE
910 M	11	12.3	84	15	---	0.06	0.04	RADIATION PNEUMONITIS
747 F	12	5.4	71	29	0.026	0.07	0.07	RADIATION PNEUMONITIS
906 F	12	6.2	88	12	0.001	0.03	0.05	RADIATION PNEUMONITIS
849 F	13	0.0007	80	15	0.20	0.04	1.6	SACRIFICE
896 F	15	4.1	81	15	0.92	0.23	0.12	RADIATION PNEUMONITIS
817 M	21	3.8	64	34	0.13	1.4	0.19	RADIATION PNEUMONITIS
815 M	25	0.074	64	32	---	0.08	0.10	SACRIFICE
829 M	26	3.2	75	19	0.79	4.2	0.45	RADIATION PNEUMONITIS
760 M	31	0.98	71	23	0.57	3.7	0.28	RADIATION PNEUMONITIS
890 F	31	2.0	55	28	2.2	13.0	0.26	RADIATION PNEUMONITIS
804 M	37	1.1	62	29	0.19	7.9	0.36	RADIATION PNEUMONITIS & LUNG TUMOR
798 F	43	0.0056	55	44	0.02	0.17	0.43	SACRIFICE
772 M	53	1.8	42	22	0.88	29	0.69	LUNG TUMOR
759 M	53	0.71	43	27	12.3	15	0.65	LUNG TUMOR
796 F	55	0.67	40	31	4.1	21	1.04	LUNG TUMOR
783 M	59	1.4	59	11	1.8	26	0.67	LUNG TUMOR
873 M	62	1.8	45	27	6.4	16	0.74	LUNG TUMOR
753 F	69	1.17	35	31	0.09	24	0.64	LUNG TUMOR
761 M	69	1.064	36	37	6.3	19	0.53	LUNG TUMOR
727 M	72	0.585	39	24	12.3	23	0.78	LUNG TUMOR
762 M	72	0.0017	51	43	0.3	0.7	0.7	SACRIFICE
837 M	72							LUNG TUMOR

[a] INCLUDES TRACHEOBRONCHIAL, MEDIASTINAL AND STERNAL LYMPH NODES

[b] INCLUDES HEPATIC, SPLENIC AND MESENTERIC LYMPH NODES

had radiographic evidence of a lung tumor for 3 mo prior to necropsy. The tumors did not metastasize. Dog 994 F died following chronic illness diagnosed as Addison's disease and dog 1191 F died due to chronic respiratory insufficiency, which did not improve with antibiotic therapy, and lesions of atypical interstitial pneumonia with chronic passive congestion. The lungs did not have the classical lesions of severe fibrosis, alveolar epithelial hyperplasia and metaplasia associated with death due to radiation pneumonitis.

In addition to the lesions associated with the cause of death, lesions in the lungs of the high dose-level dogs included focal alveolar histiocytosis, alveolitis, alveolar epithelial cell hyperplasia, alveolar emphysema, pleural fibrosis, and interstitial fibrosis. Numerous alpha stars were mainly in foci of fibrosis and single alpha tracks were

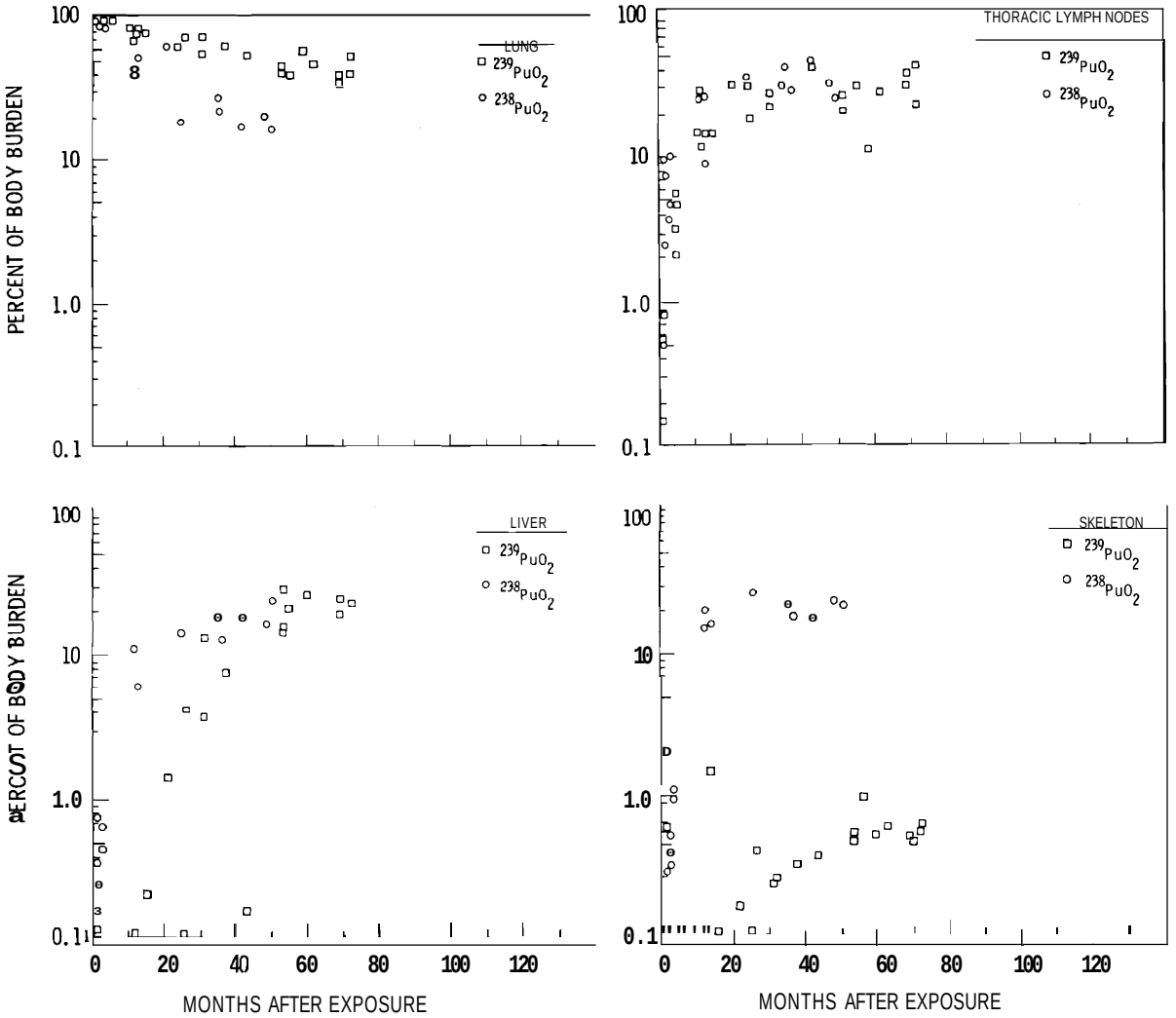

FIGURE 3.7. Tissue Distribution of Plutonium in Beagles after Inhalation of PuO_2

scattered throughout sections in foci of alveolar histiocytosis and alveolar septa. The tracheobronchial and mediastinal lymph nodes were completely obliterated with necrosis and scarring associated with high concentrations of plutonium as alpha stars. Similar but less severe lesions were seen in the hepatic lymph nodes. There were extensive alterations in bone including multiple areas of focal atrophy of bone; endosteal, trabecular and peritrabecular bone fibrosis; and osteolysis of cortical, endosteal, and trabecular bone. Radioactivity in the bone was present as single tracks generally scattered throughout the bone, cartilage and bone marrow. The liver contained foci of hepatocellular fatty change where small clusters of single tracks were seen. There was also mild focal nodular hyperplasia of hepatocytes.

Dose-related lymphocytopenia was observed in groups with mean alveolar deposition of 77 to 5200 nCi, similarly to the dogs exposed to $^{239}PuO_2$ (Figure 3.8). The lymphocyte depression was, however, more pronounced both as to magnitude and time of appearance, than observed in dogs exposed to similar doses of $^{239}PuO_2$. This effect was particularly evident in the 3-, 4-, and 5-dose level groups. As was found with ^{239}Pu, lymphocyte values in the two lowest exposure groups, i.e., 2.3 and 18 nCi, were not different from control values. A dose-related reduction in total leukocytes was evident, primarily due to the lymphocytopenia except in Groups 5 and 6 in which neutropenia was observed. No difference in monocyte values was seen in relation to dose levels. A significant and progressive reduction in eosinophils was evident only in

TABLE 3.9. Tissue Distribution of Plutonium in Beagles after Inhalation of $^{238}PuO_2$

DOG NUMBER	TIME AFTER EXPOSURE, MONTHS	FINAL BODY BURDEN, μCi	PERCENT OF FINAL BODY BURDEN					CAUSE OF DEAM
			LUNGS	THORACIC LYMPH NODES[a]	ABDOMINAL LYMPH NODES[b]	LIVER	SKELETON	
1032 M	0.25	0.15	97	0.03	0.2	1.7	0.16	SACRIFICE
921 F	1	0.0044	93	0.12	0.04	0.38	2.1	SACRIFICE
930 F	1	0.052	99	0.52	0.009	0.75	0.35	SACRIFICE
931 F	1	0.35	96	1.6	0.009	0.05	0.03	SACRIFICE
929 F	2	0.022	89	7.5	0.002	0.26	0.58	SACRIFICE
932 F	2	0.38	95	2.5	0.004	0.18	0.35	SACRIFICE
923 F	2	0.0023	85	9.4	0.03	0.09	0.44	SACRIFICE
925 M	3	0.0064	91	3.7	0.04	0.04	0.%	SACRIFICE
926 M	3	0.078	86	10	0.22	0.65	1.1	SACRIFICE
934 M	3	0.90	91	4.7	1.7	0.45	0.93	SACRIFICE
1318 M	12	0.030	45	27	0.08	11	15	SACRIFICE
1319 M	12	0.078	41	26	0.05	11	20	SACRIFICE
1214 M	13	0.014	52	9	0.32	6.2	16	SACRIFICE
1310 M	25	0.017	19	37	0.08	14	28	SACRIFICE
1317 M	25							SACRIFICE
1315 M	25							SACRIFICE
1191 F	35	0.658	26	32	0.13	18	22	PNEUMONIA
1215 M	36	0.011	22	43	0.18	13	19	SACRIFICE
994 F	42	5.025	17	45	0.49	18	18	ADDISON'S DISEASE
970 F	48	0.002	20	34	0.36	16	24	SACRIFICE
1025 M	50	10.043	16	27	7.05	24	23	LUNG TUMOR
1064 M	51							LUNG TUMOR AND BONE TUMOR

(a) INCLUDES TRACHEOBRONCHIAL, STERNAL AND MEDIASTINAL LYMPH NODES

(b) INCLUDES HEPATIC, SPLENIC AND MESENTERIC LYMPH NODES

Group 6 dogs following ^{238}Pu inhalation. No chronic effects have been observed in the red cell parameters.

The fraction of the final body burden in the lungs of the ^{238}Pu-exposed dogs 4 yr postexposure was about 20% compared to 50% in the ^{239}Pu-exposed dogs (Figure 3.7). About 30% of the plutonium was found in the thoracic lymph nodes and 20% in the liver 4 yr after exposure for both ^{239}Pu and ^{238}Pu. About 20% of the final body burden was found in the skeleton of the ^{238}Pu-exposed dogs 4 yr postexposure, compared to less than 1% in the ^{239}Pu-exposed dogs. During the 4 yr postexposure period there were no obvious differences in the plutonium tissue distribution in low-dose-level sacrifice dogs compared to the high-dose-level dogs exposed to ^{238}Pu.

After inhalation of $^{239}PuO_2$ or $^{238}PuO_2$, lymphocytopenia was the earliest observed effect, occurring after deposition of $\geq$ 80 nCi plutonium in the lungs. On a concentration basis, the 80-nCi dose level is about 40 times the 16-nCi maximum permissible human lung deposition, based on 0.3 rem/wk to the lung.

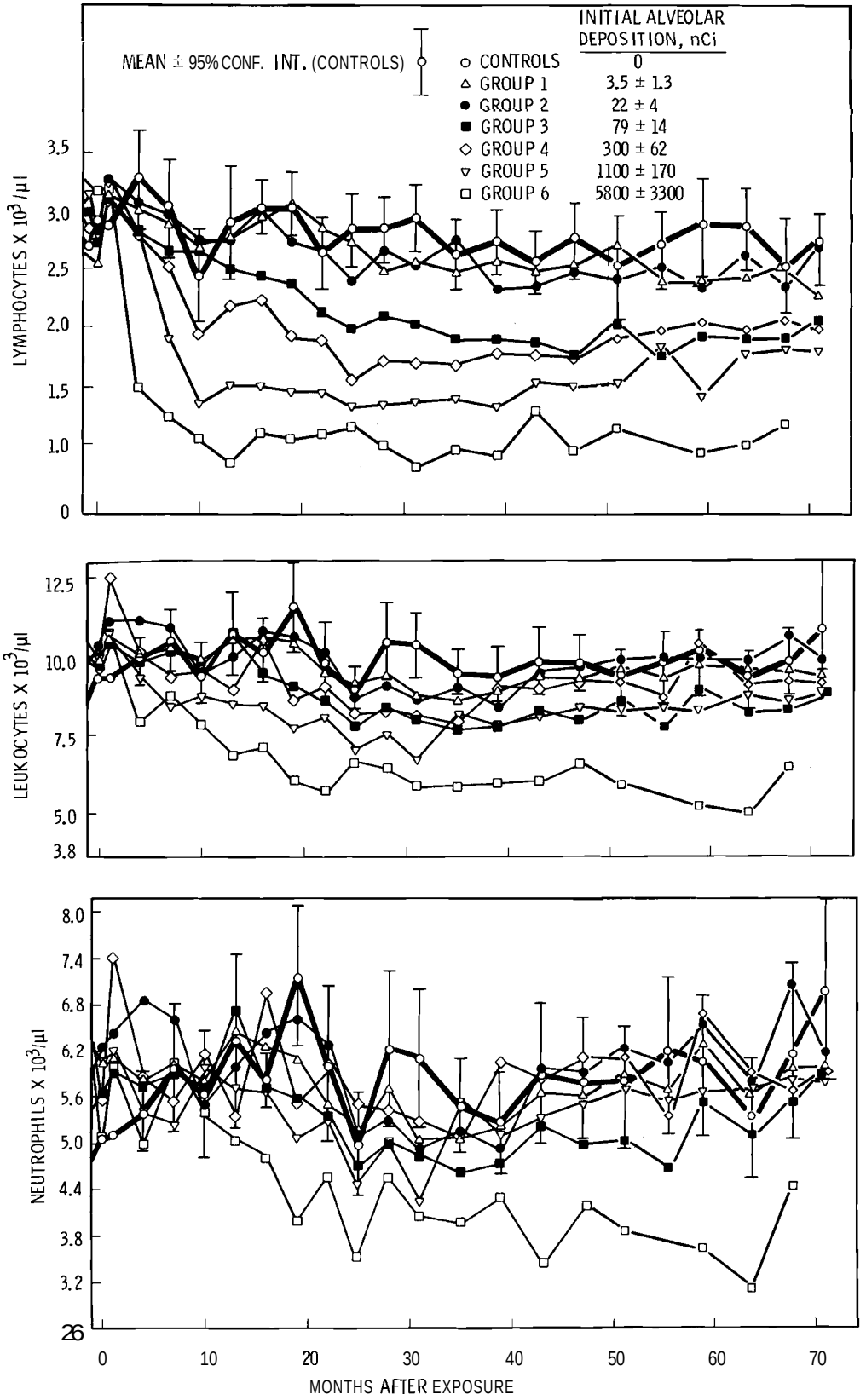

FIGURE 3.8. Mean Leukocyte Values from Dogs after Inhalation of $^{239}PuO_2$

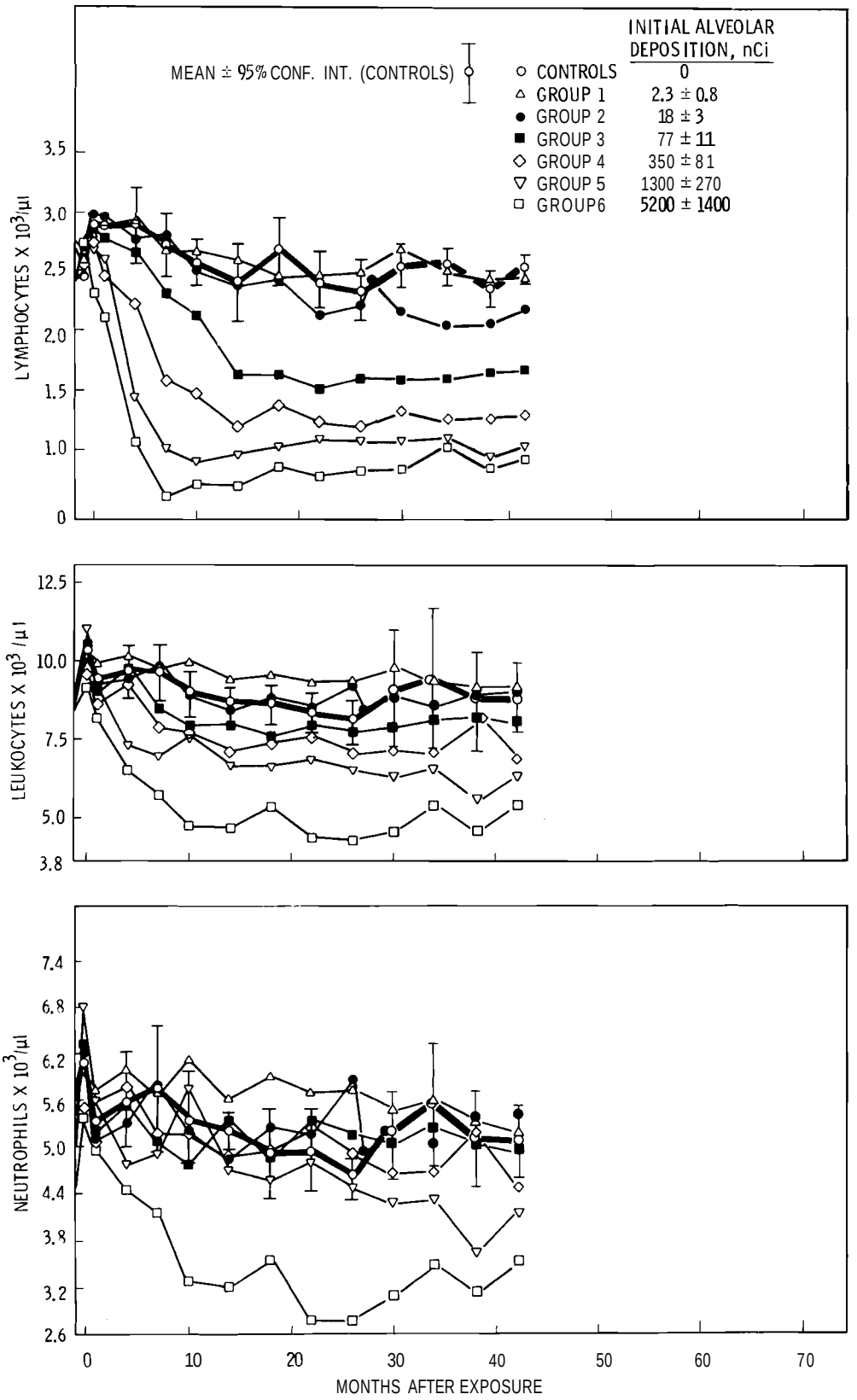

FIGURE 3.9. Mean Leukocyte Values from Dogs after Inhalation of $^{238}PuO_2$

DISPOSITION OF $^{241}AmO_2$ FOLLOWING INHALATION BY BEAGLE DOGS

Investigators:

D. K. Craig, J. F. Park, G. J. Powers, D. L. Catt, and A. C. Case

Technical Assistance:

A. J. Clary, L. R. Peters, A. L. Webb, P. J. Raney, and J. S. Barnett

Translocation of ^{241}Am from the lungs of beagles following inhalation of AmO_2 was fairly rapid, roughly equal quantities being found in the liver and skeleton at all postexposure times to 810 days. Less than 16% of the initial body burden was excreted, more than two-thirds of this in the feces.

The disposition of americium-241 in beagles was followed for up to 810 days after their inhalation exposure to $^{241}AmO_2$ aerosols having an AMAD of about 1.3 μm and a geometric standard deviation (GSD) of 1.8 for medium (40 nCi/ℓ) and high (340 nCi/ℓ) concentrations. At low concentrations (<1 nCi/ℓ), the aerosols were smaller (AMAD ~0.6 μm) and the distribution broader (GSD ~2.6). Activity in the dogs was estimated from thorax counts at 7 days; excreta were analyzed for up to 90 days postexposure and, where appropriate, during the last week before sacrifice. Cornplete tissue analyses for ^{241}Am were conducted on groups of three dogs sacrificed at 10, 30, 90, 270, and 810 days postexposure.

Forty percent of the final body burden (FBB) of ^{241}Am was located in tissues other than the lung parenchyma by 10 days postexposure and only 6% remained in the lung by 810 days postexposure. Translocation was primarily to the liver and skeleton, with roughly equal fractions of the final body burden in each at all postexposure sacrifice times (Table 3.10). These data differ significantly from those obtained in rodent studies, which show concentration in the liver peaking somewhere between 7 and 28 days postexposure and then decreasing relative to the skeletal burden. After the first week, two to eight times as much ^{241}Am was excreted in feces as in urine. There is some evidence for the translocation and excretion rate being higher for the low-level dogs, but this could be due to the smaller particle size of the aerosols to which these dogs were exposed. For the medium- and high-level dogs, a maximum of 16% of the initial lung burden was excreted. There was very little retention in thoracic lymph nodes (<1%) and virtually no ^{241}Am was found in the gonads (<0.05%). Figure 3.10 shows the mean distribution of ^{241}Am, expressed as a percentage of initial lung burden as a function of time postexposure, for lung, liver, skeleton, muscle and cumulative excreta.

Transient lymphocytopenia was observed in only two of the fifteen dogs within the first 10 days postexposure. Since this was not related to level of exposure, it was probably coincidental. For an initial lung burden of 1 μCi, approximate mean radiation doses over 800 days to lungs, liver, and skeleton of these dogs were 500, 300, and 60 rad, respectively.

TABLE 3.10. ^{241}Am **Distribution in Tissue, as Percent of Final Body Burden**

Dog No.	Final Body Burden, nCi	Lung	Liver	Skeleton	Muscle	All Other
10 L	4.36	30	3	8	3	42
10 M	142.7	76	4	8	8	5
10 H	1151	79	8	7	3	3
Mean		62	5	7	4	16
30 L	1.85	40	21	23	10	6
30 M	130.5	52	16	17	10	5
30 H	1316	53	22	16	5	3
Mean		48	20	19	8	5
90 L	1.28	17	24	33	10	13
90 M	123.7	28	38	21	10	4
90 H	1297	45	20	25	8	3
Mean		30	27	26	9	7
270 L	0.72	28	51	3	3	15
270 M	161.2	15	31	46	4	4
270 H	649.9	19	44	31	2	5
Mean		21	42	26	3	8
810 L	3.31	5	39	49	1	6
810 M	103.9	5	47	34	11	3
810 H	652.2	8	49	35	6	2
Mean		6	45	39	6	4

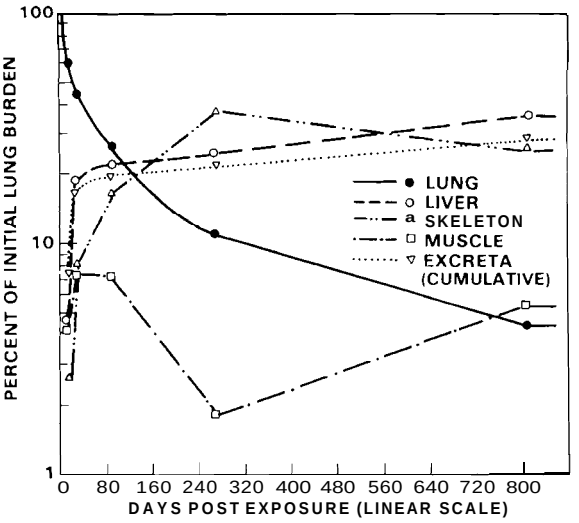

FIGURE 3.10. ^{241}Am **Distribution as a Function of Time (mean of Three Dogs at Each Sacrifice Time)**

Both rate of translocation and organ distribution as a function of time are different from those found in dogs that inhaled $^{238}PuO_2$, $^{239}PuO_2$, or $^{244}CmO_2$. Therefore it is probably not appropriate to use data derived from $^{239}PuO_2$ experiments or observations to predict the behavior of other transuranic isotopes and elements.

DISPOSITION OF $^{244}CmO_2$ FOLLOWING INHALATION BY BEAGLE DOGS

Investigators:

D. K. Craig, J. F. Park, G. J. Powers, D. L. Catt, and A. C. Case

Technical Assistance:

A. J. Clary, L. R. Peters, G. L. Webb, P. J. Raney, and J. S. Barnett

Translocation of ^{244}Cm from the lungs of beagles following inhalation of $^{244}CmO_2$ was rapid compared with other transuranic oxides, 60% of the final body burden being in tissues other than lung by 10 days postexposure. Less than one-quarter of the initial body burden of ^{244}Cm was eliminated by these dogs over 810 postexposure days, more in feces than in urine.

The disposition of ^{244}Cm in beagle dogs was followed for up to 810 days after their inhalation exposure to $^{244}CmO_2$ aerosols (AMAD 0.4 μm, geonietric standard deviation 2.3). Activity in the dogs was estimated from thorax counts at 7 days; excreta were analyzed for up to 90 days postexposure and, where appropriate, for the last week prior to sacrifice. Complete analyses for ^{244}Cm were conducted on groups of three dogs sacrificed at 10, 30, 90, 270 and 810 days, postexposure.

The ^{244}Cm was rapidly redistributed from the lung parenchyma to other tissues, primarily liver (25 to 45% of final body burden) and skeleton (25 to 35%), with 5 to 10% in muscle (Table 3.11). This material was avidly retained, with two of the three 810-day dogs excreting less than 25% of their initial lung burden. Slightly more (1 1/2 to 3 times as much) ^{244}Cm was excreted in feces than in the urine of these dogs. There was little retention of ^{244}Cm in thoracic lymph nodes (<1%) and virtually none in gonads (<0.01%). Figure 3.11 shows the retention of ^{244}Cm in several organs expressed as a function of initial lung burden (initial body burden minus first week's fecal excretion).

TABLE 3.11. ^{244}Cm Distribution in Tissue as % of Final Body Burden

Dog No.	Final Body Burden, nCi	Lung	Liver	Skeleton	Muscle	All Other
10 L	8.68	35	17	30	5	13
10 M	90.97	41	29	24	2	5
10 H	482.1	40	30	18	9	3
Mean		39	25	24	5	7
30 L	6.84	25	27	32	11	5
30 M	56.47	29	24	25	15	7
30 H	412.4	27	24	36	8	4
Mean		27	25	31	12	6
90 L	30.88	13	52	25	6	3
90 M	195.48	19	34	30	10	8
90 H	3377.87	17	47	26	4	5
Mean		16	45	27	7	5
270 L	5.64	11	37	44	3	5
270 M	88.67	9	29	34	23	4
270 H	961.76	15	42	31	6	6
Mean		12	36	37	11	5
810 L	4.61	5	33	49	7	6
810 M	52.55	4	39	31	22	5
810 H	418.5	6	53	29	9	4
Mean		5	42	36	12	5

Clearance from the lung occurs initially with a half-time of less than 10 days, decreasing thereafter to around 350 days over the last 700 days of this study. For an initial lung burden of 1 μCi, approximate mean radiation doses over 800 days to lungs, liver, and skeleton of these dogs would be 250, 250, and 55 rad, respectively. These values differ significantly from those obtained under similar conditions for $^{241}AmO_2$ in beagles (comparable lung, liver, and skeleton doses were 500, 300, and 60 rad, respectively); and for the highly insoluble $^{239}PuO_2$, where about 65% of the activity remained in the lung at 800 days postexposure, producing a lung dose of about 2400 rad.

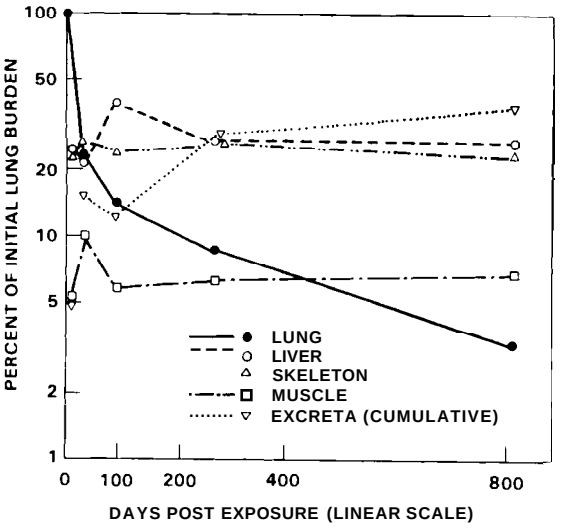

FIGURE 3.11. ^{244}Cm Distribution as a Function of Initial Lung Burden (Mean of Three Dogs at Each Sacrifice Time)

COMPARISON OF METHODS FOR SEPARATING BONE MARROW FROM BONE

Investigator:
B. J. McClanahan

Bones from a dog whose skeletal burden resulted from lung translocation following inhalation of $^{238}PuO_2$ were subjected to ultrasonic cell disruption or washing to remove the cells from marrow cavities. Ultrasonic vibrations appeared to effectively dislodge marrow cells, while flushing the bones achieved only a partial separation.

A significant component of the risk from plutonium deposited in bone may be due to the plutonium in marrow. An effective method for separation of marrow from bone would permit separate calculation of doses to bone and bone marrow, and possibly improve the prediction of effects.

A study was undertaken to develop such a method. One restriction imposed was that the method be as chemically innocuous as possible. All chemical and biochemical means of removing marrow cells present the risk of also removing measurable quantities of plutonium from bone. In our first experiments, 1- to 3-cm-long, cross-sections of rib from a dog that had inhaled $^{238}PuO_2$ were subjected to cell disruption by sonication, in either a slightly hypotonic (0.12 M) sodium chloride solution or "Hemosol" (a synthetic detergent), or were flushed with the detergent solution to remove the marrow. The results of this experiment are summarized in Table 3.12. Washing with detergent did not remove all of the cellular elements from the marrow cavity; it was possible to visually detect cells remaining after vigorous flushing. After washing, the bone was subjected to sonication to complete cell removal. It can be seen that flushing removed slightly more than half of the total amount removed by flushing and sonication combined, or by sonication alone. The wash solution appeared to stream through the larger spaces in the marrow cavity and did not build up enough pressure with the equipment employed to eject cells occupying the smaller spaces.

TABLE 3.12 ^{238}Pu Content of Bone and Bone Marrow in Canine Rib

Treatment	Percent of Total ^{238}Pu[a]	
	Bone	Marrow
Sonication	92.7 ± 0.5 (5)	7.3 ± 0.5 (5)
Wash + Sonication	92.6 (1)	4.2 W[b] (1)
		3.2 S[b] (1)

[a] Mean ± SE, number of determinations in parentheses
[b] W = wash solution; S = sonication solution

Sonication appears to be an effective means of removing the cellular elements from bones. However, it must be determined whether there is measurable release of plutonium bound to the organic or mineral fractions of bone, thereby elevating the plutonium content of the fraction designated as marrow. Additional experiments have been initiated to answer this question.

• Inhaled Plutonium Nitrate in Dogs

The objective of this project is to determine the dose-effect relationships of inhaled plutonium nitrate in life-span studies in beagle dogs. The critical tissue after inhalation of "soluble" plutonium (such as plutonium nitrate) is generally considered to be the skeleton or liver, on the assumption that such plutonium will be rapidly translocated from the lung to skeleton and liver. In several rodent studies, however, inhalation of "soluble" plutoniuni has resulted in lung tumors as well as skeletal tumors.

INHALED PLUTONIUM NITRATE IN DOGS

Investigators:

G. E. Dagle, W. C. Cannon, H. A. Ragan, C. R. Watson, D. L. Stevens, F. T. Cross, P. J. Dionne, and T. P. Harrington

Technical Assistance:

J. F. McShane, S. L. Owzarski, G. L. Webb, S. L. English, and M. C. Perkins

Beagle dogs given a single inhalation exposure to $^{239}Pu(NO_3)_4$ are being observed for life-span dose-effect relationships. Lymphopenia occurred at the two highest dosage levels as early as 1 mo following exposure and was associated with neutropenia and reduction in numbers of circulatory monocytes by 4 mo postexposure. Radiation pneumonitis developed in one dog at the highest dosage level at 14 mo postexposure. More rapid translocation to skeleton and liver occurred following inhalation of $^{238}Pu(NO_3)_4$ than after $^{239}Pu(NO_3)_4$ inhalation.

Six dosage groups of 105 dogs have been exposed to aerosols of $^{239}Pu(NO_3)_4$ for life-span observations (Table 3.13). Sixty-one of these dogs were exposed in 1976 and 44 dogs in 1977. In addition, 20 dogs were exposed to nitric acid aerosols as vehicle controls, 20 dogs were selected as untreated controls for life-span observation, 25 dogs were exposed to aerosols of $^{239}Pu(NO_3)_4$ for periodic sacrifice to study plutonium metabolism and the pathogenesis of developing lesions, and 7 dogs were selected as controls for periodic sacrifice. Twelve dogs were exposed to aerosols of $^{238}Pu(NO_3)_4$ for periodic sacrifice to study deposition and translocation up to 1 yr. The dogs were exposed in aerosol chambers using techniques described in previous Annual Reports.

A digital computer system was used to model the early translocation of inhaled $^{239}Pu(NO_3)_4$ in dogs. Fractional uptake constants and biological half-lives for the relatively soluble transuranic nuclide in various

TABLE 3.13. Inhaled Plutonium Nitrate in Dogs: Exposures in 1976 for Life-Span Observations

Number of Dogs			Aerosol Parameters		
Planned	On Study	Initial Alveolar Deposition[a] nCi	AMAD[b] (μm)	GSD[c]	Concentration nCi/ℓ
10	5	5445 ± 1841	085	2 37	534 ± 118
20	10	2293 ± 509	0.93	2.23	322 ± 66
20	13	312 ± 68	0.81	1.98	99 ± 20
20	20	56 ± 17	0.65	1.97	18 ± 4
20	20	8.2 ± 4.4	0.51	1.87	2.6 ± 0.5
20	20	2.2 ± 2.4	0.33	2.07	0.6 ± 0.3
20	17	Vehicle	—	—	—
20	20	Control	—	—	—

[a] Initial alveolar deposition estimated from thoracic count 2 wk post exposure
[b] Activity Mean Aerodynamic Diameter
[c] Geometric Standard Deviation

organs or compartments were estimated using activity levels measured in urine and fecal samples, in tissues obtained at necropsy, and external 17-keV X-ray body counts. The model prediction for each of the compartments is compared with the corresponding data and the model parameters are adjusted until a "best fit" is obtained for all compartments. The model fitting process is, by necessity, an interactive procedure since adjustments to one of the compartments will affect others. Preliminary data suggests that 0.046 of the initial alveolar deposition is excreted in feces from day 4 to day 28; this correlation is useful for comparison to dogs inhaling insoluble transuranics. Body counts for estimating initial alveolar deposition improve using the cube root of the weight of the dog. The modeling data is presently used for estimating dose (rad) to organs in dogs on life-span studies.

Preliminary data comparing the tissue distribution of $^{238}Pu(NO_3)_4$ and $^{239}Pu(NO_3)_4$ indicate that $^{238}Pu(NO_3)_4$ is more rapidly translocated to bone and liver than $^{239}Pu(NO_3)_4$ (Table 3.14). Additional tissue distribution analyses will be made on dogs killed 3 mo and 1 yr postexposure to further study the comparative distribution of $^{238}Pu(NO_3)_4$ and $^{239}Pu(NO_3)_4$. It is interesting to note the low accumulation of both isotopes in the tracheobronchial lymph nodes.

Lymphopenia was present at the two highest dosage levels at 4 wk postexposure; by 4 mo postexposure there was lymphopenia, neutropenia, and reduced numbers of circulating monocytes at the two highest dosage levels (Figure 3.12). No effects were observed on erythroid parameters.

TABLE 3.14. **Inhaled Plutonium Nitrate in Dogs**

Nuclide	Time Post Exposure	Animal Number	Total Body, nCi	Distribution, Percent			
				Lung	Skeleton	Liver	Tracheal Lymph Nodes
$^{239}Pu(NO_3)_4$	3 days	1359	78	92	3	2	0.1
		1375	72	92	5	1	0.0
		1407	84	52	19	11	0.2
	4 weeks	1336	32	71	20	6	0.2
		1341	22	65	19	13	0.1
		1344	52	59	16	22	0.1
		1329	484	70	19	8	0.1
		1346	901	77	10	10	0.2
		1347	694	72	14	9	0.3
	3 months	1522	58	55	28	12	0.4
		1529	49	52	24	18	0.3
		1539	71	53	25	19	0.2
$^{238}Pu(NO_3)_4$	3 days	1544	126	41	22	12	0.1
		1549	54	50	15	12	0.2
		1554	86	58	16	9	0.1
	4 weeks	1545	90	17	44	31	0.2
		1552	93	18	34	41	0.1
		1553	58	26	43	23	0.2

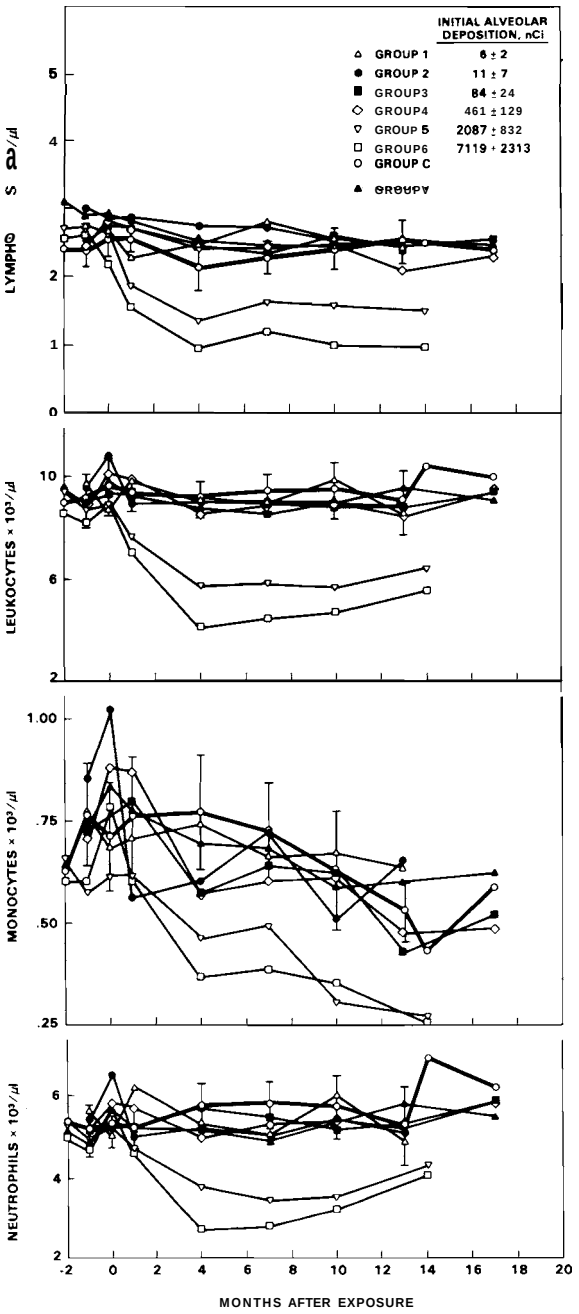

FIGURE 3.12. Mean Lymphocyte, Leukocyte, Monocyte and Neutrophil Values from Dogs after Inhalation of $^{239}Pu(NO_3)_4$

Radiation pneumonitis developed in one high-dosage dog at 14 mo postexposure. This dog had dyspnea, hypoxia, hypercapnea, and weight loss before euthanasia was performed.

• Inhaled Transuranics in Rodents

The purpose of this project is to examine in small mammals, the fate, effects and pathogenesis in the lung and elsewhere following inhalation of transuranic compounds. This project should provide data required for hazard evaluation and establishment of permissible exposure limits to man for inhaled transuranics, particularly with respect to radiation dose and dose-distribution.

EFFECTS OF REPEATED EXPOSURES TO $^{239}PuO_2$

Investigator:

C. L. Sanders

Technical Assistance:

S. L. Baker and A. W. Conklin

Preliminary evidence indicates that protraction of $^{239}PuO_2$ exposure may influence the development of lung tumors in the rat.

Individuals may be exposed to transuranic aerosols in a single, fractionated or continuous manner. Previous studies in rodents with inhaled plutonium have considered only the single, acute exposure. This study will attempt to define the influence of $^{239}PuO_2$ dose-fractionation exposure in rats on the autoradiographic distribution of PuO_2 in the lung and upon the incidence of lung tumors.

Female, Wistar, SPF rats were first exposed to $^{239}PuO_2$ aerosol at about 70 days of age. The following exposure groups of rats are being studied: (1) one exposure to PuO_2; (2) three exposures to PuO_2 at consecutive monthly intervals; (3) nine exposures to PuO_2 at consecutive weekly intervals; (4) 25 exposures to PuO_2 at consecutive weekly intervals; and (5) sham exposure of controls for 25 consecutive weeks. Estimated alveolar $^{239}PuO_2$ depositions are shown in Table 3.15.

Data discussed in last year's Annual Report were interpreted to indicate a decreased alveolar clearance of ^{239}Pu with increasing fractionation. Subsequent statistical analysis suggested that alveolar clearance rates among the exposure groups were not significantly different from each other. Plotting individual animal data for ^{239}Pu content of lung as a function of time and dose fractionation indicates no difference in rates of Pu lung clearance after the last Pu exposure (Figure 3.13).

Qualitatively, autoradiograms of exposed lungs indicate an influence of dose fractionation on $^{239}PuO_2$ particle distribution in lung. In rats given nine exposures, there appears to be a greater concentration of PuO_2 in subpleural regions of the lung than is seen with a single exposure. Attempts are currently being made to quantitate this observation.

TABLE 3.15. Early Pulmonary Lesions and Total Alveolar Deposition Following Fractionated $^{239}PuO_2$ Exposure.

	Exposures			
	Single	Monthly for 3 mo	Weekly for 9 wk	Weekly for 40 wk
Total Alveolar Deposition, nCi[a]	352	29.4	139	−2 nCi/Exposure
Total Alveolar Deposition, nCi[b]	322	21.2	135	In Progress
Days After Exposure to Last Death	432	459	431	—
Number of Life-Span Animals	65	65	65	70
Number Dead	19	7	15	—
Number with Lung Metaplasia	8	1	3	—
Number with Lung Tumors	4	1	5	—

(a) Estimated deposition based on ^{239}Pu contents + body burden
(b) Estimated deposition based on derived lung clearance curves for single exposure to $^{239}PuO_2$ (Annual Report, 1976): $Y = 41.9\ E^{-0.0886T} + 58.1\ E^{-0.00398T}$

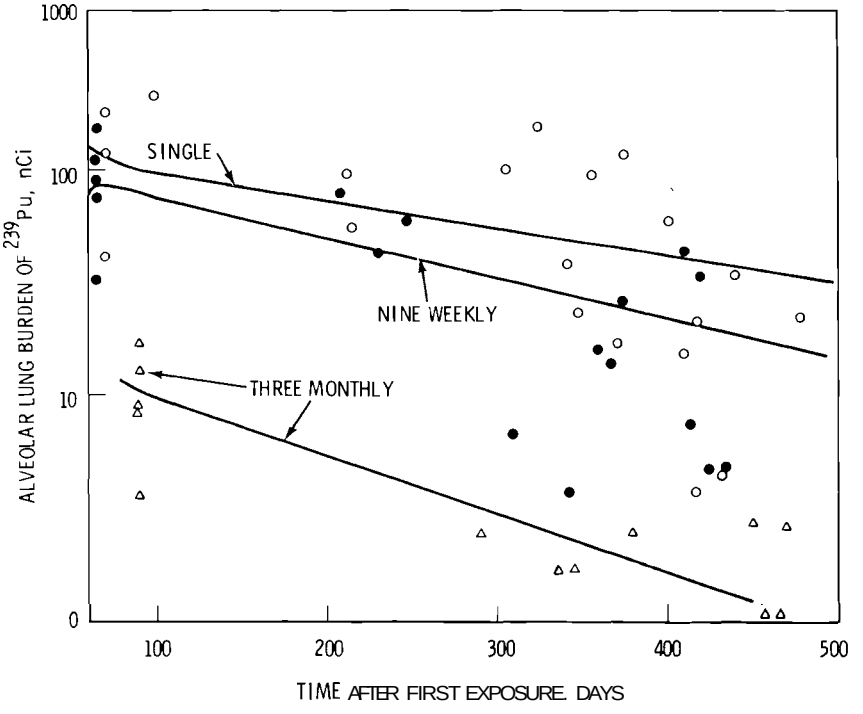

FIGURE 3.13. Amount of ^{239}Pu Present in the Lung as a Function of Dose Fractionation and Time After the First Exposure. The form of the first part of each curve was constructed from excretion data presented in last year's Annual Report. Each point represents an individual animal.

Over 40 of the exposed rats died and have been necropsied at time periods of up to 500 days after the first exposure to $^{239}PuO_2$. No lung tumors were seen in controls and only one lung tumor has been found in rats receiving three exposures. In rats receiving a single exposure, 4/19 rats developed lung tumors, none of which were squamous cell carcinomas. However, several rats in this group did display squamous cell metaplasia. Rats receiving nine ^{239}Pu exposures, amounting to only 40% of ^{239}Pu deposition seen in rats given only one exposure, developed lung tumors in 5/15 rats, to date (Table 3.12). Of these tumors, three were squamous cell carcinomas. Earlier studies with inhaled $^{239}PuO_2$ in rats demonstrated that concentration of PuO_2 in subpleural regions of the lung at high depositions of PuO_2 resulted in a preponderance of squamous cell carcinomas.

TOXICITY OF INHALED $^{241}AmO_2$

Investigators:

C. L. Sanders, W. C. Cannon, and J. G. Powers

Technical Assistance:

S. I. Baker

The metabolism and microscopic distribution of inhaled high-fired $^{241}AmO_2$ is more similar to that of inhaled $^{244}CmO_2$ than to $^{238}PuO_2$ or $^{239}PuO_2$.

Previous studies have demonstrated the influence of particle size and solubility upon the carcinogenicity of inhaled plutonium and curium oxides (Annual Reports, 1975, 1976). In this report, we will consider the metabolism of americium oxide and compare its distribution and translocation to other transuranics.

Americium-241 was obtained from beta decay of ^{241}Pu, converted to the oxalate and heated at 700°C for 4 hr to produce $^{241}AmO_2$. The material was kept in a dry state until suspended in water not more than 24 hr prior to aerosolization for animal exposure. The $^{241}AmO_2$ had an activity median aerodynamic diameter (AMAD) of 0.92 ± 0.29 μm, with a geometric standard deviation (GSD) of 0.02 ± 0.04 μm. The particle size distribution was not log normal.

Groups of female Wistar, SPF rats were exposed, nose-only, as summarized in Table 3.16. An additional 30 animals were exposed at a lung deposition level of 130 nCi for metabolism studies.

Autoradiograms of lung taken at 1 to 100 days after inhalation showed a rather uniform distribution of alpha tracks throughout the lung parenchyma. A few large particles were seen as dense stars, randomly interspersed among single tracks (Figure 3.16). This basic distribution pattern did not appear to change during the first few months following exposure.

TABLE 3.16. Distribution of ^{241}Am in Tissues at 1 Day After Exposure for the Various Life-Span Groups [a]

Group	Number of Life-Span Rats	Amount ^{241}Am in Tissue, nCi		
		Lung	Liver	Bone
1	70	<0.1 nCi[b]	<0.1 nCi[b]	<0.1 nCi[b]
2	70	1.3 ± 1.0	(c)	(c)
3	35	6.6 ± 3.7	3.6 ± 0.7	(c)
4	35	13 ± 8.5	5.2 ± 1.7	3.9 ± 2.9
5	35	26 ± 24	4.4 ± 3.5	(c)
6	35	31 ± 18	4.1 ± 5.8	(c)
7	35	650 ± 220	30 ± 14	31 ± 18

[a] Values are means ± standard deviation from 5 rats in each group
[b] Less than twice background
[c] Data not yet available

Inhaled $^{241}AmO_2$ was cleared more rapidly from the lung (Table 3.17) than was either $^{238}PuO_2$ or $^{239}PuO_2$, but more slowly than $^{244}CmO_2$. A substantial amount of the inhaled ^{241}Am was translocated to liver and bone

(Table 3.16 and 3.17). The amount of ^{241}Am in bone appears unchanged after 14 days post-exposure, while liver ^{241}Am content decreased from 14 days to 70 days postexposure.

Radiation pneumonitis was observed at the 650-nCi dose level within several hundred days postexposure. No other delayed effects were seen during the first year postexposure.

Light and electron microscopic autoradiography of ^{241}Am distribution in lung, liver, bone, and bone marrow is being investigated in a group of rats which received an estimated alveolar lung deposition of 2 μCi ^{241}Am.

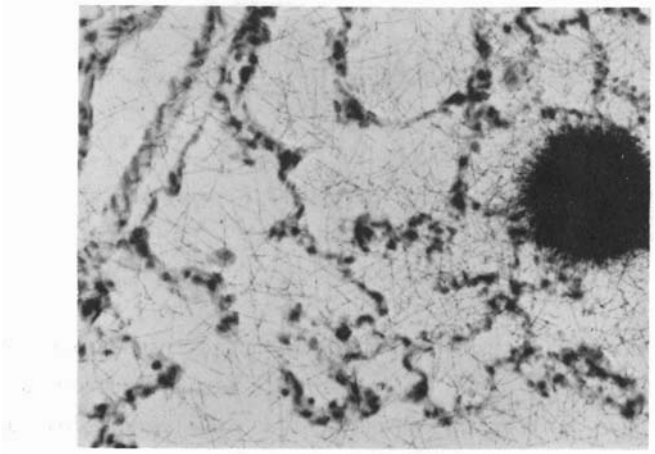

FIGURE 3.14. Autoradiogram of Lung Taken at 28 Days After Inhalation of $^{241}AmO_2$; 33 nCi ^{241}Am in Lung; 4-Wk Exposure of Autoradiogram (525X)

TABLE 3.17. Alveolar Clearance of Inhaled $^{241}AmO_2$ in Rats.

Time After Exposure (days)	Amount ^{241}Am in Tissue, nCi[a]		
	Lung	Liver	Bone
1	130 ± 30	4.4 ± 2.7	9.5 ± 6.4
7	50 ± 28	11 ± 9.1	11 ± 8.0
14	42 ± 6.3	16 ± 4.6	21 ± 7.1
28	18 ± 9.5	6.7 ± 2.9	12 ± 5.6
35	15 ± 6.9	8.0 ± 8.0	14 ± 9.5
70	14 ± 8.2	3.1 ± 1.4	21 ± 3.7

[a] Values are means ± standard deviation from 5 rats in each group

INHALATION TOXICOLOGY OF $^{241}Am(NO_3)_3$

Investigators:

J. E. Ballou and R. A. Gies

Technical Assistance:

R. L. Music

Inhaled $^{241}Am(NO_3)_3$ is cleared rapidly from the lung and translocated principally to skeleton. The rate of lung clearance exceeds that seen with similar Pu compounds, however accumulation and retention in bone is similar. Translocation to liver is initially higher than for Pu, but the loss from liver is rapid in the first few weeks after exposure.

Male Wistar rats 60 days of age were administered a single, nose-only exposure to $^{241}Am(NO_3)_3$ aerosols generated from 0.27 N nitric acid solutions with a Lovelace nebulizer. Animals were sacrificed immediately after exposure to determine initial lung burden, and after 7, 30, 60, 100, 150 and 200 days to determine retention kinetics for dosimetric purposes. Additional animals were held for life-span study of delayed biological effects. The experimental protocol and estimated cumulative radiation dose to the long-term animals is shown in Table 3.18.

Inhaled $^{241}Am(NO_3)_3$ is cleared more rapidly from the lung than an equivalent lung burden of ^{239}Pu or ^{238}Pu nitrate. Accumulation and retention in skeleton, as well as the pattern of urinary excretion, are similar for all three. Americium-241 is initially accumulated to a greater extent in liver than the plutonium isotopes; however, due to more rapid clearance, the differences are not significant after 100 days.

Estimates of accumulated radiation dose to major tissues for the two groups of

TABLE3.18. Experimental Protocol and Dose Estimates Following $^{241}Am(NO_3)_3$ Inhalation

Initial Lung Burden (nCi)	Number of Rats		Aerosol Characteristics		500-Day Accumulated Dose (rad)			
	Serially Sacrificed	Life-Span Study	AMAD	GSD	Lung	Skeleton	Liver	Kidney
8.2	10	58	0.248	1.97	12	8	0.6	0.8
95.3	40	60	0.348	2.01	145	95	8	9
51.7[a]	35	0	2.136	2.18				

[a] These rats were used in preliminary range setting and metabolism studies prior to initiating long-term biological effects study

long-term animals were based on retention parameters derived from the clearance curves shown in Figure 3.1 5. Retention in lung, kidney and liver could be described as the sum of two exponential functions. Skeletal data were fit with a linear function with slope = 0, accounting for 20% of the initial lung burden. Dose estimates will be made for individual long-term animals at the time of death, based on analyses of tissues and the tissue retention model. Late effects have not been observed during the brief (~100 days) course of this study.

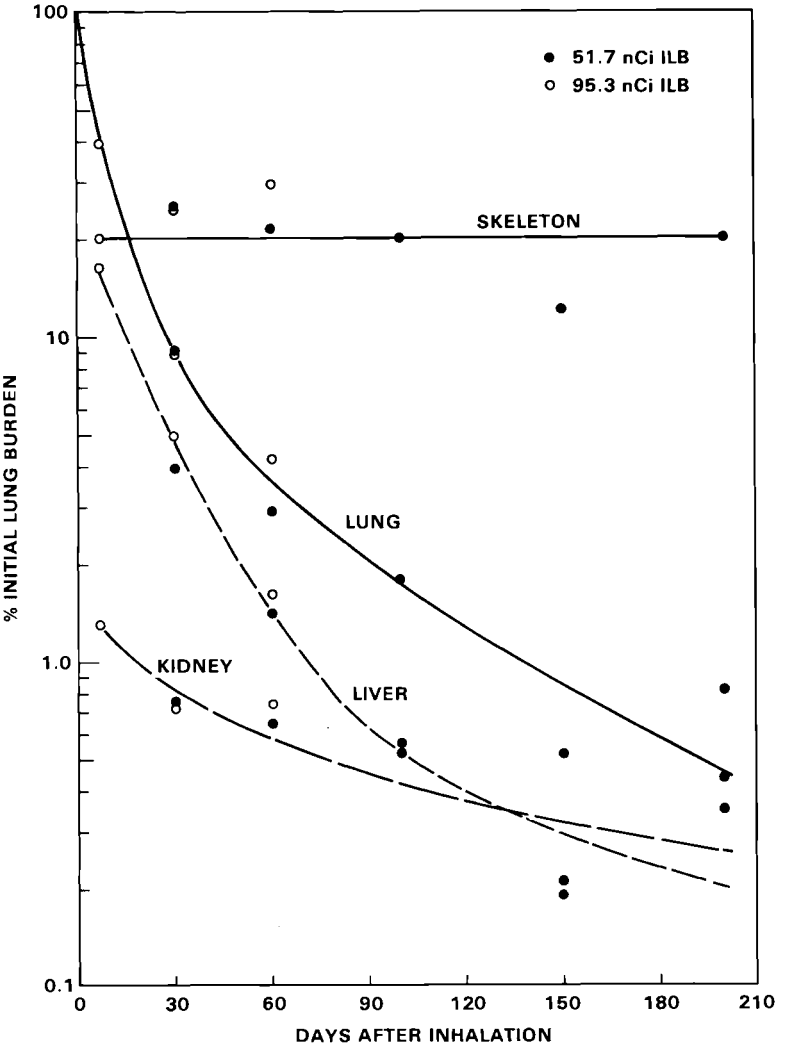

FIGURE 3.15. Retention of Inhaled $^{241}Am(NO_3)_3$ in Rat Tissues

BONE AND LUNG TUMOR RESPONSE FOLLOWING INHALATION OF TRANSURANIC NITRATES

Investigators:

J. E. Ballou, G. E. Dagle, R. A. Gies, K. E. McDonald, L. G. Smith, P. G. Doctor, and G. J. Powers

Technical Assistance:

R. L. Music

Eight-hundred five rats exposed to transuranic nitrate aerosols developed 111 lung tumors and 24 bone tumors. Results for $^{239}Pu(NO_3)_4$, $^{238}Pu(NO_3)_4$, and $^{253}Es(NO_3)_3$ were similar, and comparable to what has been shown for the more refractory transuranic oxides.

Male Wistar rats 60 days of age were exposed nose-only to graded doses of $^{238}Pu(NO_3)_4$, $^{239}Pu(NO_3)_4$, and $^{253}Es(NO_3)_3$ to determine dose-related, long-term biological effects. Interim reports in previous Annual Reports have described the experimental protocol, nietabolic, and pathologic aspects of this study. This report presents the relationship between cumulative radiation dose and incidence of lung and bone tumors.

A total of 805 rats (14 different exposure groups) were administered transuranic nitrate aerosols and held for life-span study. Animals were examined at death or sacrifice (if moribund) and all major tissues and suspicious lesions were sampled for histopathologic examination. In 100 nontreated controls and 125 vehicle controls (0.27 N nitric acid) that completed the study, 111 lung tumors and 31 bone tumors were diagnosed; 7 of the 31 bone tumors developed in the HNO_3 vehicle control group.

Tissues were analyzed for radioactivity (lung, liver, skeleton, pelt, tracheobronchial lymph nodes, and remainlng soft tissue) to enable estimation of the radiation dose accrued during the life span study. The cumulative radiation dose to lung and bone was estimated for individual rats using retention kinetics determined for each exposure group. Representative retention curves for animals exposed to Pu are shown for one exposure group in Figures 3.16 and 3.17. Half-lives and corresponding activities used in the dose calculation are indicated on the figures. Radiation dose was calculated assuming a two-exponential clearance froni lung and a single exponential fit for retention in bone. Similar retention curves were obtained for rats exposed to ^{253}Es; however, the lung burden of each rat was determined from an external body count taken 7 days after exposure and an experimentally determined relationship between total body count and the 7-day lung burden. The initial lung burden was determined by extrapolation, using the lung retention curve, and radiation dose was calculated using lung retention parameters. This procedure was necessary because the short physical half-life of ^{253}Es (20 days) precludes the reconstruction of the cumulative dose curve from the time of death.

Animals were grouped by cumulative radiation dose and the dose was related to the tumor incidence determined for each dose group. Usually, order-of-magnitude steps in dose were used (e.g., 0.01 to 0.1, 0.1 to 1, etc.), except at the two highest lung doses, where a smaller dose interval was more appropriate.

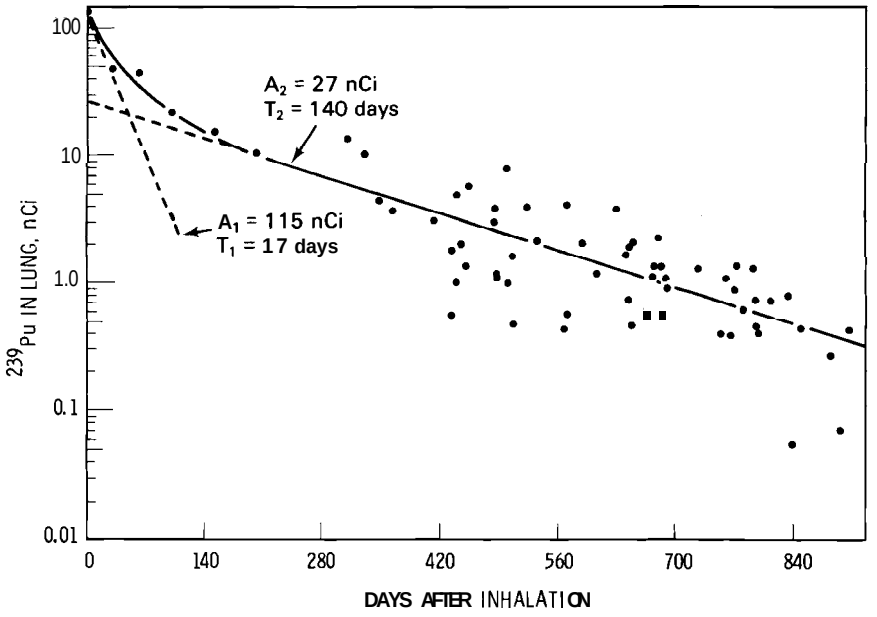

FIGURE 3.16. Retention of Inhaled ^{239}Pu Nitrate in Lung

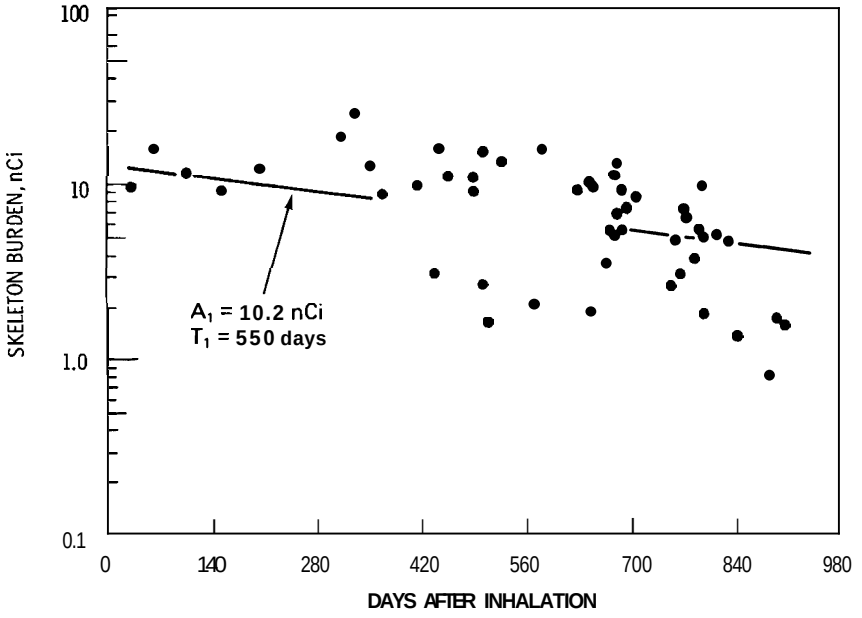

FIGURE 3.17. Retention of Inhaled ^{239}Pu Nitrate in Skeleton

Tumor incidence figures are indicated on Figures 3.18 (bone) and Figure 3.19 (lung) as fractions, with the numerator equal to the number of rats with tumors, and the denominator equal to the number of rats in that cumulativedoserange. Thefirstfractionapplies to animals exposed to $^{239}Pu(NO_3)_4$ and the second to $^{238}Pu(NO_3)_4$ animals. The three-digit numbers represent the average survival time of the ^{239}Pu and ^{238}Pu rats that fall in the indicated dose range. Tumor incidence with ^{253}Es is indicated by an asterisk.

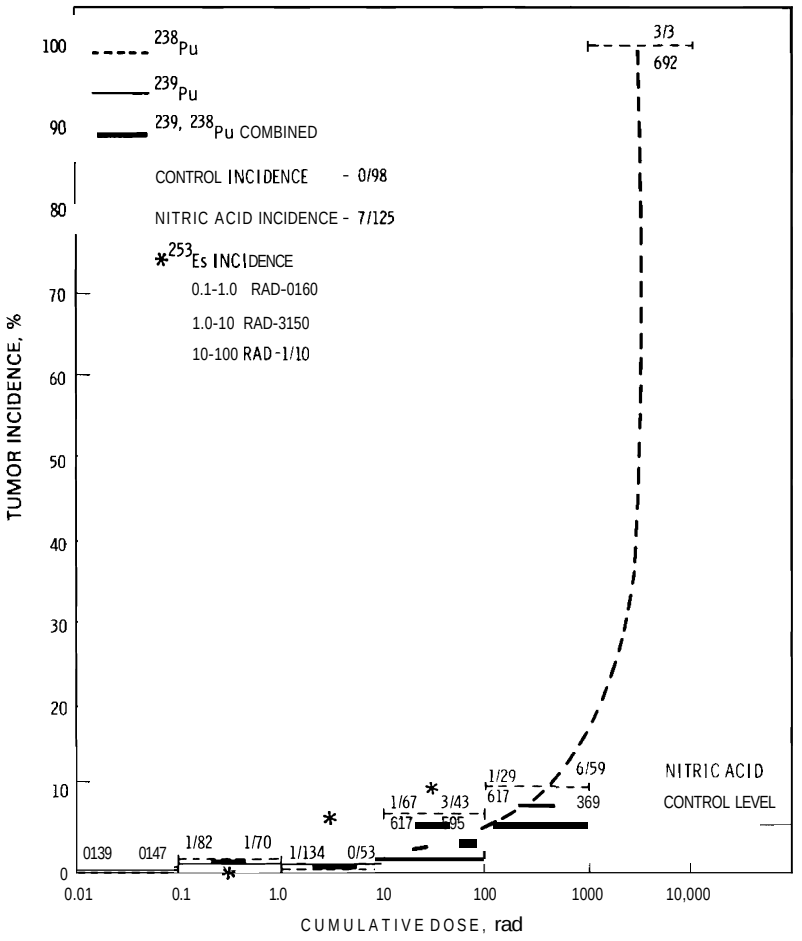

FIGURE 3.18. Bone Tumor Incidence

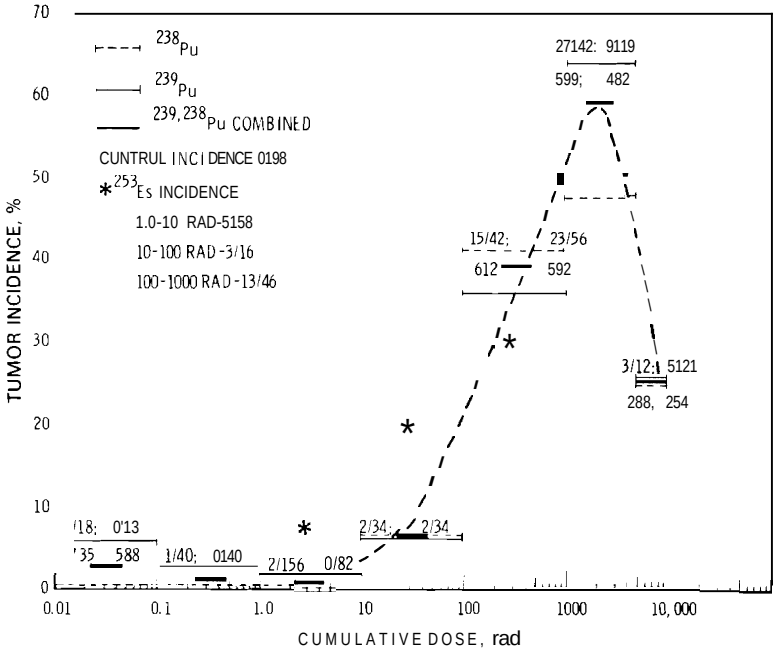

FIGURE 3.19. Lung Tumor Incidence

The mean survival time of bone tumor-bearing, was not significantly shortened, as shown in Figure 3.20. The Pu-exposed rats with lung tumors did, however, have a significantly shorter mean survival time when compared with either HNO_3-treated or nontreated control groups ($P = 5 \times 10^{-6}$ and $P = 0.017$, respectively). The results with ^{253}Es were consistent with those for Pu except that survival of the animals with lung tumors did not differ significantly ($P = 0.23$) from the nontreated controls. Also, as observed in the Pu-exposed rats, the ^{253}Es rats dying from all other causes had significantly shorter mean survival times than either of the control groups. Dose rate or the potential for recovery from alpha radiation damage had little effect on mean survival, with the possible exception of those animals dying with lung tumors.

Results of lung tumor induction with transuranic nitrates are in agreement with results from studies with the more refractory transuranic oxides. Four tumors were observed in 349 rats with estimated cumulative lung dose of 10 rad or less. The peak incidence (~60%) was observed at a dose range of 1000-5000 rad. Bone tumors were much less abundant than lung tumors, although the transuranic nitrates are translocated readily to bone. This is particularly applicable to ^{253}Es, where earlier studies using intratracheal instillation have shown a preponderance of bone tumors. A similar inhaled dose of $^{253}Es(NO_3)_3$ was acutely lethal, apparently due to a more generalized radiation pneumonitis not seen with the less uniformly distributed intratracheal dose.

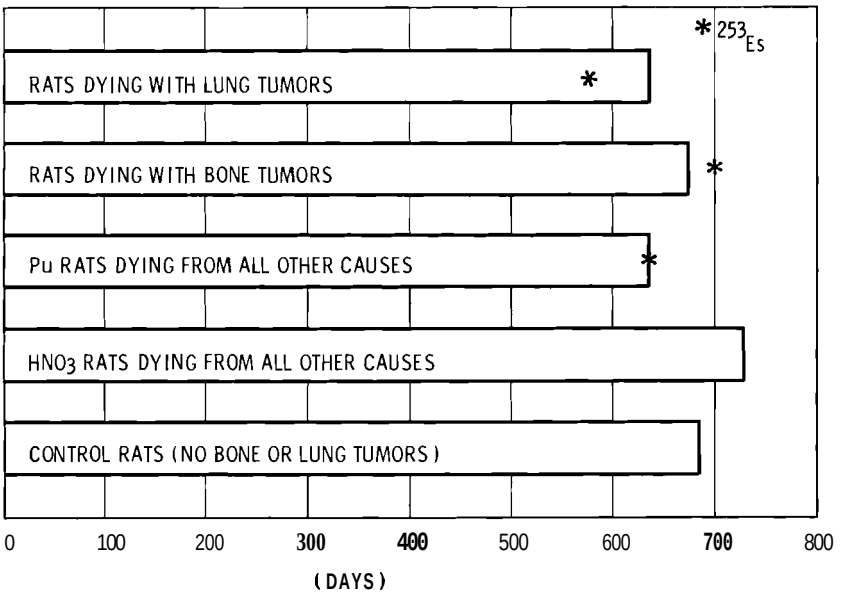

FIGURE 3.20. Average Survival Time

STATISTICAL EVALUATION OF LUNG, BONE, AND LIVER TUMORS IN RATS EXPOSED TO AEROSOLS OF $^{238}PuO_2$, $^{239}PuO_2$, AND $^{244}CmO_2$

Investigators:

J. A. Mahaffey and C. L. Sanders

The Mantel-Haenszel procedure was applied to the evaluation of tumor data from exposures to aerosols of $^{238}PuO_2$, $^{239}PuO_2$, and $^{244}CmO_2$. Significance was evident for lung tumors for all three transuranics, for osteosarcomas in animals exposed to $^{244}CmO_2$, and was suggested for liver tumors in animals exposed to $^{244}CmO_2$.

The Mantel-Haenszel procedure incorporates adjustments to equalize differences among groups for factors other than tumor incidence. Differences in survival were equalized by stratifying the data into 30-day intervals, based on time after exposure to death. The test statistic is chi-square with k-1 degrees of freedom (for comparing k groups). A chi-square with a single degree of freedom was also calculated to test for a linear trend in the data.

Table 3.19 shows the observed and expected number of tumors, (summed over the time intervals), by exposure group, for each transuranic. Expectations are based on the null hypothesis of no differences in tumor incidence for the different levels of exposure. All tumors were assumed to be fatal and animals sacrificed late in the experiment were treated as if they had died. There was no reasonable doubt as to the significant correlation of exposure with lung tumor incidence ($P < 0.000005$) Table 3.20). The chi-square values obtained from the analyses of osteosarcomas and hepatocellular carcinomas were not valid, however, because they were based on small expected values in every cell.

For the $^{238}PuO_2$ bone and the $^{244}CmO_2$ liver tumors, the exact probability of the observed tumor pattern was calculated. First, the probability of a tumor in each group was found (adjusted expected value/total number of tumors). The exact probability was then calculated to be the probability of the observed tumor pattern plus the probability of any more extreme configurations. Based on two groups (Table 3.19) the $^{238}PuO_2$ osteosarcomas occurred with probability $P = (0.51)^2 = 0.26$, not a significant result. With $^{244}CmO_2$, two hepatocellular carcinomas were observed, and $P = 2(0.292)(0.044) + (0.044)^2 = 0.028$. This is generally classified as significant, but since it is based on only two tumors, further investigation is necessary. To evaluate the $^{244}CmO_2$-exposed animals that developed osteosarcomas, it was necessary to combine the 0.54- and 4.4-nCi exposure groups and the 48- and 450-nCi groups, then recalculate the chi-square value. This was found to be $\chi^2 = 8.82$ with a single degree of freedom, which was significant ($P < 0.005$).

TABLE3.19. Observed and Expected[a] Tumors by Exposure Group

	Exposure												
	$^{238}PuO_2$				$^{239}PuO_2$				$^{244}CmO_2$				
Tumors	0.14[b]	11	220	890	0.18	5.0	45	180	0.54	4.4	48	450	1800
Lungs[c]													
Observed	0	9	16	4	0	6	30	14	1	1	7	13	0
Expected	13.1	13.6	2.3	0.1	23.9	10.9	13.1	2	6.3	7.4	6.2	2.1	0[d]
Osteosarcoma													
Observed	0	2	0	0	0	0	0	0	0	2	5	5	0
Expected	0.98	1.02	0[d]	0[d]					3.4	4	3.1	1.1	0[d]
Hepatocellular Carcinoma													
Observed	0	0	0	0	0	0	0	0	0	0	1	1	0
Expected									0.6	0.7	0.6	0.1	0[d]
Number of Animals	134	140	34	31	135	71	71	69	67	70	65	48	23

[a] Expected under the null hypothesis of no differences between exposure groups
[b] Estimated initial alveolar deposition in nCi
[c] Includes adenocarcinoma, hernangiosarcoma, squamous carcinoma, and fibrosarcoma
[d] All animals in these groups were dead when tumors in other groups were observed. Degrees of freedom must be reduced appropriately

TABLE 3.20. Values of Chi-Square from Testing Differences in Exposure Croups for Lung Tumor Incidence

	χ^2	
Exposure	Mantel-Haenszel (3 DF)[b]	Linear Trend (1 DF)
$^{238}PuO_2$	297.6[a]	104.9[a]
$^{239}PuO_2$	127.8[a]	102.2[a]
$^{244}PuO_2$	71.1[a]	40.1[a]

[a] Significant with $p < 0.000005$
[b] Degrees of freedom

METABOLIC MODELING OF INHALED $^{244}CmO_2$

Investigators:
J. A. Mahaffey, J. A. Merrill,
and C. L. Sanders

Data on ^{244}Cm content of Wistar rat organs were modeled by a weighted nonlinear least squares method. Radiation doses were estimated from these models and estimates of the variation of dose were mathematically propagated. Conclusions drawn from the dose estimates must take into account the imprecision of the estimate.

Because our purpose in metabolic modeling of radiochemical data from aerosol exposures is the estimation of radiation dose to an organ, it is important to have a measure of the precision of the model. A set of differential equations describing the entire metabolic process is usually too complicated to permit an accurate estimate of precision. Data from animals exposed to aerosols have at least two major sources of variability: (1) natural biological variation in the animals, and (2) variation based on uncontrollable differences in initial exposure. A complicated modeling system with feedback is beyond the discrimination potential in most mass exposure data sets where the second source of variation is large. Thus, simplifying yet realistic assumptions must be imposed on the system, consistent with the observed variation in the data.

In the modeling of $^{244}CmO_2$, it was found that a three-component model was the simplest that adequately described the lung data. Feedback from other organs and within-lung transfer was assumed negligible, since such phenomena could not be detected due to the variation and the time distribution of the observed data (Figure 3.21). The equation is

$$Y = 76.5e^{-1.3t} + 21.8e^{-0.060t} + 1.7e^{-0.0017t},$$

where Y is the percent of initial alveolar deposition (IAD) predicted at time t (in days) postexposure. The half-times of the three compartments (± standard deviation) are 0.5 ± 0.3, 12 ± 9, and 410 ± 440 days.

To model the other organs of interest, a differential equation was solved, the derivation of which assumed the above lung clearance curve. It was further assumed that (1) once the Cm reached the organ, elimination was similar regardless of which of the three lung compartments was identified as the source, and (2) the Cm which reaches the organ could do so indirectly and repeatedly, just as long as the ultimate percentage from each lung compartment did not exceed 100%. For the skeleton, 14% (f_1) of the first component and 36% each (f_2=f_3) of the other two lung compartments were estimated to be transferred. This is shown schematically in Figure 3.22 and can be represented by the equation:

$$Z = 11\{(1-e^{-1.3t}) - (1-e^{-0.00013t})\} + 8\{(1-e^{-0.060t}) - (1-e^{-0.00013t})\} + 1\{(1-e^{-0.0017t}) - (1-e^{-0.00013t})\},$$

where Z is the predicted percent of IAD in the skeleton at day t after exposure. Similar functions were used to model the data from the liver and the thoracic lymph nodes. All of the estimated transfer constants have a standard deviation similar in magnitude to the estimate. The half-times were estimated to be about 14 yr for skeleton, 7 days for liver and 14 days for thoraci'c lymph nodes.

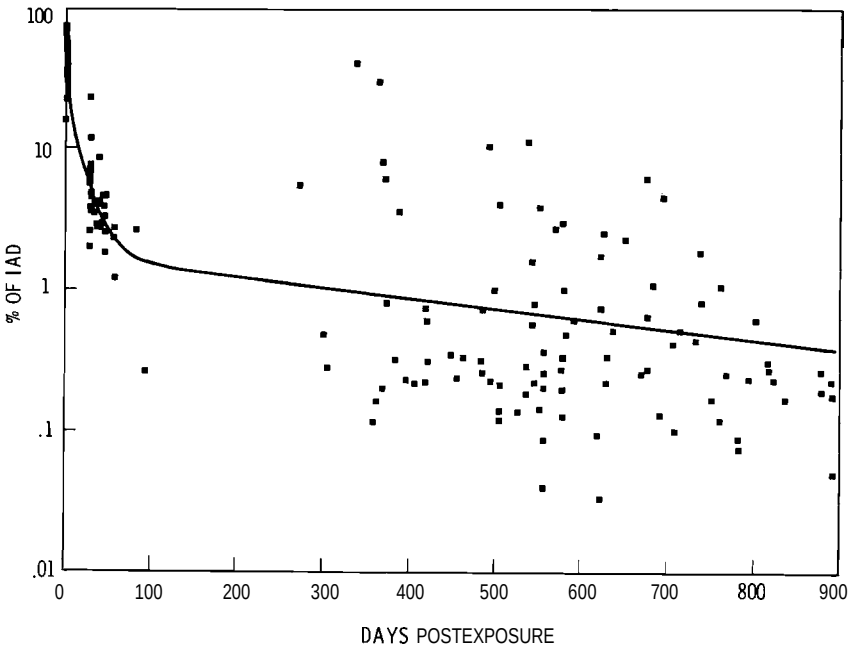

FIGURE 3.21. Lung Clearance Curve for $^{244}CmO_2$

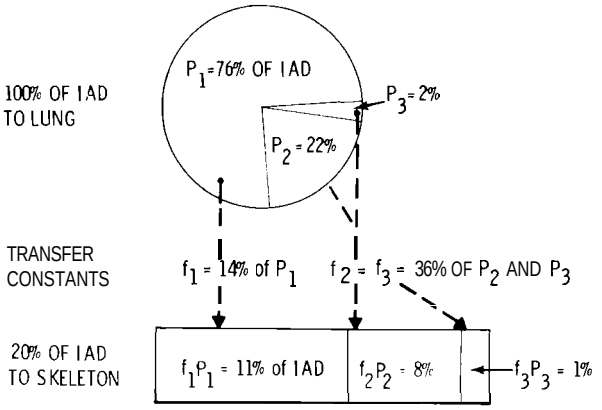

FIGURE 3.22. Transfer of $^{244}CmO_2$ from Lung to Skeleton

To use these models to estimate radiation dose it was assumed that the difference between the observed and predicted percent at death for a given animal was entirely due to variation in IAD from the group average. An individual animal's IAD was calculated to account for this difference. Dose at death (or at any specified time) is then the integral of the clearance or retention curve to this time, adjusted by a known constant (which incorporated IAD). Based on the variances and covariances of the variables in the clearance or retention curve, and using a Taylor expansion, an approximate variance of dose can be propagated. Consistently, the size of the standard deviation of dose was similar to the size of estimated dose. That is, statistically, the dose estimates cannot be said to differ from zero.

This implies that the use of dose estimates obtained by integrating clearance or retention curves is not a good choice for evaluatin response variables (often tumor incidence7. This is not to say that this should not be done, but it is important to first establish the existence of a relationship between increased response and increased exposure. The magnitude of the standard deviation of dose further implies that any extrapolation to low doses should be done with extreme care and presented with due qualification.

EXPRESSION OF LUNG TUMORIGENESIS IN THE HAMSTER CHEEK-POUCH

Investigators:

K. E. McDonald, C. L. Sanders

Technical Assistance:

K. M. Dragoo

Lung sections from hamsters exposed to $^{239}PuO_2$ aerosol were serially implanted into the cheek pouches of recipient hamsters. By histologic comparison of donor tissue with the implant after growth we hope to develop criteria for malignancy.

Adequate criteria of pulmonary malignancy are required for the classification of metaplastic and neoplastic lung lesions in hamsters exposed to alpha emitters. To establish criteria for more definitive diagnosis of these lesions, lung sections of hamsters exposed to $^{239}PuO_2$ aerosols were implanted in recipient hamster cheek pouches. Hamsters with benzo(a)pyrene-(BAP) induced neoplasnis served as positive controls to confirm the validity of the procedure. Iron (Fe_2O_3) oxide was used as a carrier control (Table 3.21).

Hamsters were exposed, nose-only, to $^{239}PuO_2$ aerosol. Two animals from each exposure group were killed one day postexposure and their lungs removed for Pu analysis; initial lung burdens ranged from 12-150 nCi. The Fe_2O_3 controls and the BAP + Fe_2O_3 positive control groups were given 15 consecutive weekly intratracheal instillations of 3 mg BAP and/or 3 mg Fe_2O_3 per instillation.

Five months after exposure the first group of animals was killed with ether, their lungs removed and placed in a sterile petri dish with Hank's balanced salt solution. Each lung was examined visually and the 10 most suspicious areas removed. These sections were subsequently bisected, with one-half placed in 10% neutral buffered formalin and the other half subcutaneously inserted by trocar into the cheek pouch of the recipient animal. These animals were killed 3 wk later, and the cheek pouch was removed and placed with the corresponding section of lung previously saved for histologic examination.

Epithelial proliferation was found in control implants, which is not unusual considering the incidence of bronchiolization of the alveolar epithelium in aged hamsters. There were no mitotic figures observed nor any abnormal increase in size of the implant sites. There was an increase in the incidence of

TABLE 3.21. Experimental Protocol

Treatment	Number of Animals Exposed	Number of Donors/Month	Number of Recipients/Month
$^{239}PuO_2$	160	10	100
BAP + Fe_2O_3	40	2	20
Fe_2O_3	40	2	20
Controls	40	2	20

epithelialization in hamsters exposed to BAP + Fe_2O_3 or to $^{239}PuO_2$. Implants without epithelialization in the corresponding lung sample lost their normal architecture, which was replaced by necrosis, dystrophic calcification and proliferative fibrosis (Figure 3.23). On the other hand, implants from lungs which exhibited epithelial proliferation of the terminal bronchioles, diagnosed as focal interstitial response or bronchiolar adenomatous hyperplasia (Figure 3.24), often exhibited acinar-type epithelial proliferations (Figure 3.25). Some of the epithelial cells in the implants were ciliated.

These studies will continue during the next fiscal year, when the value of transplantability for diagnoses of hamster lung tumors should be resolved within the limitations of this experimental design.

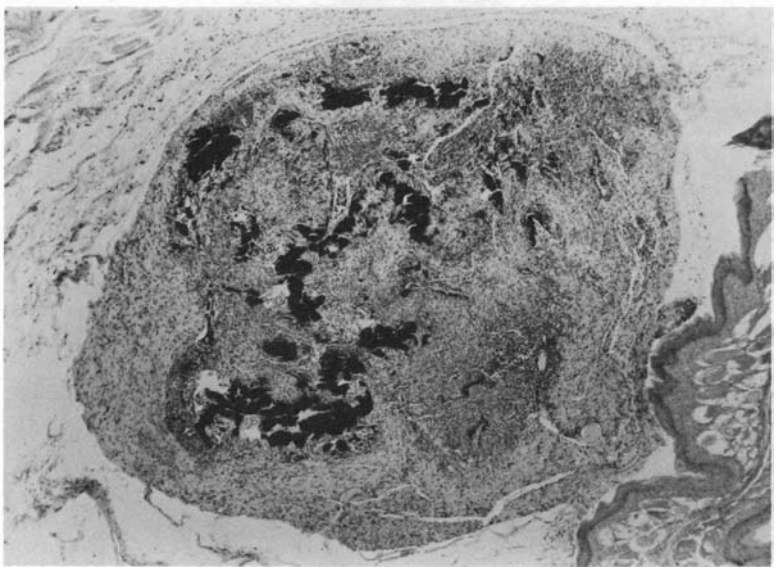

FIGURE 3.23. Hamster Cheek Pouch with Lung Implant Showing Necrosis, Calcification and Fibrosis

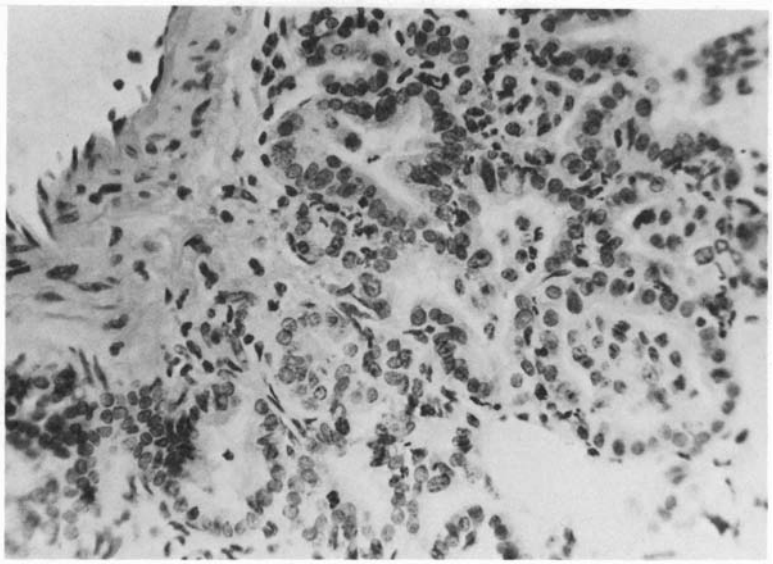

FIGURE 3.24. $^{239}PuO_2$-Exposed Hamster Lung, Showing Slight Bronchiolization of Alveolar Epithelium

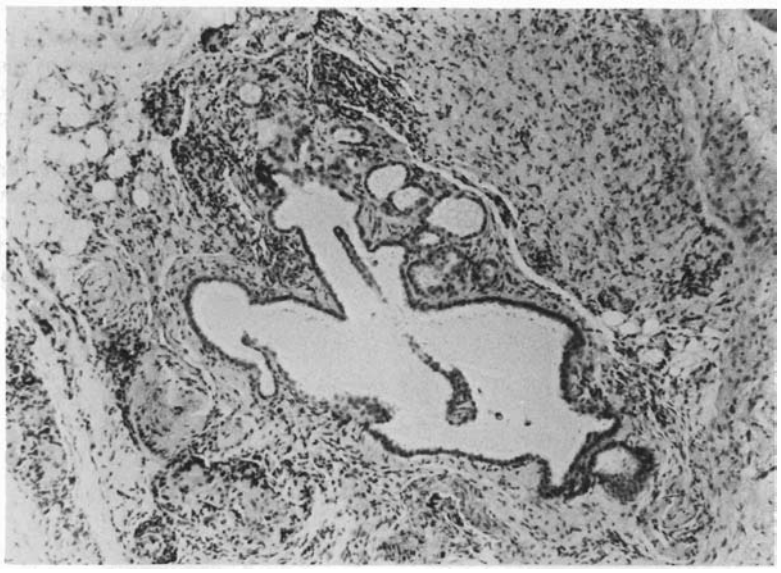

FIGURE 3.25. Hamster Cheek Pouch with Pu-Exposed Lung Implant, Showing Epithelization

ELECTRON MICROSCOPIC MORPHOMETRY OF LUNG

Investigator:
K. Rhoads
Technical Assistance:
S. I. Baker and A. W. Conklin

The volumetric and cell type distribution in alveolar lung of rat and hamster were similar, although statistically significant species differences were found for alveolar epithelium, capillary endothelium, and some noncellular interstitial components. No significant effect of inhaled $^{239}PuO_2$ on lung composition could be demonstrated within either species.

The pathologic response to inhaled $^{239}PuO_2$ in life-span studies is apparently different for rats and hamsters. At optimal doses rats develop a high incidence of primary lung tumors arising from bronchiolar or alveolar epithelium. Hamsters receiving similar doses develop epithelial lesions that do not progress to neoplasms within the normal life span of the animals. Previous autoradiographic studies showed no species differences in lung distribution of $^{239}PuO_2$, although the pattern did change with time after exposure in both species (Annual Report, 1976). The present extension of that study employs morphometric techniques at the electron microscopic level.

Twenty-four Wistar rats and 20 Syrian golden hamsters (all females) were exposed to $^{239}PuO_2$ and lung tissue from these animals and from controls was prepared for observation according to procedures described previously (Annual Report, 1976). The average initial alveolar deposition was 132 nCi for rats and 67 nCi for hamsters. Three tissue blocks, 2-3 mm^3 in volume, were selected by systematic and random sampling procedures from the lower left lung of each animal. These were embedded, sectioned, and photographed for morphometric analysis. Six micrographs were recorded for each section (a total of 18 per animal), at a final magnification of 5300X. Only alveolar lung was considered in this part of the study.

The micrographs were analyzed using a multipurpose test system, similar to that described by Weibel et al., 1966, J. Cell Biol. 30:23-38. The volumetric distribution was determined by point-counting volumetry and surface-related parameters by counting intersections of test line segments with alveolar and capillary surfaces. The cell type distribution was obtained by simple counting of cells with visible nuclear profiles.

Results of the analysis are shown in Figures 3.26 and 3.27 and Table 3.22. All of the statistically significant differences were species differences in one or both treatment groups. Neither species showed a significant change from control to exposed groups for any parameter.

The volume distribution (Figure 3.26) revealed the following statistically significant differences at the given levels: 1) Exposed rats contained a lower fraction of total epithelium than exposed hamsters ($P < 0.05$), 2) Capillary endothelium was also lower in exposed rats than in exposed hamsters ($P < 0.01$), 3) Noncellular interstitial components accounted for a greater fraction of lung in rat than in hamster in both control ($P < 0.05$) and exposed ($P < 0.01$) groups.

The only significant difference in cell type distribution (Figure 3.27) was the decreased fraction of Type I epithelial cells

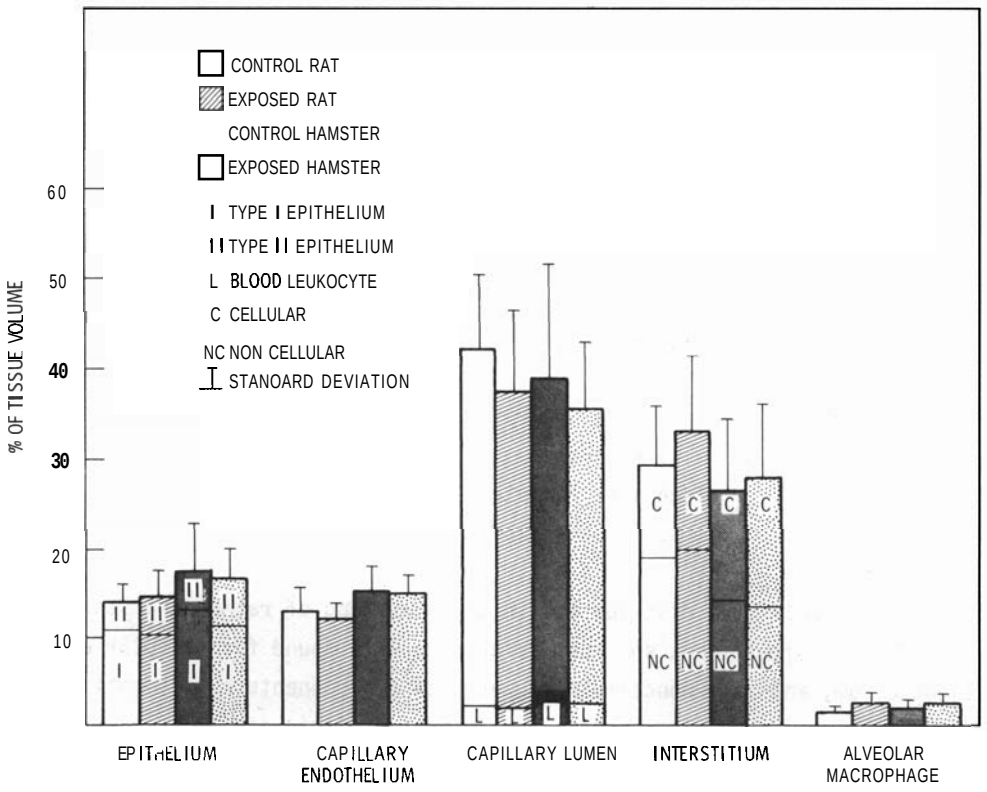

FIGURE 3.26. Volume Distribution of Alveolar Tissue Compartments

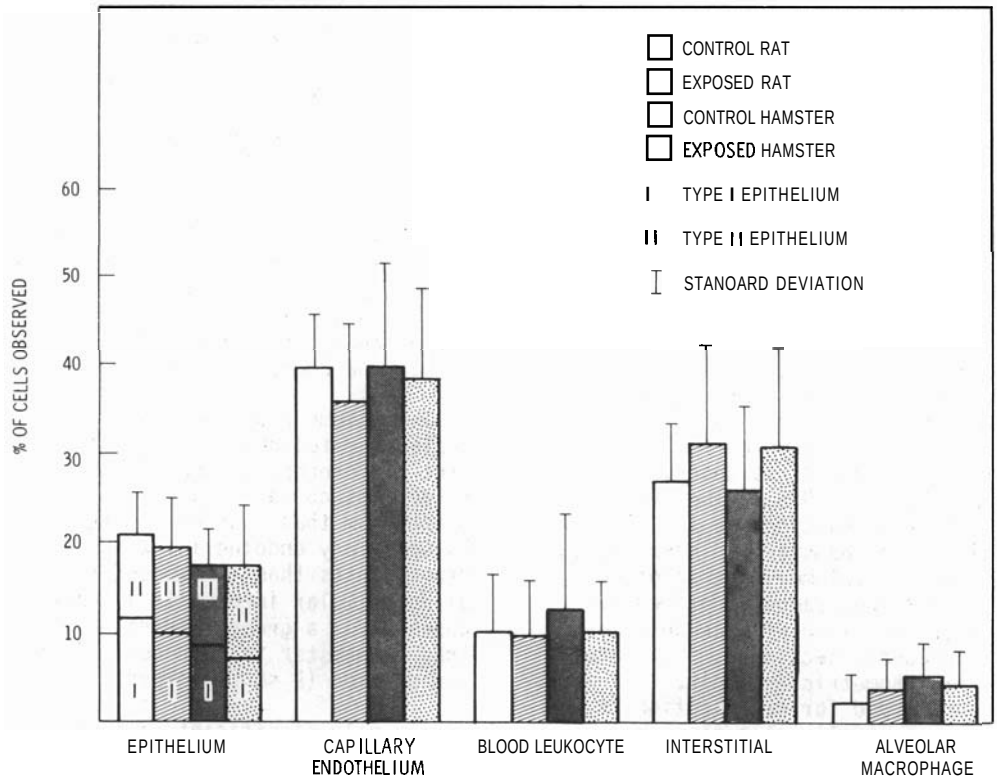

FIGURE 3.27. Alveolar Cell Type Distribution

TABLE 3.22. Surface Area Parameters (Mean + SD)

	Rats		Hamsters	
	Control	Exposed	Control	Exposed
Capillary Surface/ Volume Ratio, μ^{-1}(a)	1.1 ± 0.3	1.2 ± 0.3	1.4 ± 0.5	1.3 ± 0.2
Alveolar Septal Surface/ Volume Ratio, μ^{-1}(a)	0.67 ± 0.48	0.55 ± 0.15	0.73 ± 0.05	0.63 ± 0.15
Arithmetic Mean Thickness - Alveolar Septa, μ(b)	3.5 ± 1.1	3.9 ± 1.6	2.8 ± 0.2	3.7 + 2.8

(a) Surface/Volume Ratio = $\frac{4N}{ZP}$

(b) Arithmetic Mean Thickness = $\frac{ZP}{2N}$

where:

N = No. of intersections of test lines of length Z with surface of a structure (alveolar wall or capillary)

P = No. of test points falling on structure of interest (test points are ends of test lines of length Z)

Z = length of test line on micrographs

in exposed hamsters compared to exposed rats ($P < 0.05$). The total number of cells counted per animal was also significantly lower for control hamsters (47 + 8) than for control rats (71 + 17) ($P < 0.01$).

The values for surface-related parameters in Table 3.22 revealed no significant differences between species or treatment groups.

Although some significant species differences in lung composition were found, they were relatively few in number and did not appear to account for the dramatic difference in tumor response. The Type II epithelial cell, which has been implicated as a target cell for both chemical and radionuclide carcinogens, showed no significant difference with respect to species or treatment. Generalized pathological response in alveolar lung was minimal following inhalation of $^{239}PuO_2$ at a level which produced about 50% lung tumors in rat life-span studies.

IN VITRO STUDIES OF ACTINIDES AND ALVEOLAR MACROPHAGES

Investigators:
R. P. Schneider and A. M. Robinson

The toxicity of $^{239}PuO_2$, $^{239}Pu(NO_3)_4$, and $^{241}AmO_2$ to rabbit alveolar macrophages in culture was assessed. Comparison of toxicity of $^{239}Pu(NO_3)_4$ and $^{241}AmO_2$ at the same radiation dose level indicates toxicity is due to radiation and not the chemical form of the actinide. Investigations were begun to determine the effect of serum macrophages and DTPA on $^{241}AmO_2$ solubility.

Actinide particles phagocytized by macrophages are largely inaccessible to presently used actinide therapy techniques. We are developing an in vitro system to examine the interaction of macrophages with radionuclides and to search for improved methods and/or agents to increase the removal of radionuclides from the intracellular fraction. Previous reports (Annual Reports 1975, 1976) have described development of cell culture and cell loading techniques utilizing $^{239}PuO_2$. This report will describe the initial generation of baseline macrophage survival data for $^{239}PuO_2$, $^{239}Pu(NO_3)_4$ and $^{241}AmO_2$. Also described is the solubility of $^{241}AmO_2$ as effected by serum, DTPA, and cultured macrophages.

Plutonium polymer and hydroxide were generated by a 1/1000 dilution of $^{239}Pu(NO_3)_4$ (6N in HNO_3) in Hanks' balanced salt solution with 10% rabbit serum (HRS). This method results in a mixture probably similar to that formed when $^{239}Pu(NO_3)_4$ is introduced into body fluids. $^{239}PuO_2$ and $^{241}AmO_2$ were used as 1/1000 dilutions of aqueous stock suspensions in the media of choice.

The macrophages and actinide particles were incubated with shaking for 2 hr at 37°C. The cells and particles were placed in culture flasks and allowed to attach to the flask surface. Unattached cells and particles were washed from the flask with M-199 salts, 10% in rabbit serum (MRS) and attached cells cultured in 5% CO_2 for the remainder of the experiment. More than 90% of the attached cells were viable (as ascertained with trypan blue stain) and no significant differences in the number of attached cells between control and actinide-exposed cells was found. Cell survival was estimated by counting the cells remaining attached to the flask. Particle uptake was demonstrated by autoradiography of cell smears. $^{239}PuO_2$ uptake has been previously shown by electron microscopy (Annual Report 1976).

Data in Figure 3.28 illustrates that cell survival is dependent upon the actinide level to which the cells are exposed during incubation in suspension. A comparison of the $^{239}Pu(NO_3)_4$ and $^{241}AmO_2$ curves shows essentially similar results. Chemically, there is 55 times as much Pu as Am in the incubation mix. This would indicate that Am and Pu toxicity to the macrophage is more related to radiation dose than chemical form.

To evaluate new chelating agents and/or methods of increasing the solubility of intracellular actinides it is desirable that the test actinide particles exhibit several criterian. The particle must be taken up by macrophages, it must not kill them too quickly, it must be moderately soluble so that results can be measured with reasonable speed and ease, and dosing and size must be reproducible from experiment to experiment.

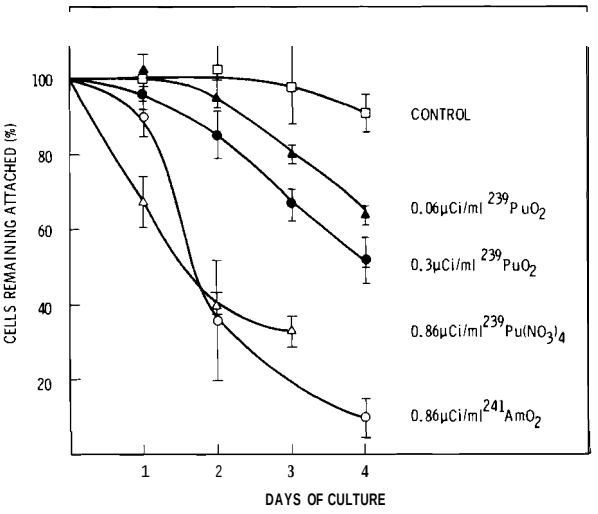

FIGURE 3.28. The Effect of Phagocytized Actinide on Survival of Rabbit Pulmonary Macrophages

$^{239}PuO_2$ exhibited all of these criteria except for solubility. After 2 wk in culture, less than 1% of the radioactivity was filterable (0.05-micron filter). This observation, coupled with the well-known resistance of $^{293}PuO_2$ to DTPA solubilization suggested that a more soluble form of actinide would be more suitable for the study.

$^{239}Pu(NO_3)_4$ placed in MRS resulted in 11% filterable (0.05-micron filter). Uptake, toxicity and solubility were satisfactory but particle size was not reproducible.

$^{241}AmO_2$ appears to fit all criteria and therefore more extensive investigation of its solubility and behavior in solution was begun. The $^{241}AmO_2$ for the experiment was a fresh aqueous suspension (less than 1 month old). Dilutions of this stock for solubility measurements and uptake were made as 1/1000 dilutions in suitable media.

The $^{241}AmO_2$ particles were partially solubilized (passed through a 0.1-micron filter) by DTPA (Table 3.20). The decrease of filterable ^{241}Am in Hanks' balanced salts is presumably due to adsorption of Am to the walls of the vessel and the formation of particulate hydroxides. The increase in the filterable fraction in the presence of serum may have been the result of binding to molecules in solution, thus preventing adsorption and precipitation as hydroxides. The addition of serum to Hanks' salt solution containing DTPA reduced the filterable fraction by two-fold. The mechanism of this antagonism is unknown; however, it seems likely that serum proteins coat the AmO_2 particles and this coat may reduce DTPA access to the particles. The presence of approximately 20 μM iron in the serum (2.0 μM in HRS) could bind the DTPA but there should be a 50-fold excess of DTPA, so this seems unlikely to decrease Am binding.

The influence of macrophages on the solubility of $^{241}AmO_2$ was examined by incubating the cells with $^{241}AmO_2$ for 2 hr and culturing the washed cells in the presence and absence of 0.1 μM DTPA. The supernatant culture medium was filtered (0.1-micron filter) initially, and after 6 days, when less than 10% of the cells were intact. The ingestion of $^{241}AmO_2$ by the cells had no detectable effect on ^{241}Am solubility. After 6 days the filterable fraction both in the presence and absence of DTPA was the same as in the 6-hr (4-day) cell-free incubation (Table 3.23).

Because it meets the desired criteria, $^{241}AmO_2$ will be used as the actinide test particle in future investigations of potential therapeutic agents and/or mechanisms. We also plan to investigate the mechanism of antagonism of DTPA chelation by serum, since body fluids contain virtually the same proteins found in serum and may reduce chelation effectiveness in vivo as well.

TABLE 3.23. Effect of Serum and DTPA on Filterability of $^{241}AmO_2$

	Percent of $^{241}AmO_2$ Filtered through a 0.1-μ Filter			
	Incubation Medium[a]			
Duration of Incubation, hr	Hanks'[c]	Hanks' + 10% Serum[c]	Hanks' + DTPA, 0.1 mM[d]	Hanks' + 10% Serum + DTPA, 0.1 mM[d]
0[b]	1.5 ± 0.4	5.2 ± 0.5	10.6 ± 0.8	8.3 ± 0.8
3	0.3 ± 0.4	5.8 ± 1.0	12.9 ± 1.1	10.3 ± 0.2
30	0.06 ± 0.02	8.0 ± 0.3	18.1 ± 1.1	11.7 ± 0.5
96	0.05 ± 0.04	6.0 ± 0.4	22.5 ± 1.3	11.9 ± 0.5

[a] Plastic centrifuge tubes containing 0.7 μCi/ml $^{241}AmO_2$ in the appropriate media, incubated at room temperature
[b] Zero hour sample taken from 0 to 20 minutes after introduction of aqueous stock solution into media
[c] Average of three samples
[d] Average of two samples

• Toxicology of Plutonium-Sodium

It has been postulated that liquid metal fast breeder reactor (LMFBR) accidents would involve the formation of sodium vapor through which plutonium and uranium oxide particles would pass enroute to release, resulting in a mixed plutonium-uranium-sodium aerosol. This project will devise methodology for the production of appropriate aerosols of fuel and sodium under several conditions, and will determine the biological characteristics of these aerosols. If preliminary results indicate it to be desirable, the biological effects of mixed fuel-sodium aerosols will be evaluated in life-span studies.

CHARACTERIZATION OF MIXED LMFBR FUEL-SODIUM AEROSOLS GENERATED BY LASER VAPORIZATION

Investigator:
M. D. Allen
Technical Assistance:
J. K. Briant

A laser is used to vaporize PuO_2-UO_2 from the surface of a rotating fuel pellet to simulate LMFBR fuel-sodium condensation aerosols. The branched, chain-like PuO_2-UO_2 aggregates are swept by argon into a sodium vapor atmosphere. The sodium condenses on the aggregates, and the mixed aerosol is diluted with 50% relative humidity air. These aerosols are being characterized according to physical appearance, crystalline structure, and aerodynamic behavior.

The mixed LMFBR fuel-sodium aerosol generation and exposure system is shown in Figure 3.29. The CO_2 laser is operated in the pulsed mode, with pulse widths ranging from 1 to 10 msec. The pulse period can be varied between 0.01 and 40 sec, depending on the concentration required. The beam can be focused to a spot diameter of 0.1 mm and can have a power density as high as 4 MW/cm^2. The beam is focused onto the surface of a specially fabricated LMFBR fuel pellet with the composition $(Pu_{0.24}\ U_{0.76})O_{1.97}$.

Zeiss particle size analyses of the PuO_2-UO_2 branched, chain-like aggregates show that the primary particle diameters within each aggregate are normally distributed with respect to the logarithm of particle diameter. Although the primary particle size is similar within any particular aggregate, e.g. GSD ≃ 1.35, the size can vary widely among aggregates. The mean primary particle diameter is usually around 25 to 35 nm.

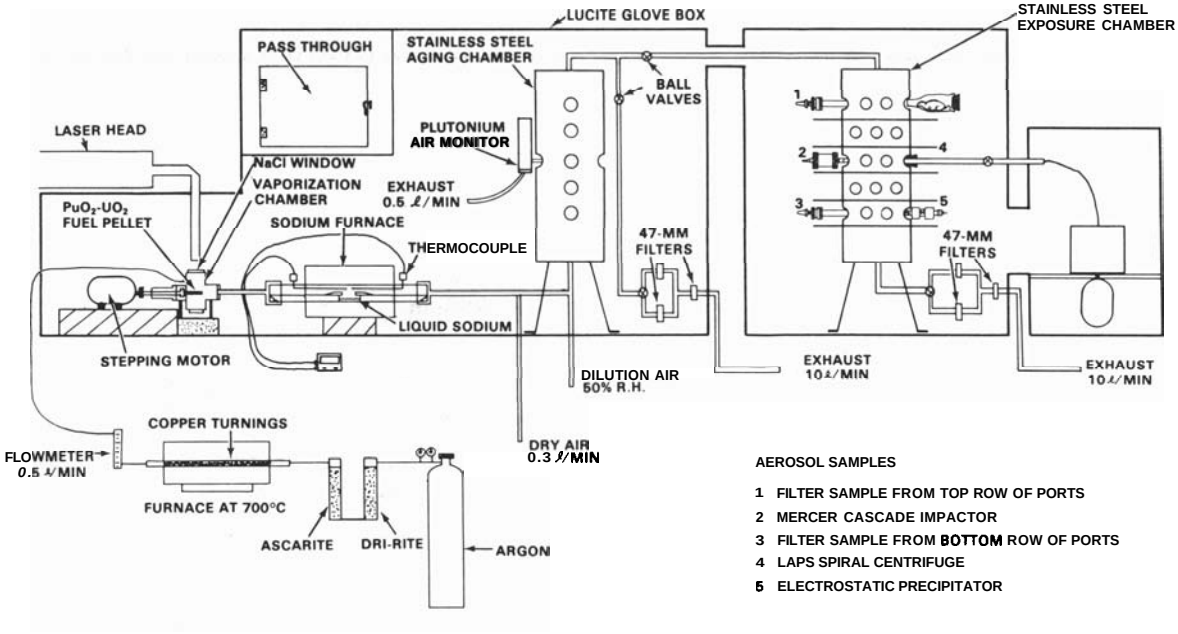

FIGURE 3.29. PuO_2-UO_2-Na Condensation Aerosol Generation System

The amount of PuO_2-UO_2 present in mixed PuO_2-UO_2-Na aerosols does not make much difference in the physical appearance of the aerosol. The branched, chain-like structure of the PuO_2-UO_2 aggregates cannot be seen in the mixed aerosol. Figure 3.30 gives an indication of what happens to the PuO_2-UO_2 aggregates as Na condenses on them.

Table 3.24 gives the results of measurements of aerodynamic size distribution of PuO_2-UO_2 aerosols, using Mercer cascade impactors and a Lovelace Aerosol Particle Separator (LAPS) spiral centrifuge. These data show that the aerodynamic size of the PuO_2-UO_2 aggregates is not strongly dependent on the energy in the laser pulse. Over the range of power and pulse widths investigated thus far, an AMAD of 0.78 μm and a GSD of 1.3 describe the aerosol fairly accurately.

Figure 3.31 shows the effect on the aerodynamic behavior of mixing PuO_2-UO_2 aggregates with sodium vapor. Without sodium present, the AMAD is usually less than 1 μm; at a 1:1 mass ratio the AMAD increases to approximately 1.6 μm, and seems to level off between 4 and 5 μm at greater than a 1000:1 ratio.

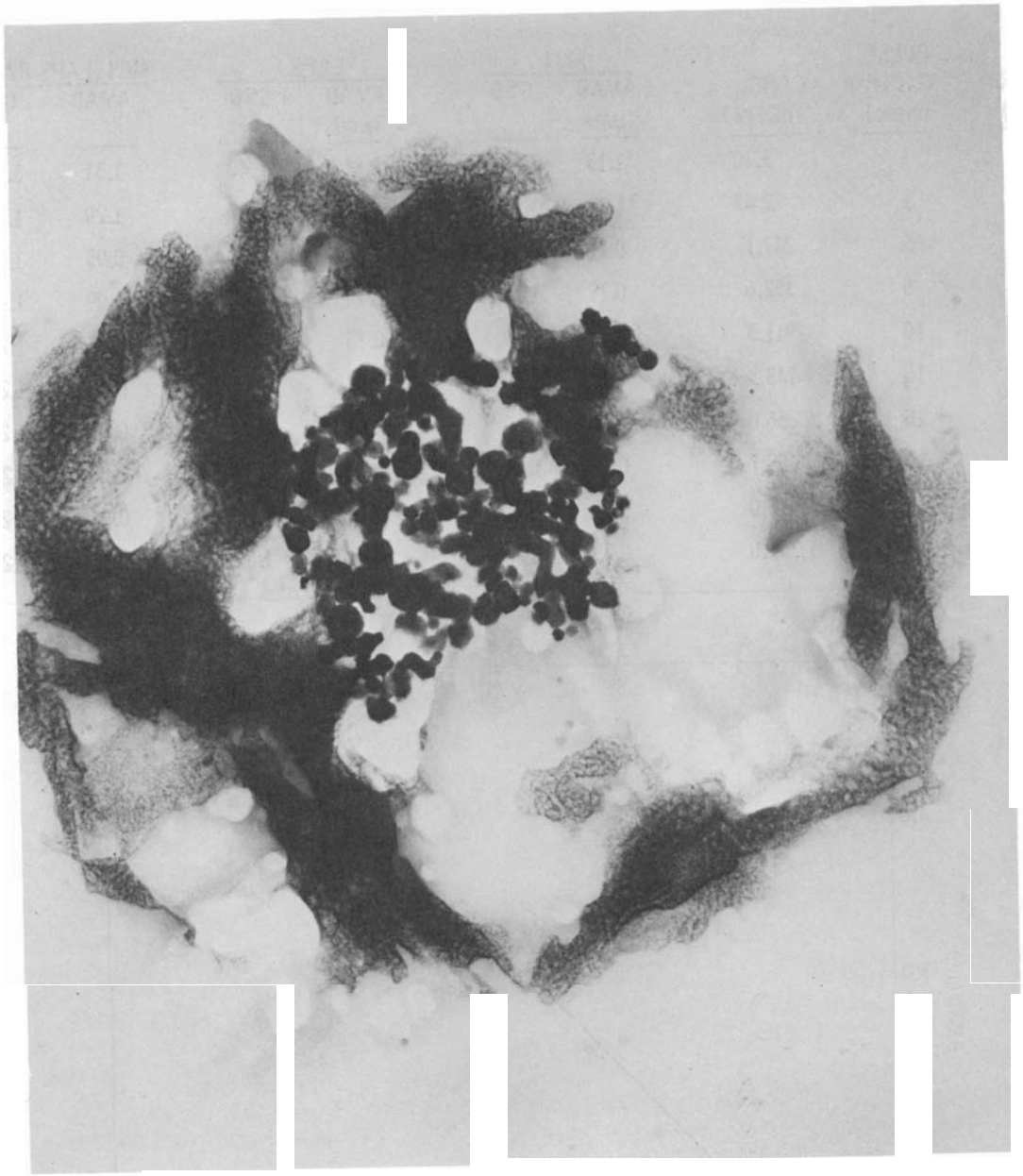

FIGURE 3.30. PuO_2-UO_2-Na **Particle with Na Coating Partially Vaporized 1:1 Na-to-Fuel Ratio**

TABLE 3.24. Comparison of the Aerodynamic Size Distributions of Chain-Like Aggregates Generated at Different Laser Powers and Pulse Widths

LASER BEAM POWER (watts)	PULSE WIDTH (msec)	CONC. (nCi/ℓ)	MCI AMAD (μm)	MCI GSD	LAPS AMAD (μm)	LAPS GSD	MCI/LAPS RATIO AMAD	MCI/LAPS RATIO GSD
220	1	3.20	1.13	1.90	0.86	1.40	1.31	1.36
220	1	2.45	1.11	1.87	0.86	1.37	1.29	1.36
220	5	247.1	0.70	1.54	0.74	1.27	0.95	1.21
220	5	352.6	0.78	1.57	0.79	1.27	0.99	1.24
220	10	911.3	0.72	1.59	0.83	1.29	0.87	1.23
220	10	748.3	0.72	1.58	0.82	1.27	0.88	1.24
110	10	256.0	0.80	1.60	0.84	1.30	0.95	1.23
110	10	152.7	0.87	1.64	0.87	1.30	1.00	1.26
340	10	1,312.0	0.73	1.51	0.79	1.24	0.92	1.22
340	10	1,243.0	0.73	1.57	0.85	1.27	0.86	1.24

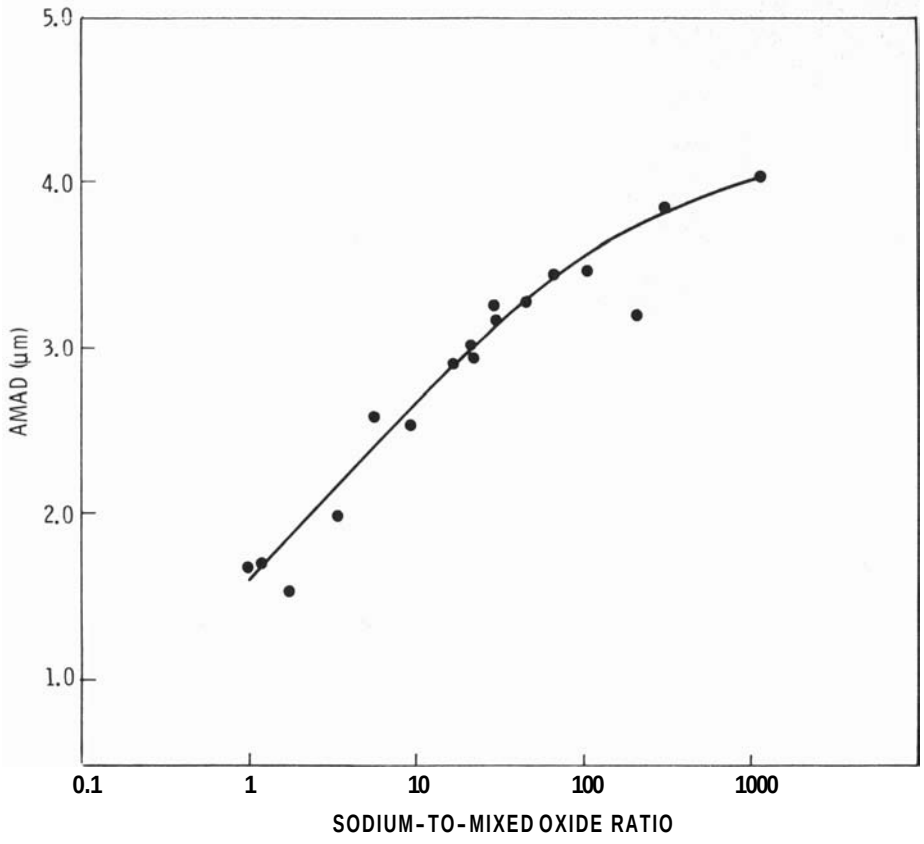

FIGURE 3.31. Activity Median Aerodynamic Diameter (AMAD) Versus Sodium Aerosol-to-Mixed Oxide Fuel Mass Ratios

TRANSLOCATION OF MIXED LMFBR FUEL-SODIUM AEROSOLS FROM THE LUNG FOLLOWING INHALATION BY RODENTS

Investigators:

D. D. Mahlum, J. O. Hess, and M. D. Allen

Technical Assistance:

M. J. Conger, L. F. Hensley, and J. K. Briant

Rats were exposed to aerosols consisting of either LMFBR fuel or mixtures of sodium and fuel. Pulmonary deposition of the mixed aerosol was usually less than that of the fuel only because of the larger size of the mixed aerosol. When the ratio of sodium to fuel was high (>32), the rate of clearance from the lung was faster than for the aerosols with low sodium-to-fuel ratios.

We have investigated the biological properties of condensation aerosols of a liquid metal fast breeder reactor (LMFBR) fuel (20% PuO_2:80% UO_2), with and without the presence of sodium. Aerosols of fuel or fuel + sodium were generated according to the methods described by Allen et al. (Annual Report, 1976). Female rats were exposed by a nose-only technique to aerosols containing sodium and fuel in ratios of 0 to 1200, for 30 min. Animals were killed at 0, 7, 30, 90, and 180 days postexposure and tissues removed for plutonium analysis.

The deposition of aerosol within the lung, as determined in animals sacrificed immediately after exposure, was higher for fuel-only than for sodium-fuel aerosols (Figure 3.32). The difference appears to be related to particle size since the values for two sodium-fuel aerosols with AMADs less than 2.1 were similar to those for fuel only.

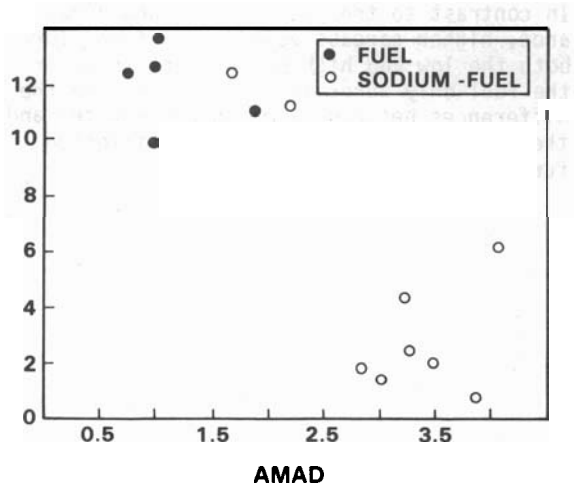

FIGURE 3.32. Effect of AMAD on Particle Deposition in Lung for LMFBR Fuel Only and Sodium-Fuel Aerosols

The influence of sodium on the clearance of Pu from the lung is illustrated in Figure 3.33. Data from several experiments have been combined to derive the three curves shown on this graph. Animals exposed to aerosols containing large amounts of sodium (sodium:fuel >32) show a more rapid clearance of Pu from the lung than do those exposed to fuel only or to aerosols containing lower ratios of sodium to fuel. The difference in clearance from the lung is probably not due to differences in particle sizes, since the aerosols containing lower sodium:fuel ratios were cleared at the same rate as the fuel-only, although the particle sizes were similar.

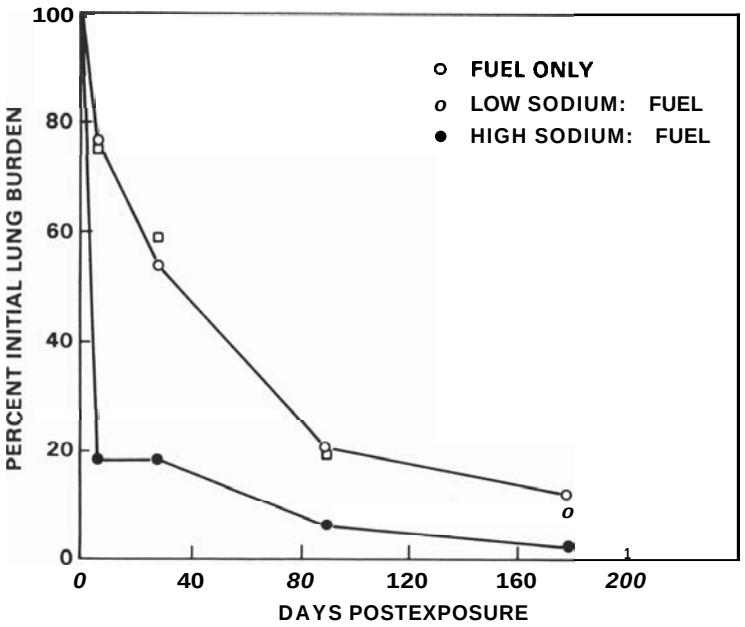

FIGURE 3.33. Clearance of ^{239}Pu for the Lung

The translocation of ^{239}Pu from the lung to other tissues (as indicated by carcass values) was greater in animals which received the sodium-fuel aerosols (Table 3.25). In contrast to the results for lung clearance, higher carcass values were found for both the low and high sodium fuel than for the fuel-only aerosols. The reason for the differences between lung clearance rates and the carcass values are being investigated further.

TABLE 3.25. ^{239}Pu Content (% of Initial Lung Burden) of Carcass After Exposure of Rats to LMFBR Fuel of Sodium-Fuel Aerosols

		Time Postexposure (days)			
Aerosol	Na:Fuel	7	28	90	180
Fuel	0	2.7	1.3	1.0	0.8
Sodium-fuel	1	3.1	3.8	5.8	5.0
Sodium-fuel	12-21	8.4	20.4	19.3	24.2

- **Toxicology of Sodium**

Large quantities of sodium will be used as a coolant for liquid metal fast breeder reactors (LMFBRs), some of which might be released in the event of an accident. This project will design and fabricate an aerosol generation system and an exposure system for rodents, which will simulate conditions that might occur in such an accident. This equipment will be employed to determine the biological response of acute whole-body exposure of adult and immature rats to different concentrations of these aerosols.

TOXICOLOGY OF SODIUM

Investigators:

G. M. Zwicker and M. D. Allen

Technical Assistance:

J. K. Briant

A system has been developed for controlled, whole-body exposure of rodents to sodium aerosols of varied concentration and chemical composition. Preliminary nose-only exposures of rats to an aerosol concentration of 65 µg/ℓ produced no clinical signs or pathological damage. Exposures conducted in rats at 1000 µg/ℓ and 2000 µg/ℓ for 40 min had a severe corrosive effect on nasal turbinates, and at 2000 µg/ℓ, the larynx was similarly affected.

Large quantities of liquid sodium will be used as the heat transfer medium in liquid metal fast breeder reactors (LMFBR). In the event of an accidental release of molten sodium metal into an air atmosphere, a dense white sodium smoke will form. Chemical composition of the aerosol will depend on the atmosphere that it encounters. Humans on-site and off-site could be exposed to the sodium aerosol cloud for several hours. The purpose of this project is to determine appropriate toxicity limits for exposure to sodium aerosols from very low-probability (e.g., once in a lifetime) accidents.

Between June 1 and December 1, 1977, a system for whole-body exposure of rodents to sodium aerosols was designed and fabricated (schematic drawing, Figure 3.34). A stainless steel chamber, containing approximately 500 g pure sodium metal, is heated inductively to 550°C. The sodium aerosol is generated by sweeping argon over the molten sodium surface. Sodium vapor, surrounded by a clean argon sheath, flows into a burning chamber with a controlled-air atmosphere, where the aerosol condenses and reacts. The aerosol flows into the aging chamber and bypasses the exposure chamber until the required concentration is obtained. The animals can then be loaded and the aerosol diverted into the exposure chamber.

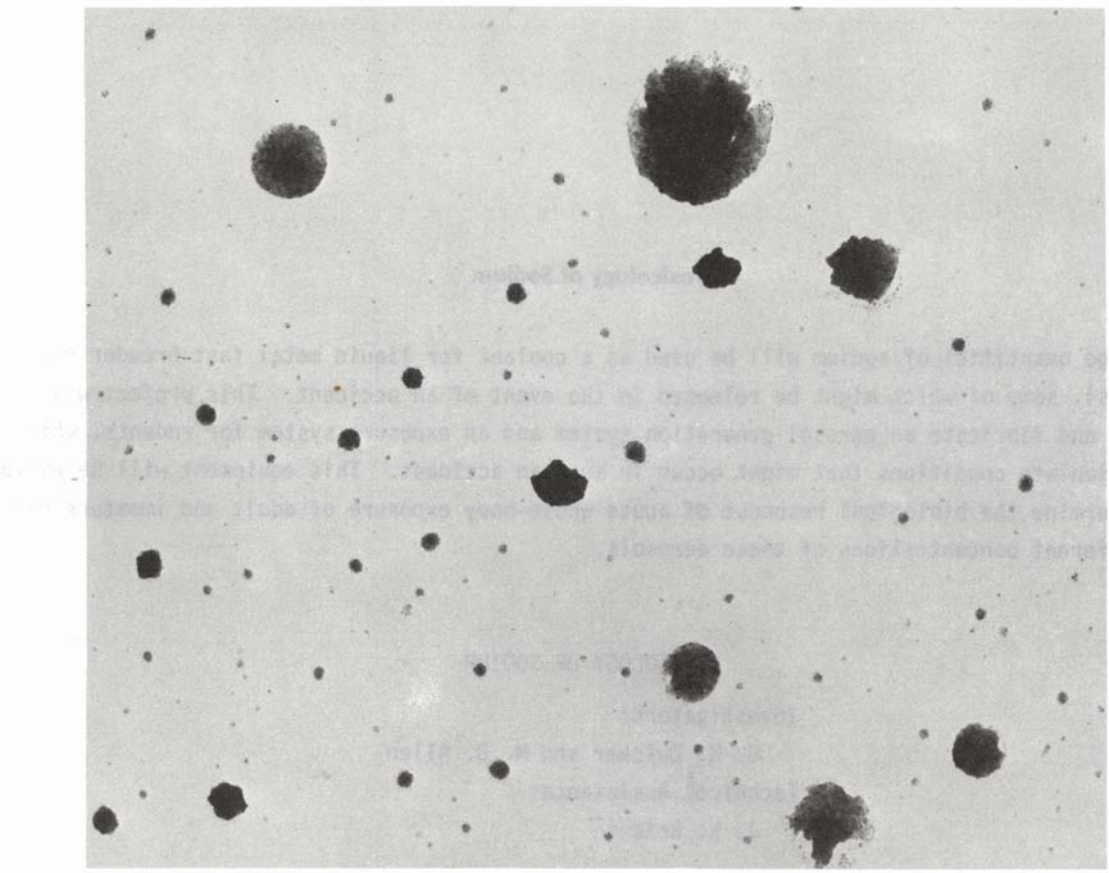

FIGURE 3.34. Transmission Electron Photomicrograph of the Sodium Aerosol

Aerosol concentration will be measured by collecting the sodium on membrane filters and analyzing the filters with an electrobalance, a flame photometer, and a sodium ion electrode. Aerodynamic size distribution will be measured using cascade impactors and a spiral centrifuge. Sodium aerosol concentration will be monitored during exposures using a low-angle, light-scattering photometer. Whole-body exposures of rodents will begin in December 1977.

To obtain preliminary toxicological data on health effects of exposure to sodium combustion products, 16 weanling and 14 adult male Wistar rats were exposed by the nose-only method for 2 hr at a sodium aerosol concentration of approximately 65 µg/ℓ. The aerosol had a mass median aerodynamic diameter of 3.4 and a geometric standard deviation of 3.. The sodium aerosol particles (Figure 3.35) are probably a mixture of NaOH, Na_2CO_3 and their various hydrates.

During the exposure, there were no clinical signs apparent such as breath holding or excitation. When animals were removed from exposure they appeared normally active, alert and healthy. One-half the animals in each group (adults and weanlings) were anesthetized by intraperitoneal administration of sodium pentobarbital, then killed by exsanguination. The other animals were killed 96 hr postexposure. At necropsy, there were no lesions observed in nose, mouth, respiratory system or digestive system

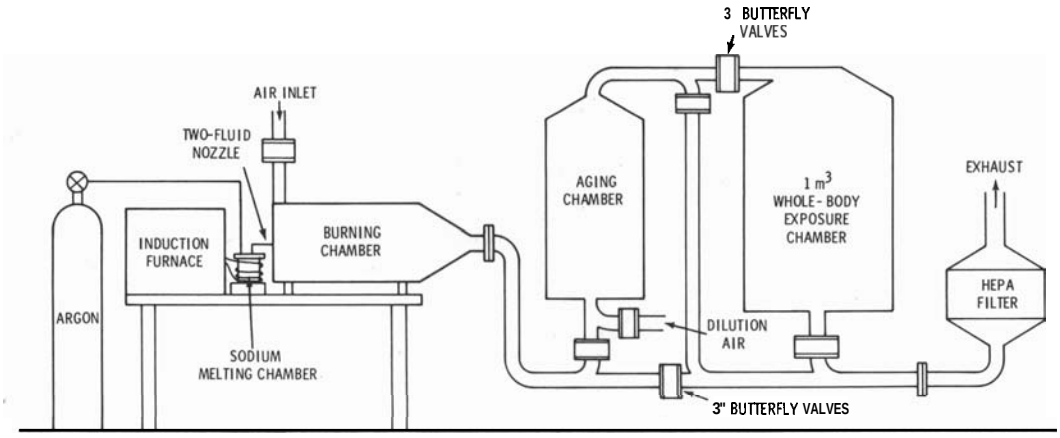

FIGURE 3.35. Proposed Sodium Aerosol Generation and Whole-Body Exposure System

associated with exposure to sodium combustion products. Tissues collected at necropsy for microscopic examination included skin of nose and face, oral mucosa, nasal turbinates, esophagus, stomach, larynx, trachea and lungs. Lungs were infused intratracheally with 10% neutral buffered formalin at 25-cm fixative pressure for 24 hr. Microscopic examination of tissues from these rats revealed no lesions with an incidence or severity pattern suggestive of an exposure effect.

We have conducted several pilot experiments using a prototype whole-body exposure system. During one pilot study we exposed one adult male Wistar rat to 1000 µg/ℓ and another to 2000 µg/ℓ, for 40 min. While exposures were in progress, the rats were not visible in the chamber because of the density of sodium combustion products. Although each rat appeared less active and less alert when removed from exposure, both returned to "normal" within 4 hr. Each rat was killed ≃24 hr postexposure and had no obvious lesions at necropsy. Microscopic examination of the respiratory tract revealed that each had moderately severe focal acute ulcerative rhinitis (turbinates) and that the rat exposed to 2000 µg/ℓ also had acute necrotizing laryngitis related to exposure. There were no exposure-associated lesions affecting the skin, trachea, lungs or gastrointestinal tract.

- **Inhalation Hazard to Uranium Miners**

This project will determine the specific biological effects of daily exposures to known levels of pathogenic uranium mine air contaminants, using both large and small experimental animal models of human respiratory disease. Lung cancer and deaths by degenerative lung diseases have reached epidemic proportions among uranium miners, but the cause-effect relationships for these diseases are based on inadequate epidemiological data. This project will identify the agents or combinations of agents and their levels which are responsible for severe respiratory tract pathology, including respiratory epithelial carcinoma, pneumonconiosis, and emphysema. Determination of actual absorbed radiological and chemical doses of inhaled materials is essential to establish cause and effect relationships.

BIOLOGICAL EFFECTS OF INHALED CIGARETTE SMOKE IN BEAGLE DOGS

Investigators:

B. O. Stuart, R. F. Palmer, R. E. Filipy, and G. E. Dagle

Technical Assistance:

W. Skinner, C. Petty, K. C. Upton, and D. Teats

A group of twenty dogs has received up to 7 yr of daily cigarette smoking (10 cigarettes per day, 5 days per week), using realistic methods of oral inhalation and nose-plus-mouth exhalation. Three dogs that received 20 cigarettes per day over 9 mo developed respiratory tract lesions, including pleural thickening, alveolar septal fibrosis, vesicular emphysema, and chronic bronchitis, more rapidly than dogs receiving 10 cigarettes per day.

These experiments (Table 3.26) were initiated to examine cause and effect relationships in the development of respiratory tract pathology as a result of lifespan daily inhalation exposures of a large experimental animal to radon daughters with uranium ore dust and cigarette smoking, both combined and separately, under conditions that closely simulate conditions of human exposure in uranium mines. This report will concentrate on effects of chronic cigarette smoking alone.

Beagle dogs were trained to accept daily smoking of 10 cigarettes (Groups 2 and 3) or to receive identical daily periods of sham smoking of unlighted cigarettes (Controls, Groups 1 and 4). Fresh smoke was inhaled using masks specifically designed to simulate human patterns of cigarette smoking; i.e., oral smoke inhalation and nose plus mouth exhalation. These dogs were not anesthetized or tranquilized during smoke exposures, and received their repeated daily

TABLE 3.26. Experimental Design

Group	Number of Animals	
1	20	600 WL Radon Daughters with Uranium Ore Dust (Carnotite) 15 mg/m³ with Sham Smoking
2	20	600 WL Radon Daughters with Uranium Ore Dust (Carnotite) with Cigarette Smoking
3	20	Cigarette Smoking
4	9	Controls, with Sham Smoking

inhalation of smoke in response to their individual respiration rates.

Carboxyhemoglobin levels in both groups of dogs that received daily cigarette exposures were markedly increased after smoking, with mean levels of 5 to 6% COHb, similar to those found in humans at these smoking levels, and apparently with less variability. As a possible additional index of smoke constituent deposition, plasma thiocyanate levels were determined. Mean values obtained from cigarette smoking dogs were nearly double those from control dogs or sham-smoking dogs inhaling radon daughters with uranium ore. Differences were not significant between presmoking and postsmoking levels for each group.

Minimal changes had occurred in the respiratory tracts of the sham-exposed control dogs that were examined. One control dog was sacrificed after 52 mo of sham exposure for comparison of histopathologic data with that from the large number of dogs from Groups 1 and 2 requiring sacrifice due to respiratory distress. The respiratory tract of this dog was generally normal in appearance. There were a few small foci of subpleural interstitial fibrosis with associated alveolar epithelial hyperplasia and metaplasia in the lungs. Those lesions are considered spontaneous, and are commonly found in older beagle dogs.

Pulmonary changes in three control dogs killed after 65 mo of sham exposure included slight subpleural vesicular emphysema in two, and slight focal mononuclear cellular infiltration in all three dogs. Lungs of all three dogs also contained slight to moderate degrees of subpleural interstitial fibrosis with associated alveolar epithelial hyperplasia and metaplasia. All three dogs had very slight degrees of basal cell hyperplasia, as well as slight glandular hyperplasia, in both tracheal and laryngeal mucosa.

In one dog from Group 3, killed after 49 mo of exposure, there was seen in alveolar macrophages a relatively small amount of exogenous brownish-yellow pigment, considered to be associated with cigarette smoking. Tracheobronchial lymph nodes contained large amounts of phagocytized exogenous yellow pigment in histiocytes. Pulmonary lesions in this dog included slight vesicular emphysema, and occasional foci of subpleural interstitial fibrosis with associated alveolar epithelial hyperplasia and metaplasia.

One dog from Group 3 died, after 60 mo of daily cigarette exposure, from foreign body pneumonia subsequent to vomition during smoke exposure. In lung sections, numerous alveolar macrophages adjacent to small blood vessels and bronchioles contained black pigment, probably particulate material from cigarette smoke. Slight dilation of bronchial mucous glands and a slight degree of subpleural vesicular emphysema were also present. Extensive inflammatory changes were seen, including numerous microgranulomata. These lesions are associated with cigarette smoking and have not been observed in the lungs from Group 1 dogs.

Three other dogs from Group 3 were killed after 65 mo of exposure to cigarette smoke. Moderate bronchiolitis in one dog was characterized by a mononuclear inflammatory infiltrate surrounding respiratory and terminal bronchioles, and extending into surrounding alveolar septa, forming an associated chronic alveolitis. The smoke-exposed dogs had an increased amount of phagocytized yellow pigment, primarily in peribronchiolar and perivascular areas. There was a tendency toward more subpleural vesicular emphysema in the smoke-exposed dogs than in the sham-exposed dogs. Focal interstitial pneumonitis, focal mononuclear cellular infiltration, subpleural interstitial fibrosis with associated alveolar epithelial cell hyperplasia, and focal calcification occurred in both smoke-exposed and sham-exposed dogs. The tracheobronchial lymph nodes of all three smoke-exposed dogs had lesions clearly related to treatment. Two dogs had moderate amounts of yellow pigment, apparently the same as the smoke-related pigment found in the lungs. Moderate reactive lymphoid hyperplasia in the tracheobronchial lymph nodes and moderate histiocytosis in the mediastinal lymph nodes of one smoke-exposed dog were probably related to chronic inflammatory changes in the lungs.

In an ancillary study, three dogs were exposed to smoke from 20 cigarettes per day for only 9 mo--double the dose rate of the dogs described above, and equivalent to four

packs per day smoked by man, as evidenced from comparative lung volumes, and measured COHb and nicotine levels. Pathology developed more rapidly in the respiratory tracts of these dogs. Focal areas of pleural thickening, alveolar septal fibrosis, and subpleural chronic inflammation were present in all three dogs (Figure 3.36). Vesicular emphysema (Figure 3.37), ranging in severity from very slight in one of the dogs to slight-to-moderate in another, was a feature of the lungs of this group of dogs; it was grossly visible in one dog. Two dogs had large areas of acute interstitial pneumonitis. Additional changes observed in the pulmonary parenchyma included numerous focal granulomata (Figure 3.38), which appeared to contain fat cells. Slight-to-moderate chronic bronchitis and bronchiolitis were present in the lungs of each of the three dogs (Figure 3.39), changes seen to a lesser degree in lungs of Group 3 dogs.

Lesions of the upper respiratory tract of the three 20 cigarette/day dogs included an ulceration of the tracheal mucosa in two cases, and focal, slight squamous metaplasia of the tracheal epithelium in all three dogs. A subepithelial inflammatory focus in the larynx was found in one of the dogs, although the surrounding epithelium was essentially normal in appearance.

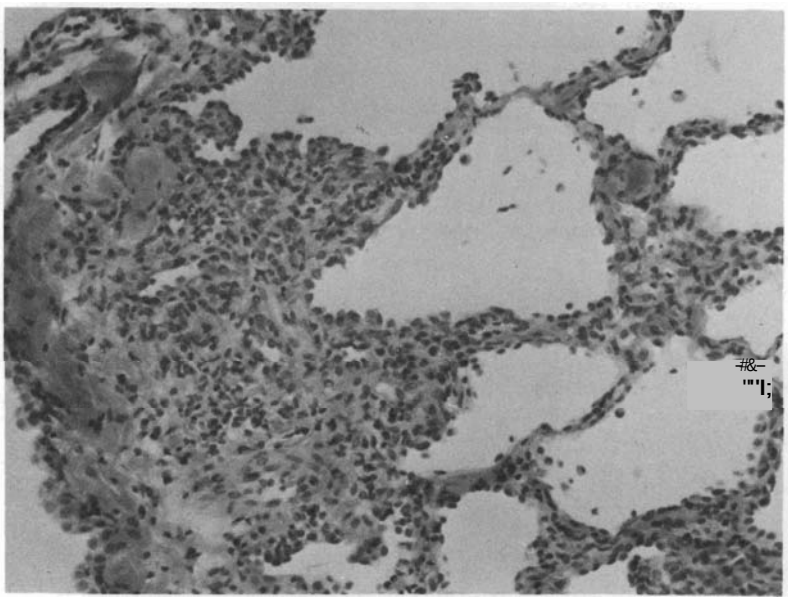

FIGURE 3.36. A Focus on Pleural Thickening, Subpleural Inflammation, Alveolar Septal Fibrosis, and Vesicular Emphysema, from a Dog that had Smoked 20 Cigarettes per Day for 9 Months. (H&E 200X)

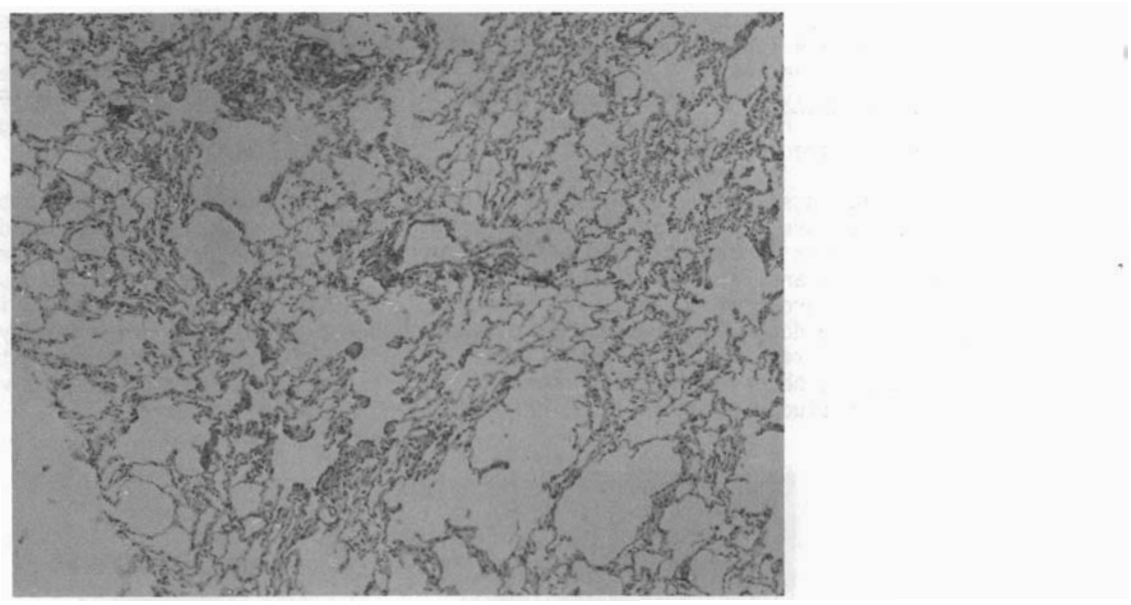

FIGURE 3.37. Vesicular Emphysema in a Section of the Same Lung Shown in Figure 3.35. (H&E 80X)

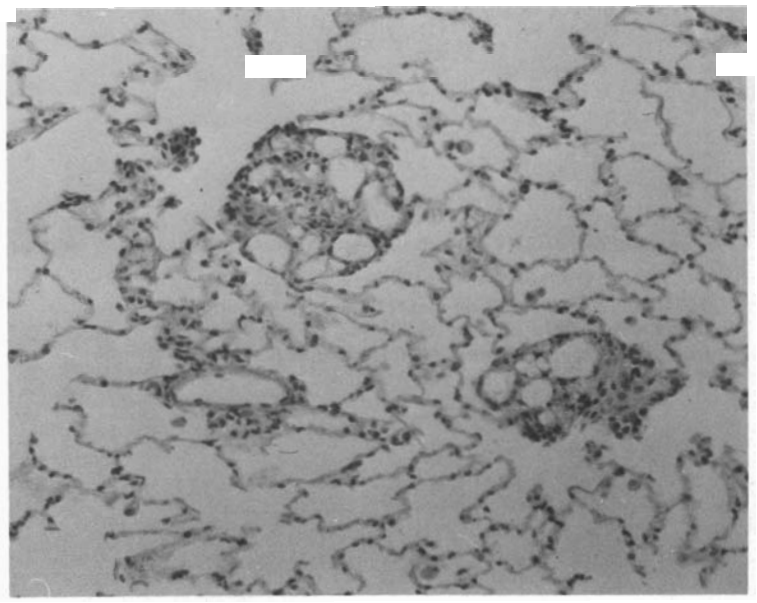

FIGURE 3.38. Focal Granulomata in a Lung Section from a Dog that had Smoked 20 Cigarettes per Day for 9 Months. (H&E 200X)

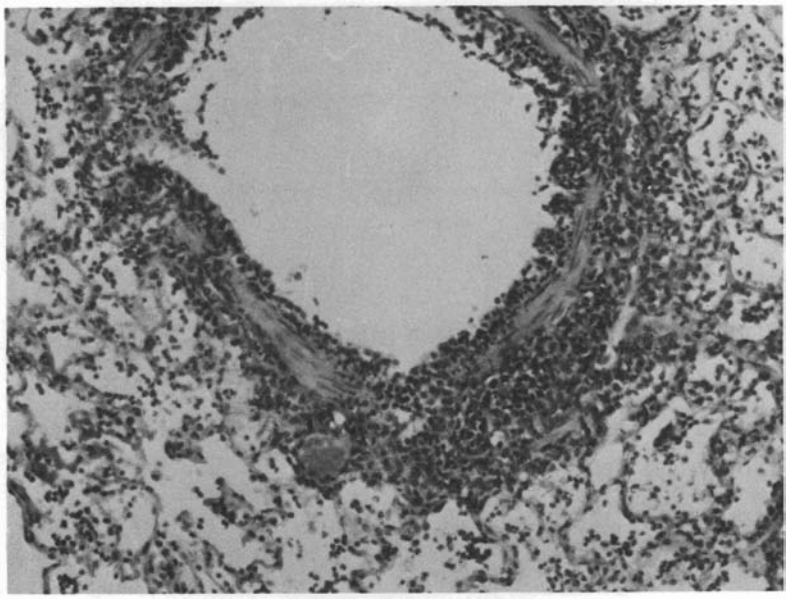

FIGURE 3.39. Chronic Bronchiolitis in a Lung Section from a Dog that had Smoked 20 Cigarettes per Day for 9 Months. (H&E 200X)

INHALED RADON DAUGHTERS AND URANIUM ORE DUST IN RODENTS

Investigators:

B. O. Stuart, R. F. Palmer, R. E. Filipy, and J. Gaven

Technical Assistance:

K. Mapstead

Male SPF rats are receiving daily inhalation exposures to radon daughters, with and without uranium ore dust. These studies will determine the dose rate dependence of pulmonary neoplastic or degenerative disease associated with inhaled radon daughters, and will define the possible physical, physiologic, or pathologic role of concomitantly inhaled aerosols of uranium ore dust.

Several studies are underway to determine the responsible agents (and their interactions) that cause respiratory tract carcinogenesis in uranium miners. These include studies described below, which exanine the influence of altered radiological dose rate and the physiologic or pathogenic role of uranium ore dust in neoplastic response.

Studies of altered carcinogenic and non-neoplastic response caused by inhaled radon daughters as a function of changing dose rate and total dose involve daily inhalation exposure of groups of male SPF Wistar rats to several concentrations (dose rates) and total doses (duration of exposures) of radon daughters. Epidemiological studies suggest that lung cancer in uranium miners is more prevalent following shorter, higher-level exposures, but this has not been shown in previous beagle dog studies. We have recently found that rats exposed to radon daughters at 900 WL[a] with ore dust for 15 mo at 30 hr/wk had a 10% incidence of pulmonary squamous carcinoma, but that rats receiving 900 WL with ore dust for 5-1/2 mo at 84 hr/wk showed 60% incidence of squamous carcinoma and adenocarcinoma (Table 3.27). Table 3.28 shows the protocol of current experiments, designed to test the hypothesis that shorter, more intense exposures to radon daughters with ore dust provide a significantly greater risk of developing lung cancer than do more protracted exposures (lower dose rate) accumulating the same total dose. If this hypothesis is disproved, and it is found that protracted exposures are more carcinogenic, uranium miners who are presently exposed at lower dose rates under a fixed limit of total exposure dose will be at greater risk of developing lung cancer than were those early miners whose cases were used to derive the present limits for uranium miner exposure.

In addition to the markedly increased risk of lung cancer (6-fold greater than normal incidence for age-correlated cohorts) in uranium miners, recent epidemiological studies have shown a 5.3-fold increase in uranium miner deaths due to chronic respiratory insufficiency, including pneumoconiosis, pulmonary fibrosis, and emphysema. These findings may be related to concomitant inhalation exposure to silica-bearing uranium ore dust present in mine air.

We have observed massive fibrosis and bullous emphysema, as well as respiratory tract neoplasia, in beagle dogs after 2 to 5-1/2 yr of daily exposures to radon daughters with uranium ore, with and without concurrent cigarette smoking; and in hamsters and rats following chronic exposures to radon daughters with uranium ore dust.

(a) WL = Working Level: any combination of short-lived radon daughters per liter of air that will result in a total alpha decay of 1.3×10^5 MEV.

TABLE 3.27. Incidence of Lesions of Hamsters and Rats Following Exposure to Radon Daughters With and Without Uranium Ore Dust.

	Exposure Conditions	Results Following Exposures[a]		
Croup 1		Nasopharnyx	Trachea	Lung
34 Hamsters	Laboratory Air Controls	N	N	N
32 Rats		N	N	N
Croup 2				
34 Hamsters	1200 Radon Daughters	34 Squamous Metaplasia	N	31 Slight Bronchiolization
		1 Squamous Carcinoma	5 Slight Hyperplasia	17 Slight Radiation Pneumonitis
32 Rats		32 Squamous Metaplasia	7 Squamous Metaplasia	32 Moderate Bronchiolization
		2 Squamous Carcinoma		16 Moderate Radiation Pneumonitis
				10 Adenomatosis
				2 Squamous Carcinoma
				1 Squamous Carcinoma and Bronchioloalveolar Carcinoma
Croup 3				
34 Hamsters	12 WL Radon Daughters with Uranium Ore Dust (Carnotite, 15 mg/m³)	14 Very Slight Squamous Metaplasia	N	32 Slight-Moderate Bronchiolization
				2 Extensive Fibrosis
				Adenomatosis
				Emphysema
32 Rats		26 Squamous Metaplasia	N	17 Squamous Carcinoma
				1 Adenocarcinoma
				1 Squamous Carcinoma and Adenocarcinoma

[a] N = normal

TABLE 3.28. Comparison of Dose Rate Versus Total Dose in Animals Exposed to Radon Daughters.

Group	Number of Animals	Exposure Regimen	Total Exposures, WLM
1	48[a]	900 WL Radon Daughters 15 mg/m³[b]	320/640
2	48	450 WL Radon Daughters 15 mg/m³	320/640
3	48	225 WL Radon Daughters 15 mg/m³	320/640
4	48	Controls	

[a] Six of these animals per group are sacrificed semiannually to assess developing pulmonary pathology, leaving 30 animals per group after 28 months, allowing a 0.96 probability of observing at least 3 neoplasms if the true incidence is 20% at 450 WL

[b] Concentration of uranium ore dust

We are testing the hypothesis that the presence of the ore dust may provide a physical or physiological interaction essential to pathogenesis by comparative carcinogenic studies using male SPF Wistar rats exposed to radon daughters with and without uranium ore dust. Our studies in uranium mines and using test chambers have shown that particle concentrations can be greatly reduced in the range of 10^6/cc to 10^5/cc without significantly altering the uncombined fraction (or attachment fraction) of radon daughters. This allows the study of the pathogenic role of the ore dust per se, without changing the physical behavior (hence deposition site) of the airborne radon daughters, as described in Table 3.26.

Pathology results from the first sacrifice schedule will be available in FY 1978.

TABLE 329. Role of Uranium Ore in Radon Daughters Carcinogenesis.

Croup	Number of Animals	Exposure Regimen	Total Exposure, WLM
I	48[a]	900 WL Radon Daughter 15 mg/m³[b]	310/1280
2	48	900 WL Radon Daughter 3 mg/m³[c]	320/1280
3	48	Controls	

[a] Six animals per group are sacrificed semiannually
[b] Concentration of uranium ore dust
[c] To determine the role of minimal ore dust levels while still maintaining very low fractions of unattached radon daughters, as found in present underground uranium mine operating conditions

- Toxicology of Krypton-85

This project is concerned with evaluating the biological effects of exposure to ^{85}Kr in rodents and larger animal species. Included are both short-term and chronic exposure studies to determine tissue distribution and retention kinetics for metabolic modeling purposes, as well as long-term biological effects, for purposes of defining the tissues at risk. Also included are dose-effect studies to determine tumorigenicity, teratologic potency, and capacity to induce changes in lung biochemistry, pulmonary function, and hematopoiesis.

DISPOSITION AND BIOLOGICAL EFFECT OF INHALED ^{85}Kr

Investigators:

D. H. Willard, J. E. Ballou,

H. A. Ragan, and A. J. Gandolfi

Technical Assistance:

H. S. DeFord, C. A. Shields,

S. L. English, and R. L. Music

Half-lives of approximately 5, 30, and 100 min were obtained for whole-body clearance of inhaled ^{85}Kr in beagle dogs. Analysis showed the highest partition coefficients in lungs, bone marrow and fat. Circulating blood elements were not lowered permanently after ^{85}Kr exposures.

Adult beagle dogs were exposed to ^{85}Kr atmospheres according to three different exposure regimens to determine total body retention kinetics, tissue distribution and hematologic effects due to ^{85}Kr irradiation of the lungs. All exposures employed a breathing mask with unanesthetized dogs sitting in a ventilated box separated by about 15 ft from the main source of ^{85}Kr to minimize external radiation exposure.

Tissue partition coefficients, calculated from the steady state ^{85}Kr concentration ($\mu Ci/g$) in tissues determined at death, divided by the ^{85}Kr concentration ($\mu Ci/ml$) in the exposure atmosphere, are shown in Table 3.30. The calculated dose rates for these tissues, if exposed to the unrestricted MPC_a level for ^{85}Kr (3×10^{-7} $\mu Ci/ml$) are also shown. The lung dose is highest since at the time of sacrifice, the lung volume was filled with the ^{85}Kr atmosphere. The value for pelt was inordinately low because the body was protected from external ^{85}Kr exposure. The high value for bone marrow is undoubtedly due to its high fat content. Lymph nodes represent a mixed sample of pulmonary, visceral, and systemic nodes. The only high values associated with the gastrointestinal tract were observed in the contents

TABLE 3.30. Partition Coefficients and Radiation Dose tor ^{85}Kr in Dog Tissues[a]

Tissue	Partition Coefficient μCi/g/μCi/ml	Tissue Dose for Chronic Exposure to MPCa, μrad/yr
Lung	0.477	599
Bone Marrow	0.254	319
Fat	0.205	258
Jejunum Content	0.137	173
Adrenals	0.130	163
Lymph Nodes	0.108	136
Ileum Content	0.094	118
Pelt	0.082	103
Pancreas	0.065	82
Thyroid	0.064	80

[a] Average of 6 dogs

of the jejunum and ileum. Compact bone had the lowest partition coefficient of 0.008. The results of this study do not confirm the high ^{85}Kr concentration found in the intestinal contents of rats exposed to ^{85}Kr atmospheres.

Breath samples were analyzed from three dogs at predetermined times after exposure to determine the rate of "washout" via respiration (Figure 3.40). Most ^{85}Kr is exhaled during the first 5 min after exposure, followed by a much slower removal process, reflecting the diffusion of ^{85}Kr from tissues into blood, then to lungs.

Using an array of 4 NaI crystals, total body retention of inhaled ^{85}Kr was measured in unanesthetized dogs, held in a fixed counting position. A typical retention curve for one dog (Figure 3.40) could be described as the sum of three exponentials, with half-lives of 2, 30, and 155 min. Average half-lives and standard deviation for 10 dogs were 5.2 ± 3.4, 31.2 ± 19, and 103 ± 38 min.

The hematologic effect of ^{85}Kr radiation of the lungs is of interest because studies with inhaled plutonium have described a dose-related leukopenia or lymphopenia as the earliest measurable biological effect. Inhaled ^{85}Kr radiation can be confined largely to the lungs since translocation from lungs to tissues is not appreciable (total body partition coefficient ∿ 0.1). Thus, studies with ^{85}Kr may help elucidate the cause of the radiation-induced blood changes seen with other forms of radiation.

Circulating blood elements of 6 dogs were counted before and after each of three consecutive exposures to inhaled ^{85}Kr, as summarized in Table 3.31. There were no significant differences between control and experimental values for lymphocytes, neutrophils, and monocytes in those dogs given a total of 1390 rad. Similar negative results were obtained with five consecutive exposures totaling 634 rad, or 13 exposures totaling 1640 rad.

Both blood and lung tissues were analyzed for hydroxyproline, noncollagenous amino acids and acid phosphatase after exposure to the ^{85}Kr regimens described above. There were no significant differences that could be attributed to ^{85}Kr inhalation.

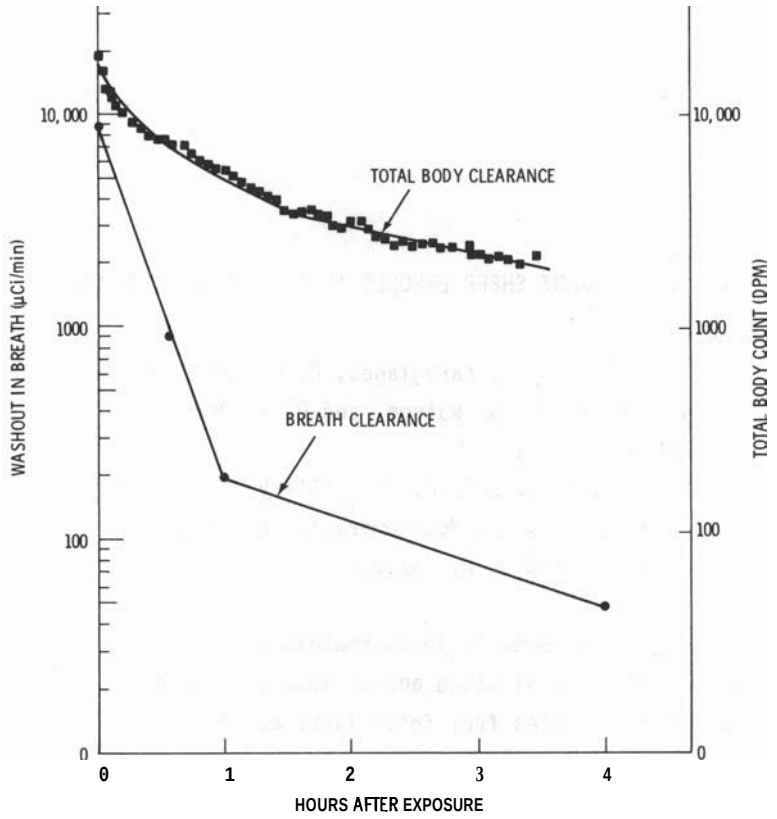

FIGURE 3.40. Clearance of Inhaled ^{85}Kr in the Beagle Dog

TABLE 3.31. Hematologic Effect of ^{85}Kr Inhalation and Sham Exposure[a]

Lung Dose, rad	340	Sham	512	Sham	538
WBC					
Before[b]	11.3	9.8	9.5	9.0	9.7
After	9.5	8.3	8.2	8.1	8.9
Neutrophils					
Before	7.12	5.49	5.89	4.41	5.79
After	6.56	5.64	5.74	5.59	6.30
Lymphocytes					
Before	3.62	3.80	3.14	3.96	3.57
After	2.57	2.32	2.13	1.94	2.23
Monocytes					
Before	0.11	ND[c]	ND[c]	ND[c]	ND[c]
After	0.10	0.08	0.08	0.08	ND[c]

[a] Values are average for 6 dogs, expressed as 10^3 cells/mm^3
[b] "Before" and "after" refer to the time blood was sampled, i.e., immediately before ^{85}Kr inhalation and 2 hr after exposure was terminated
[c] None detected

STUDIES IN PREGNANT SHEEP EXPOSED TO KRYPTON-85 ATMOSPHERES

Investigators:

F. D. Andrew, M. T. Karagianes, M. R. Sikov, J. E. Ballou, D. H. Willard, C. R. Watson, and P. G. Doctor

Technical Assistance:

J. O. Hess, H. S. DeFord, A. J. Clary, V. D. Tyler, L. F. Hensley, L. D. Montgomery, M. J. Conger, R. F. Myers, R. L. Music, and S. L. Owzarski

Inhalation exposure of pregnant ewes to approximately 50 nCi/ml ^{85}Kr in air resulted in equilibrium concentrations in maternal blood and in most tissues of approximately 1 nCi/g. Corresponding blood and tissue samples from fetal lambs at 94-123 days of gestation had generally similar values.

Investigations of absorption, tissue distribution, and retention kinetics of inhaled ^{85}Kr in the pregnant ewe and fetoplacental unit (FPU) were undertaken to provide quantitative data for determining the relative hazard to the fetus, which is known to be more radiosensitive than the adult. The results of this study in sheep will be supplemented with comparable data from rats, a species with marked differences in duration of pregnancy, in placentation, and in degree of maturity at term. These data will provide a basis for developing a model for estimating the likelihood of producing deleterious effects on the conceptus by inhalation of ^{85}Kr during pregnancy.

Maternal and fetal veins and arteries were cannulated 1-2 days before exposure of 14 gravid ewes (73 to 123 days of gestation). The ^{85}Kr atmosphere (50 nCi/ml) in air was administered via a face mask to nonanesthetized ewes for a period of 1.5-2.0 hr. Blood samples were collected for radioanalysis via the cannulas at intervals during accumulation, equilibration, and subsequent clearance periods. To minimize loss of ^{85}Kr, radioactivity was measured by liquid scintillation counting as soon as possible after removal of samples.

Mean values for five representative exposures are shown in Figure 3.41. Maternal and fetal blood concentrations attained equilibrium levels of approximately 1 nCi/ml at about 1 hr of exposure, regardless of sampling site. The apparent relative rates for reaching this steady-state value were such that maternal artery > maternal vein > fetal artery. The same order was seen in the clearance phase. Time required for concentrations to drop to 10% of maximum were approximately 9 min for maternal artery, 32 min for maternal vein, and 60 min for fetal artery.

One or 2 days after blood studies were completed, most ewes were re-exposed to ^{85}Kr and killed after attaining equilibrium to provide maternal and fetal tissue samples. The mean ^{85}Kr concentrations in adult tissues decreased in the order: lung > adipose (fat) > lymphoid > adrenal > liver = diaphragm = skeletal muscle (limbs) = kidney = ovary = small intestine > uterus > large intestine (Figure 3.42). With few exceptions, tissues from the 16 fetal lambs had similar concentration and were more uniform than those of adults. This high level of ^{85}Kr found in adult lung is artifactual, since the airway was occluded immediately after the last breath so that it contained the ^{85}Kr exposure atmosphere. The

fetal lung levels were not elevated over those of most other fetal tissues. Concentrations of ^{85}Kr in fetal fat from pericardial and subcutaneous sites were markedly lower than in adult fat. However, perirenal fat appeared to demonstrate a similar affinity for ^{85}Kr in fetal and adult tissues. The ^{85}Kr concentration in placental samples was significantly higher than in any of the fetal tissues, which was inconsistent with the concentration in the other elements of the FPU (membranes and amniotic fluid). We have no explanation for the elevated level of ^{85}Kr in sheep placenta.

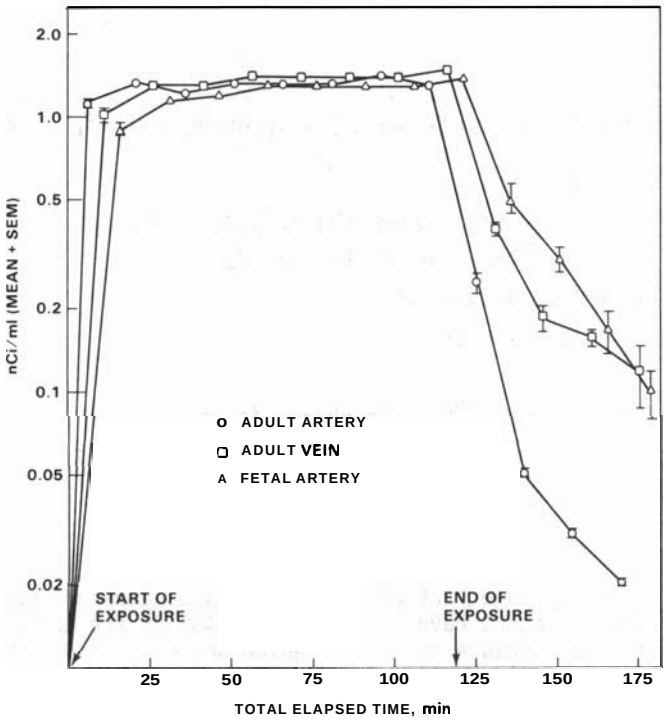

FIGURE 3.41. ^{85}Kr Concentration in Adult and Fetal Sheep Blood. Blood concentrations are expressed as nCi/ml (mean ± SEM) for 5 representative exposures during which samples were obtained from maternal arteries (0), maternal veins (□), and fetal arteries (A). Inhalation exposure to ^{85}Kr (50 nCi/ml in air) was limited to the first 120 min of the sampling period.

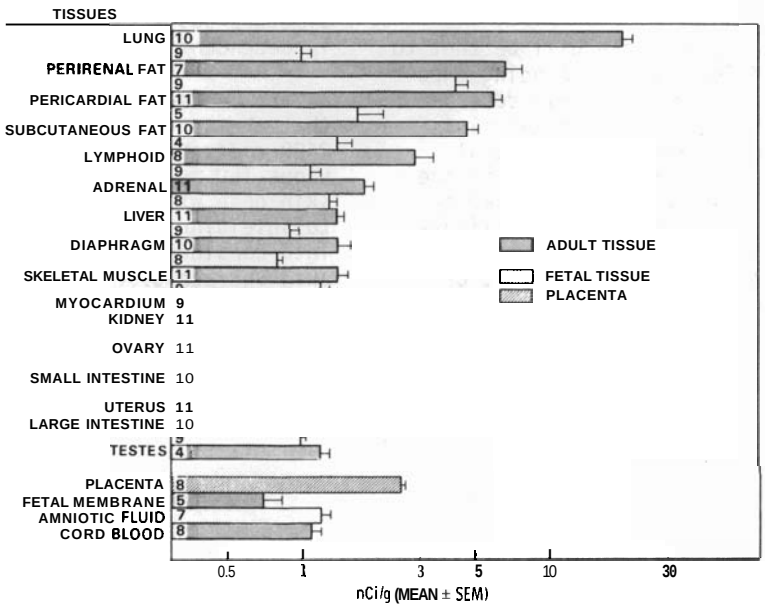

FIGURE 3.42. ^{85}Kr concentration in adult and fetal sheep tissues. Tissue concentration expressed as nCi/g (mean ± SEM) for most of the 14 ewes and 16 lambs exposed to ^{85}Kr (50 nCi/ml in air). The actual number of samples per tissue is indicated at the base of each bar.

PRELIMINARY STUDIES WITH CHRONIC KRYPTON-85 EXPOSURE CHAMBERS

Investigators:

H. S. DeFord, D. H. Willard, J. E. Ballou,

F. T. Cross, and W. R. Endress

Technical Assistance:

F. N. Eichner

Estimation of the skin dose from ^{85}Kr atmospheres is complicated by the nonuniform shielding effect of the animal cages and components of the cage rack. The extent of dose reduction due to shielding was estimated using thermoluminescent dosimeters.

Four 225-cu-ft lucite chambers, each accommodating a self-flushing animal cage rack of 20 cages housing five rats per cage, have been constructed for lifetime exposure of rats to ^{85}Kr atmospheres. Three levels of ^{85}Kr exposure and a control atmosphere will be maintained; the low-level chamber atmosphere will contain 3×10^{-5} μCi $^{85}Kr/cm^3$ air (100 times the present MPCa unrestricted value for ^{85}Kr); the midlevel and high-level chambers will have 10 and 100 times the ^{85}Kr concentration of the low-level chambers.

The highest radiation dose will be that to pelt that derived from the surrounding exposure atmosphere. Calculating this dose is complicated by the fact that the animal is partially shielded by the expanded metal sides of the cage and the components of the cage rack. This dose reduction imposed by shielding was measured using thermoluminescent dosimetry (TLD). Dosimeters were exposed, either shielded by the rat cages, or suspended in an empty chamber in the same relative positions as the caged dosimeters. The resulting reduction in shielded TLDs showed 43% of the empty chamber response, which was considered to be a measure of the dose reduction imposed by the cage and rack. It was estimated that the dose to the rat surface would be 1/2 the dose received by a dosimeter, since the dosimeter responds to dose from all sides. This was verified by exposing dosimeters fixed to the sides and top of simulated rats (horizontally positioned 500-ml beakers). The response from these dosimeters was also shown to be not significantly dependent on the orientation of the beaker.

From this information, we have estimated that the surface dose to a caged rat will be 2400 rad/year in the high-level chamber. Previous TLD measurements have indicated that the skin dose will be 83% of the surface dose due to shielding from the animal fur. Taking this into consideration, we have estimated that the skin surface dose in the high-level chamber will be about 2000 rad/year.

• Toxicity of Thorium Cycle Nuclides

The uranium-thorium breeder reactors proposed for nuclear power production, and other thorium fuel systems in conventional reactors, utilize fuels and fuel recycle process solutions that have not been evaluated for biological hazard. This project emphasizes studies of the metabolism of the oxide fuels and the nitrate solutions of the major radionuclides, following inhalation, ingestion or cutaneous application in rodents. The influence of specific activity, amount of radioactivity, and composition of various fuels and process solutions on the toxicology will be determined.

RETENTION AND TRANSLOCATION OF INHALED URANYL NITRATE (^{233}U and ^{232}U) IN RATS

Investigators:

J. E. Ballou, R. A. Gies, and N. A. Wogman[a]

Technical Assistance:

R. L. Music

Prelmininary data are reported for the clearance of inhaled $^{233}UO_2(NO_3)_2$ and $^{232}UO_2(NO_3)_2$ from the lung and their translocation to skeleton.

The experimental protocol and preliminary metabolic results for rats exposed to uranyl nitrate aerosols were described in the Annual Report for 1976. Additional results reported here for ^{232}U analyses in tissues supplement the earlier report.

Tissues from male Wistar rats sacrificed after exposure to $^{233}UO_2(NO_3)_2$ and $^{232}UO_2(NO_3)_2$ aerosols were analyzed by liquid scintillation counting (^{233}U) or with an anticoincidence-shielded Ge(Li) diode detector (^{232}U). Retention curves for major tissues (Figure 3.43) were analyzed to obtain parameters for estimating radiation dose and describing retention kinetics. Results suggest that lung and skeleton may be the major target tissues for biological effects following inhalation of the high-specific-activity uranium isotopes. Comparatively less uranium is translocated and retained in kidney; however, the kidney is known to be uniquely sensitive to uranium poisoning.

[a] Physical Sciences Department

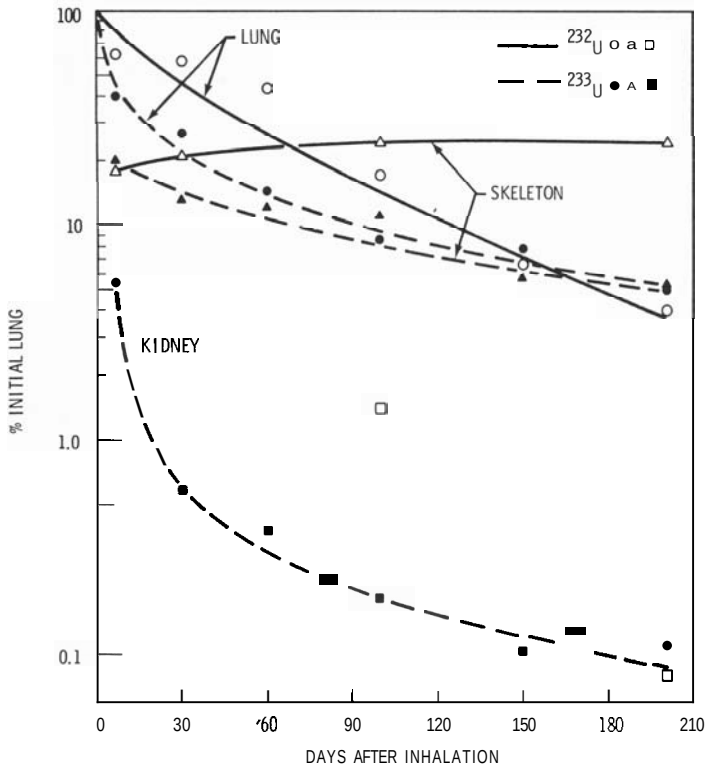

FIGURE 3.43. Retention and Translocation of Inhaled Uranyl Nitrate

LONG-TERM EFFECTS OF INHALED URANYL NITRATE IN RATS

Investigators:
J. E. Ballou, R. A. Gies,
G. E. Dagle, and R. L. Music

Rats exposed to graded doses of ^{233}U and ^{232}U nitrate aerosols have been on experiment 530 days. Approximately 20% of the animals have died, some with lung tumors; no bone tumors have been observed.

Male Wistar rats 60 days of age were exposed to graded doses of uranyl nitrate aerosols according to the protocol shown in Table 3.30, and held for life-span study of biological effects. Since the study has been in progress for only 530 days (approximately 20% mortality), only partial results are available.

Table 3.32 shows cumulative dose estimates for the uranium isotopes. These are somewhat different from earlier published estimates because more complete results are now available for the distribution and retention kinetics of the inhaled radionuclides. The distribution of the ^{232}U decay products has not yet been determined in sufficient detail to permit calculation of their contribution to the radiation dose. Preliminary results of decay product analyses suggest that the alpha dose to lung and skeleton may be increased

TABLE 3.32. Estimated Accumulated Radiation Dose to Rats Exposed to ^{232}U and ^{233}U Nitrate Aerosols

	Initial Lung Burden, nCi[a]	No. Rats	Estimated 500-day Accumulated Dose, rad		
			Lung	Skeleton	Kidney
$^{233}UO_2(NO_3)_2$	0.63	65	2	0.2	0.04
	10	65	35	3	0.6
	36	65	125	12	2
$^{232}UO_2(NO_3)_2$	0.74	65	5	0.7	0.07
	5.85	65	40	6	0.6
	53	65	350	50	5
Controls					
0.27N HNO_3		65			
Nontreated		45			

(a) Determined as the average of 5 rat lungs from animals sacrificed immediately after the 30-min nose-only inhalation exposure

by a factor of 2 or more when the alpha-emitting daughter products are taken into consideration. Early pathologic findings show lung tumors only in the high-level ^{232}U dose group. No bone tumors have been observed. Since the study is still in progress, the relative effects of uranium deposition in lung, skeleton and kidney cannot be evaluated. It is expected that lung and skeleton will be major target tissues, based on the dose estimates in Table 3.32.

DISPOSITION OF ^{232}U DECAY PRODUCTS FOLLOWING INHALATION OF $^{232}UO_2(NO_3)_2$ AEROSOLS

Investigators:

J. E. Ballou, R. A. Gies, and N. A. Wogman(a)

Technical Assistance:

R. L. Music

Uranium-232 is cleared more rapidly from the lung than its imnediate daughter product, ^{228}Th. More distant daughters in the decay chain (^{224}Ra, ^{212}Pb) accumulate principally in bone. Steady-state relationships among the decay products are apparently not established by 200 days postexposure.

Evaluation of the biological response to ^{232}U requires consideration of the radiation dose associated with the decay progeny. The decay chain includes seven alpha emitters (^{232}U, ^{228}Th, ^{224}Ra, ^{220}Rn, ^{216}Po, ^{212}Bi, and ^{212}Po) and beta-gamma emitters, including ^{212}Pb, ^{208}Tl and ^{212}Bi. The more significant internal emitter hazard is associated with the alpha-emitting radionuclides. This report describes work in progress to determine the amounts of the major decay products in tissues at the time of sacrifice. The short physical half-lives of several of the daughter products require immediate analyses, without chemical separations, to assure accurate estimation of the in vivo concentrations. Results are shown for analyses of fresh tissue samples, using an anticoincidence-shielded Ge(Li) diode detector system.

Results of analyses of rat lungs after inhalation of $^{232}UO_2(NO_3)_2$ aerosols are shown in Table 3.33. The ratio of Th/U in the aerosolized material was 0.03, representing a 30 day-ingrowth of ^{228}Th into ^{232}U. The Th/U ratio of 0.12 at day zero apparently results from preferential translocation of ^{232}U from the lung during the 30-min inhalation exposure period and the 5- to 10-min delay while the rats were removed from the chamber and killed. The Th/U ratio continued to increase with time after inhalation exposure, illustrating the greater mobility of ^{232}U compared to ^{228}Th. Others have observed a similar metabolic separation of uranium and thorium in the lung following inhalation of uranium ores. After 417 days the Th/U ratio in lung increased about 20-fold over the ratio in the starting material. Buildup of ^{228}Th through radioactive decay of ^{232}U would yield a ratio of 0.36, or only 12 times the starting ratio.

TABLE 3.33. Clearance of ^{232}U and ^{228}Th from Lung

Days After Inhalation	Radioactivity in Lung, dis/min		Ratio
	^{232}U	^{228}Th	Th/U
0	**117,500**	**13,500**	**0.12**
7	74,600	11,100	0.15
30	68,400	15,900	0.23
100	20,700	5,800	0.28
200(a)	3,400	1,500	0.44
417(a)	1,700	950	0.56 (0.36)(b)

(a) Value for one rat. Other values are averages of 5 rats
(b) (0.36) = ratio of Th to U expected from radioactive decay alone

(a) Physical Sciences Department

The distribution of ^{232}U and several decay products in lung, skeleton and kidney after 100 and 200 days postexposure is shown in Table 3.34. The amount of ^{232}U in the major tissues equaled or exceeded the amount of any individual decay product at these time points, as expected, since the starting material was only 3% equilibrated with ^{228}Th. After 100 days ^{224}Ra ($T_{1/2}$ = 3.64 days) should be in equilibrium with the immediate parent, ^{228}Th, however there is only about 1/2 the equilibrium level in lung and more than the equilibrium level in skeleton. The results suggest rapid clearance of ^{224}Ra from lung and translocation to bone, in agreement with the reported metabolism of this element. The value for ^{212}Pb in lung is difficult to predict, since one of the precursors is a radioactive gas, ^{220}Rn ($T_{1/2} \simeq 1$ min). Since ^{220}Rn is lost through expiration, we can assume that the value for ^{212}Pb in lung should be less than the value for ^{224}Ra, the immediate parent of ^{220}Rn. This is the case in lung but not in skeleton, where ^{212}Pb exceeds ^{224}Ra by a factor of 3. It is reasonable to expect greater retention of ^{220}Rn in skeleton because of the lower diffusion coefficient in compact bone. The value for ^{212}Pb is unexpectedly higher than the supporting precursor, ^{224}Ra, a finding for which we have no satisfactory explanation.

TABLE 3.34. Distribution of Major Decay Products in Lung, Kidney and Skeleton.

Tissue	Days After Inhalation	Radioactivity in Tissue, dis/min[a]			
		^{232}U	^{228}Th	^{224}Ra	^{212}Pb
Lung	100	20,700 ± 2,000	5,800 ± 300	2,380 ± 80	980 ± 100
	200	3,400 ± 600	1,500 ± 200	310 ± 60	260 ± 50
Skeleton	100	28,200 ± 3,000	5,400 ± 1,200	11,200 ± 1,800	34,000 ± 4,000
	200	28,000 ± 6,000	3,000 ± 1,400	4,400 ± 900	4,000 ± 800
Kidney	100	1,600 f 300	160 ± 60	44 ± 8	200 ± 50
	200	100 ± 80	100 ± 65	56 ± 10	42 ± 8

[a] Values are for one rat, with standard deviation based on counting statistics at each time point

- **Fetal and Juvenile Radiotoxicity**

Many of the biological parameters used to calculate permissible levels of exposure of adults to radioactive materials are inappropriate for the rapidly growing infant or child or for the pregnant female. These differences, when considered in conjunction with the greater intrinsic radiosensitivity of the immature organism, emphasize the need for more detailed information on the metabolism and toxicity of radionuclides in the prenatal and juvenile mammal. The objective of this project is, therefore, to obtain the information needed to establish appropriate exposure limits for the radionuclides of the greatest potential hazard to these age groups.

LONG-TERM EFFECTS OF PERINATALLY ADMINISTERED PLUTONIUM-239

Investigators:
M. R. Sikov, G. W. Zwicker,
J. O. Hess, and D. D. Mahlum

Prenatal, newborn, weanling, and adult rats were exposed to monomeric ^{239}Pu and studied until death or 30 mo of age. Histopathologic examination of the osseous lesions observed in these animals has now been completed, essentially confirming earlier indications that the younger rats were less sensitive on an μCi/kg basis, but more sensitive on the basis of total cumulative radiation dose to bone. The earlier observations of sites of bone tumor development relative to age also remains valid in terms of histologically confirmed tumors.

We previously described the protocol employed to study the long-term response of rats injected at various ages with ^{239}Pu citrate (Annual Report 1972). The alterations in median survival times produced by plutonium in the different age groups was compared (Annual Report, 1973), bone tumor incidences based upon gross observation were reported in relation to estimated radiation dose (Annual Report, 1974). Histopathologic examination of the osseous lesions has now been completed, resulting in some quantitative differences in the incidences presented earlier. Corrected incidence values for the various injected doses at the several ages are presented in Table 3.35. These data, based on approximately 50 rats per age-dose group, confirm earlier observations that when bone tumor incidence is expressed in terms of injected dose, sensitivity to bone tumor induction is inversely related to age at the time of injection. The only notable exception is in the case of those animals whose mother was injected with the highest dose during pregnancy and the offspring transferred to control mothers following birth.

Because of the age-related differences in the cumulative radiation dose, a markedly different picture appears when the incidence is plotted as a function of radiation dose

TABLE3.35. Influence of Age at the Time of Injection of ^{239}Pu on the Incidence of Histologically Confirmed Bone Tumors.

Croup Designation	Injected Dose, Ci/kg								
	0	0.3	1	3	6	10	20	30	60
Adult	0	10	37	60					
Weanling	2	4	23	39					
Newborn	4			15		18		17	
Prenatal	2				4		10		6
Cross-Fostered (in utero exposure)									27
Cross-Fostered (milk exposure)									3

(Figure 3.44). The exact relationships are dependent on the time interval for which the cumulative dose to bone is calculated. The weanlings appear to be more sensitive on the basis of the 2-yr radiation dose (although not when the 9-mo dose is used). The newborns show a rapid rise in incidence with increasing dose followed by a plateau; the newborn curves intersect the adult curves at about 500 rad. The prenatally exposed animals showed a rapid rise in incidence at the two lower doses but the incidence declined at the higher dose. The cross-fostered animals that were exposed in utero and nursed by control mothers showed a greater incidence of bone tumors than rats exposed to the same dose and kept with their mothers; in fact, the cross-fostered animals had the greatest incidence of any group in the lower dose range.

Although not yet completely quantitated, it is apparent that the incidence of non-neoplastic alterations of the skeleton (primarily osseous hyperplasia and exostosis) was elevated in the rats exposed prenatally. These lesions were also seen in the rats exposed to the higher doses at birth, although the increased incidence was not as striking.

The earlier reported age-related differences in the anatomical distribution of tumors has been substantiated using lists logically confirmed tumor data.

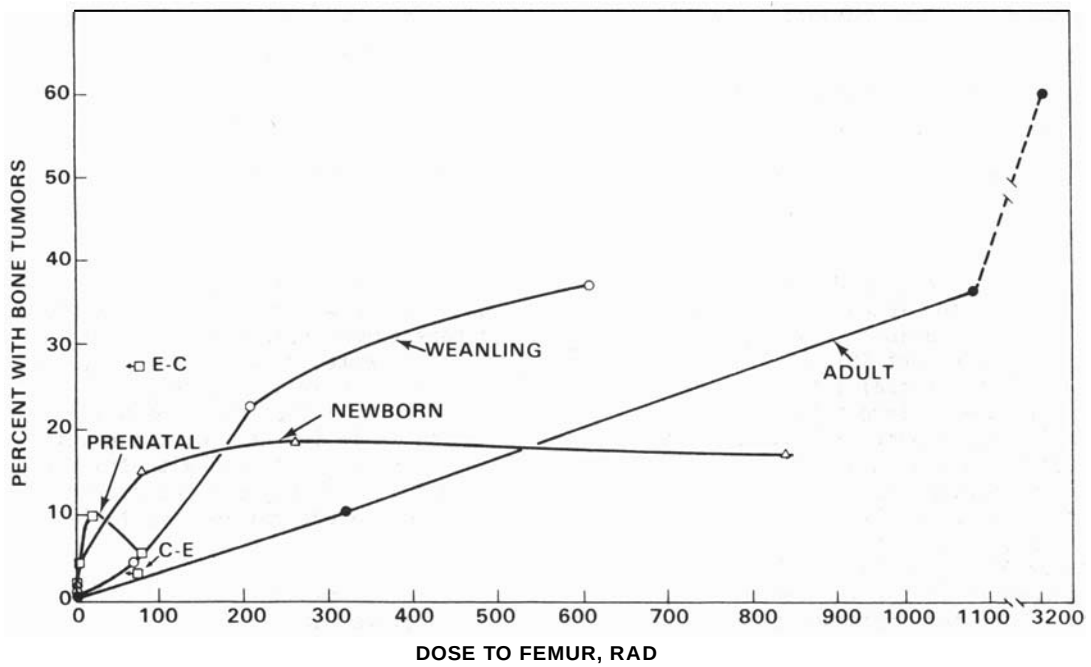

FIGURE 3.44. Bone Tumor Incidence Versus 24-Mo Radiation Dose

CROSS-PLACENTAL TRANSFER OF PLUTONIUM-239 IN GRAVID BABOONS

Investigators:

M. R. Sikov, F. D. Andrew,

R. L. Berstine, and D. D. Mahlum

Technical Assistance:

J. O. Hess, L. D. Montgomery, M. J. Kujawa,

R. F. Myers, and M. J. Conger

The crossplacental transfer of intravenously injected ^{239}Pu citrate and its distribution in the fetoplacental unit and the dam were studied in the baboon. Although there was marked variability because of the small numbers of animals used for each gestational age, the data are generally similar to those obtained in comparable experiments with rats.

A number of studies have been performed in this laboratory to investigate the cross-placental transfer of plutonium in the rat and its distribution within the fetoplacental unit, as well as the effects produced by such exposure. It has been consistently found that the concentration of plutonium in the fetoplacental unit was greatest in the fetal membranes with lesser concentrations in the placenta and in the embryo or fetus. To increase the confidence with which these data might be extrapolated to the human, studies have been performed in pregnant baboons, which have placentae similar to those of the human. In an attempt to obtain comparability of gestational ages, two baboons were studied at 22 and 23 days of gestation (comparable to the 9-day rat); two at 38 and 39 days, for comparison with the 15-day rat; and three at 106 days of gestation, as representative of the late fetus, rather than for strict comparability to the 19-day rat fetus previously studied.

Plutonium citrate solutions were filtered through 0.22-μm filters and a dose of 10 μCi/kg injected via the arm vein. The animals were kept in a restraining chair, blood and excreta collected, and a hysterectomy performed at 24 hr postinjection. Samples of uterus and the fetoplacental unit were obtained at that time and, except for one case, the mother was maintained for an additional 2–6 days to obtain adult tissues for analysis. The 106-day fetuses were dissected and tissue samples prepared for radioanalysis or autoradiography.

Concentration of Pu in the various components of the fetoplacental unit varied among the two or three animals studied at each time of gestation (Table 3.36). Nevertheless, the relative concentrations in the three major components were similar to those observed in the rat and were, in fact, quantitatively similar if previous rat data were normalized to the same injection dose used in the baboon. The autoradiographic distribution throughout the fetoplacental unit was also similar to that observed in the rat.

Because of differences in size and the small fraction of the dose entering the fetus it is difficult to compare the distribution in the fetus at 106 days of gestation with that in the dam. Accordingly, the data have been normalized by dividing the percent of the dose per gram of each organ, by the average body burden. This thus provides the organ concentration relative to the average

TABLE 3.36. Concentrations of ^{239}Pu (nCi/g) in the Fetoplacental Unit at 24 hr After Intravaneous Injection of 10 μCi/kg in Pregnant Baboons.

Days of Gestation	Structure		
	Placenta	Membranes	Embryo
22, 23	39, 69[a]	6.8,	30[b]
38, 39	7, 8	13, 67	0.52, 1.4
106	48-70[c]	39-148	0.09-0.41

[a] Individual values for the two fetoplacental units studied
[b] Combined membrane - embryo value
[c] Range of values for three fetoplacental units

concentration in the body (Table 3.37). The data for the fetuses are presented as means, and standard deviations have been calculated even though there were only three fetuses. The values for individual dams sacrificed at specific times, i.e., 3 and 7 days, as well as one which died at 1 day following hysterectomy, are shown. The mean value in the fetal liver is substantially less than that in the dams sacrificed at 3 and 7 days. The value in the baboon which died shortly after hysterectomy is probably aberrant, since the animal had hepatic pathology. The splenic values were substantially higher and the renal values slightly lower in the fetuses than in the dam. Skeletal values tended to

TABLE 3.37 Distribution of ^{239}Pu in 106-dg[a] Baboon Fetuses at 24 hr Postinjection and in Their Dams at Stated Times.[b]

	Fetuses	Dams		
		1 day[c]	3 days	7 days
Liver	2.1 ± 0.8	8.1	13.7	5.4
Spleen	7.5 ± 2.6	2.2	1.6	2.6
Kidney	1.3 ± 0.7	3.7	2.2	2.3
Femur	4.2f1.1	1.1	1.0	1.0
Calvarium	1.9 ± 1.3	0.3	0.4	0.7
Vertebrae (Lumbar)	2.1 ± 0.8	1.8	4.2	4.4
Rib (Calcified)	3.3 ± 0.8	2.0	1.7	0.7

[a] Day of gestation
[b] Values expressed as mean normalized concentration ± SD (see text) for fetuses and as individual normalized concentration for dams
[c] Died

be higher in some fetal bone (femur and calvarium) than those in the dam, although lumbar vertebrae and ribs had similar values in fetuses and dams.

The generally similar data obtained in comparable experiments with baboons and rats lends confidence to the extrapolation of these data to man.

Modifying Radionuclide Effects

Studies of radionuclide metabolism and effects have usually involved a single nuclide administered under optimally controlled conditions. People who may be exposed to radionuclides do not, however, live under such ideal conditions and it is important to define and quantitate some of the factors that may influence radionuclide metabolism and toxicity. Potentially important factors that have been identified for study include the effect of pregnancy and lactation, iron deficiency, alcohol ingestion, and protein deficiency.

ALCOHOL AND RADIONUCLIDE METABOLISM

Investigators:
D. D. Mahlum and J. O. Hess

The effect of ethanol administration on the deposition and retention of polymeric ^{239}Pu and ^{241}Am citrate has been studied in the rat. Only in the case of polymeric Pu was there an effect of alcohol administration.

Excessive use of alcohol can produce a number of physiologic disturbances, including alteration of liver function. Since the liver has an important role in the metabolism of a number of radionuclides, we have investigated the effects of alcohol administration on the metabolism of plutonium and americium.

In the first experiment, rats were fed either 12.5 or 25% ethanol in 25% sucrose solution for 1 or 6 wk. They were then injected intravenously with a suspension of polymeric ^{239}Pu, continued on their respective treatments, and six animals from each treatment group killed either 1 or 41 days later. The percent of the administered dose of ^{239}Pu deposited in liver, lung, and femur are shown in Table 3.38. At 1 day postinjection, the animals given ethanol for 6 wk before Pu injection appeared to have somewhat more ^{239}Pu in the liver than did controls, although the differences had disappeared by 41 days. Lungs of rats given ethanol for 6 wk had lower Pu values than controls. In contrast, animals which received ethanol for only 1 wk prior to Pu administration had an enhanced deposition of Pu at 1 day postinjection compared to controls. These differences were still apparent at 41 days postinjection. There was little effect of treatment on the deposition or retention of Pu in the femur.

The administration of ethanol in 25% sucrose did not result in gross damage to the liver. Two other experiments were therefore performed in which ethanol was administered without sucrose. In the first, 10% ethanol was fed to rats in drinking water for 2 or 8 wk. Americium citrate was then injected intravenously, treatment was continued, and animals were killed at 1, 7, or 28 days to obtain tissues for analysis.

Hepatic deposition of ^{241}Am was greater in females (60%) than in males (49%). In

TABLE 3.38. Distribution of Polymeric ^{239}Pu in Ethanol-Fed Rats

	% of injected Dose					
	Liver		Lung		Femur	
Treatment	1 day	41 days	1 day	41 days	1 day	41 days
Control	33.8 ±4.0(a)	32.8 ±1.0	19.4 ±4.8	13.0 k2.6	0.63 ±0.03	0.94 ±0.11
12.5% Alcohol (6 wk)	50.2 ±6.7	40.0 ±5.5	10.7 ±4.7	5.6 ±2.7	0.53 ±0.4	0.99 ±0.05
25% Alcohol (6 wk)	44.2 ±5.8	35.6 ±4.0	10.5 ±3.7	6.5 ±2.0	0.42 ±0.09	0.90 ±0.11
12.5% Alcohol (1 wk)	32.0 ±2.5	33.5 ±4.6	34.7 ±2.58	17.5 ±1.5	0.38 ±0.01	0.77 ±0.11
25% Alcohol (1 wk)	39.8 k2.8	31.4 24.4	26.3 ±1.4	19.7 ±2.6	0.60 ±0.05	0.77 ±0.11

(a) Standard error

contrast, the uptake of ^{241}Am by the kidney was greater in the male. However, the alcohol treatment did not influence the deposition or subsequent retention by liver, kidney, or any other tissue in either sex.

In the second experiment rats were given an acute dose of ethanol (5 mg/kg body weight) and injected with ^{241}Am citrate 24 hr later. Animals were killed at 1 or 14 days postinjection to provide tissues for analysis. Again, no effect of ethanol treatment on deposition or retention of ^{241}Am was found.

In contrast to these results, Cohen et al. (Progress Report, Institute of Environmental Medicine, NYU, 1977) have recently reported that alcohol increased fecal excretion of Am in the baboon at 90–150 days postinjection.

• Gut-Related Radionuclide Studies

This project is concerned with the behavior of radioactive materials of importance in the nuclear industry that may be ingested as a consequence of a reactor accident or of unavoidable occupational exposure, or after release to the environment and incorporation into the food chain. Current emphasis is directed toward evaluating hazards from ingested actinides as a function of animal age, animal species, or chemicophysical state of the radionuclide. This includes information on the disposition of nuclides that are ingested as particulates of various sizes or in combination with animal or plant tissue in which they become incorporated.

GASTROINTESTINAL ABSORPTION AND RETENTION OF PLUTONIUM-238 IN NEONATAL RATS AND SWINE

Investigator:
M. F. Sullivan
Technical Assistance:
L. S. Gorham and T. M. Graham

Neonatal rats gavaged with ^{237}Pu or ^{238}Pu retained a substantial quantity in gut mucosa for a week but absorbed only 2.9% of the ^{237}Pu. After 140 days the amount retained fell to half that initially deposited. Newborn swine also retained large amounts in the gut and absorbed about 40% of the dose.

Previous Annual Reports (1975 and 1976) reported data showing that intestines of newborn rats incorporated a substantial fraction of gavaged transuranic radionuclides and that most of that fraction was eventually excreted in feces. Similar observations were made in newborn swine after gavage with ^{106}Ru. Results of more recent experiments indicate that the behavior of ^{238}Pu in the swine GI tract is quite different from that of ^{106}Ru; a substantial fraction of the Pu stored in the gut mucosa is eventually absorbed.

Acid solutions of Pu (IV) nitrate were adjusted to pH 2 and administered either by gavage in a 1.0-ml volume to day-old pigs or by gavage in a 0.1-ml volume to 1- or 2-day-old rats. Two separate litters of swine were gavaged, one with a high dose (400 μCi/kg), and the other with a low dose (25 μCi/kg). The latter were bottle fed because their dam died during farrowing. At various intervals animals were killed and analyzed by wet-ashing and scintillation spectrometry to determine the location of retained radioactivity.

The distribution of ^{238}Pu in neonatal rats following gavage is shown in Table 3.39. At 3 days, 75% of the dose remained in the gut and only 1.18% was deposited in liver and

TABLE 3.39. Distribution of ^{238}Pu in Rats Gavaged with a Nitrate Solution at 2 Days of Age (Average ± SEM, from 5 to 11 Rates)

Age at Necropsy, days	Dose, μCi/kg	Content as Percent of Gavaged Dose				
		Skeleton	Liver	Intestine		Total Retained[a]
				Wall	Contents	
3	180	1.1 ± 0.07	0.16f0.004	58 ± 4	28 ± 5	1.2 ± 0.06
10	180	1.56 ± 0.1	0.21 ± 0.02	0.93 ± 0.11	1.7 ± 0.3	1.8 ± 0.1
20	180	1.66 ± 0.1	0.24 ± 0.01	0.03 ± 0.0	0.01 ± 0	1.7 ± 0.09
140	280	0.53 ± 0.03	0.027 ± 0.004			0.56 ± 0.03
140	110	0.65 ± 0.03	0.019 ± 0.002			0.67 ± 0.03

[a] Entire carcass, excluding GI tract and content

skeleton; at 10 days, only 2.7% remained in the gut, and there was only a small increase in deposition in liver and skeleton.

Whole-body counts of bottle-fed pigs did not decline as rapidly as those of the suckled pigs during the first few days because the former lost weight while adapting to the bottle. There was no difference between the groups in the percent of dose retained at the end of a week; 1 wk after treatment about one-fourth of the dose was still retained in the body, but very little of it remained in the gut. Distribution of absorbed ^{238}Pu (Table 3.40) shows that 15-25% of the gavaged dose was still in the gut of the high-dose, suckled swine at 10 days, while 51% was present in a bottle-fed animal that died at 3 days. About half the ^{238}Pu absorbed was deposited in the skeleton, and about one-fourth in the liver. Half as much of the gavaged dose was deposited in the liver of the high-dose, suckled pigs as was deposited in the liver of bottle-fed pigs. This could be related to the large difference in the Pu dose (400 vs 25 μCi/kg) or to the feeding regime.

From these results it appears that ^{238}Pu absorption from the GI tract of neonatal swine is much higher than in neonatal rats. Closure of the intestine to the passage of macromolecules occurs within a day after birth in swine, as it does in man; while for the rat, closure takes 3 wk. Further research with swine is essential to answer the many questions arising from these limited data.

TABLE3.40. Distribution of ^{238}Pu in Neonatal Swine Gavaged at 1 Day of Age

	Percent of Gavaged ^{238}Pu Dose					
Time of Necropsy, days	3	7	9	10	12	21
Dose, μCi/Kg	25	29	480	355	27	26
No. of Pigs	1	1	2	2	2	2
Tissue						
Skeleton	15	14			13 ± 1.4	16 ± 5.0
Liver	6.7	6.9	3.4 ± 0.25	3.45 ± 0.75	5.0 ± 0.6	6.4 ± 0.5
Muscle	4.7	5.1			4.0 ± 0.13	1.67 ± 1.32
Kidneys	0.62	0.43	0.15[b]		0.28 ± 0.01	0.23 ± 0.05
Spleen	0.20	0.15			0.14 ± 0.02	0.13 ± 0
Heart	0.15	0.05			0.06 ± 0	0.10 ± 0.01
Lungs	0.51	0.49	0.06[b]		0.48 ± 0.05	0.61 ± 0.11
Testes	0.04	0.02	0.02[b]	0.01	0.02[b]	0.04[b]
Lymph Nodes					0.65 ± 0.15	0.90 ± 0.19
Skin	3.3	2.2			1.4 ± 0.13	1.5 ± 0.02
GI Tract	51[c]	4.1	15 ± 0.9	27 ± 4.5	1.4 ± 0.19	0.79 ± 0.03
GI Content		1.6	9.1 ± 6.4	2.3	0.08 ± 0.05	0
Carcass[a]			75 ± 10	38 ± 13		
Total ^{238}Pu Retained (excluding GI tract)	31	30	79	41	26	29

[a] Entire carcass, excluding GI tract and contents
[b] Single measurements
[c] GI tract, including content

ABSORPTION OF TRANSURANIC NITRATES BY RATS, GUINEA PIGS, AND DOGS

Investigator:

M. F. Sullivan

Technical Assistance:

L. S. Gorham and T. M. Graham

Absorption of ^{238}Pu and ^{241}Am from the gastrointestinal tract was found to be quite similar for rats, guinea pigs, and dogs. Different oxidation state mixtures of ^{238}Pu nitrate (95% versus 65% Pu IV) were absorbed to about the same extent.

The 1976 Annual Report gives data on the absorption of alfalfa-incorporated ^{238}Pu by rats and guinea pigs. Continuing this program, directed toward determining the effect of dietary combinations with actinides on transport across the gastrointestinal (GI) tract, we have used guinea pigs (herbivorous) and beagle dogs (carnivorous) to study absorption of plant-incorporated actinides.

These studies were designed to compare actinide absorption from the GI tract of rats, guinea pigs and beagle dogs. Nitric acid solutions of ^{238}Pu and ^{241}Am were adjusted to pH 1.5 with NaOH, and either injected intragastrically into rats and guinea pigs or mixed in a 100-g bolus of meat and fed to dogs. All animals were maintained in metabolism cages, where urine and feces were collected separately. After necropsy all bones of guinea pigs and dogs treated with Pu were picked clean of tissue. All tissue and exreta were ashed and counted for radioactivity by scintillation spectrometry. Results are shown in Tables 3.41 and 3.42.

Absorption of ^{238}Pu did not differ appreciably among any of the species (Table 3.41). Absorption was somewhat higher in guinea pigs gavaged with 95% IV-valent Pu, as compared with 65% IV-valent Pu, but the opposite effect was observed in dogs suggesting that these differences may not be due to oxidation state. Twice as much americium as plutonium was absorbed by rats, but absorption by guinea pigs was about the same for both radionuclides.

Distribution of absorbed ^{238}Pu in dogs is shown in Table 3.42. Concentration of ^{238}Pu in testes was higher than in any tissue except skeleton. The large amount of plutonium in the muscle of the males was unexpected. Skeletons contained only 1/3 as much as muscle.

TABLE 3.41. Gastrointestinal Absorption of Transuranic Nitrates by Adult Rats, Guinea Pigs and Dogs

Radionuclide	Dose, μCi	Interval Until Sacrifice	Species	No. of Animals	Content as Percent of Administered Dose: Skeleton	Liver	Urine	Total
^{238}Pu(a)	5	7	Rat	21	0.010 ± 0.002(c)	0.001 ± 0.0002	0.018 ± 0.006	0.029
^{238}Pu(a)	7	3	Guinea Pig	10	0.011 ± 0.002(e)	0.008 ± 0.015	0.008 ± 0.002	0.027
^{238}Pu(b)	6	3	Guinea Pig	5	0.018 ± 0.004(e)	0.027 ± 0.012	0.010 ± 0.003	0.055
^{238}Pu(b)	300	3	Dog	2	0.007 ± 0.003(e)	0.0006 ± 0.001	0.028 ± 0.011	0.036
^{238}Pu(b)	300	3	Dog	4	0.002 ± 0.0004(e)	0.0005 ± 0.0001	0.21 ± 0.018	0.032
^{241}Am	4	7	Rat	11	0.014 ± 0.004(c)	0.003 ± 0.0005	0.044 ± 0.006	0.061
^{241}Am	5	3	Guinea Pig	9	0.006 ± 0.002(d)	0.008 ± 0.002	0.021 ± 0.004	0.035
^{241}Am	15	3	Guinea Pig	6	0.004 ± 0.001(d)	0.007 ± 0.001	0.006 ± 0.001	0.017

(a) 65% Pu (IV), as determined by TTA extraction
(b) 95% Pu (IV), as determined by TTA extraction
(c) Femur radioactivity x 23
(d) Femur radioactivity x 28
(e) Total skeleton radioactivity

TABLE3.42. Distribution of Gastrointestinally Absorbed Plutonium-238 in Dogs

	Percent of Ingested Dose, x 10^3 ISEM: Females(a)	Males(b)
Skeleton	7 ± 3	2.21 ± 0.50
Liver	0.65 ± 0.13	0.58 ± 0.08
Kidneys	0.04 ± 0	0.03 ± 0.01
Spleen	0.02 ± 0	0.02 ± 0.04
Lung	0.02 ± 0	0.03 ± 0.01
Adrenal	0.01 ± 0.02	0.001 ± 0.004
Testes	—	0.04 ± 0.02
Muscle	0.76 ± 0.41	6.49 ± 2.93
Blood		0.02 ± 0.01
Urine	28 ± 11	21 ± 18
Feces	96,000 ± 2,000	97,000 ± 24,000
Total Percent Recovered	96.5	97.5

(a) Two dogs, killed 4 days after ingestion of ^{238}Pu (65% IV-valent, as determined by TTA extraction)
(b) Four dogs, killed 3 days after ingestion of ^{238}Pu (95% IV-valent, as determined by TTA extraction)

ABSORPTION AND RETENTION OF INORGANIC AND ORGANICALLY INCORPORATED TECHNETIUM-95 BY RATS AND GUINEA PIGS[a]

Investigators:

M. F. Sullivan, T. M. Graham, D. A. Cataldo[b], and R. G. Schreckhise[b]

Technical Assistance:

L. S. Gorham, D. Stewart[c], T. McVey, and K. M. McFadden[b]

Transport of ^{95m}Tc, administered in both an inorganic and organically incorporated form, was measured across the gastrointestinal tracts of rats and guinea pigs. Absorption of Tc incorporated in either animal or plant tissue was about half that of inorganic pertechnitate administered by gavage. The form in which it was administered did not alter elimination rates. When Tc was administered to newborn rats by gavage, 50% remained in carcasses at 1 wk, mostly associated with the pelt, whereas only about 10% was retained by adults.

Technetium-99 (half-life = 2.1 x 10^5 yr, fission yield ≈ 6%) may become a major environmental contaminant from nuclear fuel cycles. The short half-life isotope, ^{95m}Tc (half-life = 60 days), was used to determine the absorption and excretion patterns of inorganically and organically incorporated Tc in adult and neonatal rats and in adult guinea pigs.

To determine the excretion and tissue distribution patterns of gavaged Tc, a nitrate solution of the pertechnitate, pH 6.6, was administered to twelve rats. Urine and feces were collected separately for 5 days. Five of the rats, fitted with external bile duct cannulae 24 hr earlier, were maintained in cylindrical wire-mesh restraining cages while bile was collected. Technetium distribution between urine, feces and bile is shown in Figure 3.45. Approximately 80% of the dose was excreted in the urine and feces during the first 5 days following ingestion of the Tc. The amounts were about equally divided between the urine and feces. Only about 8% of the dose appeared in the bile.

Twelve 2 day old rats and eight adult rats were gavaged with Tc and retention measured by whole-body counting. Single adult rats were killed at 1 and 2 days, while half the neonates were killed at 1 wk and the remainder at 3 wk to determine if the retained Tc was absorbed or if it remained within the gut mucosa. Ninety percent of the Tc was excreted by the adult during the first few days but 50% remained in the neonates at 1 week (Figure 3.46). At 2 wk after gavage, retention in both adult and neonatal rats was less than 10% of the dose.

Tissue distribution data are shown in Table 3.43. Most of the retained radioactivity in the adult and in the neonate was in the pelt, where it was probably associated with plasma protein. The gut of the neonate also contained a substantial quantity at 3 days postgavage.

Seven neonatal rats gavaged with Tc at 10 days of age were killed 5 hr later and fed to adult rats. Retention of ^{95m}Tc fed in this form was approximately half that measured in

(a) Supported by Waste Management funds.
(b) Ecosystems Department
(c) NORCLS

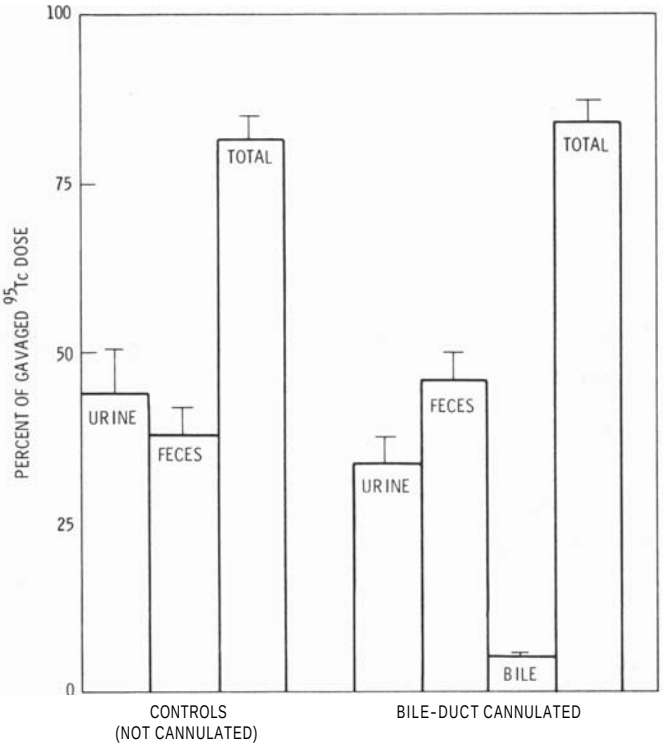

FIGURE 3.45. Five-Day Excretion of ^{95m}Tc by Bile-Duct Cannulated and Noncannulated Rats Administered Pertechnitate in a Nitrate Solution by Gavage. SEM is shown.

three rats gavaged with inorganic Tc. Fecal excretion of Tc was increased following feeding of neonatal tissues, suggesting that the organically incorporated Tc was not as well absorbed from the GI tract. By subtracting fecal Tc from the administered Tc dose in both groups we approximated the absorbed dose and calculated whole-body retention as a function of that dose. These data, shown in the upper curves in Figure 3.47, indicate no difference in the retention of inorganic or organically bound Tc.

The absorption of Tc from plant material was measured in groups containing eight rats and eight guinea pigs by feeding them soybean tissue containing incorporated ^{95m}Tc. Soybeans were grown hydroponically in a modified Hoagland's solution. They were transferred at 40 days to 450 ml of 0.5 mM $CaCl_2$ solution (pH 6.5) containing 5.6 µCi $^{95m}TcO_4^-$ (248 ng Tc). The nuclide was quantitatively accumulated by the plants in 72 hr. Shoot tissues were oven dried (60°C), ground, and pressed into 500-mg pellets.

Another group of eight animals were fed ground soybean shoots which were "spiked" with ^{95m}Tc in a nitrate solution. Whole-body retention data for rats are shown in Figure 3.48. There was little difference in the absorption and retention of Tc between "inorganic" and "spiked" groups. However, retention by the "organically incorporated" group was about 10 times less. Approximately 80% of the administered dose was excreted in the feces of the "organically incorporated" group, while only half that much appeared in the feces of the "spiked" or "inorganic" groups. When retention was considered as a fraction of the absorbed dose, there were no substantial differences among the three groups (Figure 3.48).

Similar results were obtained with guinea pigs (Figure 3.49). Despite the fact that guinea pigs are herbivores, they absorbed even less of the "organically incorporated" Tc than rats. Elimination rates were also faster in the guinea pigs. There appeared to be no difference in retention of the absorbed dose among three groups, each containing eight guinea pigs.

An experiment designed to evaluate effects of prompt or delayed treatment with DTPA showed that it was ineffective in removing Tc from rats.

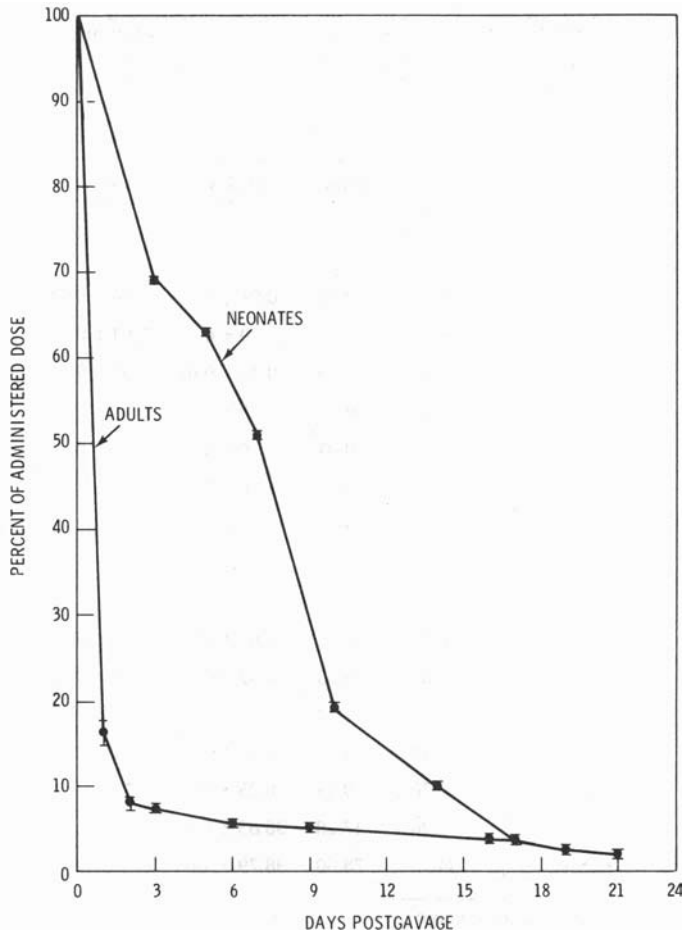

FIGURE 3.46. Whole-Body Retention of ^{95m}Tc in Adult and Neonatal Rats Following Gavage. SEM is shown.

TABLE 3.43. Distribution of Technetium-95 in Adult and Neonatal Rats Following Gavage (% of administered dose, $\bar{X}$ r SEM).

	Adults			Neonates
Tissue	1 day[a] (1)[b]	2 days (1)	14 days (5)	3 days (11)
Carcass				3.67 ± 0.29
Liver	0.49	0.18	0.04 ± 0.01	0.74 ± 0.03
Femur	0.01	0.01	0 ± 0	0.01 ± 0
Kidney	0.86	0.39	0.12 ± 0.01	1.56 ± 0
Spleen	0.01	0	0 ± 0	0.01 ± 0
Lungs	0.03	0.01	0 ± 0	0.05 ± 0
Heart	0.01	0	0 ± 0	—
Adrenals	0	—	—	—
Brain	0	—	0 ± 0	—
Ovaries	0.01	0	—	—
Thyroid	0.04	0.03	0.02 ± 0	0.06 ± 0
Gut	1.04	0.83	0.02 ± 0	16 ± 0.53
Blood	0.95	0.14	—	—
Pelt	4.53	1.11	3.33 ± 0.36	53.70 ± 2.45
Muscle	0.78	0.14	0.25 ± 0	—
Urine	5.20	17.20	36.83 ± 0.90	—
Feces	34	78.50	38.79 ± 1.68	—

[a]Time after gavage
[b]Number of animals in parentheses

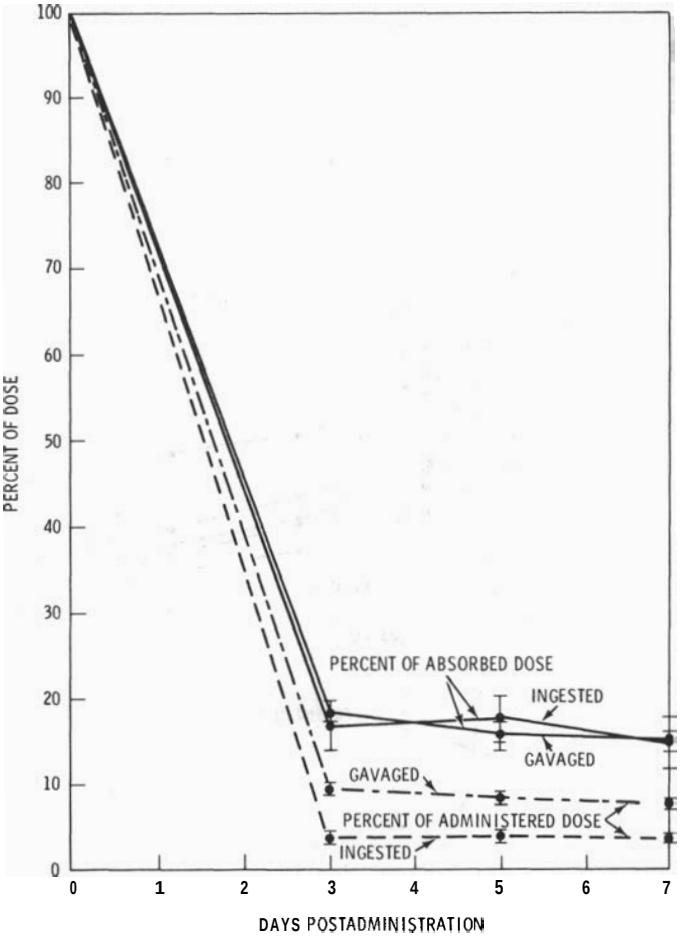

FIGURE 3.47. Whole-Body Retention of ^{95m}Tc by Adult Rats After Ingestion of Biologically Incorporated ^{95m}Tc or Gavage with a Nitrate Solution of ^{95m}Tc. Results are presented as percent of administered or absorbed dose. SEM is also shown.

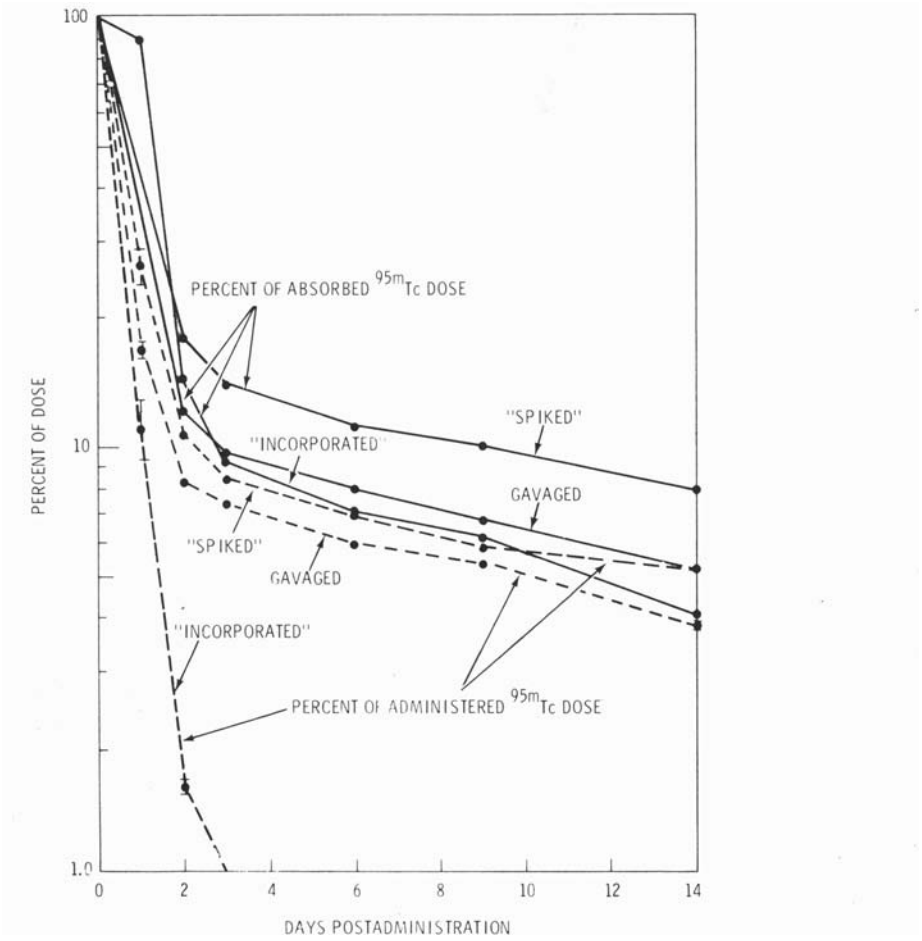

FIGURE 3.48. Whole-Body Retention of ^{95m}Tc by Rats Administered Soybean- "Incorporated", or Soybean- "Spiked", or "Inorganic-" ^{95m}Tc. Results are presented as percent of administered or absorbed dose. SEM is shown.

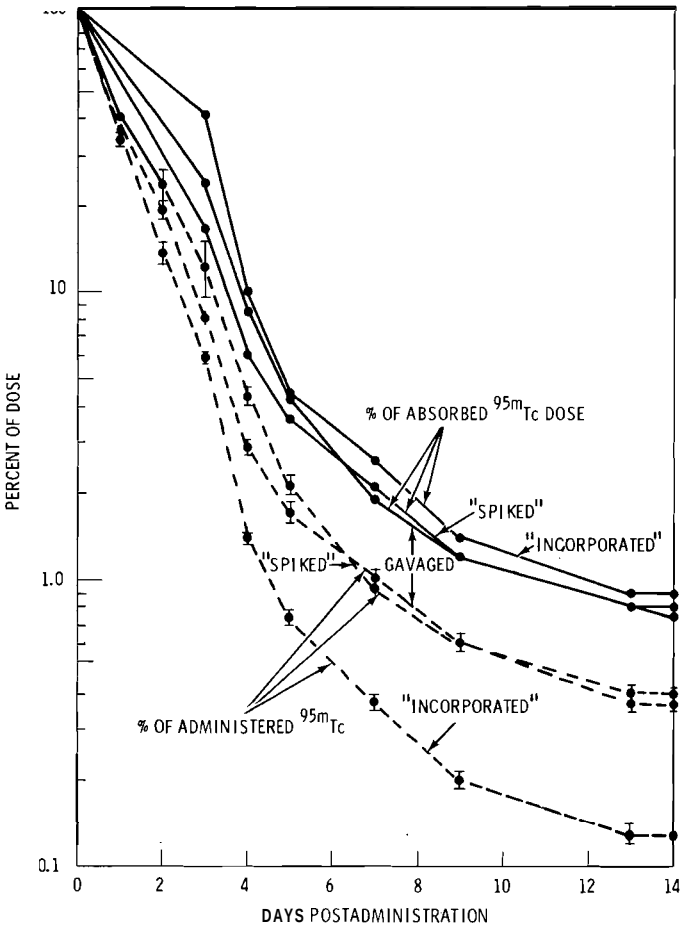

FIGURE 3.49. Whole-Body Retention of ^{95m}Tc by Guinea Pigs Administered Soybean- "Incorporated", Soybean; "Spiked", or Inorganic ^{95m}Tc. Results are presented as percent of administered absorbed dose. SEM is shown.

• Removal of Deposited Radionuclides

The objective of this project is to decrease the damage potential from inhaled, skin- or wound-absorbed, or ingested radionuclides. While primarily addressed to the needs for worker protection in the nuclear industries and laboratories, it also looks to the possible treatment needs arising from exposure of larger segments of the population. The approach is to develop methods that will prevent absorption, hasten excretion, improve decontamination, or alter translocation of the radionuclides--all for the purpose of minimizing radiation dose to sensitive tissues.

ACUTE TOXICITY OF INHALED Ca-DTPA TO THE RAT LUNG

Investigators:

V. H. Smith, G. E. Dagle, and H. A. Ragan

Technical Assistance:

R. A. Gelman

No lung pathology was observed in female rats 21 or 42 days after the one-time inhalation of Ca-DTPA at the estimated absorbed dose equivalent to that intravenously administered to man (HID). In contrast to a previous study, no emphysema was found attributable to the inhalation of 12 daily exposures to Ca-DTPA aerosols at 0.4, 0.8, 1.4, and 2.2 times the HID dose. There was a fivefold increase of incidence (compared to that in controls) of a low-grade (+1) histiocytosis in rats given the 12 consecutive exposures.

A previous test of the safety of inhaled calcium trisodiuni diethylene-triamine-pentaacetate (Ca-DTPA) (Annual Report, 1973) resulted in no lesions, except for a small incidence of what was called "transient emphysema". This term caused some confusion, since emphysema is not usually thought of as a reversible lesion. However, the data clearly showed that no emphysema was found in either rats or hamsters examined after a recovery period greater than 3 weeks. Because of the obvious advantages of the inhalation route in the prompt treatment of possible actinide exposures, and the lack of confirmatory findings by others of emphysema following Ca-DTPA inhalation, more data was needed on this point.

Female Wistar-strain, adult rats, 20/group, were exposed (total body) to aerosols generated from 10, 20, or 40% Ca-DTPA or 0.9% NaCl solutions. The treated and control groups are shown in Table 3.44. Aerosols typically had mass median aerodynamic diameters of 2.8 μm (σ_g 2.8 μm). Despite very dense, fog-like aerosols in the chamber (from Retec® Model 7301 nebulizers; maximum measured concentration, 2 mg Ca-DTPA/ℓ), the rats showed

TABLE 3.44. Summary of Ca-DTPA Inhalation Treatment and Various Control Groups (20 Rats/Groups)

Group	Nebulized Solution	Duration of Exposure, hr	Number of Exposures	DTPA Dose per Exposure[a]		Cumulative Ca-DTPA Inhaled,[c] mg/kg
				μmoles/kg	Relative to HID[b]	
Cage Control	None	None	None	0	—	—
Chamber Control[d]	None	4	12	0	—	—
Aerosol Control	0.9% NaCl	2	12	0	—	—
Single Dose	40% Ca-DTPA	2	1	28	~1.0	14
10% Ca-DTPA	10% Ca-DTPA	2	12	11	~0.4	69
20% Ca-DTPA	20%	2	12	24	~0.8	143
40% Ca-DTPA	40% Ca-DTPA	2	12	40	~1.4	239
High Dose	40% Ca-DTPA	4	12	63	~2.2	376

[a] DTPA dose absorbed from the rat lung based on measured aerosol concentration, minute volume of 0.1 ℓ/min, 30% retention of inhaled aerosol and average rat weights

[b] Hamster intravenous dose; 1 g Ca-DTPA/70 kg, 28.7 μmoles/kg

[c] The human lung weighs about 1000X the rat lung so converting these numbers to grams would represent an equivalent cumulative amount of Ca-DTPA in the human lung

[d] Rats were subjected to all exposure conditions except that no aerosol was created

no evidence of discomfort. Following each exposure the rats were washed with water to prevent Ca-DTPA being licked off the fur and contributing to the dose. Ten animals were sacrificed 21 days and 42 days following the last treatment. Lungs were weighed, then fixed at 25 cm H_2O pressure with Plumel's cacodylate fixative; their volumes were determined by the Archimedean displacement principle. Rats were weighed weekly. Blood samples for serum chemistry were taken 24 hr before sacrifice and for erythroid parameters at the time of sacrifice, as were bone marrow smears.

Rats from groups other than shelf controls and single-dose groups (Table 3.44) lost weight during the treatment period. The high-dose group rats lost an average of 20 g and did not recover weight equivalent to control rats' growth during the 8 weeks of the experiment; the other treatment groups lost less weight and recovered, essentially, to the control level. One high-dose group rat died 1 day after the 12th exposure but autolysis precluded necropsy examination.

Ratios of lung weights/lung volumes showed no significant differences among the various groups of rats. Erythroid parameters, serum chemistry measurements and bone marrow smears were normal in samples from 10 rats each from the 20% and 40% Ca-DTPA and the 0.9% NaCl groups, taken 6 weeks following their last treatment.

Histopathology found in the lungs of the animals is summarized in Table 3.45. There were no severe pathological lesions in any of the animals and only histiocytosis, characterized by the accumulation of histiocytes in alveoli, was found in higher incidence ($P = 0.02$) in the Ca-DTPA treated animals (27%) than in controls (5%). This lesion apparently was being repaired, since the greater incidence ($P = 0.05$) in rats killed 21 days following treatment (28%) was statistically different from the 10% for those killed at 42 days.

There was no difference in incidence of emphysema in control and Ca-DTPA treated groups. Two foreign body granulomas were associated with what appeared to be plant-like material, perhaps derived from food or bedding. There were no pathological consequences attributable to the one-time inhalation of Ca-DTPA.

TABLE 3.45. Incidence and Severity of Lesions in Lungs of Rats 21 and 42 Days Following Various Treatments

Lesion		Control Groups[c]			Incidence[b] in all Control Rats	Treatment Groups[c]					Incidence[b] in all DTPA-Treated Rats
		Cage Controls	Chamber Controls	Saline Aerosol Control		Single Dose	10% Ca-DTPA	20% Ca-DTPA	40% Ca-DTPA	High Dose	
Cellular Infiltration											
No. with Lesions	21 days	10	10	10		10	10	10	10	9	
	42 days	8	9	10	0.95	7	9	10	6	10	0.91
Grade[a]		(1.0)	(1.0)	(1.0)		(1.0)	(1.0)	(1.0)	(1.0)	(1.3)	
Fibrosis											
No. with Lesions	21 days	7	10	10		10	7	10	10	10	
	42 days	7	10	10	0.90	6	9	10	10	10	0.92
Grade		(1.1)	(1.2)	(1.4)		(1.1)	(1.1)	(1.6)	(1.4)	(1.8)	
Histiocytosis											
No. with Lesions	21 days	0	2	1		0	2	4	5	8	
	42 days	0	0	0	0.05	0	1	3	3	1	0.27
Grade		(—)	(1.0)	(1.0)		(—)	(1.0)	(1.0)	(1.1)	(1.1)	
Emphysema											
No. with Lesions	21 days	0	2	1		0	1	2	1	0	
	42 days	0	2	4	0.15	0	0	4	3	4	0.15
Grade		(—)	(1.5)	(1.4)		(—)	(1.0)	(1.0)	(1.0)	(1.2)	
Foreign Body Granulomas											
No. with Lesions	21 days	0	0	0		0	0	0	0	0	
	42 days	0	0	0	0	0	0	0	1	1	0.02
Grade		(—)	(—)	(—)		(—)	(—)	(—)	(2.0)	(1.0)	

(a) Average grade of lesion = lesion grades/number of rats with lesion. Lesions were ranked 1 = very slight, 2 = slight, ...5 = very severe. No lesions were found deserving a grade designation >2 in this study. One rat in High Dose group died but was not examined

(b) Fraction of rats among all control or among all treated rats with lesion

(c) See Table for dose and treatment information

REMOVAL OF PLUTONIUM FROM THE NEONATAL RAT

Investigators:

V. H. Smith and M. F. Sullivan

Technical Assistance:

R. A. Gelman and L. S. Gorham

Plutonium bound to neonatal rat gut was readily mobilized by Ca-DTPA. A single dose of Ca-DTPA, 7-10X the usual human intravenous dose level (HID = 28.7 μmol/kg), given by gavage 2 hr after 2-day-old rats received 1.46 μCi $^{238}Pu(NO_3)_2$ by gavage, lowered Pu bound to the gut by 82% as compared to untreated animals. Rats similarly treated 5 days after gavage with 1.89 μCi ^{238}Pu lost a similar amount (85%). Prompt treatment with Ca-DTPA reduced Pu in most tissues to one-third and delayed treatment reduced Pu to one-half, compared to control tissue content. The two treatment routes (gavage and intraperitoneal) were comparably effective except that removal of Pu from the skeleton, as represented by femur levels, was greater by the parenteral route.

More plutonium (100X) is absorbed from neonatal than from adult rat gut, with a large fraction of the administered dose retained for at least a week in the small bowel. The plutonium is primarily incorporated in mucosa, and most is gradually excreted with feces; some is absorbed into the body. DTPA is poorly absorbed from the gut of adult rats and does not readily cross cell membranes. Administration of DTPA by gavage or injection might indicate whether Pu is tightly bound to neonatal gut (inaccessible for chelation), as well as providing data on the effectiveness of DTPA in removing Pu from the neonatal rat.

Rats from two litters (average weight 10 g) were used in each part of the experiment. At 2 days of age the rats in the first part of the experiment received 0.10 ml, and those in the second part 0.05 ml, of a pH 2 solution of $^{238}Pu(NO_3)_4$. Radionuclide dose to rats in each group was 146 and 189 μCi/kg, respectively. In the first (prompt treatment) part of the experiment 0.287 mmol/kg Ca-DTPA in 0.1 ml solution was given 1 hr after the Pu by either gavage or intraperitoneal injection. In the second (delayed treatment) part of the experiment 0.2 mmol/kg in 0.05 ml of solution was similarly administered 5 days after the Pu. Rats were killed 6 or 7 days after Pu administration. Tissues were removed for separate radioanalysis. The Pu found in the head and remains primarily represent that in bone, although as analyzed they still contained some muscle, skin, and a few glandular elements. The femur was cleaned of tissue before analysis. Nitric acid digestion was used to prepare tissues for alpha assay by scintillation counting procedures.

Typically, treated and control rats gained about 11 g from the time of Pu administration until sacrifice. Promptly administered Ca-DTPA decreased Pu in or on the gut 6-fold, and delayed treatment decreased it 9-fold, regardless of route of administration (Figure 3.50). Less Pu was retained in gut contents at sacrifice when the DTPA was gavaged. As is the case with adult rats, prompt treatment was more efficacious by factors of 3 and 2, respectively, than delayed treatment for removing or preventing deposition in bone and soft tissue. Prompt treatment mainly reduced the quantity of Pu deposited in tissues without affecting distribution, while

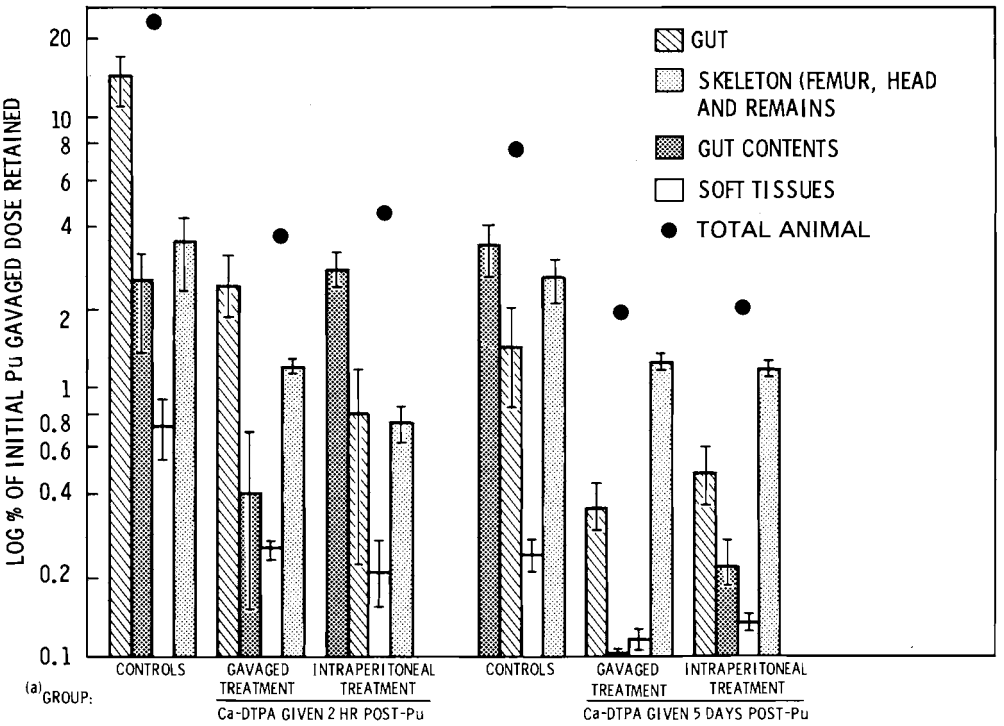

(a) SEE TABLE 1 FOR DOSAGE INFORMATION ON TREATMENT GROUPS.

FIGURE 3.50. Retention of Gavaged Pu in Nontreated (Control) or Ca-DTPA Treated Neonatal Rats. Retention measured 5 days after Pu administration and at 7-8 days after birth.

delayed treatment resulted in greater assymmetric removal of Pu from tissues, giving a different Pu distribution pattern from that in control rats (Figure 3.51). The change in Pu distribution from the pattern in control rats is likely due to the greater resistance to DTPA chelation of Pu already tightly bound to bone.

Effectiveness of treatment, in terms of retention of Pu compared with control tissues, is shown in Figure 3.52. Except for the greater degree of removal of Pu from skeleton with delayed treatment (represented on the figure by the bars for femur, head and remains) and about a 50% greater removal from gut, the results are quite similar to those observed in adult rats. DTPA-chelated Pu would be expected to be more lipid-soluble than more highly charged inorganic forms. The 100% increase in content of the brain of promptly treated rats compared to control rats suggests the chelon carried Pu into that organ. However, when treatment was given 5 days after the Pu, Pu was removed from the brain.

As with adult rats, DTPA treatments resulted in only minor changes in concentration of Pu in kidneys. Concentration ($\bar{x} \pm s_{\bar{x}}$) after prompt treatnient was 7.3 $\pm$ 1.1 μCi/g; after delayed treatment, 3.2 $\pm$ 0.41 μCi/g. This was statistically indistinguishable from Pu concentration in control rat kidneys of 9.2 $\pm$ 2.2 and 4.0 $\pm$ 0.62 μCi/g, respectively. Concentrations in kidney after treatment were the highest of the soft tissues examined, equivalent to concentrations in the femur.

The equally effective oral and parenteral DTPA treatments for removal of Pu from neonatal rat gut demonstrate that Pu is loosely bound to the mucosa, is readily chelatable and then excreted. The neonatal rat gut may permit more facile DTPA absorption than that of the adult where the removal of Pu caused by parental and oral treatments is markedly better by the former route.

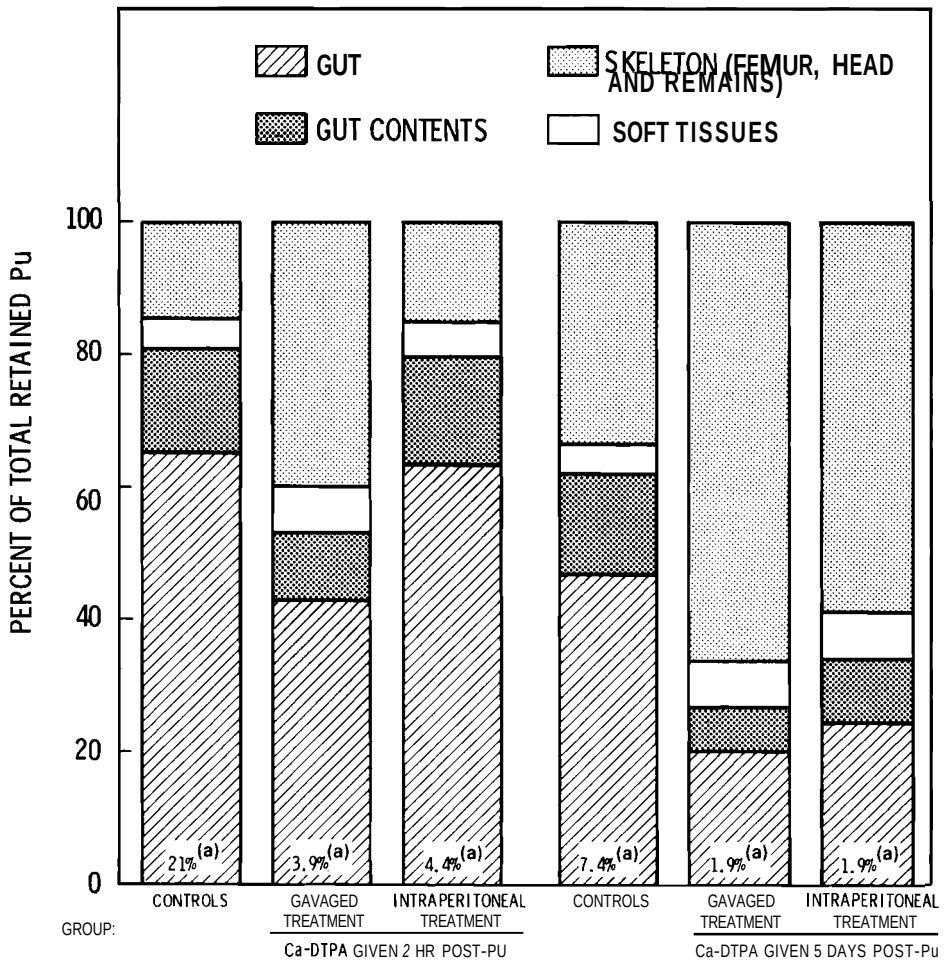

FIGURE 3.51. Distribution of Retained, Gavaged Pu in Nontreated (Controls) and Ca-DTPA Treated Neonatal Rats. Pu distribution determined 5 days after Pu administration and at 7-8 days after birth.

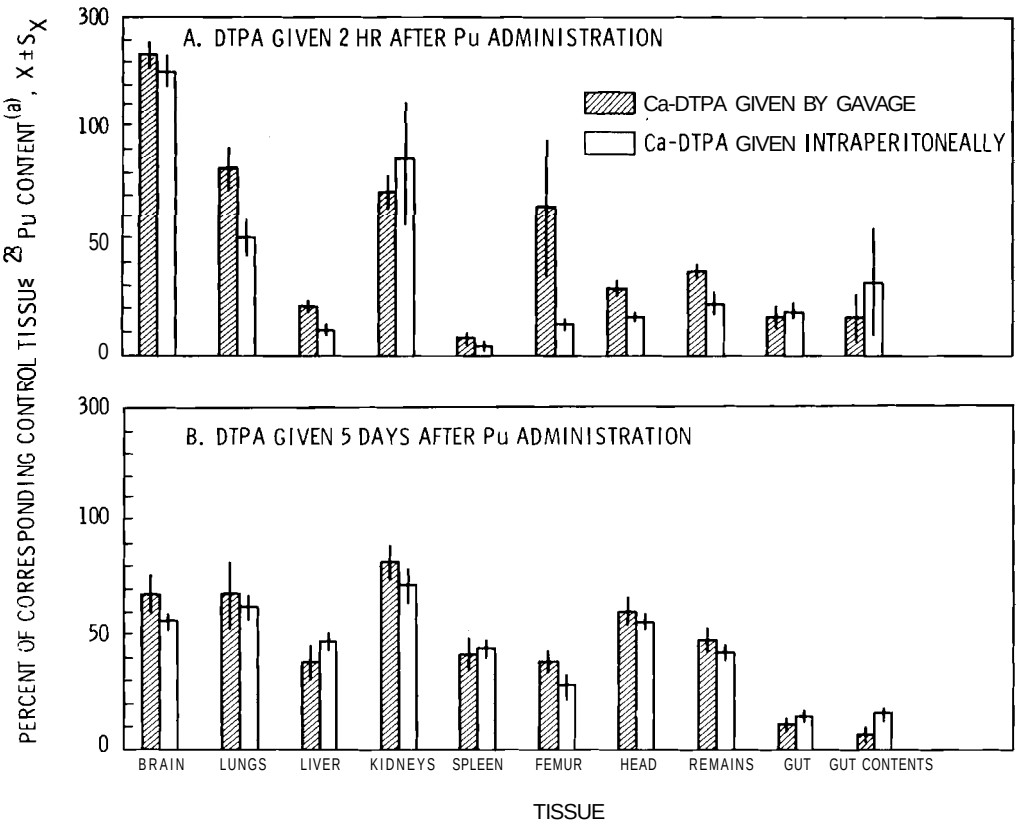

(a) THE SCALE ON THE ORDINATE IS COMPRESSED 4 FOLD ABOVE 110%

FIGURE 3.52 Effects of DTPA Treatments on Plutonium Content of Neonatal Rat Tissues Relative to Comparable Control Rat Tissues.

• Viral and Radiation Carcinogenesis

The studies included under this project are concerned with basic biological and biochemical indices that may aid in the detection and understanding of the primary effects of radiation insult and the initiation of the observed malignancies. A primary objective is to determine the role of virus in "radiation-induced" malignancies and in the process to identify those changes (biochemical, virological, immunological, etc.) which might serve to monitor the oncogenic process. Specific efforts include studies of leukemia induced by the B-emitter ^{90}Sr, and lung and bone tumors induced by inhalation of the a-emitters ^{238}Pu and ^{239}Pu.

RADIATION-INDUCED MALIGNANCIES IN BEAGLES: STATUS OF VIRUS STUDIES

Investigators:

M. E. Frazier and M. J. Hooper

Technical Assistance:

T. K. Andrews and B. B. Thompson

In the 1975 Annual Report we reported DNA polymerase activity with the properties of viral reverse transcriptase in tumor tissues from beagles with plutonium-induced bone tumors, but not in lung tumor material. Since then we have examined additional samples from unexposed dogs, from plutonium-exposed dogs without tumors and from plutonium-exposed beagles with tumors.

To be considered a virus-like DNA polymerase, the material investigated in these studies had to be present as a cytoplasmic particulate fraction of the size (50S-90S) and buoyant density (1.14-1.16 g/ml) of known oncornaviruses. If this condition was met, the RNase sensitivity of the DNA polymerase was monitored by following the kinetics of incorporation of ^{3}H TTP into acid-insoluble product. The RNase had to inhibit at least 50% of the incorporation of ^{3}H TTP when compared to the control reaction carried out in the absence of RNase. In addition, synthesis of an acid-insoluble material must require a divalent cation (Mg^{++} or Mn^{++}) and all four deoxyribonucleotide triphosphates (dATP, dGTP, dCTP and TTP). The product of this polymerase was then subjected to analysis on a glycerol velocity gradient to determine the size and nature of the labeled product, and whether the newly synthesized ^{3}H DNA was bound to a high-molecular-weight RNA. By including the appropriate controls this test simultaneously detected the high molecular weight RNA component and the DNA polymerase activity.

A further analysis of the product of the virus-like DNA polymerase was carried out using cesium sulfate density gradients. This analysis of the untreated reaction product and the product following heat denaturation, sodium hydroxide denaturation, or partial digestion with RNase provided proof that the product of the reaction mixture was ^{3}H DNA. These experiments also showed the newly synthesized ^{3}H DNA was associated with an RNA molecule. Such a finding implicates a virus-like reverse

transcriptase in the formation of the observed ^{3}H DNA:RNA hybrid molecule. Results of these studies are summarized in Table 3.46.

Results to date show that a retrovirus is associated with plutonium-induced bone tumors. The retrovirus continues to be produced in vitro by cell cultures established from bone tumor tissues. Retrovirus and/or virus-like DNA polymerases have not been found in normal tissue samples, or in plasma samples from plutonium-exposed or control animals. Likewise, no polymerase activity has been detected in plutonium-induced lung tumors, However, experiments with cell cultures prepared from plutonium-induced lung tumors have revealed the presence of a virus-like DNA polymerase associated with a cytoplasmic particulate fraction having a buoyant density of 1.20-1.18 g/ml. The higher density of these particles may indicate an endogenous retrovirus with a B-type (analogous to mouse mammary tumor virus) or D-type (similar to Mason Pfizer monkey virus) morphology.

In addition to kinetic analysis, simultaneous detection tests, and tests with cesium sulfate gradients, we have carried out an in vitro labeling study of canine lung tumor cell cultures with ^{3}H uridine. In these experiments a ^{3}H RNA component coincides with the peak of endogenous virus-like DNA polymerase activity in the 1.20-1.18 g/ml region of the density gradient. While experiments have ruled out the possibility of mycoplasma contamination there is still the possibility that these cells were infected by an exogenous retrovirus. Electron microscopic evaluation of these preparations is in progress.

TABLE 3.46. Association of Virus-Like DNA Polymerase with Radiation-Induced Malignancies in Beagle Dogs.

Status of Animal	Tissue	Kinetic Analysis	Simultaneous Detection	Cs_2SO_4 Analysis	Electron Microscopy
Unexposed	Lung	0/2[b]	0/2	NT[a]	0/2
	Spleen	0/2	0/2	NT	NT
	Lymph node	0/2	0/2	NT	NT
	Plasma	0/9	0/9	NT	NT
	Cell culture	0/2	0/2	NT	0/2
^{238}Pu - Exposed	Lung	0/2	0/2	NT	NT
	Spleen	0/2	0/2	NT	NT
	Bone tumor	5/8	8/8	3/3	0/8
	Cell culture (Bone tumor)	5/5	5/5	5/5	ENC[d]
	Plasma	0/8	0/8	NT	NT
^{239}Pu - Exposed	Lung	0/2	0/2	NT	NT
	Lung tumor	0/5	0/5	NT	NT
	Spleen	0/2	0/2	NT	NT
	Plasma	0/5	0/5	NT	NT
	Cell culture (Lung tumor)	2/3[c]	2/3[c]	1/1[c]	ENC
^{249}Cf - Exposed	Bone tumor	1/1	1/1	1/1	NT
^{241}Am - Exposed	Bone tumor	1/2	2/2	1/1	NT

(a) Not tested
(b) Number positive samples/total number of samples examined
(c) DNA polymerase from lung tumor cell cultures is associated with a more dense particle (1.20 - 1.18 g/ml). These same samples were all negative for Type C retrovirus (buoyant density, 1.14 - 1.16 g/ml)
(d) Evaluation not completed

PORCINE RETROVIRUS: AN IN VITRO MODEL

Investigators:

M. E. Frazier, F. Akiya, and M. J. Hooper

Technical Assistance:

T. K. Andrews and B. B. Thompson

Virus replication in cell cultures from swine with myelogenous leukemia, myeloid metaplasia, and from normal animals exposed to ^{90}Sr has been shown to be related to the severity of disease. The viral DNA polymerase produced in cell cultures from leukemic swine is characterized. The cofactors and conditions necessary for optimal DNA synthesis are the same as for the viral DNA polymerase produced in tissues from leukemic swine.

Previous studies at this laboratory (Annual Report, 1976) have shown that a retrovirus is present in miniature swine with ^{90}Sr-induced myelogenous leukemia and myeloid metaplasia. Furthermore, the virus titer was related to the disease status of these animals.

Since a continuing source of ^{90}Sr swine is no longer available, it has been necessary to propagate cell lines producing virus in order to carry out necessary immunological investigations and nucleic acid hybridization experiments. Several cell lines were studied to determine which allowed porcine virus replication. Viral production was evaluated, using the standard techniques for virus detection and quantitation described in earlier annual reports (Annual Report, 1975). These tests include viral reverse transcriptase assays, electron microscopic evidence of the presence and number of C-type particles, and the hybridization of purified viral RNA with ^{3}H-labeled poly dT to give an estimate of virus titer. The results of these studies indicate that virus production is generally correlated to the disease status of the animal from which the cell line originated. In other words, cell cultures from animals with myeloid metaplasia are producing oncornavirus at lower titers than cell cultures from animals with myelogenous leukemia. These cell lines thus provide both a source of virus (potentially more than one virus class) and an in vitro model for studying the relationship between observed pathology and virus production.

Attempts to explain the observed differences in virus production must begin with the careful characterization of the individual viruses. Two cell lines from animals with myelogenous leukemia were selected for the initial aspects of this study. The virus from these cell lines was purified and the DNA polymerase from these viruses was investigated to determine the cofactor requirements and reaction conditions necessary for optimal DNA synthesis.

The basic requirements of the endogenous viral DNA polymerase from both cell lines were essentially the same (Table 3.47). The marked decrease in DNA synthesis with the omission of dATP, dCTP, or dGTP indicates that a heteropolymeric polydeoxynucleotide is being synthesized that requires all four deoxyribonucleotides. Omission of the oligo dT_{12-18} primer causes a markedly limited reaction, as does the absence of a divalent cation. The DNA synthesis is sensitive to RNase. In contrast, the absence of actinomycin D and distamycin A from the reaction mixture results

TABLE 3.47. Requirements of Endogenous DNA Polymerase from Porcine Oncornavirus.

Conditon	^{3}HTTP Incorporated[a] CPM x 10^{-3}
Complete reaction mixture[b]	17.9
Minus dATP	2.1
Minus dGTP	1.8
Minus dCTP	2.3
Minus divalent cation (Mg++ or Mn++)	3.8
Minus oligo dT_{12-18}	7.3
Plus RNase A and T_1	3.2
Minus actinomycin D and Distamycin A	38.2
Complete reaction mixture (culture fluid from uninfected porcine culture)	1.9

(a) The amount of ^{3}HTTP incorporated into acid insoluble DNA product in a 10-μl aliquot from the reaction mixutre. Reactions were incubated at 37°C for 60 min

(b) Approximately 0.5 μg of purified virus (based on protein determinations) is solubilized by the addition of Triton X-100 to a concentration of 0.005%. The complete reaction mixture (100 μl) contains the solubilized virus and the following concentration of reagents: Tris HCl (pH 8.3), 50 mM; $MnCl_2$ 3mM, KCl 80 mM; dithiothreitol 0.8 mM; 200 μM each dGTP, dATP, dCTP and 50 μM ^{3}H-TTP (50 Ci/m mole); actinomycin D (100 μg/ml); distomycin A (50 μg/ml); and oligo dT_{12-18}

in at least 100% more synthesis. Previous studies indicate that these antibiotics selectively inhibit synthesis of the DNA(+) strands; thus only DNA(-) synthesis is taking place in our standard reaction mixture.

Finally, experiments were carried out to determine the optimal conditions for synthesis of DNA by the viral DNA polymerases produced in cell cultures from leukemic swine. While the enzyme synthesizes DNA in the presence of either Mn^{++} (2-5 mM) or Mg^{++} (10-20 mM), there is a consistently higher rate of synthesis in the presence of 2-5 mM Mn^{++} (Figure 3.53A). In addition, the polymerase shows a peak of activity when the virus is solubilized in very low concentrations of Triton X-100, and synthesis is virtually eliminated by detergent concentrations above (0.05%) (Figure 3.538).

This low and narrow range of Triton X-100 (around 0.005-0.01%) is consistent with previous observations for the porcine oncornavirus. Rather broad ranges of activity were observed for both KCR concentration (Figure 3.53C) and buffer pH (Figure 3.53D).

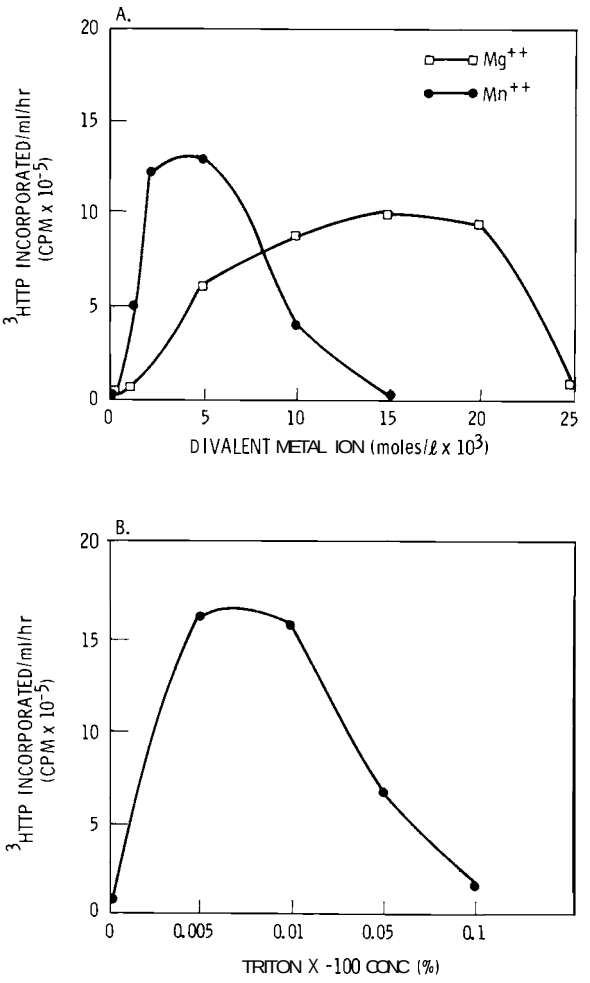

FIGURE 3.53. Reaction Conditions for Optimal Polymerase Activity. Polymerase assays were performed as described earlier except that the concentration of divalent cations (Mg++ or Mn++), detergent (Triton X-100), KCQ, and the pH of the reaction mixture were varied as indicated. (A) dependence of polymerase activity on divalent cation [Mn* or Mn++], (B) detergent concentration. C and D on following page.

The conditions and cofactors for optimal DNA synthesis by the virus present in cultured cells from leukemic animals are basically the same as for virus from tissues of leukemic swine (Annual Report, 1976). Similar studies with virus in cell cultures from normal swine exposed to ^{90}Sr and from animals with myeloid metaplasia are being carried out to determine if polymerase activity is the same for all these viral isolates.

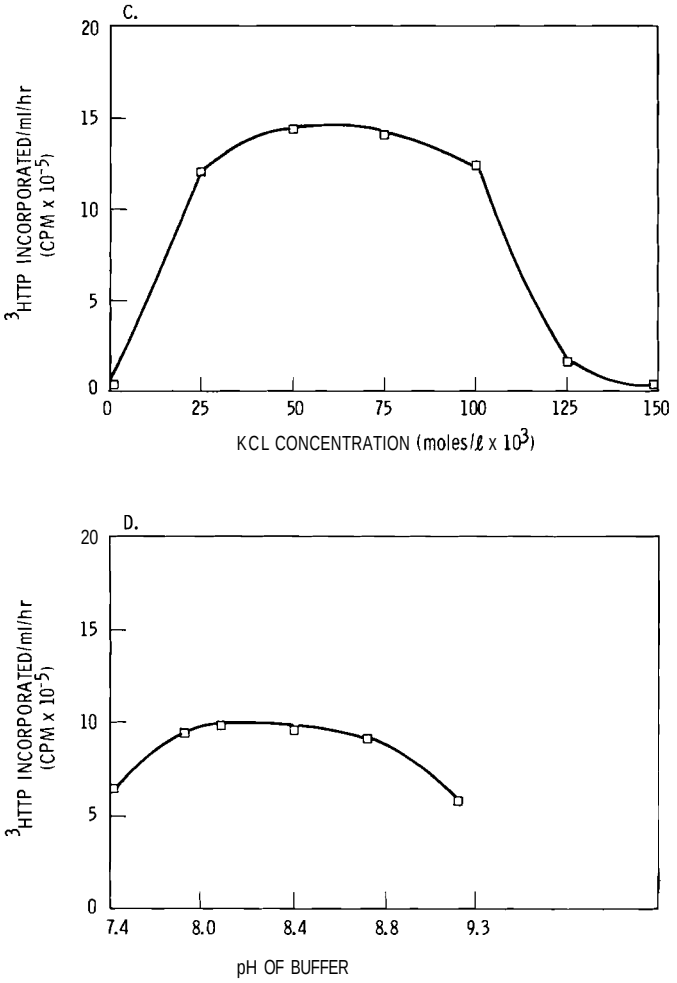

FIGURE 3.53. (C) [K+], and (D) pH of the reaction mixture

PORCINE RETROVIRUS: HYBRIDIZATION STUDIES

Investigators:

M. E. Frazier, F. Akiya, and M. J. Hooper

Technical Assistance:

T. K. Andrews and B. B. Thompson

Tritium-labeled porcine retrovirus (PoRV) was isolated and purified, and kinetics of hybridization of this RNA with DNA from various sources was determined. Results indicate that PoRV is an endogenous porcine virus.

Porcine retrovirus-infected cell cultures were fed NCTC 135 medium containing 10% fetal bovine serum and ^{3}H-5 uridine, ^{3}H-2 adenosine and ^{3}H-5 cytidine, respectively. Medium was changed at 8-hr intervals and centrifuged to remove cells and cellular debris. The virus was pelleted by centrifugation then purified on a sucrose density gradient. The labeled viral material banding at a density of 1.14-1.16 g/ml was collected and pelleted. Viral RNA was extracted by the phenol SDS method, precipitated with ethanol and layered over a 5-20% sucrose gradient. High-niolecular-weight (HMW) RNA was separated from low-molecular-weight RNA by centrifugation (Figure 3.54). From the $\sim$2 x 10^{12} virus particles we obtained approximately 8 µg of HMW RNA, equivalent to a little more than 50% of the available material present. Minimum specific activity of the labeled RNA was 10^6 cpm/µg.

The purified PoRV ^{3}H-labeled HMW RNA was then used to study the kinetics of hybridization of PoRV with DNA from various sources. The hybridization mixture contained ^{3}H-labeled HMW RNA, DNA fragments in phosphate buffer and 0.05% SDS. Before mixing these components the DNA was boiled 1 min to denature it to single-stranded DNA; the hybridization mixture was then prepared, and the solution was incubated at 68°C until needed; 500-µl aliquots were then removed and diluted. The sample was divided in half and two RNAse were added to one or the other halves of the sample. Tubes were incubated at 37°C for 30 min, then placed in an ice bath for 10 min precipitated with 10% trichloroacetic acid. After 30 additional min at 4°C the acid-insoluble material was collected on 0.45-micron nitrocellulose filters.

Hybridization between the tritium-labeled PoRV HMW RNA fraction and DNA extracted from either leukemic or nonleukeniic swine reached a maximum of about 74% and 70%, respectively (Figure 3.55).

The kinetics of reaction of the PoRV RNA with DNA from swine may contain a biphasic element. If this proves to be the case then some sequences ($\sim$40%) are present in a higher frequency than the remaining sequences. This more rapidly annealing fraction (below a Cot of 500) may be present in as many as 200 copies/cell. The slower-annealing fraction (above 500) would represent only 1-2 copies/cell.

If, on the other hand, the kinetics of PoRV RNA hybridization to porcine cell DNA is not biphasic, the Cot 1/2 valve for reassociation would be about 300. This would indicate that there are on the order of 10 copies of the viral genome present in each cell.

No hybridization was observed at Cot values of up to 30,000 when the PoRV ^{3}H RNA was hybridized to the DNA isolated from dog liver or calf thymus. A small amount of hybridization (11%) was seen with RLV infected Balb/c mouse spleen.

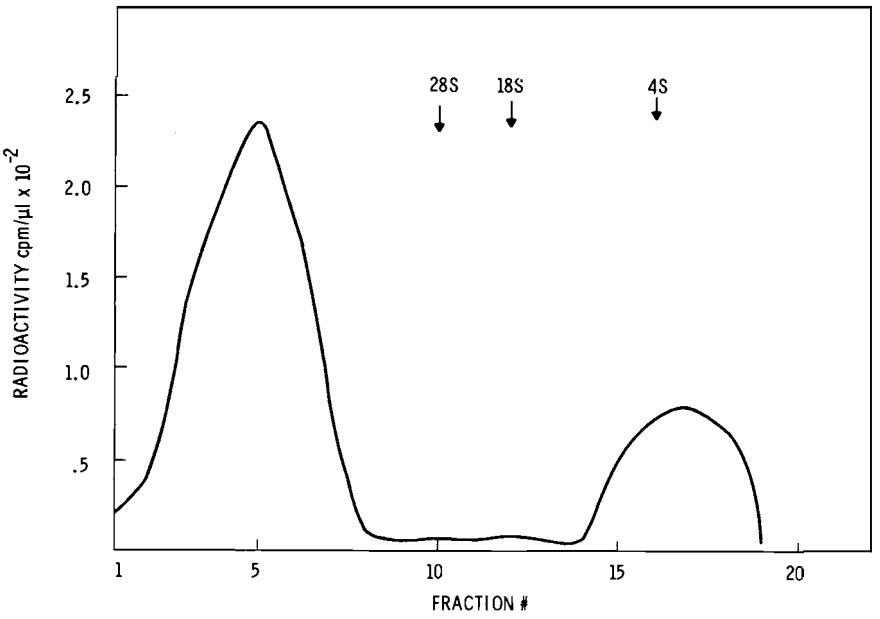

FIGURE 3.54. Sedimentation Velocity Analysis of PoRV ^{3}H RNA. The RNA was sedimented in a 10-30% glycerol gradient and fractions collected dropwise. The high-molecular-weight RNA peak of the gradient was determined by monitoring the trichloroacetic acid-precipitable radioactivity. ^{3}H-labeled RNA from HeLa cell ribosomes served as external markers of RNA size.

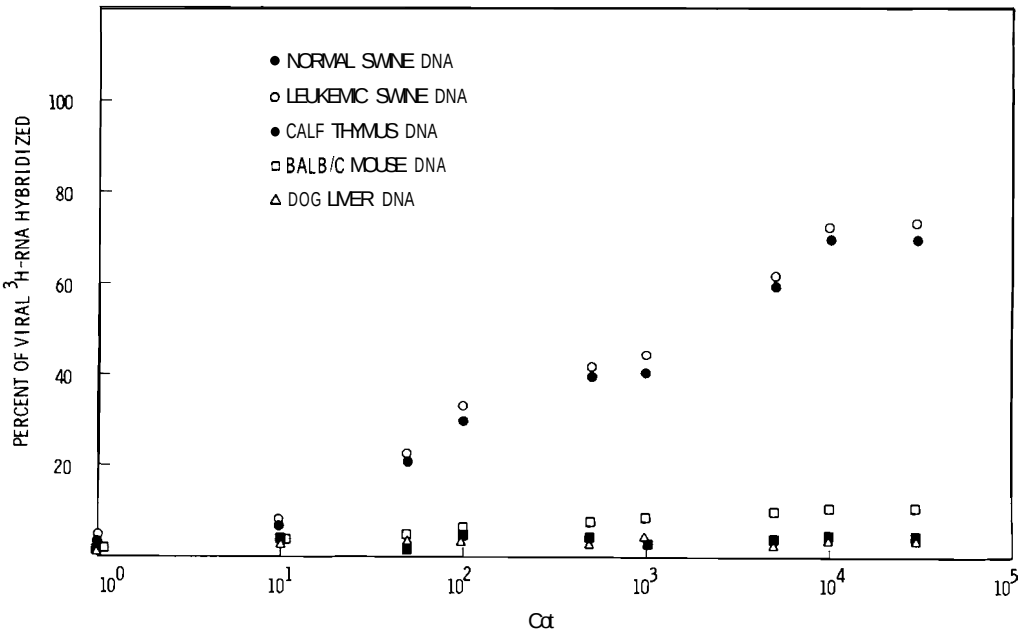

FIGURE 3.55. Kinetics of Hybridization of PoRV ^{3}H RNA with DNA from Various Sources. Percent hybridization at each time point was determined by deducting the zero times background sample from the untreated sample and dividing cpm present in the RNase treatment sample by cpm present in the untreated sample. Values are expressed at Cot, the product of the time of hybridization (in seconds) multiplied by the concentration (in moles per liter).

The final hybridization value for the leukemic DNA preparation is only 2-4% greater than that of the nonleukemic DNA. This probably represents only experimental differences; however, these slight differences could also indicate that a small part of a given set of sequences may be absent from the DNA of at least some of the cell types from a normal pig.

The bulk of the evidence indicates that PoRV is a class I virus. Class I viruses constitute the endogenous virus class (e.g., RD_{114} of cats). Generally speaking, class I viruses are less oncogenic than class II viruses. According to current thought, a cell-replicating class I virus should contain in its DNA genome all the genetic information of the virus being produced. However, we have noted less difference in the percent of hybridization and the mean thermal elution temperature of hybrids between virus and leukemic cell DNA than with hybrids of virus and normal cell DNA (Annual Report, 1976). Therefore, it is not yet possible to state categorically that DNA from a normal cell codes for the present form of the virus. It is possible that the endogenous class I virus from swine has undergone a mutation as the result of radiation insult that has increased its oncogenic potential.

EFFECTS OF INHALED $^{239}PuO_2$ ON THE PRIMARY IMMUNE RESPONSE OF BEAGLE DOGS

Investigator:
J. E. Morris
Technical Assistance:
L. S. Winn

Effects of inhaled $^{239}PuO_2$ on the humoral component of the immune system were measured by intravenous immunizations of beagle dogs with keyhole limpet hemocyanin (KLH). With this T-cell-dependent antigen, a significant decrease ($P = < 0.01$) in primary antibody response was observed in exposed versus unexposed dogs.

Inhaled plutonium oxide has been shown to induce a dose- and time-dependent lymphopenia prior to tumor formation in beagle dogs. The lymphopenia has been characterized as being a decrease in peripheral blood levels of both T- (thymus dependent) and B- (thymus independent) lymphocytes with greater reduction in B-cell populations. In this report we will consider in vivo hunioral immunological effects of inhaled plutonium as it relates to the primary antibody response of exposed beagle dogs.

For the antibody response study, keyhole limpet hemocyanin (KLH, molecular weight 3×10^6) was chosen as the antigen because of its high antigenicity and the possibility that the dogs had not previously been immunologically exposed to it. It is known that KLH is T-cell-dependent because functional T-cells, as well as B-cells, are required to mount a humoral response to KLH.

A group of 6 dogs exposed to a mean initial deep lung deposition of 1.2 ± 0.9 µCi $^{239}PuO_2$, 2.5 yr previously, and 5 unexposed dogs were used in the study. Peripheral lymphocyte levels in exposed and unexposed dogs were $1.2 \pm 0.5 \times 10^6$ and $2.2 \pm 0.4 \times 10^6$, respectively, per milliter of blood at primary immunization. Dogs were immunized intravenously with 0.5 mg KLH/kg body weight. Daily blood samples were drawn and antibody titers to KLH were measured using a direct-binding radioimmunoassay. Typical antibody titer precipitation curves for both an exposed and unexposed dog (11 days post primary immunization) are shown in Figure 3.56. The curves were generated by mixing 100 µl of immune dog serum with increasing amounts of KLH ranging from 1.3 µg to 169.9 µg. To compare the antibody content in the serum of the immunized dogs, the 5.3 µg point was chosen.

A plot of the percent of 5.3 µg KLH precipitated by the antibody present in 100 µl of immune dog serum is shown in Figure 3.57. The binding and precipitation curves indicate that plutonium exposure induced a significant functional decrease ($P > 0.01$) in the primary antibody response of exposed dogs to KLH. This reduced response suggests that impairment of immune mechanism may play a role in tumorigenesis in animals exposed to $^{239}PuO_2$.

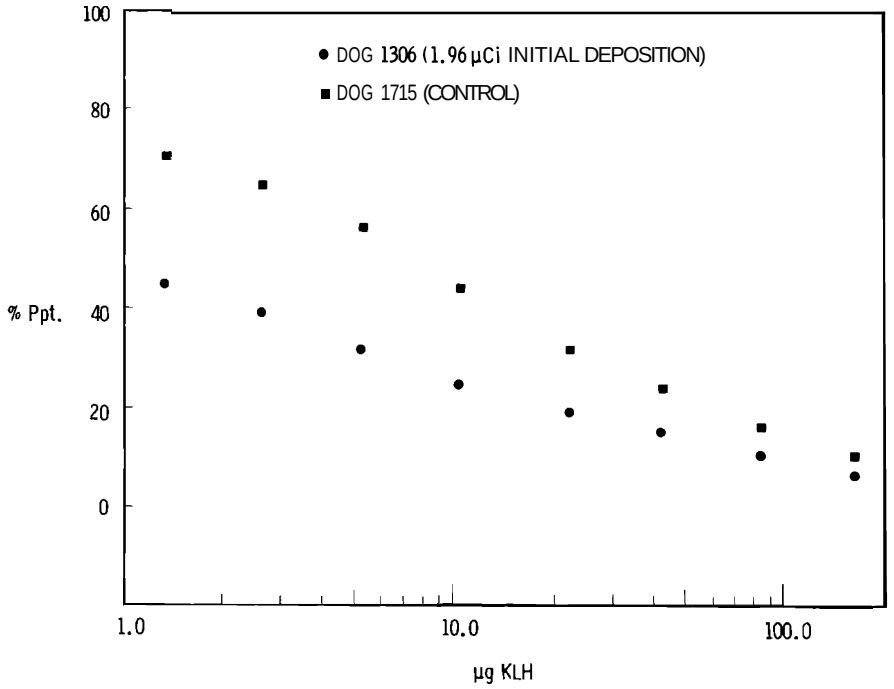

FIGURE 3.56. Antibody Titration Curve at 11 Days after Primary Immunization

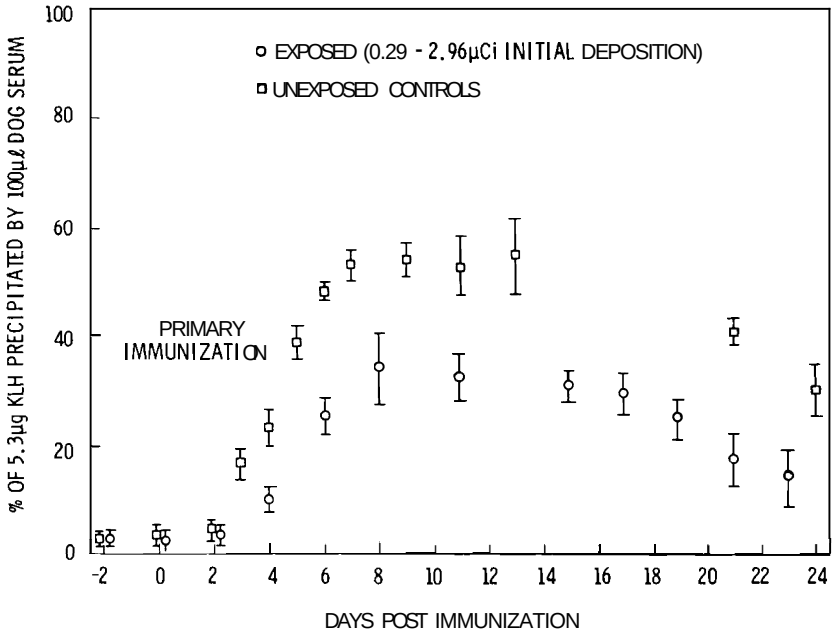

FIGURE 3.57. Serum Antibody Measurement in $^{239}PuO_2$-Exposed and Unexposed Beagle Dogs

LYMPHOCYTE MOBILIZATION BY DEXTRAN SULFATE IN BEAGLES

Investigators:

H. A. Ragan and K. H. Debban

Technical Assistance:

S. L. English and M. C. Perkins

Dogs manifesting ^{239}Pu-induced lymphopenia responded to the lymphocyte-mobilizing agent, dextran sulfate, to a degree similar to that observed in control dogs. No life-threatening increase in prothrombin times or hemorrhagic tendencies were observed.

Dogs exposed to a single inhalation of $^{239}PuO_2$ develop a dose-related and prolonged lymphopenia. It has been speculated that the lymphopenia results primarily from continuous irradiation of circulating lymphocytes via thoracic lymph nodes, but this pathogenesis has not been clearly defined. It was of interest to determine whether dogs with lymphopenia still have mobilizable pools of lymphocytes, or whether all available lyniphocytes are already in circulation.

Several polyanions have been found to induce lymphocytosis following injection in rats and primates, due mainly to mobilization of lymphocytes from lymphoid organs. Dextran sulfate (DS) was selected as a lymphocyte-mobilizing agent in this experiment because of its ready availability and lack of serious side effects.

Dogs with average initial lung burdens of ∿ 2.5 μCi $^{239}PuO_2$ 18 mo postexposure had blood lymphocyte concentrations ∿ 55% those of age-related control dogs. Dogs from both groups were given 5 mg/kg body weight sterile DS by intravenous injection, and blood samples were taken 0, 0.5, 1.0, 2.0, 3.0 and 5.0 hr later. From these samples the total leukocyte count was determined and blood smears were made for leukocyte differential counts. Since dextran interferes with clotting, plasma prothrombin times were also assayed.

The results of DS injection on blood lymphocyte, neutrophil, and monocyte concentrations, calculated as the ratio of cells at time $_x$/cells at time are shown in Figure 3.58. Although absolute lymphocyte concentrations were reduced in $^{239}PuO_2$-exposed dogs, the percent of lymphocytes mobilized after DS injection was comparable in lyniphopenic and control dogs, both as to time and degree of maximum response. Only a niodest increase in neutrophils was observed in either treatment group. Interestingly, the percent of monocytes mobilized by DS was greater in lymphopenic than in control dogs, even though the preinjection monocyte values were about equal, ($400 \pm 130/mm^3$ in the former versus $460 \pm 120/mm^3$ in the latter).

Maximal prolongation of prothrombin time occurred at the 0.5-hr sample in both groups. Mean value at that time was 1.8 times the zero-hr value, so did not represent a serious compromise of the clotting mechanism.

From the results of this study it appears that dogs manifesting prolonged ^{239}Pu-induced lymphopenia have a reserve pool of mobilizable lymphocytes. However, a major unanswered question remains: Why is a feed-back mechanism not stimulated by the prolonged lymphopenia that would return lymphocyte levels toward normal? Studies to help answer this question are being planned.

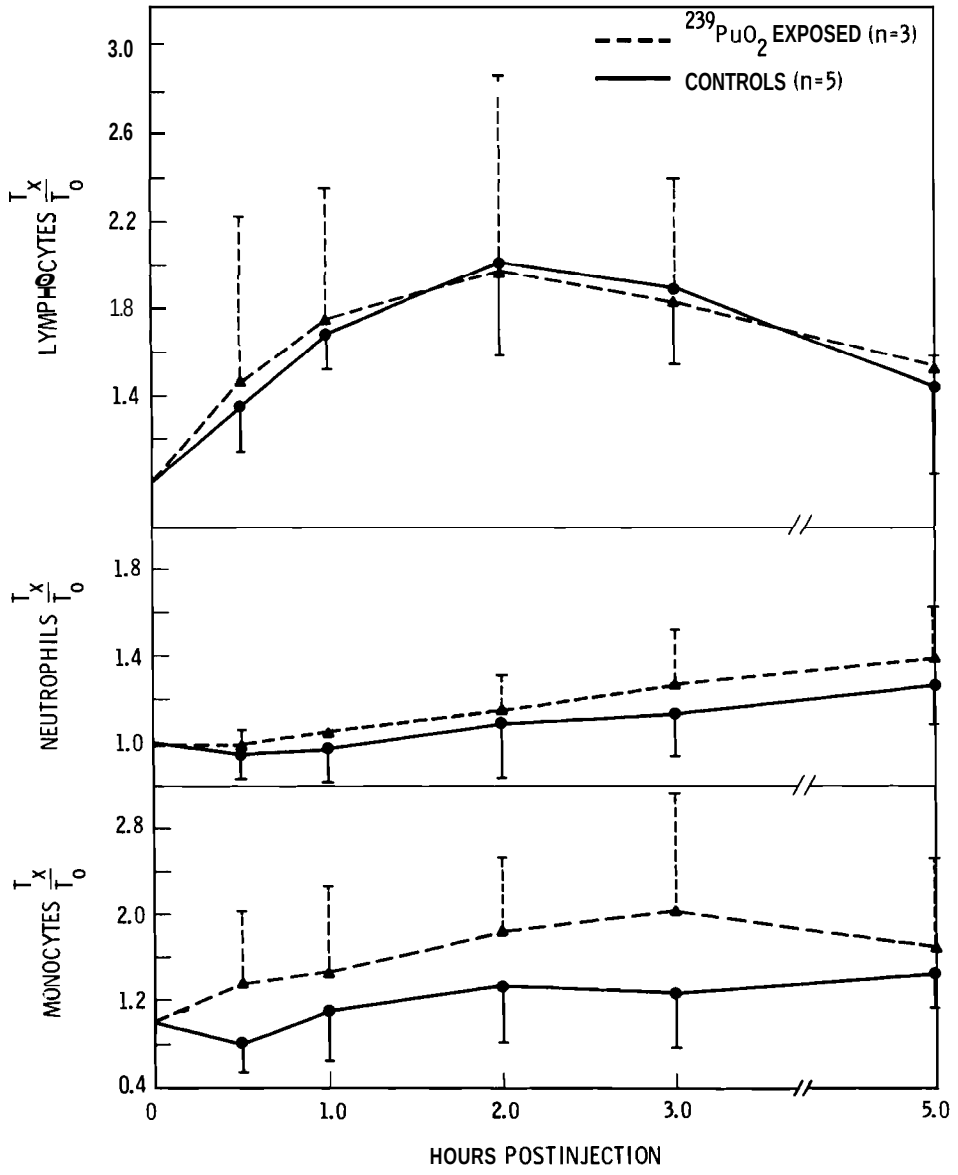

FIGURE 3.58. Leukocyte Mobilization in Dogs Following Intravenous Injection of Dextran Sulfate, Ration of cells at time x (mean ± SD)

- **Development of Blood Irradiator**

Extracorporeal irradiation of blood, using repeated brief exposures, has been shown to suppress rejection of tissue transplants and to inhibit progression of chronic lymphocytic leukemia. This project is designed to study the basic processes by which blood irradiation produces such effects, to establish the conditions of dose administration which optimize therapeutic effect, and to improve the technique of blood irradiation through the development of improved and portable blood irradiators.

PROGRESS IN DEVELOPMENT OF A PORTABLE BLOOD IRRADIATOR

Investigator:
F. P. Hungate

Hardware problems associated with maintaining a nonthrombogenic environment for blood flow appear to be largely solved. The new technique of spin casting the blood interface layer continues to provide irradiator units that produce no evidence of thrombus initiation internally.

Earlier connectors had surface discontinuities at the point of butt joining due to nonconcentricity and occasional differential shrinkage of the teflon liner from the body of the connector. With knowledge of these problems, the vendor (Quinton Instruments) prepared a series of connectors cast from other materials, with no internal teflon liner, which were tested in animals with arteriovenous shunts in place.

One of the materials, Tefzel, showed evidence of thrombus initiation on the connector wall within 24 hr. A second material, polyvinylchloride, deformed within 24 hr to the point of discontinuity at the joint, although no thrombus was observed on the connector wall. No evidence of thrombus induction was observed in a polyethylene-polyvinylchloride copolymer, polyformaldehyde, or polypropylene units during 24-hr tests. Because of slightly better physical conformance, polyformaldehyde units were used in subsequent shunts and have performed well over a period of many months, even when shunts were repeatedly opened for blood sampling or irradiator replacement.

Activation of units has been a continuing problem due to reactor operation scheduling and difficulties in getting units into the area of high neutron flux. The reactor tube normally used gives a flux of 10^{14} neutrons cm^{2}, but early in the year saniples failed to attain their typical radiation level. Tests indicated tube blockage, even when higher gas pressures were used for inserting the samples. At the scheduled fall reactor outage, this tube was cleaned and converted from a pneumatic to a hydraulic system. Recent tests indicate that access via this tube is still obstructed, and there is no consensus about how to rectify the problem. In the meantime, a new carrier was constructed so that units can be irradiated in a tube yielding 10^{13} neutrons cm^{-2}. The lower irradiation level in this tube requires a longer period of activation (about a month) and lower activity levels are attained.

Biological testing of the irradiators has confirmed earlier suppression of lymphocyte levels by relatively low levels of irradiation. Our continued failure to observe typical rejection sequelae has been disappointing. On the supposition that this might be due to some quirk of common genotype, reciprocal grafts were made between full-size goats obtained locally and an inbred strain of African Pygmy goats maintained at this laboratory. When we still observed no distinct rejection syndrome, reciprocal grafts were made between the goats and a sheep, with similar lack of success in identifying a distinctive rejection pattern. Biopsies taken through the graft area indicated lack of vascularization. To overcome this lack of vascularity, split skin grafts are now being tested. Although biopsies have not yet been examined, there was no visual evidence of immunologic reaction.

It was reported last year that clotting problems during irradiator testing had been resolved by use of dicoumarol with aspirin. While this was effective therapy, very large doses of dicoumarol were required to counteract the intake of vitamin K in alfalfa feed. Three cases of dicouniarol overdosage occurred when animal feed intake varied. Injection of vitamin K was successful in reversing the problem in only one case; the other two succumbed to internal bleeding. Consequently, we now routinely inject low doses of heparin twice daily. Since heparin is noncumulative this regimen also allows for temporary cessation of treatment just prior to skin grafting.

Preliminary discussions on preclinical irradiator testing in baboons were held with Dr. E. D. Thomas. We hope to initiate this testing during the coming year so that evaluation on human patients can follow.

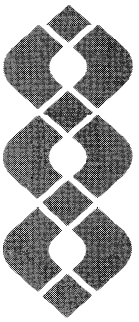

4.0 Fusion

FUSION

• Biomagnetic Effects

The development of magnetic fusion power sources will undoubtedly result in the occupational exposure of personnel to magnetic fields of varying strengths and geometries. The Division of Magnetic Fusion Energy (DMFE), ERDA has, therefore, expressed the need for information on the biological effects of magnetic fields to aid them in their evaluation of fusion reactor designs.

There have been a number of investigations of the biological effect of magnetic fields, using several experimental systems. The results have often been equivocal, the effects noted being small or nonreproducible by different investigators. Nonetheless, evidence that biomagnetic effects do occur is sufficient to indicate the need for systematic, well-controlled studies to obtain information suitable for the establishment of reasonable exposure limits. For these reasons, the studies described in the following reports have been undertaken.

EXPOSURE OF PRIMARY AND ESTABLISHED CELL LINES TO MAGNETIC FIELDS

Investigators:

T. K. Andrews, M. E. Frazier and B. B. Thompson

Technical Assistance:

C. White and M. J. Hooper

Experiments were initiated to replicate and, if possible, quantitate the reported effect of magnetic fields on cultured cells. Since the W138 and L929 cells previously employed are less than ideal choices for use in quantitative studies of this nature, we have included three additional cell lines to help in evaluating the potential effects of magnetic fields on cultured cells.

Malinin et al. (Science 194: 844-846, 1976) reported that strong magnetic fields markedly inhibited the growth rate of cultured cells. In addition, these same cells reportedly underwent a morphological and physiological transformation as a result of their exposure to magnetic fields. These results, if verified, represent a significant scientific finding. Unfortunately, only subjective criteria were used in evaluating these cell lines. For example, the actual growth rates were not determined for either the exposed or the control cultures. Furthermore, neither cell size measurements

nor objective determinations of cell transformation (i.e., growth in soft agar or animal transplantation experiments) were attempted. Because of the implications of these findings and the incompleteness of the data it seemed imperative that this study be repeated and extended.

Table 4.1 lists the cell lines being used in our current study. The L929 and W138 cells used in the original investigation are included, together with three additional cell lines. Hamster embryo cells were chosen because they represent a diverse population of fairly differentiated cells with limited life span (unless they become transformed); they are widely used as indicator cells in transformation studies and results with these cells could be more easily interpreted by the scientific community. The C_3H 10T1/2 cells represent a continuous cell line that is also widely used as an indicator cell for chemical carcinogens; they display strict contact inhibition until they become transformed. The VERO cells were included because their ingrowth parameters have been well characterized in our laboratory and even very subtle changes in growth characteristics are readily discernible.

TABLE 4.1. Identification of Cell Lines Used to Evaluate Magnetic Effects in Cultured Cells

Cell Line	Source
WI38	Human Lung (fibroblast)
L929	Mouse Fibroblast
VERO	Monkey Kidney
HEC	Secondary Hamster Embryo
C_3H 10T1/2	Mouse Prostate

Cells were exposed in a frozen state (as in Malinin's experiment) to either 5000 or 10,000 gauss magnetic field for 4, 8, or 24 hr. Cells were then thawed, washed with fresh medium, and grown, using standard cell culture techniques. Periodic evaluations of cell viability, growth rate, cell size, cell morphology, and cell transformation frequency of exposed and control cultures were carried out according to the plan outlined in Table 4.2.

L929 cells exposed to 10,000 gauss for 4 or 8 hr have been studied for 80+ days in culture and the morphological and growth characteristics described by Malinin et al. have not yet been observed. However, L929 cells exposed at 10,000 gauss for 8 hr have increased significantly in size. Studies with hamster embryo cells have been uniformly negative, these cultures began dying after the 6th passage, indicating they had not been malignantly transformed by exposure to magnetic fields. Studies with VERO, WI38, and the C_3H 10T1/2 cells are still in progress.

TABLE 4.2. Experimental Parameters for Evaluation of Cells Exposed to Magnetic Fields

Parameter	Method of Evaluation
A. Cell Viability	1. Trypan Blue 2. Cloning Efficiency
B. Growth Rate	1. Elkind's 2. Total Protein
C. Cell Size	1. Photomicrographs
D. Cell Morphology	1. Phase Contrast Microscopy 2. Stained Slide Preparations
E. Cell Transformation	1. Morphology a) Loss of Contact Inhibition b) Random Crowth Patterns c) Change in Morphology 2. Crowth in Soft Agar

RESPONSE OF ARTIFICIAL MEMBRANES AND GELS TO MAGNETIC FIELDS

Investigators:
D. R. Kalkwarf[a] and J. C. Langford[a]

Gelation temperatures of aqueous 1.4% agarose solutions were found to increase linearly with applied magnetic field, from 37.4 ± 0.2°C at 0 tesla to 38.8 ± 0.2°C at 1 tesla. Gels formed in a 1-tesla field were also found to be 10% more permeable to DNA than were control gels. The effect was attributed to magnetically induced alignment of agarose chains in the liquid state prior to gelation. No change in the permeability of phospholipid-bilayer membranes to fluoride ions was found even at magnetic fields of 1 tesla.

Most biochemicals are diamagnetic and can be expected to align their major molecular axes parallel to an applied magnetic field. The reported clarification of turbid, organic "liquid crystals" when placed in a magnetic field is a vivid illustration of this process. In such cases, the orienting effect of the magnetic field couples with the short-range binding forces within the individual "swarms" of liquid crystals to create long-range order in spite of thermal agitation. Conversely, a rapidly changing magnetic field would be expected to aid thermal agitation in disrupting preformed structures. In cells, stabilization or disruption of loosely bound microstructures such as aqueous gels or phospholipid-bilayer membranes could initiate more extensive biological effects. It is the purpose of this study to search for magnetically induced changes in model gels and membranes that might suggest experiments to reveal more overt biomagnetic effects.

Aqueous solutions containing 1.4% agarose were used as models for investigating the effects of magnetic fields on gel structure. Agarose is a high-molecular-weight, linear polysaccharide consisting of alternate D-galactose and 3,6-anhydro-L-galactose units. When a solution of agarose cools, it forms a firm gel; this transition is accompanied by a slight increase in turbidity. A small turbidimeter and thermistor assembly was constructed to accurately measure the temperature of this transition in samples held within the 2.75-in. air-gap of an electromagnet. As a sample cooled, the gelation temperature was indicated by a sharp break in the recorded plot of transmitted light intensity versus temperature. These temperatures were found to increase linearly with magnetic field from 37.4 ± 0.2°C at 0 tesla to 38.8 ± 0.2°C at 1 tesla (Figure 4.1). The statistical limits shown are 95% confidence intervals, each based on at least nine separate determinations.

These data suggest that magnetic fields can align linear chains of agarose in the liquid state so that they can form a solid structure at higher temperatures. Additional evidence for magnetically induced alignment was found by comparing the electrophoretic mobilities of high-molecular-weight, bacterial DNA through 1.4% agarose gels allowed to solidify in either a 0- or 1-tesla field. The DNA moved 10% faster through gels formed in the 1-tesla field, suggesting that this field created a more ordered gel structure with less circuitous paths for the migrating DNA molecules.

[a] Physical Sciences Department

Spherical vesicles bounded by single bilayers of either dipalniitoyl- or dioleoyl-phosphatidylcholine were used as models to investigate the effects of magnetic fields on biological membranes. Vesicles were prepared by sonicating aqueous suspensions of the phospholipids in 0.1 M NaF and passing the product through a gel filtration column to remove all fluoride ion from the solution between vesicles. Release of fluoride from the vesicle interior was then measured with a selective fluoride-ion electrode, as a function of time, to evaluate disruption of bilayer structure. Fluoride-release rates were measured at constant temperature over the range 15 to 30°C in the presence or absence of an applied magnetic field. A constant 1-tesla field or 0.17-Hz field was applied. Neither field caused a significant alteration in rates at the 95% confidence level.

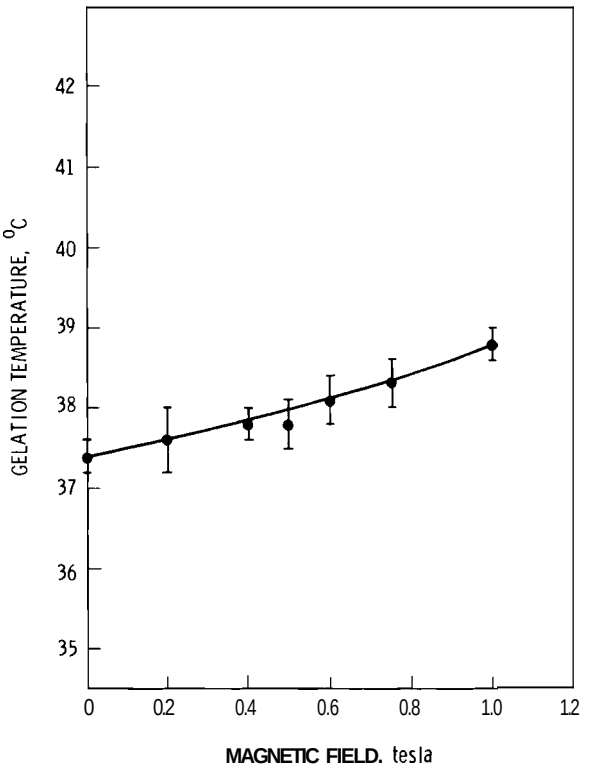

FIGURE 4.1. Effect of Magnetic Fields on Gelation Temperature of 1.4% Agarose Solutions. Data are presented as 95% confidence intervals, each based on at least 9 separate determinations.

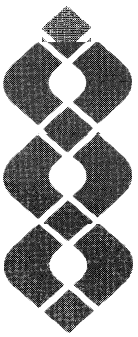

5.0
Oil Shale

5.0 OIL SHALE

Potential biomedical concerns in the area of oil shale fuel technology are being investigated, in part, by a tiered testing approach utilizing the Ames assay and mammalian cell transformation, followed by more standard toxicologic procedures. Studies in this area have resulted in derivatives of the basic Ames assay that appear to allow better definition of the mutagenic potential of toxic mixtures. Fractions of potential importance, as defined by the Ames assay, are presently being utilized in development of a quick and quantitative assay for pulmonary carcinogenesis.

Techniques for administering (via the inhalation route) and analyzing effects of spent and oil-bearing shale dust were developed in this past year.

OIL SHALE

• Late Effects of Oil Shale Pollution

The purpose of this study is to investigate the potential health hazards associated with exposure to dusts and other effluents released during the processing of oil shale. Potential exists for occupational exposure to oil shale and spent shale particulates, crude shale oil, processed shale oil, and waste water. Polycyclic aromatic hydrocarbons (PAH), including carcinogens, are present in all of the above pollutants.

GENERATION AND CHARACTERIZATION OF OIL SHALE AND SPENT SHALE AEROSOLS FOR ANIMAL INHALATION

Investigators:

W. C. Cannon and D. W. Phelps

Technical Assistance:

B. F. Garrity, J. R. Laidler, and K. R. Hanson

The Wright Dust Feed Mechanism was evaluated as a generator of oil shale and spent shale aerosols for animal inhalation experiments. Oil shale concentrations of 197 mg/m^3 were obtained, of which 68% was respirable; spent shale concentrations of 86 mg/m^3 were obtained (79% respirable). Both oil shale and spent shale aerosols had particle size-dependent conipositions.

Oil shale and spent shale aerosols were generated from pulverized chunk material by a Wright Dust Feed Mechanism (WDFM) into a 222-R plastic aerosol chamber, with a cyclone elutriator interposed in the line to remove larger particles. Aerosol properties are summarized in Table 5.1.

Aerosol samples included gravimetric filter samples for total aerosol concentration, MRE respirable dust samples for respirable concentration and Andersen cascade impactor samples for particle size distribution.

Particle size dependence of composition was demonstrated by analyses of samples collected on the first seven stages of an Andersen cascade impactor. Metallic element analyses were performed on acid-digested samples (Table 5.2). Samples of oil shale were desiccated at room temperatures, then heated at 300°C until weight stable and percent weight loss was determined (Table 5.3). Weight loss of spent shale samples by this procedure were too small to measure. The weight lost from oil shale samples is considered to be largely organic material, but probably does not indicate total organic content. The generally greater weight losses from smaller particle fractions may have resulted from the larger surface area per unit mass, rather than from a difference in composition.

Oil shale materials were obtained from the Laramie Energy Research Center (LERC); spent shale materials were obtained from Lawrence Livermore Laboratory.

TABLE 5.1. Aerosol Properties Using the Wright Dust Feed Generator.

	Oil Shale	Spent Shale
Generator Data		
Gear Ratio	1:2	1:2
Air Flow ℓ/min	20	20
Recommended Packing Pressure Kg/cm²	44	175
Pack Density g/cm³	1.41 ± 0.10	1.92 ± 0.05[a]
Aerosol Data		
Chamber Air Flow ℓ/min	141.5	141.5
Chamber Volume liters	222.3	222.3
Aerosol Concentration mg/M³ (Filter Paper)	197 ± 39	86 ± 16[a]
Respirable Concentration mg/M³	135 ± 23	68 ± 4
MMAD[b]	0.99	1.46
GSD	2.60	2.68

[a]Mean ± SD
[b]Mass Median Aerodynamic Diameter

TABLE 5.2. Metal Content[a] of Raw and Spent Oil Shale Aerosol Samples (μg Metal/Mg Shale)

	Andersen Stages							
	1	2	3	4	5	6	7	
(urn)	> 7.1	(4.8-7.1)	(3.3-4.8)	(2.1-3.3)	(1.05-2.1)	(0.64-1.05)	(0.45-0.64)	Bulk
Oil Shale Metals								
Al	5	5	37	122	430	137	209	60 ± 8
Ca	—[b]	80	58	430	60	27	—	74 ± 7
Fe	38	54	37	30	45	35	48	41 ± 2
Spent Shale Metals								
Al	46	42	25	38	44	31	25	Not Analyzed
Ca	154	174	123	169	180	120	72	Not Analyzed
Fe	35	30	31	45	100	103	187	Not Analyzed

[a]All values are in μg metal/mg shale
[b]Below detection limits

TABLE 5.3. Weight Loss of Oil Shale Heated to 300°.

	Andersen Stage							
	1	2	3	4	5	6	7	Bulk Sample
AED[a] μm	> 7.1	4.8-7.1	3.3-4.8	2.1-3.3	1.05-2.1	0.64-1.05	0.45-0.64	—
Percent Weight Loss Test #1	19	21	19	18	23	28	33	17.3 ± 0.2[b]
Percent Weight Loss Test #2	—	12	12	14	17	20	21	18.1 ± 0.2

[a]Aerodynamic Equivalent Diameter
[b]Mean ± Standard Deviation

FIBROGENIC POTENTIAL OF RAW AND SPENT SHALE PARTICULATES

Investigators:

R. A. Renne, L. G. Smith and K. E. McDonald

Technical Assistance:

K. M. Dragoo

Rats exposed to raw oil shale, spent shale or quartz by intratracheal instillation developed granulomatous pneumonia with fibrosis and alveolar proteinosis over a postexposure period of 8 mo. Fibrosis was most severe in the quartz-exposed rats and progressed with time in these groups. Alveolar proteinosis, also more severe in the quartz-exposed rats, progressed with time in all exposed groups.

A study of the potential fibrogenic activity of raw and spent shale was initiated in February, 1977, using the protocol indicated in Table 5.4. Rats were given 3 weekly intratracheal instillations of 30 mg particulate shale. Quartz (fibrogenic positive control) was given in two concentrations: one at a dosage equal in mass to the particulate shale (30 mg), the other at a dosage equal to the concentration of silica in the instilled shale (5 mg silica/30 mg dose).

TABLE 5.4. Experimental Design

Exposure Group	Number of Rats Examined at Each Sacrifice Period[a]				
	0 mo	3 wk	7 wk	4 mo	8 mo
Raw Shale (30 mg)	6	10	10	10	10
Spent Shale (30 mg)	6	10	10	10	10
Quartz (30 mg)	6	10	10	10	10
Quartz (5 mg)	6	10	10	10	10
Vehicle Control	6	10	10	10	10
Shelf Control	6	10	10	10	10

[a] Tissues from 4 rats in each group were examined microscopically; 6 were utilized for biochemical studies

Shale samples were obtained from Laramie Energy Research Center (LERC), Laramie, Wyoming: raw shale was from Colorado; spent shale was from the 10-ton experimental retort at LERC. The shale material, ground in a ball mill, had particle sizes ranging from 0.5 μ to 1.5 μ, with a mean particle diameter of 0.9 μ.

Tissue response to the injected materials was similar in rats sacrificed 3 wk, 7 wk and 4 mo after initial exposure. There was a granulomatous pneumonia present in response to the injected shale or quartz; the predominant cellular response was the presence of intra-alveolar aggregates of alveolar macrophages containing lipoprotein and particulate shale or quartz (Figure 5.1). There was infiltration of heterophils, mononuclear inflammatory cells, and varying amounts of fibrosis around aggregates of particulate material. Although fibrosis was more severe in the quartz-exposed rats, the progressive increase and maturation of fibrous tissue observed in human silicosis was not evident until 8 mo postexposure (Figure 5.2). There

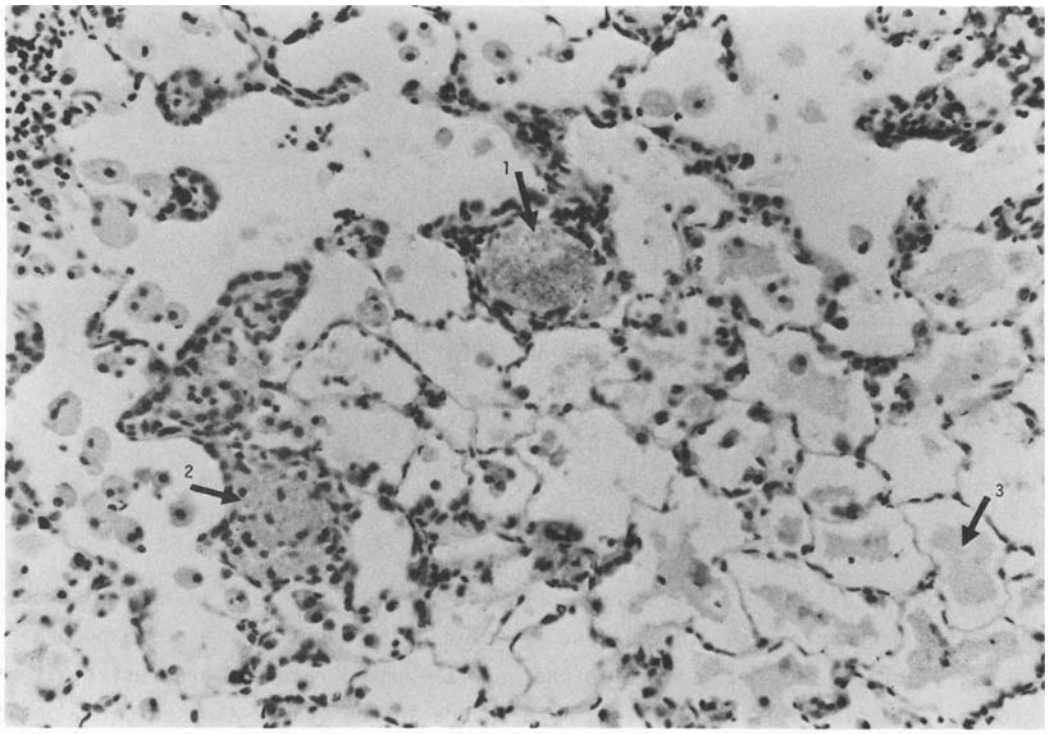

FIGURE 5.1. Rat Lung Containing Raw Shale in Large Clumps Surrounded by a Mild Inflammatory Response (1), and Within Macrophages (2). Lipoprotein is visible in adjacent alveoli (3).

was no apparent increase in fibrosis with time in either raw shale or spent shale-exposed groups of rats.

One of the most striking lesions observed in both shale- and quartz-exposed rats was alveolar lipoproteinosis, consisting of aggregates of pink-staining, eosinophilic lipoprotein material in alveoli. This lesion was most severe in the higher-dose quartz-exposed group, and appeared to increase in severity with time. This material was PAS-positive, but did not appear to be metachromatic with toluidine blue stains, as is observed in human pulmonary alveolar lipoproteinosis.

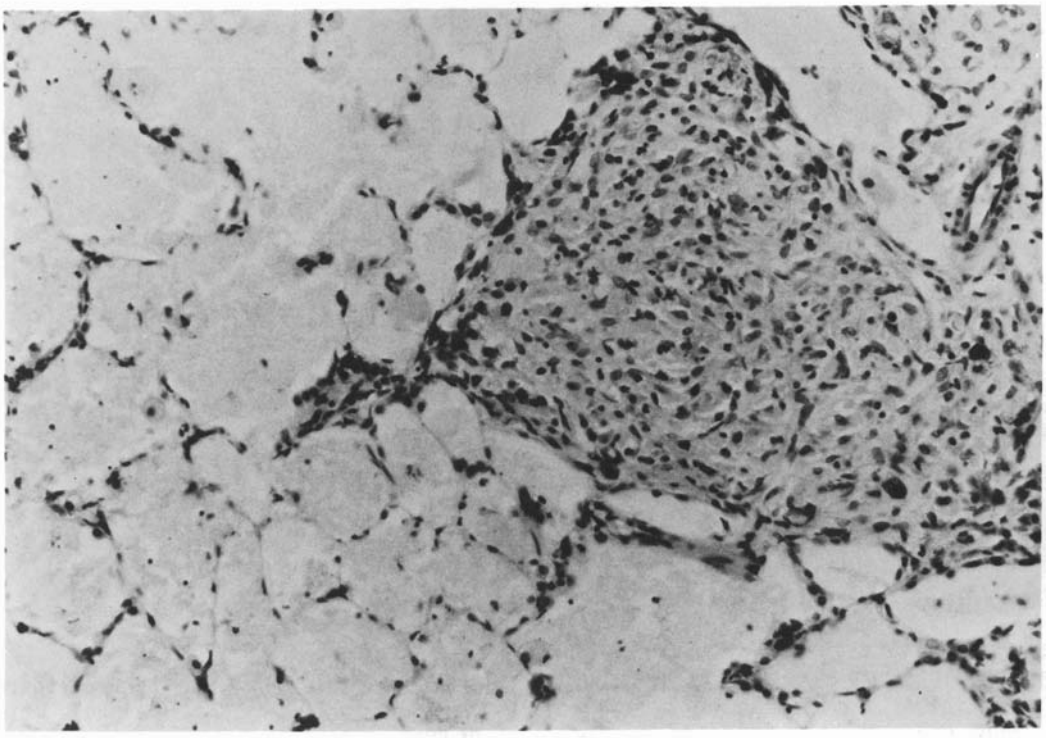

FIGURE 5.2. Granuloma with Prominent Fibrous Component in Lung Section from Rat Exposed to Quartz; 8 mo Postexposure. Lipoprotein is visible in adjacent alveoli.

CARCINOGENIC POTENTIAL OF RAW AND SPENT SHALE PARTICULATES

Investigators:

R. A. Renne, K. E. McDonald and L. G. Smith

Technical Assistance:

K. M. Dragoo

Rats and hamsters exposed to raw or retorted shale developed a granulomatous response with alveolar epithelial hyperplasia 12 mo after the first exposure. Rats also developed alveolar proteinosis. No evidence of a neoplastic response was observed.

In March, 1976, a study of the carcinogenic potential of intratracheally instilled raw or spent oil shale was initiated, using rats and hamsters of both sexes. The experiment design for this study is outlined in Table 5.5.

Shale samples were obtained from Laramie Energy Research Center (LERC), Laramie, Wyoming; raw shale was from Colorado; spent shale was obtained from the small experimental retort at LERC. The shale material, ground in a ball mill, had particle sizes ranging from 0.5 μ to 1.5 μ, with a mean particle diameter of 0.9 μ.

TABLE 5.5. Experimental Design

Exposure Group[a]	Number of Rats Examined at Each Sacrifice Period			
	0 mo	12 mo	18 mo	24 mo
Raw Shale (20 mg)	10	10	10	40
Raw Shale (5 mg)	10	10	10	40
Spent Shale (20 mg)	10	10	10	40
Spent Shale (5 mg)	10	10	10	40
BaP - Fe_2O_3 (3 mg)	—	—	—	40
Vehicle Control (saline)	—	10	10	40
Shelf Control	—	10	10	40

(a) Rats were given 5 bimonthly intratracheal instillations of shale; the positive control group (BaP-Fe_2O_3) was given 5 biweekly instillations.

Rats and hamsters were given five bimonthly intratracheal instillations of particulate raw or spent shale in two concentrations (20 mg or 5 mg). A positive control group of each species was given benzo(a)pyrene and ferric oxide (BaP-Fe_2O_3). The experimental design is indicated in Table 5.5.

Histopathology is complete on rats sacrificed at 12 mo after the first exposure (4 mo after the last exposure), and examination of tissues from animals sacrificed at 18 mo (September 1977) is in progress. The final (24-mo) sacrifice is scheduled for March 1978. The principal cellular response of the lung to the presence of particulate shale at 12 mo was aggregation of large numbers of alveolar macrophages and minimal to mild hyperplasia of alveolar epithelium. Alveolar epithelial hyperplasia was slightly more noticeable in rats exposed to spent shale. In addition to the cellular response, alveolar lipoproteinosis was present in lungs of many shale-exposed animals, similar to that observed in shale- and quartz-exposed animals in the fibrosis study (elsewhere in this Annual Report). Further investigation of the nature of this material is in progress. The degree of tissue response in the lungs of rats administered 5 mg/dose was less than those given 20 mg/dose in both the raw

and spent shale groups. No evidence of a neoplastic response to shale was observed at the 12-mo sacrifice.

The hamster portion of the study was terminated 14 mo after the first exposure due to a high mortality rate in all groups, including controls. Histopathologic examination of these animals is in progress. In the animals examined to date, the response to both raw and spent shale has been aggregation of alveolar macrophages, minimal to mild hyperplasia of alveolar epithelium, and minimal to mild interstitial fibrosis of alveolar septa.

RESPONSE OF LUNGS TO INTRATRACHEALLY ADMINISTERED OIL SHALE DUSTS

Investigators:

A. J. Gandolfi and C. A. Shields

Technical Assistance:

C. T. Resch

Rats were dosed intratracheally with suspensions of oil shale, spent shale, or quartz. The animals were sacrificed periodically over the next 8 mo, and their lungs analyzed for several biochemical/physical alterations. In the lungs of the oil shale/spent shale-treated animals, there was initial inflammation, with increases in lung weight, characterized by a doubling in collagen content, and an almost threefold increase in soluble lipoprotein.

This report describes measures of some pulmonary biochemical effects of acute intratracheal exposure to spent shale, oil shale, and quartz particulates (0.9 μMMAD) and accompanies a pathologic study on similarly treated animals (see Renne et al., this Annual Report). The oil shale and spent shale were obtained from the 10-ton experimental retort at the Laramie Energy Research Center (LERC), using Colorado oil shale. Since this is an experimental unit, data reported should not be considered as representative for all running conditions of the retort, nor representative of other oil shale extraction methods.

Male Wistar rats, 50 per group, were dosed intratracheally at three weekly intervals with particulates suspended in 1 ml saline to produce the following total dose: 30 mg spent shale, 30 mg oil shale, 5 and 30 mg quartz. Animals were dosed repeatedly and with a large volume (1 ml) to assure an even distribution of this high dose. Six animals per group were then sacrificed, along with appropriate controls, at 1, 2, 4, and 8 months after the initial dose and their lungs removed for analysis. Lungs were analyzed by standard techniques for the following pulmonary parameters: lung weight, total hydroxyproline, total noncollagenous amino acids, soluble protein, soluble lipid phosphate, soluble acid phosphate, mitochondrial succinic dehydrogenase, and proline hydroxylase.

All lung weights in groups receiving the 30-mg total of particulates (3 doses at 10 mg/dose) were elevated ($P < 0.01$) at the first sacrifice and remained elevated throughout the study (Figure 5.3). At the last sacrifice period, the group receiving 30 mg of quartz almost doubled its lung weight in four months; lung weights of oil shale and spent shale-dosed groups were also elevated ($P < 0.01$). Whole-body weights for controls versus treated animals did not vary significantly at any of the sacrifice periods except for the quartz-5 mg group, which had a slight reduction in body weight (see Renne et al., this Annual Report).

Two months after the initial dose, there was a nonsignificant elevation in total pulmonary hydroxyproline in the higher dose groups, which is a reflection of the collagen content (Figure 5.4). By four months after dosing, the total hydroxyproline in the oil shale and spent shale-dosed animals was significantly increased ($P < 0.01$). A proliferation in collagen occurred in the quartz-30 mg group between the 4- and 8-month sacrifices ($P < 0.001$).

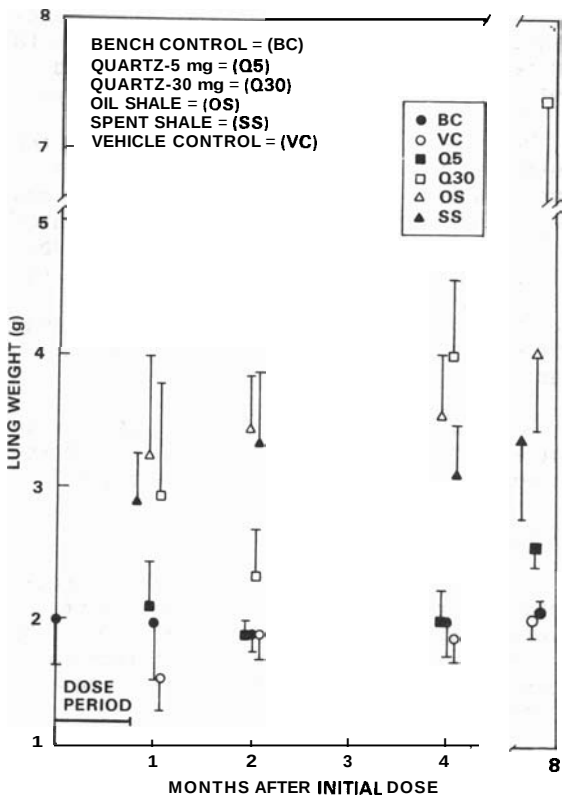

FIGURE 5.3. Lung Weights of Rats Intratracheally Exposed to Oil Shale Dusts

In the 30-mg total dose groups there was immediate proliferation of proteins (not related to collagen), as reflected by the increase in pulmonary noncollagenous amino acid equivalents (Figure 5.5). The increases are significant ($P < 0.005$); even the quartz-5 mg group is elevated at the last sacrifice period ($P < 0.02$). The quartz-30 mg group again had a large increase between the 4- and 8-month sacrifice periods, but not as large as its increase in hydroxyproline. These increases in noncollagenous amino acid equivalents in total lung were found not to be sedimented by centrifugation, indicating increases in soluble protein content.

Coinciding with the increase in soluble protein was a corresponding increase in lipid phosphate (Figure 5.6). Pathologic studies support these findings (see Renne, et al., this Annual Report).

Pulmonary tissue was also analyzed for acid phosphatase, as an indication of inflammation, and for mitochondria1 succinic dehydrogenase, as an indicator of alterations in bioenergetics. At the first sacrifice there was a significant (50%) increase ($P < 0.01$) in the specific acid phosphatase content of groups receiving 30 mg of particulates. This was the only significant alteration in

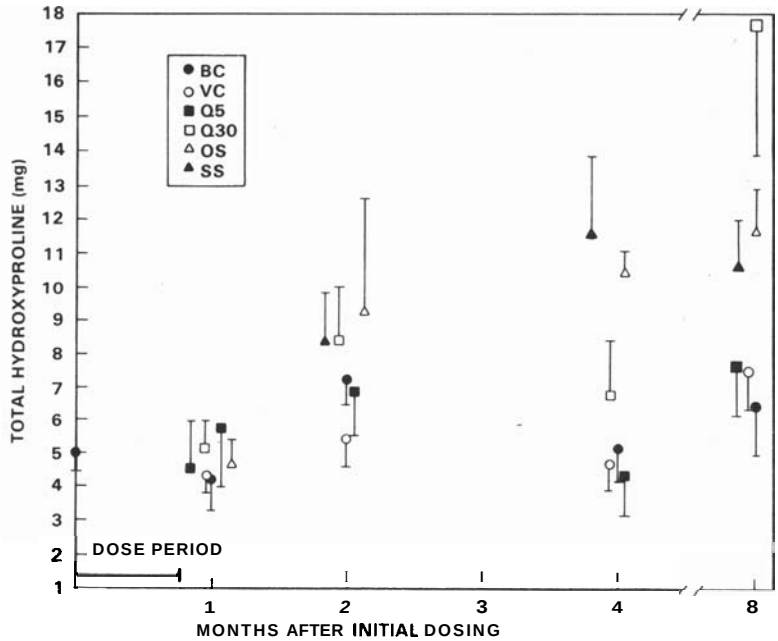

FIGURE 5.4. Total Pulmonary Hydroxyproline

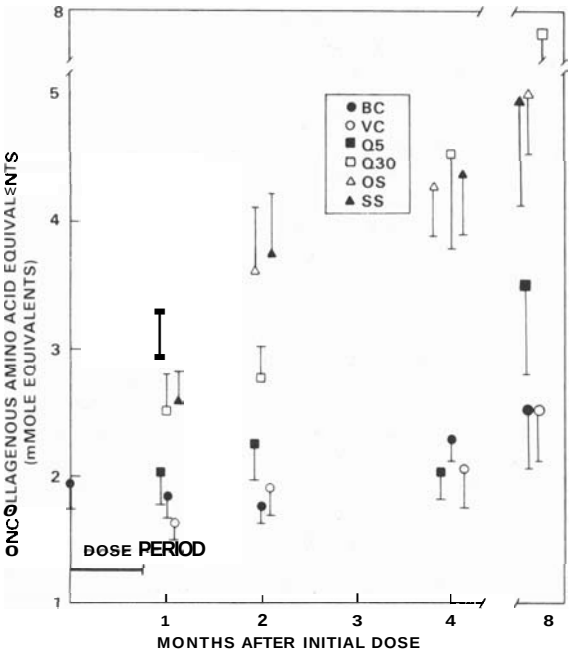

FIGURE 5.5. Total Noncollagenous Amino Acid Equivalents

acid phosphatase throughout the study. Succinic dehydrogenase, which has been shown to increase prior to pulmonary fibrosis, did not change significantly during the study.

Proline hydroxylase, an indicator for the potential for collagen synthesis, was measured in lung tissue (Table 5.6). There was an initial elevation in level in all treated animals and in vehicle controls, which subsided by the second sacrifice period but was again elevated at the 4-month sacrifice. Recent technical difficulties with the assay prevent us from presenting values for the last sacrifice.

Given the changes in lung weights, specific activity for all biochemical parameters showing increases either varied erratically as a function of exposure time or did not change significantly.

Biochemical results reported here correlate with pathologic findings: a slight fibrotic condition, and accumulation of proteinaceous material similar to that observed in alveolar lipoproteinosis (see Renne et al., this Annual Report).

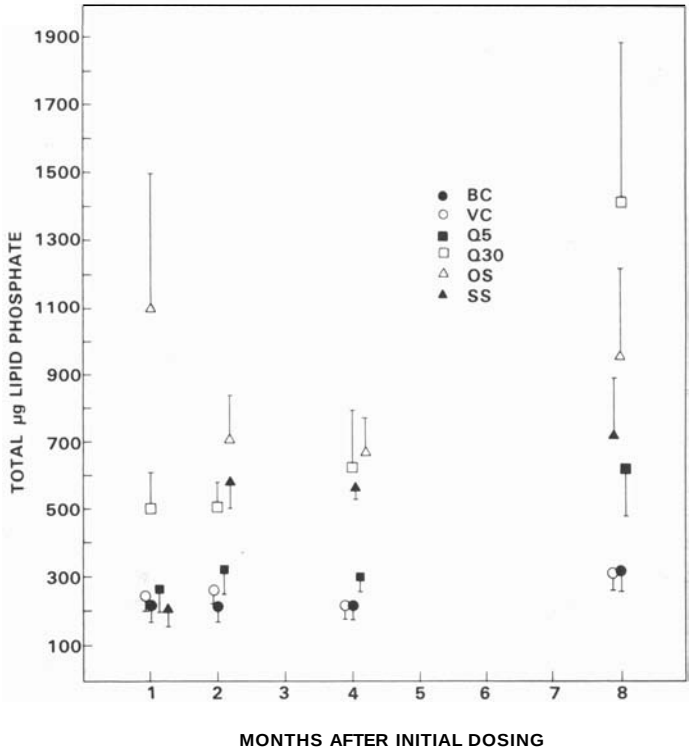

FIGURE 5.6. Total Soluble Lipid Phosphate

TABLE 56. Total Pulmonary Proline Hydroxylase (relative activity) (a)

Treatment	Months After Dosing		
	0	1	4
Bench Control	0.91 ± 0.18	1.00 f0.18	1.00 ± 0.21
Vehicle Control		1.13 ± 0.20	0.83 ± 0.15
Quartz (5 mg)		1.28 ± 0.28	1.10 ± 0.33
Quartz (30 mg)		1.45 ± 0.43	1.77 ± 0.40(b)
Oil Shale		1.92 ± 0.63(b)	1.44 ± 0.17(c)
Spent Shale		2.11 ± 0.60(c)	1.57 ± 0.16(c)

(a) Mean value of six animals normalized versus bench control
(b) Significant difference from control, $p < 0.1$
(c) Significant difference from control, $p < 0.01$

LUNG PELLET CARCINOGENESIS ASSAY OF SHALE OIL IN RATS

Investigators:

G. E. Dagle, K. E. McDonald, and L. G. Smith

Technical Assistance:

K. M. Dragoo and J. F. McShane

A preliminary 4-wk study showed metaplastic changes around the implanted pellets suggestive of an early effect of carcinogens. A chronic study was initiated to study the progression of these changes.

Lung pellet implantation has emerged as a useful and relatively inexpensive procedure for evaluating potential pulmonary carcinogens. The material to be evaluated is mixed with a beeswax-tricaprylin vehicle, and when implanted in the lungs of rats forms a pellet, with potential carcinogens slowly leaching into the surrounding pulmonary parenchyma. This technique has been successfully used to study pulmonary carcinogenesis in rats exposed to cigarette smoke condensates and methylcholanthrene.

A preliminary 4-wk toxicity study was performed to determine the highest concentration of shale oil and shale oil fractions tolerated with minimal toxic effects. Laramie Energy Research Center (LERC) whole shale oil from the 10-ton retort, and its neutral, basic, and polynuclear aromatic (PNA) fractions, were mixed with equal parts of melted beeswax and tricaprylin. For comparison with oil field material, samples of Wilmington California crude petroleum were similarly prepared. Methylcholanthrene (MCA) was used as a positive control. Young adult female Wistar rats were anesthetized with ether and 0.2 ml of pellet material, melted at 76°C, was implanted in the left lung, which was exposed by thoracotomy. All rats were sacrificed at 4 wk postinjection and the implant site in the left lung was examined histologically.

Rats tolerated the procedure well. Most rats showed a net weight increase. The PNA-, MCA-, and Crude Petroleum-treated rats gained less than the others.

Histopathologic examination of the implant site showed an apparent cavity where the pellet was dissolved during routine preparation of the slides. The vehicle produced a granulomatous reaction and a fibrous capsule surrounding this cavity (Figure 5.7). It appeared that the pellet material would interrupt the continuity of a bronchiole at some point, resulting in a tendency for growth and extension of bronchiolar epithelium along the inside lumen of the cavity. This epithelium then underwent squamous metaplasia (Figures 5.8 and 5.9). The squamous metaplasia was considerably more severe in those groups of rats with active materials added to the vehicle (Table 5.7).

The feasibility and potential value of a chronic study were indicated by the results of the preliminary study. The rats tolerated all levels of the test materials well and all materials (except vehicle) produced a significant amount of pulmonary squamous metaplasia around the pellet site. The lack of any clear dose response relationship with the shale oils was probably related to the closeness of the dosage groups; a more evident dose response relationship was obtained with the California Crude Petroleum, where there was a larger range of dosage. In previous studies employing this technique, squamous metaplasia occurred prior to the development of lung cancer.

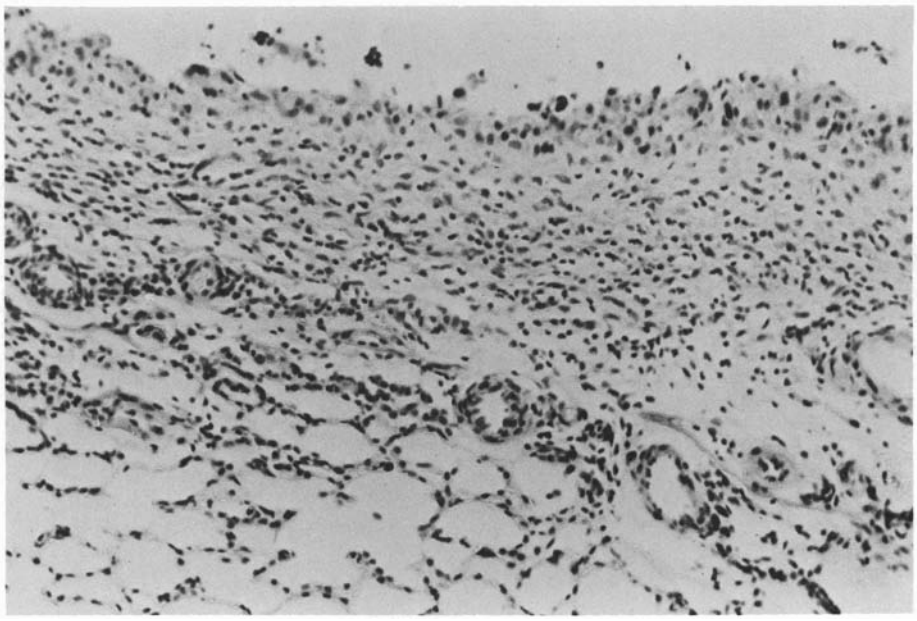

FIGURE 5.7. Lung Section Through the Pellet Site, Showing a Granulomatous Reaction to the Vehicle

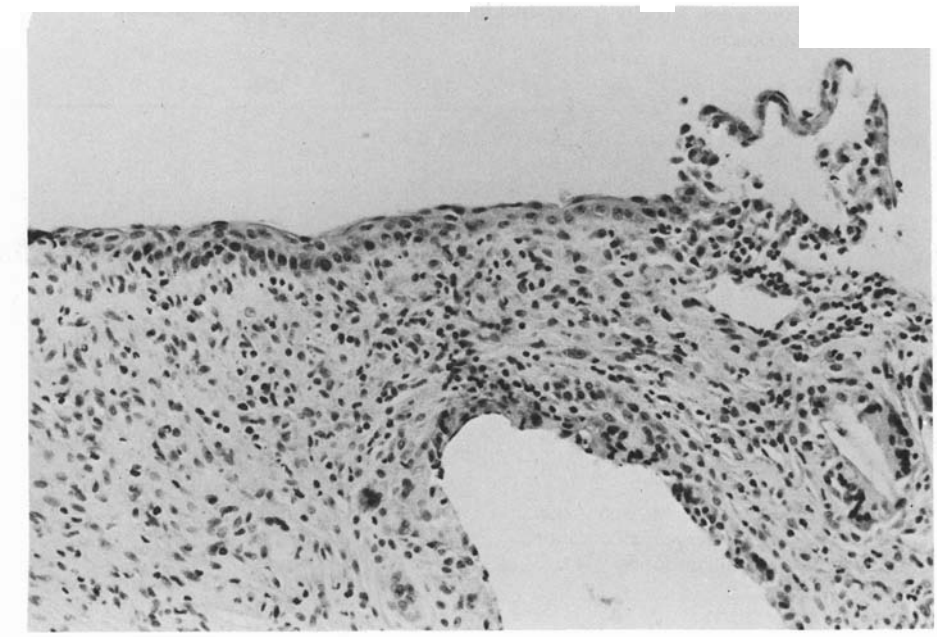

FIGURE 5.8. Lung Section Showing Squamous Metaplasia Partially Lining the Pellet Site

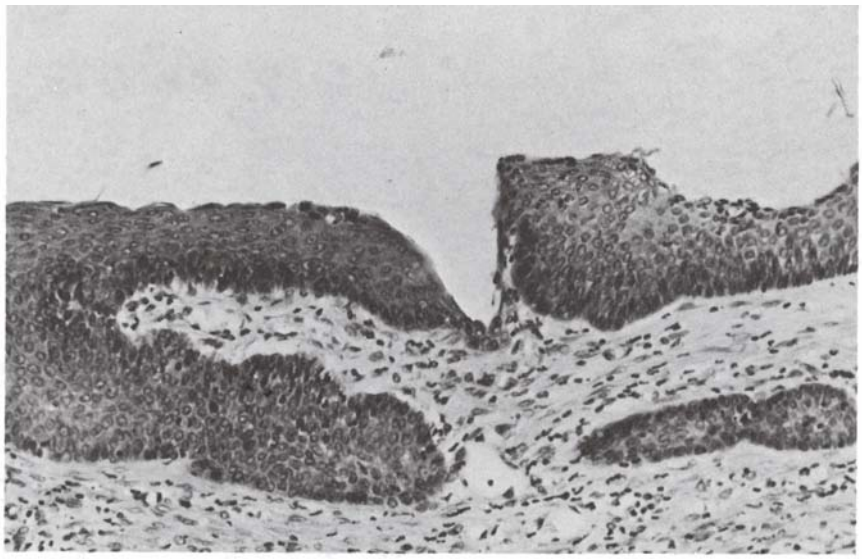

FIGURE 5.9. Lung Section Showing Squamous Metaplasia of Epithelium Extending into the Capsule of an Implanted Lung Pellet

TABLE 5.7. Four-week Toxicity Study: Incidence of Squamous Metaplasia at Lung Pellet Implant Sites.[a]

Treatment[b] (mg)	60	27	15	6.0	0.6	1.0	0
Laramie Whole Shale Oil	2.4 ± 0.6	2.6 ± 0.9	2.8 ± 0.4	—	—	—	—
Neutral Fraction	2.6 ± 0.6	1.8 ± 0.8	1.6 ± 0.6	—			—
Basic Fraction	3.5 ± 0.6	2.6 ± 0.6	2.8 h0.4	—	—		—
PNA Fraction	2.8 ± 0.4	2.7 ± 0.5	3.0 ± 0.7	—		—	—
Methylcholanthrene	—	—	—	—		2.8 ± 0.4	—
Vehicle	—	—	—	—		—	0.6 ± 0.6
Wilmington California Crude	3.0 ± 0.0	—	—	2.2 ± 0.8	1.6 ± 0.6	-	—

[a] Mean ± SD with 5 rats in each group
1 = very slight (or very small amounts)
2 = slight (or small amounts)
3 = moderate
4 = marked
5 = extreme

[b] Each rat received an 0.2-ml pellet in left lung

• Mutagenicity of Oil Shale

Utilization of oil shale as a fuel source will release to the atmosphere many organic and inorganic materials. Many of these materials, especially the polyaromatic compounds and aromatic aniines, are potentially carcinogenic. This project will test oil shale chemicals for potential carcinogenicity, using microbial and mammalian tissue-culture bioassays.

AMES TEST EVALUATION OF MUTAGENICITY OF SHALE OIL FRACTIONS

Investigators:
R. A. Pelroy and M. R. Petersen

A raw shale oil, and its basic, polynuclear aromatic, and tar subfractions, were shown to be mutagenic against S. typhimurium, TA98 and/or TA100. Mutagenicity was microsomally mediated. Although the basic and PNA fractions were about equally mutagenic when assayed separately, these fractions exerted very different effects on the mutagenicity of added chemicals.

Raw shale oil, obtained from the small retort (125 kg) at the Lawrence Livermore Laboratory, was generated by simulated, modified in situ pyrolysis of Anvil Point oil shale in run S-11, and is designated as shale oil S-11 in this report. This is a research material for use in physical-chemical and biological experimentation, and cannot be considered as a representative sample from a pilot plant or from a commercially oriented process.

Shale oil S-11 was separated into five fractions, representing classes of chemically different compounds: acidic, basic, neutral, polynclear aromatic (PNA) and a residual or tar fraction. Each of these coniplex fractions was then assayed for mutagenicity against Salnionella typhimurium strains TA100 and TA98. Figure 5.11 shows mutagenicity data obtained using strain TA100. In the experiment the microsonial (S9) enzymes were added directly to the top agar layer along with the Salmonella test strain and the crude fraction. In this technique (standard Ames Assay), cells are continuously exposed to the shale oil fraction and to mutagens formed by the S9 enzymes for the length of time that the microsomes are active.

As can be seen in Figure 5.10, the basic tar and PNA fractions, and the crude shale oil, were mutagenic against TA100, with the basic fraction the most active (1 revertant colony/μg). The acidic and neutral fractions showed little or no mutagenicity against any of the test strains (data not shown).

In the modified assay, a variant of the Ames assay was developed (data shown in Figure 5.11), in which S9 enzymes, plus either crude shale oil, complex fraction, or pure chemicals, were added to a liquid medium in a preincubation step. This was followed by addition of the Salmonella test strain (TA98) in the exposure step and dilution of the ex-

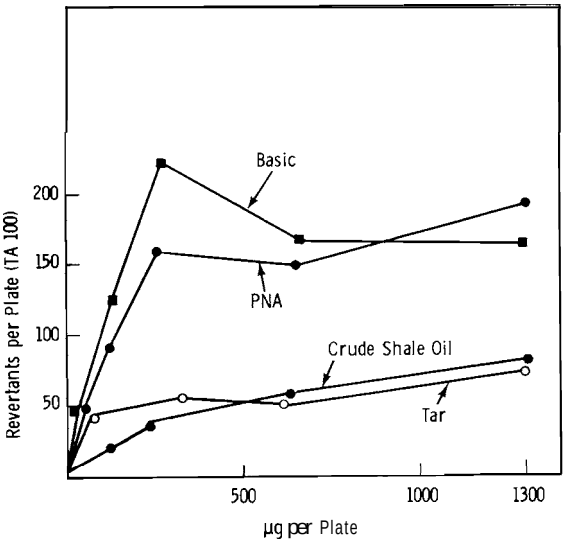

FIGURE 5.10. Mutagenicity of Shale Oil S-11 Against Salmonella *typhimurium,* TA100. Spontaneous revertants of about 70 per plate have been subtracted. Concentration of S9 protein was 1500 µg per plate.

posed cells into the molten top agar for plating, as in the standard Ames assay. Results derived from this assay are shown in Figure 5.11. While the tar fraction was slightly mutagenic in the standard assay, it showed a comparatively strong response in the modified assay. These data suggest that the modified assay is preferable for demonstrating the mutagenicity of the tar fraction of shale oil S-11, and, perhaps, for analyses of other mixtures of high toxicity to the Ames strains.

One method of estimating the importance of the composition of complex mixtures on the Ames assay is to add a chemical mutagen to a complex fraction, then compare the mutagenicity of mixed-system (chemical + fraction) with the mutagenicity of the chemical alone. This experimental approach was used with the basic and PNA fractions of shale oil S-11 as representative complex materials, and 2-aminoanthracene, benzanthracene, as the known chemical mutagens (ie., premutagens). The parameter of interest in each of these experiments is the ratio of µg complex fraction to µg chemical. This value was controlled in two ways: First, the concentration of the chemical was held at a constant level and different amounts of complex fraction were added to the system. In the second method, the concentration of the complex fraction was held constant and the chemical was varied.

From the first method it can be seen that the mutagenicity of 25 µg benzanthracene in the standard Ames assay decreased sharply with increasing concentrations of the PNA fraction (Figure 5.12). At a ratio of 10:1 (PNA fraction to benzanthracene), the number of revertant colonies per plate fell by approximately 50%. Increasing this ratio to 50:1 resulted in approximately a 94% decrease in the number of revertant colonies formed. Using the second method, the effect of the basic fraction on the mutagenicity of the nitrogen-containing premutagen, 2-aminoanthracene, was determined. The maximal mutagenic response was approxiniately the same in the presence or absence of the basic fraction (Figure 5.13). However, the rate of mutagenesis (revertant colonies per µg chemical) was somewhat reduced by the basic fraction.

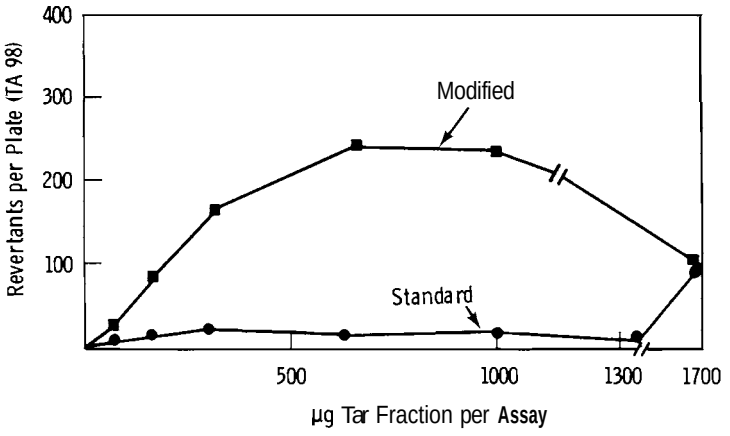

FIGURE 5.11. Comparison of Modified Versus Standard Assay: Tar fraction from Shale Oil S-11. Each sample contained 500 µg of S9 protein in the top agar or in the liquid pre-incubation mix. The background number of spontaneous revertant colonies was subtracted from the total.

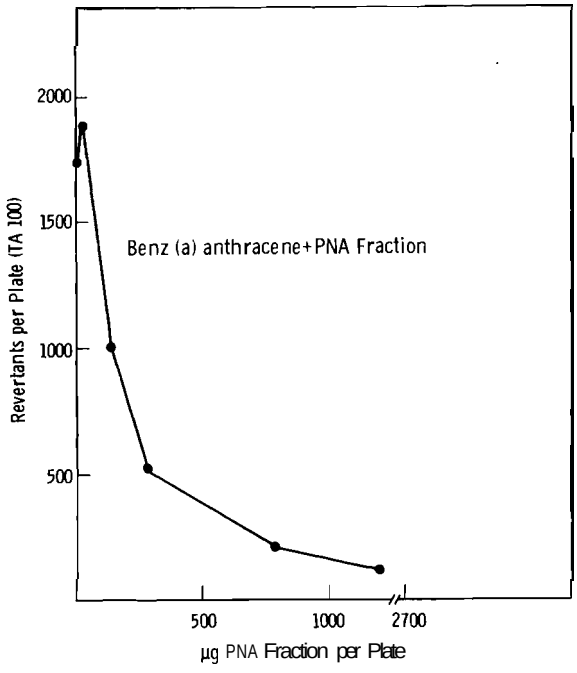

FIGURE 5.12. Effect of PNA Fraction on Mutagenesis by Benz[a]anthracene. Concentration of benz[a]anthracene was fixed at 25 µg per plate. Spontaneous revertant colonies estimated at 90 per plate were subtracted. Each plate contained approximately 2000 µg of S9 protein.

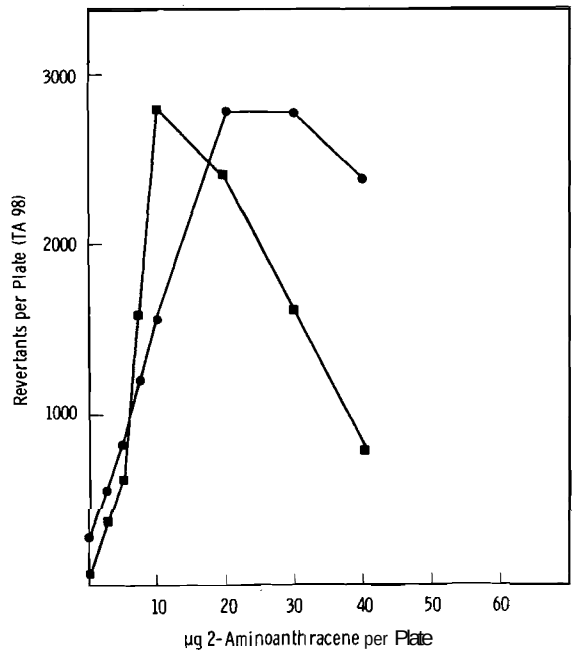

FIGURE 5.13. Effect of Basic Fraction on Mutagenesis by 2-aminoanthracene spontaneous revertant colonies estimated at 100 per plate were subtracted. Each plate contained approximately 2000 µg S9 protein. Concentration of basic fraction per plate was fixed at 1295 µg, ●. Response curve for 2-aminoanthracene alone is designated by ▪.

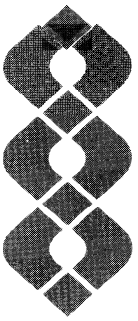

6.0 Multitechnology

MULTITECHNOLOGY

• Toxicology of Inhaled Acid Aerosols

Acid aerosols are present in many industrial processes as well as being common industrial effluents or secondary effluents formed from gaseous products released into the atmosphere. Although acute effects following exposure to strong mineral acids are generally well recognized, there is little information on the long-term hazard of subacute exposures to such aerosols. This project will investigate the long-term biological effects in rats following inhalation of inorganic acid aerosols generated from solutions of nitric acid, sulfuric acid, and hydrochloric acid.

LATE EFFECTS OF ACID INHALATION

Investigators:

J. E. Ballou, R.A. Gies, G. E. Dagle

F. G. Burton and O. R. Moss

Technical Assistance:

R. L. Music and K. D. Wiemers

Studies with nitric acid aerosols have not confirmed earlier findings of bone tumor induction with this agent. Neither bone tumors nor lung tumors have been observed during a 375- to 650-day period following exposure to nitric, sulfuric or hydrochloric acid aerosols.

Earlier studies with rats exposed to trans-uranic nitrate aerosols showed that bone tumors developed in a treated control group exposed only to 0.27 N nitric acid aerosols (Annual Report, 1976). The present study repeats the earlier nitric acid exposure and extends the scope to include animals exposed repeatedly to varied concentrations of nitric acid, sulfuric acid and hydrochloric acid aerosols.

The protocol for studies now in progress is summarized in Table 6.1. Values for estimated deposition were derived from the aerosol particle size distribution and assumed values for ventilation parameters and fractional deposition. Various groups in this study have been in progress for 375 to 650 days without producing an osteosarcoma. Benign lesions in bone (osteoarthritis) have been seen in both control and acid-exposed animals. There has been no gross pathology indicative of lung tumor induction.

Treatment with acid aerosols at the levels indicated in Table 6.1 has resulted in mortality ranging from 9 to 25% during the 375- to 650-day course of the study. Daily observation, periodic weighing and pathologic examination of tissues will continue throughout the life-span study.

TABLE 6.1. Protocol for Acid Aerosol Exposures.

Agent	Number of Rats	Chamber Concentration		Estimated Total Deposition, mg
		mg/ℓ	Fraction TLV	
HNO_3	62[a]	0.034	7 ± 2	0.1
	50	0.049	10 ± 2	6.8
	50	0.018	4 ± 1	2.3
	50	0.013	3 ± 1	2.0
HCl	50	0.022	3 ± 1	2.5
	50	0.009	1 ± 0.6	1.3
	50	0.005	0.7 ± 0.4	0.7
H_2SO_4	50	0.156	160 ± 50	26
	50	0.023	23 ± 4	3.2
	50	0.004	4 ± 1	0.7
Controls				
Treated				
Nontreated	45			

[a] Rats exposed 30 minutes, nose only, to 0.27 N HNO_3 using Lovelace nebulizer. All other groups were exposed for 6 hr per day on alternate weekdays for a total 6 exposures using a Retec nebulizer.

[b] Water aerosol

• Mobilization of Deposited Metals

This project seeks to develop treatments for overexposure to toxicants, particularly metallic or organometallics, that humans may encounter during energy or fuels research, development and production. Associated with this is identification of the toxic agents, their effects, mechanisms of toxicity, development of suitable test models and exposure procedures, and use of information from these studies in developing and recommending treatment to alleviate or decrease potentially toxic effects from both acute and chronic exposures.

PRODUCTION AND PURIFICATION OF SIDEROCHROMES

Investigator:
A. V. Robinson

The method of producing pure siderochromes, reported last year, was refined and scaled up to produce milligram quantities of siderochronies Md II and Md III from Micrococcus denitrificans. The method is being extended to three more strains of catechol-producing microorganisms, Bacillus subtilis, Klebsiella aerogenes, and Escherichia coli. The use of chelex 100 (a metal-binding resin) in the culture flask was found to significantly increase siderochrome production in E. coli and B. megaterium (hydroxamate producer). K. aerogenes catechol production was not increased.

In last year's Annual Report we described the development of an analytical method to purify siderochromes from crude media. This method has been refined and scaled up to produce milligram quantities of siderochromes (Md II and Md III) from M. denitrificans. The method is also being extended to other catechol-producing microorganisms, E. coli, K. aerogenes, and B. subtilis. Production of siderochromes is complicated by the procedures necessary to exclude iron from the growth media. Tentative investigations have indicated the potential usefulness of chelex 100 (a chelating resin, BioRad Laboratories) as a media constituent during growth, limiting iron availability.

The purification of Md II and Md III was accomplished. In various runs, 2-5 ℓ of cell-free M. denitrificans media containing 30-54 mg catechol were then placed on the column. The effluent was assayed for catechol and showed none. Adsorbed catechol was then washed with distilled H_2O before being eluted with a two-step gradient of tetrahydrofuran (THF): methanol (MeOH):5% ammonium acetate (AA) (1:1: 1, V/V/V), followed by THF/MeOH/10% AA (1:1:1, V/V/V).

A UV_{254} trace and assayed catechol content of the eluate from one run is shown in Figure 6.1. The tubes at the junctions marked were run on polyamide TLC plates in the 5% AA solvent and indicated no cross contamination. TLC of fractions 2 and 6 on both polyamide and cellulose supports indicated purity for these fractions and contained 62% and 22%, respectively, of the recovered catechol.

Results of elemental analysis of Md II and Md III are given in Table 6.2, and compared to values published for the same materials from a M. denitrificans strain. The differing elemental analyses may be due to use of different microbial strains for siderochrome production (we employ ATCC 19367; study quoted utilized NCIB 8944).

To test the applicability of the polyamide purification system on other catechol producing bacteria, B. subtilis, K. aerogenes, and E. coli were subjected to polyamide TLC. The purification of siderochromes from these microorganisms appears quite analogous to the M. denitrificans Md II and Md III purification.

The production of siderochromes from iron-deficient bacterial cultures often requires the reduction of ferric iron to levels of 0.1 ppm or less. Many techniques are described in the literature to accomplish this. We may have developed a new, simple technique that appears to lower iron concentration and/or alter media conditions such that siderochromes are produced in significant yield.

The chelating resin chelex 100 was added to the growth medium of B. megaterium, K. aerogenes, and E. coli. In the case of E. coli, catechol production was increased by approximately 2X; B. megaterium hydroxamate production was increased from 0 to 7 mg/ℓ. K. aerogenes catechol production was not increased by this method. This method of deferrating media is much simpler than other currently used methods, and will be used whenever feasible to increase yield.

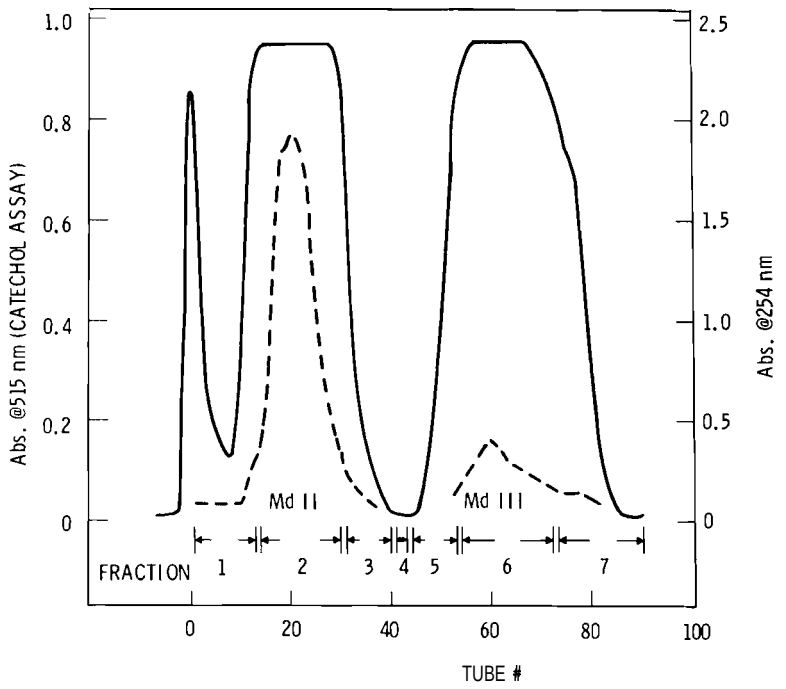

FIGURE 6.1. Preparative Chromatographic Purification of Micrococcus denitrificans Siderochromes, Md II and Md III

TABLE 6.2. Elemental Analysis of Purified Md II and Md III and Comparison with Published Values.

Element	% in Md II[a]	% Expected[b]	% in Md III	% Expected
C	40.8	60.4	47.1	60.0
N	8.2	10.1	6.6	8.8
H	5.6	6.5	5.7	6.6
O[c]	45.8	23.0	40.6	24.6

(a) Average of 2-3 analyses
(b) Based upon assumed identity with compounds isolated by Tait, *Biochem. 146:*191-204, 1975.
(c) Extrapolated value based upon C, N, H percentages

EVALUATION OF THE TOXIC EFFECTS OF HEAVY METALS AND CHELATING AGENTS IN VERO CELLS

Investigators:

M. E. Frazier, T. K. Andrews,

B. B. Thompson, and M. A. Wincek

Technical Assistance:

C. White and M. J. Hooper

An in vitro assay for determining toxicity of metallic compounds is described. A relative ranking of metal toxicity in tissue culture cells is reported and compared to the toxicity of metallic compounds in vivo.

Last year (Annual Report, 1976) we reported the development of an inexpensive and rapid in vitro assay for determining metal and chelon toxicity. The compounds under test at varying concentrations are added to a known number of VERO (monkey kidney) cells and the degree of clone (colony) formation relative to control cultures is observed.

The test material is diluted in culture medium (RPMI 1640, supplemented with 10% fetal bovine serum) and the VERO cells are grown in this milieu throughout the experiment. Any cluster of eight cells present at the end of the experiment is scored as a clone. The relative plating efficiency (the number of colony-producing cells in the experimental wells plus test material divided by the number of colony-producing cells in the control well minus test material) is used as the measure of toxicity. Toxicity for these compounds has been determined over a wide range of values, but only the RPE_{50} (the point where the relative plating efficiency equals 50%) is shown in Table 6.3. Based on these findings, the scale of metal toxicity in vitro is: Cr > V > Ru > Cd > Hg > Co > Cu > Ni > Zn > Pb > Fe >> Ca. This ranking appears to be largely consistent with the relative hazard rating of these same compounds under industrial conditions. RPE_{50} values are similarly reported for several potential chelating agents. Information on the relative toxicity of these compounds in humans and animals is seldom available.

In a further attempt to evaluate our assay system we have plotted in Figure 6.2 our RPE_{50} values against metal concentrations that result in a lethal dose for 50% of exposed experimental animals (LD_{50}). There is a positive correlation (0.73) between RPE_{50} and LD_{50} values. This correlation coefficient derives from only eight data points, but it suggests that the comparison of RPE_{50} with LD_{50} values may be a reasonable means, with further development, of estimating toxicity to higher organisms from cell culture data. It should be noted that uncertainty attaches to the LD_{50} values for metal toxicity; e.g., the relative toxicity ranking of metals based on the LD_{50} data would be: Cu > Cd > Hg > Ni > Zn > Fe > Pb; however, the preponderance of scientific literature does not support the contention that copper is more toxic than either cadmium or mercury.

TABLE 6.3. Comparison of In Vitro Toxicity to Industrial Toxicity Ratings.

Test Agent	RPE_{50}[b] Dose, g/ml[d]	Relative Hazard[c] Rating
Metal Ions[a]		
Cr	0.006	3
V	0.03	V
Ru	0.1	U
Cd	0.6	3
Hg	2.44	3
Co	2.7	1
Cu	6.6	1-2
Ni	8.0	1-3
Zn	14.4	V
Pb	37.0	0-3
Fe	59.0	1
Ca	>1000.0	0
Chelating Compounds		
8-hydroxyquiniline	<0.01	NA[e]
1-pyrolidine carbodithiothoic acid	0.1	NA[e]
Ca-DTPA	28.0	NA[e]
Siderochromes I, II, and III	~50.0	NA[e]
Dihydroxybenzene	90.0	2-3
Na-EDTA	365.0	1-2
Zn-DTPA	4000.0	NA[e]

(a) All metals were tested as chloride salts except Cr, which was tested as chromate

(b) That concentration of metal ion resulting in a 50% reduction in the number of eight cell clones following a 5-day exposure

(c) Dangerous Properties of Industrial Materials, 4th Ed., N. Irving Sax. Van Nostrand Reinhold Company, New York, NY, 1975. Toxic Hazard rating: 0 - none, 1 - slight, 2 - moderate, 3 - high, U - unknown, V - variable

(d) The metal concentrations are estimates, based on dilutions. Ultrafiltration experiments have been carried out and the actual concentration of available metal ion will be determined using analytical procedures

(e) Rating not available

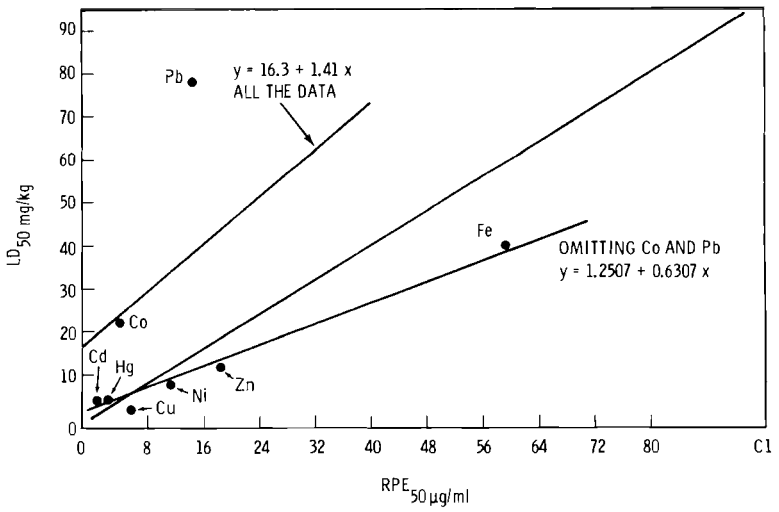

FIGURE 62. LD_{50} Values are Plotted Versus RPE_{50} Values. If all eight data points are included the correlation is equal to 0.733. If Co and Pb are omitted as potential outliers, a correlation of 0.994 is obtained. LD_{50} values are from Bienvenu, et al. CR Acad Sci (Paris) 256:1043.

• Metal-Membrane Interactions

The ionic forms of most toxic metals penetrate cell membranes slowly and it seems likely that their primary effects are exerted at the membrane level. Information on the interaction of metals with defined membrane functions may therefore be expected to aid in predicting potential effects of trace metals derived from fossil-fuel combustion. In its present stage, the research is attempting to define the role of membranes in regulating cellular synthetic activity and cell division and to study membrane alterations which accompany cell transformation to the neoplastic state.

ATPase OF AVIAN MYELOBLASTOSIS VIRUS AND THE HOST CELL MEMBRANE

Investigator:
R. P. Schneider
Technical Assistance:
L. M. Butcher

Gel electrophoresis with SDS has shown that ATPase-containing particles from avian myeloblastosis contain seven major polypeptides, two of which are virus-specific glycoproteins. This suggests that ATPase is associated with surface projections of the virus. The level of ATPase activity on the external surface of the host cell appears to be correlated to the rate at which the cell produces virus. These observations suggest that synthesis and assembly of the enzyme is closely linked to virus production.

The lipid-protein envelope of Avian Myeloblastosis Virus (AMV) contains an ATPase which presumably originates in the host-cell membrane and is transferred to the virus during its maturation. The ATPase may be a useful tool for investigation of virus control over the composition of the host-cell membrane and, thus, for identification of cancer cells. Previous efforts have been directed towards characterization of the virus enzyme; extraction of the virus with cholate and subsequent centrifugation yields a particle in which the enzyme is purified about tenfold, compared to whole virus. Further purification has not been possible since activity is lost upon solubilization (Annual Report, 1976).

During the past year we have examined the cholate-extracted particles with polyacrylamide gel electrophoresis in the presence of sodium dodecyl sulfate (SDS). This technique separates proteins which have been dissolved

in a detergent (SDS) according to their molecular weight.

The four major bands in gels of intact virus particles (Figure 6.3), known to be internal structural polypeptides (p27,p19, p15,p12), are present in much lower concentrations in gels of ATPase particles (Figure 6.4). The particles, however, are enriched in proteins, found in two complexes (p37-p35 and p77-p75), each of which contains a virus-specific glycoprotein. The particles are also enriched in three additional polypeptides (p100, p95, and p64). Since specific activity of the particles is ten times that of the virus, it follows that one or more of the seven enriched polypeptides possesses the ATPase activity. These proteins are all part of a stable complex which includes the glycoprotein spikes and knobs seen protruding from the virus in electron micrographs. Thus ATPase is a component of a virus-specific structure rather than a portion of the host-cell membrane, suggesting that it is derived from or controlled by the virus genome.

Leukemia cells that produce the virus possess ATPase activity on the exterior surface of the cell membrane, which is presumably the source of viral enzyme. As can be seen in Table 6.4, intact cells have a higher activity than broken cells. Since ATP cannot penetrate cell membranes, this suggests that most of the activity of the cells is on the outside of their membranes and, further, that more then one-half is lost by membrane folding, which prevents access to substrate after cell disruption. Enzyme activity of cells increased approximately threefold following culture for 3 days. After 47 more days of culture, activity decreased by 69%, and rate of virus production decreased by 75%. The correlation between ATPase activity and virus production suggests that synthesis of the enzyme is coupled to that of the virus. In both 3-day and 50-day cultures, virus production in 1 day accounted for loss of one-half of the total cellular ATPase activity.

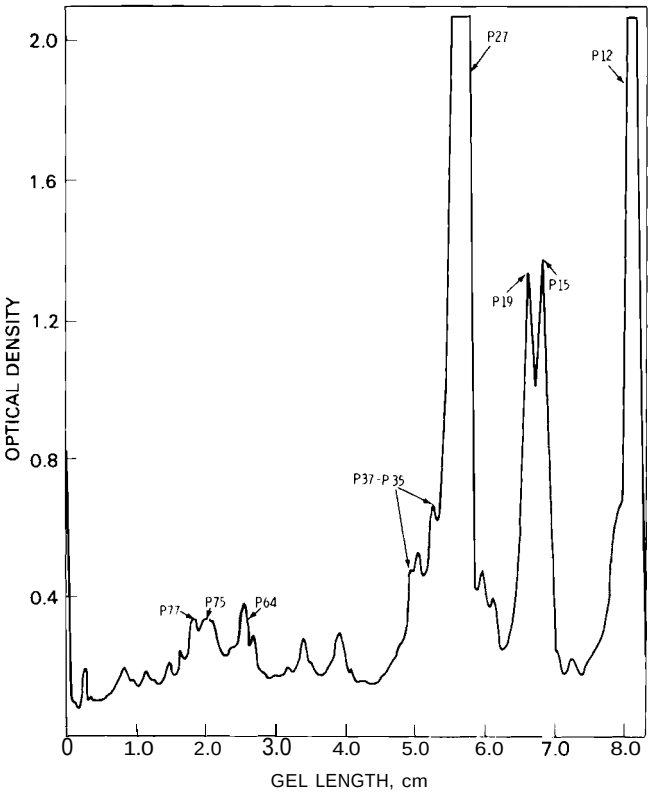

FICURE6.3. Optical Density Scans of Polyacrylamide Electrophoresis Gels of Whole Avian Myeloblastosis Virus Dissolved in 1% SDS and 5% Mercaptoethanol

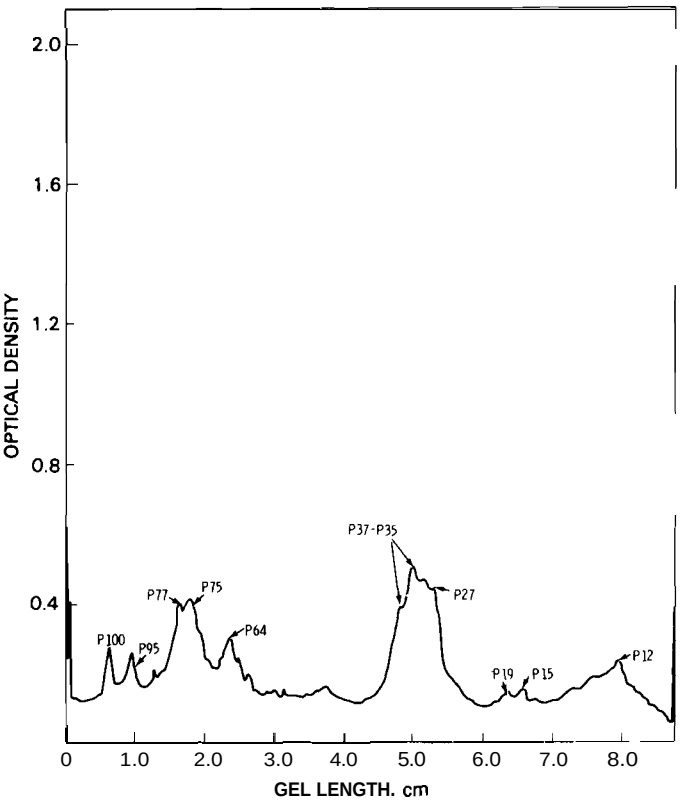

FIGURE 6.4. Electrophoresis Gels (SDS) of Purified ATPase Particles Isolated by Cholate Treatment of Avian Myeloblastosis Virus and Separated by Centrifugation. These particles were dissolved in 1% SDS and 5% mercaptoethanol for gel electrophoresis.

TABLE 6.4. ATPase Activity of Myeloblast Cells

Cell Source	Treatment	Viability (%)	ATPase Activity μmoles $(1 \times 10^9)^{-1}$min^{-1}
Leukemic Chick	Ringer's	95	77
	Distilled Water	<1	22
	Freeze-Thaw	<1	12
Culture (3-day)[a]	Ringer's	95	200
Culture (50-day)[b]	Ringer's	94	62

[a] Cells produced 4779 virus cell^{-1} day^{-1}
[b] Cells produced 1176 virus cell^{-1} day^{-1}

MORPHOLOGICAL CHANGES AND EXOCELLULAR PROTEASE SIS IN NEUROSPORA CRASSA

Investigator:
H. Drucker
Technical Assistance:
L. C. Neil

Spheroplasts prepared by enzymic stripping of cell walls from Neurospora crassa appear to be incapable of exocellular protease biosynthesis. When cell wall structure is regained, Neurospora crassa recovers its ability to synthesize and secrete exocellular protease.

The slime mold variant of Neurospora crassa posesses little or no cell wall structure, although it may possess some cell wall material. Previous work demonstrated that this spheroplastic mutant of N. crassa, unlike the wild-type organism, would not induce exocellular protease when placed on a medium where the protein bovine serum albumin (BSA) was sole carbon and energy source. Both these spheroplastic cells, and membrane vesicles prepared from the cells, possessed a cell-bound inactive protease that could be renioved from the cells and activated by the bacterial protease, thermolysin. The wild-type strain of N. crassa possessed a similar cell-wall or membrane-bound proteolytic enzyme.

One could hypothesize that this inability of the slime mold variant to induce exocellular protease, even though possessed of what we consider a necessary precursor for protease release (the membrane or cell-wall-bound enzyme) could be due to 1) the role of the cell wall in secretion of exocellular protease or 2) pleiotrophic effects which alter the metabolism of the cell in a non-specific fashion such that exocellular protease cannot be synthesizedlsecreted.

To differentiate between these two possibilities, wild-type cells of N. crassa, strain 74A, were treated with the enzyme(s) glusulase, which removes the cell wall of the organism, yielding spheroplasts. If cell wall structure is an obligate requirement for protease induction/secretion, these cells, when stripped of wall material, should not be capable of protease induction. If glusulase is removed from the cells and cell wall synthesis is allowed to resume, the ability of the cells to make exocellular protease should be regained. The degree to which induction occurs would then be a function of the number of cells possessing cell wall.

When N. crassa was treated with glusulase for 2 hr with the addition of the protease thermolysin in a medium where spheroplast lysis was minimal, and where BSA was sole carbon and energy source, no exocellular protease was induced by the cells (Figure 6.5) If the cells were treated with glusulase for 2 hr, washed free of the enzyme by filtration, then placed into a medium containing thermolysin and protein substrate, the ability to synthesize exocellular protease appeared to return (Figure 6.6). Microscopic examination of the cells after glusulase treatment (but before transfer to the protein-containing medium) suggested that primarily protoplastic cells were present. After 5 hr of growth in the transfer medium, the majority of cells present had what appeared to be intact cell walls.

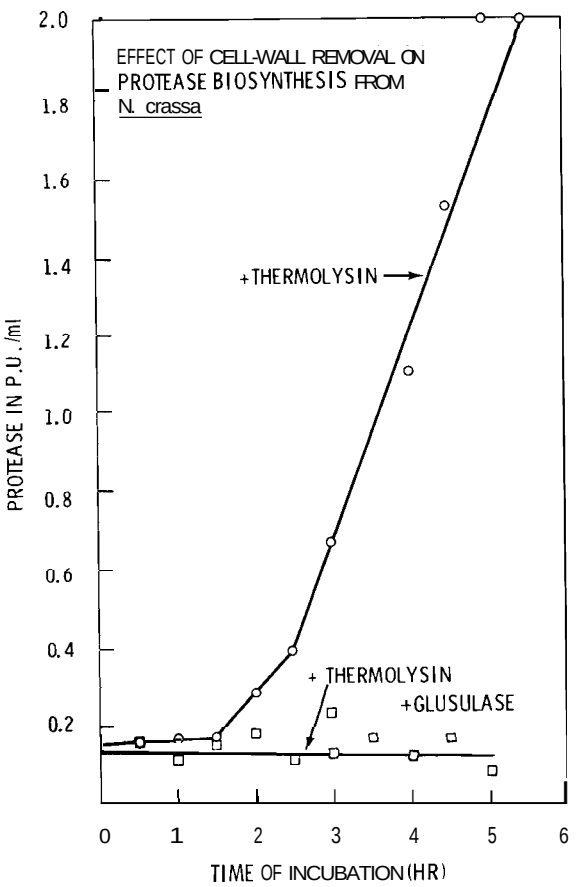

FIGURE 6.5. Effect of Cell Wall Removal on Protease Biosynthesis from N. crassa. 0—0, cells of N. crassa were placed in a medium containing the protein bovine serum albumin (1%) and 0.06 μg/ml of the bacterial protease, thermolysin. Protease was measured in the cell-free filtrate as a function of time of incubation in the medium. O—O cells of N. crassa were placed in a medium consisting of a protein substrate (1% BSA) and bacterial protease, thermolysin, was added to a concentration of 0.06 μg/ml in addition to the cell wall lytic enzyme, glusulase (0.04 ml/ml media). Protease was measured in the cell-free filtrate as a function of time of incubation in the medium.

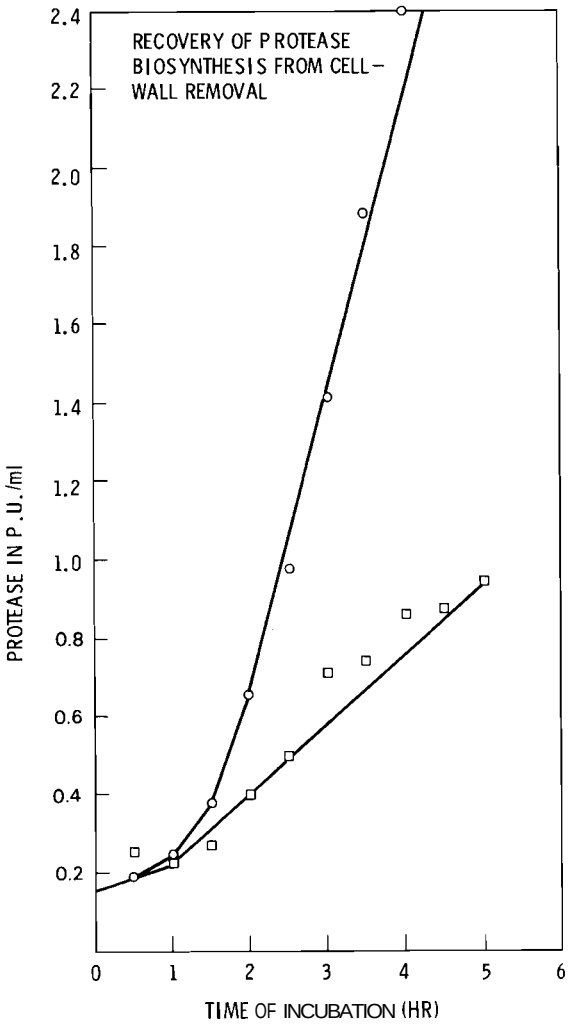

FIGURE 6.6. Recovery of Protease Induction from N. crassa After Removal of Cell Wall by Glusulase. 0–0, cells were incubated for 2 hr in a medium containing glucose as carbon and energy source, medium, then transferred to a medium containing 1% BSA as carbon and energy source, and 0.06 μg/ml of the bacterial protease, thermolysin. O--O, cells were incubated in complete medium containing 0.4 ml/ml medium of glusulase. After 2 hr, cells were transferred to a medium containing 1% BSA and 0.06 μg/ml of the bacterial protease, thermolysin. The zero time point is the level of protease in exocellular filtrate immediately after transfer of cells to inducing medium.

We found that the concentration of glusulase in the preincubation step appeared to control the number of spheroplasts at 2 hr and also the degree of "abnormality" in the mycelia of the cells. This was correlated with the number of spheroplasts and number of normal-appearing rnycelia after recovery in the transfer medium. In terms of protease induction, glusulase concentration in the preincubation was negatively correlated with rate of protease biosynthesis and level of enzyme produced after 5 hr (Figure 6.7). That is, extent and rate of protease biosynthesis appeared to be a function of number of cells possessing cell walls or, in a negative sense, of number of spheroplasts; these, in turn, were a function of glusulase concentration. If protease release from the cells before protease induction is determined (a measure of inactive cell-bound protease), it appears to remain constant at all glusulase concentrations. This suggests that numbers of cells, and spheroplasts capable of responding to thermolysin in terms of enzyme release, are constant at time 0 of induction; an observation which correlates with microscopic examination.

These results suggest that cell wall or some cell wall components may be involved in either synthesis or secretion of exocellular protease in N. crassa. There are a number of possible roles that cell wall could play in the process of protease biosynthesis. We consider three possibilities as most likely:

- Cell wall is required for attachment of protein inducer.
- Cell wall is required for secretion of protease once it is synthesized in the cell and passed to the cell membrane.
- Cell wall regulates, in some way, membrane conformation, and certain configurations of membrane are necessary in order for secretion of induced protease to occur.

Experiments examining these three possibilities are now in progress.

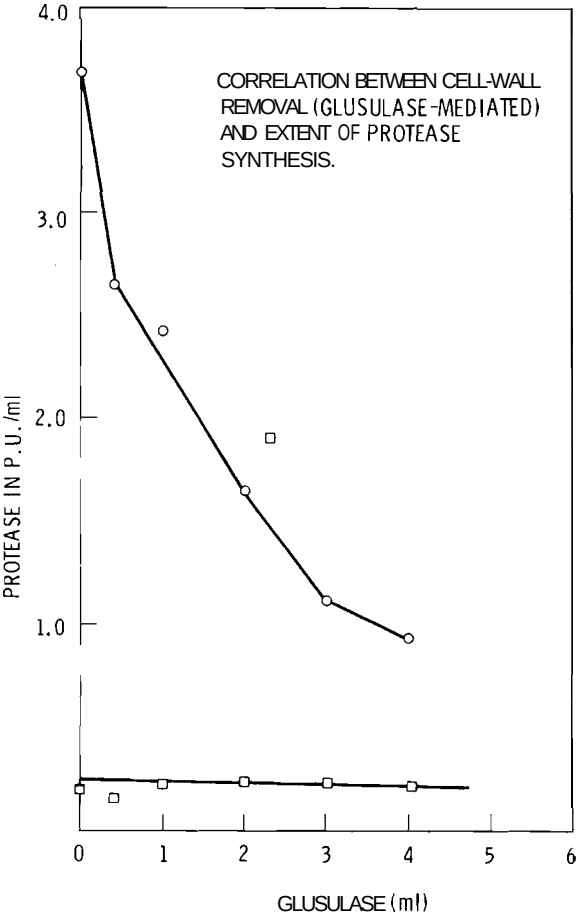

FIGURE 6.7. Effect of Glusulase Concentration on Protease Induction from N. crassa. Experimental conditions were as in Figure 6.6. 0—0, protease levels in cell-free filtrate 5 hr after transfer to inducing medium. □—□ protease levels in medium at zero time of transfer to inducing medium.

CALCIUM-MEDIATED MOLECULAR TRANSITIONS OF S-100 PROTEIN: RELATIONSHIP TO S-100 SYNTHESIS IN RAT GLIAL CELLS

Investigators:

L. E. Anderson, J. M. Morris, L. S. Winn, and W. R. Wiley

S-100 protein can be isolated in several macromolecular forms which vary in their immunoreactivity with anti-S-100. In the radioimmune assay, subunits of S-100 exhibit a response which is less than 5% that of the larger, presumably native form. Calcium appears to stabilize the protein in a trimeric conformation.

A clonal rat glial cell line, C_6, has been shown to regulate synthesis and/or accumulation of a brain-specific protein, S-100, as a function of the growth cycle (Annual Report, 1976). The amount of S-100 protein per cell, measured radioimmunologically, decreases during exponential growth and increases to a maximal level in confluent cultures. Subclones isolated from the parental C_6 cell line by an independent genetic selection process failed to accumulate S-100 in all phases of the growth cycle (Annual Report, 1976).

The implications of these and other studies are that S-100 accumulation was induced by cell-cell contact or by entry of cells into the G_1 phase of growth. In order to obtain additional evidence in support of this theory, it was necessary for us to examine the biochemical mechanisms involved in the control of S-100 accumulation. Three hypotheses (not mutually exclusive) can be evoked to explain the differential accumulation of S-100 by C_6 cells: 1) synthesis of S-100 could be repressed and/or derepressed as a function of the cell cycle; 2) specific degradation of the protein could be induced as a function of growth cycle, thereby decreasing accumulation with no change in rate of synthesis; and 3) since S-100 protein is measured immunologically, it is possible that the physical state of the molecule is altered as a function of the cell cycle, rendering it immunologically unreactive during exponential growth and reactive during stationary growth.

In FY-1977 we have obtained data which suggest that S-100 undergoes molecular transformations in vitro which are not recognized by antibody specific to "native" S-100 protein. The implication is that differential accumulation, as measured immunologically, may be due to changes in the physical state of the molecule due to physiological changes in cells as they progress from one cell cycle stage to another.

S-100 protein can be isolated in several macromolecular forms, depending upon the isolation conditions. In its "native configuration," the protein is composed of three subunits that are crosslinked by intramolecular disulfide bonds. The protein readily undergoes dissociation in the presence of reducing agent, e.g., 0.02 M 2-mercaptoethanol, to the monomeric state. The transition between trimeric and monomeric forms is shown in Figure 6.8. The molecular forms of the protein were separated by gel filtration in the presence or absence of reducing agent. The different forms of the protein were evaluated for relative amounts of S-100

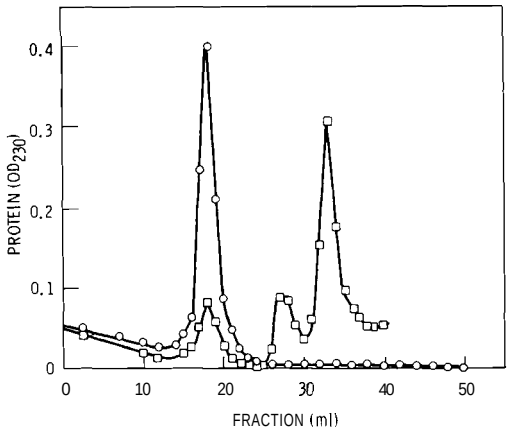

FIGURE 6.8. Gel Filtration of S-100 Protein on Sephadex G-50. (□—□) S-100 incubated in 0.02 M 2-mercaptoethanol, 1 hr, 60°C.

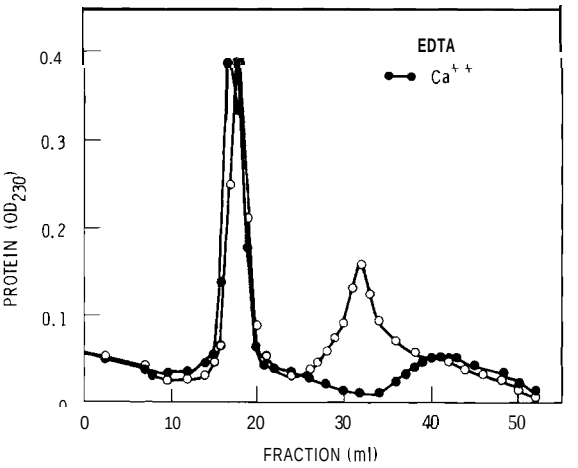

FIGURE 6.10. Gel Filtration of S-100 Protein on Sephadex G-50. (0—0) S-100 dialyzed in 0.03 M EDTA; (●—●) S-100 dialyzed in 0.002 M $CaCl_2$.

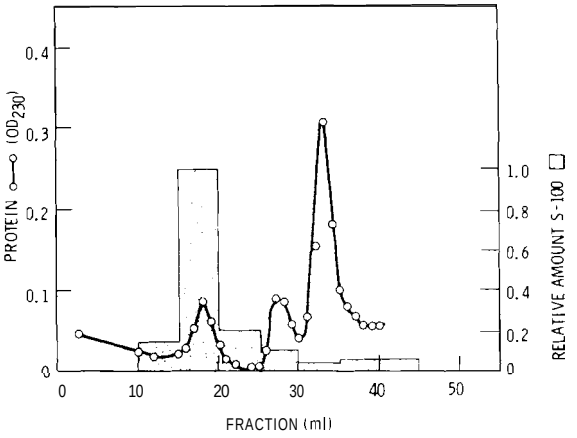

FIGURE 6.9. Gel Filtration of S-100 Protein on Sephadex C-50 Following Incubation in 0.02 M 2-mercaptoethanol, 1 hr, 60°C (0—0). Relative amounts of immunologically reactive S-100 as measured by radioirnmune assay (bar graphs).

ininiunoreactivity, using a radioimmune assay described previously (Annual Report, 1976). As shown in Figure 6.9, subunits exhibit much lower immunologic activity than the larger, presumably native, form.

The addition of 0.002 M calcium appears to stablize S-100 protein in the trimeric conformation (Figure 6.10). Reassembly of the protein from subunits can be accomplished by incubation in an oxidizing environment. The reassembled protein, however, exhibits less than 20% of the immunologic activity of the native protein.

Experiments are in progress to develop methods which stabilize the molecule in its native form. We have achieved partial stabilization of the protein in its native form by incubation of S-100 in the thiol reagent, 5,5'-dithio-bis(2-nitrobenzoic acid). This process is modulated by calcium ion, with calcium apparently stabilizing the protein and favoring the reaction of S-100 with the thiol reagent. Studies on the reassembly and stabilization of the protein in its native form are necessary to differentiate between the three alternative mechanisms for the regulation of S-100 accumulation in vivo.

In addition to the experiments described above, we have improved the sensitivity and decreased the variability of the double-antibody radioimmune assay for S-100 protein previously described (Morris et al., Annual Report, 1976). The reproducibility of the assay was improved considerably by the introduction of a second radiolabel, ^{22}Na, into the assay. The additional label provided an internal control and volume marker. Inclusion of 0.002% nonidet-40, a nonionic detergent, in each assay eliminated background problems due to S-100 protein adhering to the walls of the assay tubes. An increase in the antibody titer of both goat and horse resulted in a 20-fold improvement in the sensitivity of the assay. A 60% precipitation of S-100 is now obtained in the assay (80-100% precipitation is theoretically possible). As discussed above, the factors limiting reactivity of S-100 with S-100 antibody appears to be related to physical characteristics of the molecule. Additional work is required to determine if the in vitro experiments with

S-100 protein are applicable to the in vivo situation. However, it is of interest to point out the similarities between the aggregation and disaggregation of microtubules as a function of cell cycle and the Ca^{+2}-mediated molecular transformation of S-100 reported here. Aggregation of microtubules appears to be favored in cells trapped in the G_1 phase of the cell cycle.

APPENDIX

APPENDIX

DOSE-EFFECT STUDIES WITH INHALED PLUTONIUM IN BEAGLES

On the following pages data are presented for all dogs employed in current life-span dose-effect studies with inhaled $^{239}PuO_2$, $^{238}PuO_2$, and ^{239}Pu nitrate. Information is presented on the estimated initial alveolar deposition, based on external thorax counts at 14 and 30 days postexposure and on estimated lung weights (0.011 x body weight) at time of exposure. Information is also provided on the current interpretation of the most prominent clinical-pathological features associated with the death of animals. These data represent information presently available, and are presented as reference material for scientists who desire to follow in detail the progress of these experiments.

These computer-generated tables were produced by SNOOPY, the biomedical data base management system described previously in these reports. Since last year's report, there have been no major changes in the format of these tables. There have been several deaths in the $^{239}PuO_2$ studies and new animals have been added to the ^{239}Pu nitrate study.

DOSE-EFFECT STUDIES WITH INHALED PU-239 OXIDE IN BEAGLES

DOSE GROUP	DOG NUMBER	SEX	INITIAL ALVEOLAR DEPOSITION NCI	NCI/G LUNG	NCI/KG	INHALATION EXPOSURE WEIGHT (KG)	AGE* (MO)	DATE	DATE OF DEATH	MONTHS SINCE INHALATION 9/30/77	DEATH	COMMENTS ON DEAD DOGS
CONTROL	738	F	0	0.00	0.00					101.2*		
CONTROL	740	F	0	0.00	0.00					101.2*		
CONTROL	749	F	0	0.00	0.00					99.9*		
CONTROL	755	M	0	0.00	0.00					99.8*		
CONTROL	766	M	0	0.00	0.00					99.5*		
CONTROL	775	F	0	0.00	0.00					99.1*		
CONTROL	785	M	0	0.00	0.00					98.4*		
CONTROL	789	M	0	0.00	0.00					98.1*		
CONTROL	792	M	0	0.00	0.00				04/28/76		79.5*	ORAL TUMOR
CONTROL	800	F	0	0.00	0.00					95.3*		
CONTROL	801	M	0	0.00	0.00					95.3*		
CONTROL	811	F	0	0.00	0.00					94.2*		
CONTROL	846	M	0	0.00	0.00					93.4*		
CONTROL	861	M	0	0.00	0.00					93.0*		
CONTROL	868	F	0	0.00	0.00					91.7*		
CONTROL	872	F	0	0.00	0.00					91.6*		
CONTROL	878	M	0	0.00	0.00					89.7*		
CONTROL	882	M	0	0.00	0.00					89.5*		
CONTROL	885	F	0	0.00	0.00					88.9*		
CONTROL	903	F	0	0.00	0.00					86.6*		
CONTROL SACRIFICE	701	F	0	0.00	0.00					102.5*		
CONTROL SACRIFICE	703	M	0	0.00	0.00				03/24/77		96.2*	SACRIFICED
CONTROL SACRIFICE	724	M	0	0.00	0.00					102.0*		
D-1 LOWEST	756	M	0	0.00	0.00	13.0	19.5	01/19/71		80.4		
D-1 LOWEST	762	M	0	0.00	0.00	11.5	19.3	01/19/71	01/24/77		72.2	SACRIFICED
D-1 LOWEST	847	M	0	0.00	0.00	13.0	18.5	07/06/71		74.8		
D-1 LOWEST	858	M	0	0.00	0.00	13.0	18.2	07/06/71		74.8		
D-1 LOWEST	865	F	0	0.00	0.00	9.0	17.4	07/06/71		74.8		
D-1 LOWEST	879	M	0	0.00	0.00	14.5	17.9	10/07/71		71.8		
D-1 LOWEST	886	F	0	0.00	0.00	10.5	18.2	11/10/71		70.7		
D-1 LOWEST	907	F	0	0.00	0.00	11.5	15.9	11/10/71		70.7		
D-1 LOWEST	825	F	1	0.01	0.12	11.5	18.1	06/08/71		75.8		
D-1 LOWEST	849	F	1	0.01	0.10	10.0	21.3	10/07/71	10/26/72		12.6	SACRIFICED
D-1 LOWEST	904	F	1	0.01	0.07	10.0	15.9	11/10/71		70.7		
D-1 LOWEST	832	F	2	0.02	0.24	8.5	16.5	04/26/71		77.2		

* INDICATES , IN MONTHS SINCE BIRTH ALL OTHER AGES ARE IN MONTHS SINCE EXPOSURE

DOSE-EFFECT STUDIES NITH INHALED PU-239 OXIDE IN BEAGLES

DOSE GROUP	DOG NUMBER	SEX	INITIAL ALVEOLAR DEPOSITION NCI	NCI/G LUNG	NCI/ KG	INHALATION EXPOSURE WEIGHT (KG)	AGE* (MO)	DATE	DATE OF DEATH	MONTHS SINCE INHALATION 9/30/77	DEATH	COMMENTS ON DEAD DOGS
D-1 LOWEST	900	M	3	0.02	0.22	13.0	16.0	11/10/71		70.7		
D-1 LOWEST	870	F	4	0.03	0.32	12.0	16.9	07/06/71		74.8		
D-1 LOWEST	899	F	4	0.03	0.31	11.5	16.0	11/10/71		70.7		
D-1 LOWEST	867	M	5	0.04	0.41	11.5	17.4	07/06/71		74.8		
D-1 LOWEST	891	M	6	0.04	0.41	14.0	16.0	11/10/71		70.7		
D-1 LOWEST	850	F	5	0.05	0.59	8.5	21.3	10/07/71		71.8		
D-1 LOWEST	853	M	8	0.05	0.51	15.0	21.3	10/07/71		71.8		
D-1 LOWEST	875	M	8	0.05	0.54	14.0	16.8	07/06/71		74.8		
D-1 LOWEST	770	F	6	0.06	0.63	9.5	19.1	01/19/71		80.4		
D-1 LOWEST	788	M	8	0.06	0.62	13.0	18.7	02/09/71		79.7		
D-1 LOWEST	893	M	9	0.06	0.61	14.0	14.9	10/07/71		71.8		
D-1 LOWEST	807	F	8	0.07	0.73	11.0	14.6	02/09/71		79.7		
D-1 LOWEST	841	F	6	0.07	0.75	8.0	17.7	06/08/71		75.8		
D-1 LOWEST	908	M	9	0.07	0.77	11.0	15.9	11/10/71		70.7		
D-2 LOW	776	M	10	0.07	0.74	13.5	20.2	03/04/71		78.9		
D-2 LOW	767	M	10	0.08	0.83	12.0	18.2	12/21/70		81.3		
D-2 LOW	842	M	10	0.08	0.83	12.5	18.6	07/06/71		74.8		
U-2 LOW	920	M	11	0.08	0.92	12.0	16.0	06/08/72	07/07/72		1 0	SACRIFICED
D-2 LON	862	M	13	0.09	1.00	13.0	17.3	06/08/71		75.8		
D-2 LOW	871	M	13	0.09	0.96	13.5	16.9	07/06/71		74.8		
D-2 LON	874	M	16	0.11	1.24	13.0	16.8	07/06/71		74.8		
D-2 LOW	754	M	22	0.15	1.69	13.0	19.5	01/19/71		80.4		
D-2 LOW	845	F	19	0.15	1.63	11.5	17.6	06/08/71		75.8		
D-2 LOW	748	F	14	0.16	1.75	8.0	19.5	01/19/71		80.4		
D-2 LON	798	F	16	0.16	1.78	9.0	15.6	02/09/71	08/29/74		42.6	SACRIFICED
D-2 LON	826	F	19	0.16	1.81	10.5	19.1	07/06/71		74.8		
D-2 LOW	831	F	21	0.18	2.00	10.5	17.9	06/08/71		75.8		
D-2 LOW	881	F	19	0.19	2.09	9.0	17.7	10/07/71		71.8		
D-2 LON	780	F	24	0.22	2.40	10.0	18.2	01/19/71		80.4		
D-2 LOW	859	M	35	0.22	2.41	14.5	18.2	07/06/71		74.8		
D-2 LON	757	M	36	0.23	2.57	14.0	18.5	12/21/70		81.3		
D-2 LOW	876	F	19	0.23	2.51	7.5	17.9	10/07/71		71.8		
D-2 LOW	806	F	26	0.25	2.74	9.5	15.3	03/04/71		78.9		
D-2 LOW	813	F	32	0.28	3.05	10.5	15.1	03/04/71		78.9		
0-2 LOW	877	F	34	0.29	3.24	10.5	17.9	10/07/71		71.8		

• INDICATES AGE IN MONTHS SINCE BIRTH, ALL OTHER AGES ARE IN MONTHS SINCE EXPOSURE

DOSE-EFFECT STUDIES WITH INHALED PU-239 OXIDE IN BEAGLES

DOSE GROUP	DOG NUMBER	SEX	INITIAL ALVEOLAR DEPOSITION NCI	NCI/G LUNG	NCI/ KG	INHALATION EXPOSURE WEIGHT (KG)	AGE* (MO)	DATE	DATE OF DEATH	MONTHS SINCE INHALATION 9/30/77	MONTHS SINCE INHALATION DEATH	COMMENTS ON DEAD DOGS
D-2 LOW	769	F	28	0.32	3.50	8.0	18.2	12/21/70		81.3		
D-2 LOW	802	M	40	0.33	3.64	11.0	18.1	04/26/71		77.2		
D-3 MED-LOW	781	F	48	0.38	4.17	11.5	17.3	12/21/70		81.3		
D-3 MED-LOW	771	F	44	0.40	4.40	10.0	19.2	01/20/71		80.3		
D-3 MED-LOW	782	M	62	0.42	4.59	13.5	19.0	02/10/71		79.6		
D-3 MED-LON	786	M	62	0.42	4.59	13.5	19.5	03/04/71		78.9		
D-3 MED-LOW	752	M	62	0.43	4.77	13.0	18.6	12/21/70		81.3		
D-3 MED-LOW	823	M	65	0.44	4.81	13.5	16.8	04/26/71		77.2		
D-3 MED-LOW	883	M	63	0.44	4.85	13.0	17.7	10/07/71		71.8		
D-3 MED-LOW	778	M	74	0.46	5.10	14.5	20.2	03/04/71		78.9		
D-3 MED-LOW	838	M	56	0.46	5.09	11.0	17.8	06/08/71		75.8		
0-3 MED-LOW	795	F	54	0.52	5.68	9.5	15.0	01/20/71		80.3		
D-3 MED-LOW	815	M	68	0.52	5.67	12.0	16.8	04/26/71	05/22/73		24.9	SACRIFICED
D-3 MED-LON	851	F	53	0.54	5.89	9.0	21.3	10/07/71		71.8		
D-3 MED-LON	918	M	74	0.58	6.43	11.5	16.0	06/08/72	07/06/72		0.9	SACRIFICED
D-3 MED-LOW	834	F	67	0.68	7.44	9.0	17.8	06/08/71		75.8		
D-3 MEU-LON	797	F	85	0.70	7.73	11.0	16.4	03/04/71		78.9		
D-3 MED-LOW	848	F	75	0.72	7.94	9.5	21.3	10/07/71		71.8		
D-3 MED-LOW	827	F	89	0.81	8.90	10.0	16.7	04/26/71		77.2		
D-3 MED-LOW	697	M	140	0.85	9.33	15.0	19.5	10/30/70		83.0		
D-3 MED-LOW	750	M	118	0.93	10.26	11.5	19.6	01/20/71		80.3		
D-3 MED-LOW	834	M	123	1.12	12.30	10.0	17.8	10/08/71		71.8		
D-3 MED-LON	844	F	135	1.23	13.50	10.0	17.6	06/08/71		75.8		
D-3 MED-LOW	905	F	127	1.44	15.88	8.0	15.9	11/10/71		70.7		
D-4 MEDIUM	809	F	151	1.25	13.73	11.0	15.3	03/04/71		78.9		
D-4 MEDIUM	866	M	200	1.35	14.81	13.5	17.4	07/06/71		74.8		
D-4 MEDIUM	764	F	138	1.37	15.05	10.5	18.2	12/21/70		81.3		
D-4 MEDIUM	835	F	163	1.48	16.30	10.0	16.4	04/26/71		77.2		
D-4 MEDIUM	839	F	189	1.49	16.43	11.5	16.3	04/26/71		77.2		
D-4 MEDIUM	814	F	140	1.50	16.47	8.5	15.1	03/04/71		78.9		
D-4 MEDIUM	836	M	256	1.66	18.29	14.0	17.8	06/08/71		75.8		
D-4 MEDIUM	dl9	F	163	1.74	19.18	8.5	18.2	06/08/71		75.8		
D-4 MEDIUM	888	M	274	1.78	19.57	14.0	17.1	10/08/71		71.8		
D-4 MEDIUM	824	F	227	1.79	19.74	11.5	18.1	06/08/71		75.8		
D-4 MEDIUM	8b0	M	254	1.85	20.32	12.5	17.3	06/08/71		75.8		

• INDICATES AGE IN MONTHS SINCE BIRTH, ALL OTHER AGES ARE IN MONTHS SINCE EXPOSURE

DOSE-EFFECT STUDIES WITH INHALED PU-239 OXIDE IN BEAGLES

DOSE GROUP	DOG NUMBER	SEX	INITIAL ALVEOLAR DEPOSITION NCI	NCI/G LUNG	NCI/ KG	INHALATION EXPOSURE WEIGHT (KG)	AGE* (MO)	DATE	DATE OF DEATH	MONTHS SINCE INHALATION 9/30/77	DEATH	COMMENTS ON DEAD DOGS
D-4 MEDIUM	833	F	248	2.37	26.11	9.5	16.5	04/26/71		77.2		
D-4 MEDIUM	810	F	302	2.39	26.26	11.5	15.3	03/04/71		78.9		
D-4 MEDIUM	794	M	444	2.60	28.65	15.5	17.7	03/04/71		78.9		
D-4 MEDIUM	854	M	465	2.64	29.06	16.0	21.3	18/08/71		71.8		
D-4 MEDIUM	478	M	298	2.71	29.80	10.0	64.0	10/09/70	10/16/70		0.2	SACRIFICED
D-4 MEDIUM	d08	F	270	2.73	30.00	9.0	14.6	02/10/71		79.6		
D-4 MEDIUM	805	F	257	3.12	34.27	7.5	18.5	06/08/71		75.8		
D-4 MEDIUM	812	M	438	3.19	35.04	12.5	17.1	04/26/71		77.2		
D-4 MEDIUM	857	M	486	3.40	37.38	13.0	17.3	06/08/71		75.8		
D-4 MEDIUM	892	M	494	3.59	39.52	12.5	16.0	11/18/71		70.7		
D-4 MEDIUM	816	M	398	3.62	39.80	10.0	16.8	04/26/71	05/11/71		0.5	SACRIFICED
D-4 MEDIUM	777	M	546	3.97	43.68	12.5	20.2	03/04/71		78.9		
D-4 MEDIUM	803	M	547	4.32	47.57	11.5	18.1	04/26/71		77.2		
D-5 MED-HI	787	M	651	4.73	52.08	12.5	19.5	03/04/71		78.9		
D-5 MED-HI	840	F	703	4.92	54.08	13.0	17.7	06/08/71		75.8		
D-5 MED-HI	727	M	733	5.33	58.64	12.5	18.8	10/26/70	11/10/76		72.5	LUNG TUMOR
D-5 MED-HI	898	F	711	5.39	59.25	12.0	16.0	11/18/71		70.7		
0-5 MED-HI	759	M	809	6.13	67.42	12.0	18.3	12/21/70	06/02/75		53.4	LUNG TUMOR
D-5 MED-HI	864	F	801	6.62	72.82	11.0	17.4	07/07/71		74.8		
D-5 MED-HI	909	M	737	6.70	73.70	10.0	15.9	11/18/71		70.7		
D-5 MED-HI	734	M	914	6.92	76.17	12.0	19.2	11/10/70	04/01/71		4.7	SACRIFICED
D-5 MED-HI	856	F	818	7.08	77.90	10.5	18.2	07/07/71		74.8		
D-5 MED-HI	837	M	1283	8.04	88.48	14.5	18.8	07/07/71	07/21/77		72.5	LUNG TUMOR
D-5 MED-HI	863	F	Y80	8.48	93.33	10.5	17.4	07/07/71		74.8		
0-5 MED-HI	820	F	847	8.56	94.11	9.0	18.2	06/08/71		75.8		
D-5 MED-HI	852	F	1187	9.38	103.22	11.5	21.3	10/08/71		71.8		
D-5 MED-HI	880	F	840	9.55	105.00	8.0	17.8	10/08/71		71.8		
D-5 MED-HI	889	F	1089	9.90	108.90	10.0	16.0	11/18/71		70.7		
D-5 MED-HI	783	M	1394	10.14	111.52	12.5	18.9	02/09/71	12/03/75		57.8	LUNG TUMOR
D-5 MED-HI	804	M	1344	10.18	112.00	12.0	20.5	07/07/71	08/18/74		37.4	LUNG TUMOR RADIATION PNEUMONITIS
D-5 MED-HI	873	M	1767	10.71	117.80	15.0	16.8	07/07/71	09/03/76		61.9	LUNG TUMOR
D-5 MED-HI	760	M	1378	10.89	119.83	11.5	19.3	01/20/71	08/15/73		30.8	RADIATION PNEUMONITIS
D-5 MED-HI	796	F	1318	11.41	125.52	10.5	15.6	02/09/71	09/17/75			
D-5 MED-HI	761	M	1460	12.07	132.73	11.0	19.3	01/20/71	11/02/76		69.4	LUNG TUMOR

* INDICATES AGE IN MONTHS SINCE BIRTH, ALL OTHER AGES ARE IN MONTHS SINCE EXPOSURE

DOSE-EFFECT STUDIES WITH INHALED PU-239 OXIDE IN BEAGLES

DOSE GROUP	DOG NUMBER	SEX	INITIAL ALVEOLAR DEPOSITION NCI	NCI/G LUNG	NCI/ KG	INHALATION EXPOSURE WEIGHT (KG)	AGE* (MO)	DATE	DATE OF DEATH	MONTHS SINCE INHALATION 9/30/77 DEATH	COMMENTS ON DEAD DOGS
D-5 MED-HI	709	M	1726	12.55	138.08	12.5	19.6	11/10/70	03/31/71	4.6	SACRIFICED
D-5 MED-HI	772	M	1896	14.99	164.87	11.5	19.8	02/09/71	06/26/75	52.5	LUNG TUMOR
D-5 MED-HI	702	F	1682	15.29	168.20	10.0	19.8	11/18/70	03/31/71	4.6	SACRIFICED
D-5 MED-HI	739	F	1511	17.17	188.88	8.0	18.5	11/10/70	04/01/71	4.7	SACRIFICED
D-6 HIGH	753	F	2448	23.43	257.68	9.5	18.5	12/21/70	10/02/76	69.4	LUNG TUMOR
D-6 HIGH	817	M	3164	23.97	263.67	12.0	19.2	07/07/71	03/26/73	20.6	RADIATION PNEUMONITIS
D-6 HIGH	829	M	3515	24.58	270.38	13.0	19.1	07/07/71	09/13/73	26.3	RADIATION PNEUMONITIS
D-6 HIGH	890	F	3101	31.32	344.56	9.0	16.0	11/10/71	06/13/74	31.1	RADIATION PNEUMONITIS
D-6 HIGH	435	F	3840	33.25	365.71	10.5	75.5	11/05/70	11/12/70	0.2	SACRIFICED
D-6 HIGH	913	M	4900	35.64	392.00	12.5	17.4	07/19/72	08/18/72	1.0	SACRIFICED
D-6 HIGH	986	F	6632	63.46	698.11	9.5	15.9	11/18/71	11/22/72	12.4	RADIATION PNEUMONITIS
D-6 HIGH	dY6	F	5515	66.85	735.33	7.5	16.0	11/18/71	02/12/73	15.1	RADIATION PNEUMONITIS
D-6 HIGH	747	F	7476	97.09	1068.00	7.0	19.6	01/20/71	01/13/72	11.8	RADIATION PNEUMONITIS
D-6 HIGH	910	M	14267	103.76	1141.36	12.5	15.9	11/18/71	18/12/72	11.1	RADIATION PNEUMONITIS

* INDICATES AGE IN MONTHS SINCE BIRTH, ALL OTHER AGES ARE IN MONTHS SINCE EXPOSURE

DOSE–EFFECT STUDIES WITH INHALED **PU-238** OXIDE IN BEAGLES

DOSE GROUP	DOG NUMBER	SEX	INITIAL ALVEOLAR DEPOSITION NCI	NCI/G LUNG	NCI/ KG	INHALATION EXPOSURE WEIGHT (KG)	AGE* (MO)	DATE	DATE OF DEATH	MONTHS SINCE INHALATION 9/38/77	DEATH	COMMENTS ON DEAD DOGS
CONTROL	939	M	0	0.00	0.00					76.9*		
CONTROL	949	F	0	0.00	0.00					76.7*		
CONTROL	978	M	0	0.00	0.00					76.6*		
CONTROL	990	F	0	0.00	0.00					76.2'		
CONTROL	996	F	0	0.00	0.00					76.0*		
CONTROL	1005	M	0	0.00	0.00					76.0*		
CONTROL	1007	F	0	0.00	0.00					76.0*		
CONTROL	1024	M	0	0.00	0.00					75.5*		
CONTROL	1038	M	0	0.00	0.00					73.4*		
CONTROL	1045	M	0	0.00	0.00					73.4*		
CONTROL	1054	F	0	0.00	0.00					73.1*		
CONTROL	1061	F	0	0.00	0.00					73.0*		
CONTROL	1093	M	0	0.00	0.00					69.3*		
CONTROL	1097	F	0	0.00	0.00					68.6*		
CONTROL	1112	M	0	0.00	0.00					68.4*		
CONTROL	1116	F	0	0.00	0.00					68.1*		
CONTROL	1186	F	0	0.00	0.00					61.5*		
CONTROL	1197	M	0	0.00	0.00					61.0*		
CONTROL	1209	M	0	0.00	0.00					60.7*		
CONTROL	1225	F	0	0.00	0.00					59.9*		
CONTROL SACRIFICE	966	M	0	0.00	0.00				04/30/77		71.6'	SACRIFICED
CONTROL SACRIFICE	1011	F	0	0.00	0.00					75.9*		
CONTROL SACRIFICE	1013	F	0	0.00	0.00					75.9*		
CONTROL SACRIFICE	1087	M	0	0.00	0.00				12/14/76		60.0*	SACRIFICED
CONTROL SACRIFICE	1118	M	0	0.00	0.08				01/13/76		47.5'	SACRIFICED
CONTROL SACRIFICE	1223	M	0	0.00	0.00				05/15/75		31.9'	SACRIFICED
CONTROL SACRIFICE	1227	M	0	0.00	0.00				12/01/76		49.9*	SACRIFICED
CONTROL SACRIFICE	1228	M	0	0.00	0.00					59.9*		
D-1 LOWEST	998	M	0	0.00	0.00	10.5	19.6	01/18/73		56.4		
D-1 LOWEST	1003	M	0	0.00	0.00	14.0	19.6	01/18/73		56.4		
D-1 LOWEST	1023	F	0	0.00	0.00	12.5	19.2	01/18/73		56.4		
D-1 LOWEST	1039	M	0	0.00	0.00	11.0	17.0	01/18/73		56.4		
D-1 LOWEST	11144	F	0	0.00	0.00	11.5	17.0	01/18/73		56.4		
D-1 LOWEST	1055	M	0	0.00	0.00	13.0	16.8	01/18/73		56.4		
D-1 LOWEST	1063	M	0	0.00	0.00	14.5	16.7	01/18/73		56.4		

* INDICATES AGE IN MONTHS SINCE BIRTH, ALL OTHER AGES ARE IN MONTHS SINCE EXPOSURE

DOSE-EFFECT STUDIES WITH INHALED PU-238 OXIDE IN BEAGLES

DOSE GROUP	DOG NUMBER	SEX	INITIAL ALVEOLAR DEPOSITION NCI	NCI/G LUNG	NCI/ KG	INHALATION EXPOSURE WEIGHT (KG)	AGE* (MO)	DATE	DATE OF DEATH	MONTHS SINCE INHALATION 9/38/77	DEATH	COMMENTS ON DEAD DOGS
D-1 LOWEST	1105	F	0	0.00	0.00	10.0	16.4	05/31/73		52.0		
D-1 LOWEST	1194	F	0	0.00	0.00	10.5	19.8	04/18/74		41.4		
D-1 LOWEST	1215	M	0	0.00	0.00	15.5	19.3	04/18/74	04/26/77		36.3	SACRIFICED
D-1 LOWEST	1230	M	0	0.00	0.00	12.5	18.4	04/18/74		41.4		
D-1 LOWEST	951	M	2	0.01	0.14	14.0	19.3	12/19/72		57.4		
D-1 LOWEST	1008	M	2	0.01	0.15	13.5	19.6	01/18/73		56.4		
D-1 LOWEST	1193	F	2	0.01	0.16	12.5	19.8	04/18/74		41.4		
D-1 LOWEST	959	M	3	0.02	0.22	13.5	19.2	12/19/72		57.4		
D-1 LOWEST	1069	F	2	0.02	0.24	8.5	18.1	05/31/73		52.0		
D-1 LOWEST	1095	F	2	0.02	0.19	10.5	16.6	05/31/73		52.0		
D-1 LOWEST	921	F	3	0.03	0.31	10.0	19.5	11/38/72	12/27/72		0.9	SACRIFICED
D-1 LOWEST	923	F	3	0.03	0.35	8.5	19.5	11/38/72	01/26/73		1.9	SACRIFICED
D-1 LOWEST	989	F	3	0.03	0.32	9.5	18.8	12/19/72		57.4		
D-1 LOWEST	925	M	5	0.04	0.40	12.5	19.5	11/30/72	02/27/73		2.9	SACRIFICED
D-1 LOWEST	993	F	6	0.04	0.46	13.0	18.8	12/19/72		57.4		
D-1 LOWEST	1204	M	6	0.04	0.43	14.0	17.7	02/26/74		43.1		
D-1 LOWEST	970	F	6	0.05	0.55	11.0	19.2	12/19/72	01/04/77		48.5	SACRIFICED
D-1 LOWEST	1106	F	5	0.05	0.50	10.0	16.4	05/31/73		52.0		
D-1 LOWEST	1310	M	54	0.34	3.72	14.5	18.5	03/04/75	04/01/77		24.9	SACRIFICED
D-1 LOWEST	1312	M	58	0.34	3.74	15.5	18.5	03/04/75		30.9		
D-1 LOWEST	1311	M	54	0.36	4.00	13.5	18.5	03/04/75		30.9		
D-1 LOWEST	1317	M	72	0.41	4.50	16.0	18.1	03/04/75	04/01/77		24.9	SACRIFICED
D-1 LOWEST	1309	M	60	0.44	4.80	12.5	18.5	03/04/75		30.9		
D-1 LOWEST	1318	M	67	0.45	4.96	13.5	18.1	03/04/75	03/08/76		12.2	SACRIFICED
D-1 LOWEST	1316	M	84	0.53	5.79	14.5	18.1	03/04/75		30.9		
D-1 LOWEST	1315	M	90	0.55	6.00	15.0	18.1	03/04/75	03/31/77		24.9	SACRIFICED
D-1 LOWEST	1319	M	99	0.67	7.33	13.5	18.1	03/04/75	03/09/76		12.2	SACRIFICED
D-2 LOW	1065	F	6	0.05	0.60	10.0	18.3	05/31/73		52.0		
D-2 LOW	1082	M	11	0.06	0.69	16.0	18.0	05/31/73		52.0		
D-2 LOW	1188	M	11	0.06	0.71	15.5	18.4	02/26/74		43.1		
D-2 LOW	1084	M	13	0.07	0.74	17.5	17.5	05/31/73		52.0		
D-2 LOW	1090	F	10	0.10	1.05	9.5	17.3	05/31/73		52.0		
D-2 LOW	1222	M	15	0.10	1.11	13.5	19.0	04/18/74		41.4		
D-2 LOW	971	F	13	0.11	1.24	10.5	19.2	12/19/72		57.4		
D-2 LOW	999	F	11	0.11	1.16	9.5	18.7	12/19/72		57.4		

* INDICATES AGE IN MONTHS SINCE BIRTH, ALL OTHER AGES ARE IN MONTHS SINCE EXPOSURE

DOSE-EFFECT STUDIES WITH INHALED PU-238 OXIDE IN BEAGLES

DOSE GROUP	DOG NUMBER	SEX	INITIAL ALVEOLAR DEPOSITION NCI	NCI/G LUNG	NCI/ KG	INHALATION EXPOSURE WEIGHT (KG)	AGE* (MO)	DATE	DATE OF DEATH	MONTHS SINCE INHALATION 9/38/77	DEATH	COMMENTS ON DEAD DOGS
D-2 LOW	1229	M	16	0.11	1.23	13.0	16.8	02/26/74		43.1		
D-2 LOW	1070	M	22	0.12	1.33	16.5	18.1	05/31/73		52.0		
D-L LOW	1214	M	17	0.12	1.36	12.5	19.3	04/18/74	05/12/75		12.8	SACRIFICED
D-2 LON	955	M	17	0.14	1.55	11.0	19.2	12/19/72		57.4		
D-2 LOW	1033	M	17	0.14	1.55	11.0	19.1	02/22/73		55.2		
V-2 LON	1036	F	16	0.14	1.52	10.5	18.2	02/22/73		55.2		
0-2 LOW	1216	M	23	0.16	1.77	13.0	19.3	04/18/74		41.4		
0-2 LOW	1060	F	22	0.18	2.00	11.0	17.8	02/22/73		55.2		
D-L LOW	981	M	30	0.21	2.31	13.0	19.0	12/19/72		57.4		
D-2 LOW	1046	M	27	0.22	2.45	11.0	18.1	02/22/73		55.2		
D-2 LOW	1050	F	22	0.22	2.44	9.0	18.1	02/22/73		55.2		
D-2 LOW	1078	F	29	0.22	2.42	12.0	18.0	05/31/73		52.0		
D-2 LOW	1207	F	22	0.24	2.59	8.5	17.6	02/26/74		43.1		
D-2 LOW	1196	F	28	0.25	2.80	10.0	17.9	02/26/74		43.1		
D-2 LOW	1189	M	38	0.26	2.81	13.5	20.0	04/18/74		41.4		
D-L LOW	930	M	3d	0.27	2.92	13.0	19.2	11/30/72	12/28/72		0.9	SACRIFICED
D-3 MED-LOW	1066	M	54	0.31	3.38	16.0	18.3	05/31/73		52.0		
D-3 MED-LOW	1089	F	41	0.31	3.42	12.0	17.3	05/31/73		52.0		
D-3 MED-LON	972	F	40	0.33	3.64	11.0	19.2	12/19/72		57.4		
D-3 MED-LOW	1219	F	46	0.40	4.38	10.5	19.0	04/18/74		41.4		
D-3 MED-LON	1158	M	73	0.43	4.71	15.5	17.7	11/06/73		46.8		
D-3 WED-LOW	1165	M	76	0.43	4.75	16.0	17.3	11/06/73		46.8		
D-3 MED-LOW	929	F	41	0.50	5.47	7.5	19.2	11/30/72	01/25/73		1.8	SACRIFICED
D-3 MED-LOW	960	M	68	0.54	5.91	11.5	19.2	12/19/72		57.4		
D-3 MED-LOW	1072	M	98	0.54	5.94	16.5	18.1	05/31/73		52.0		
D-3 MED-LOW	1190	F	71	0.54	5.92	12.0	18.1	02/26/74		43.1		
D-3 MED-LOW	926	M	75	0.55	6.00	12.5	19.5	11/30/72	02/28/73		3.0	SACRIFICED
0-3 MED-LOW	9d2	M	76	0.58	6.33	12.0	19.0	12/19/72		57.4		
D-3 MED-LOW	1040	M	84	0.64	7.00	12.0	18.2	02/22/73		55.2		
D-3 NED-LOW	1059	F	71	0.65	7.10	10.0	17.8	02/22/73		55.2		
D-3 NED-LOW	1108	F	34	0.69	7.64	11.0	16.4	05/31/73		52.0		
D-3 MED-LOW	1000	F	70	0.71	7.78	9.0	ld.7	12/19/72		57.4		
D-3 MED-LOW	1056	M	97	0.71	7.76	12.5	17.9	02/22/73		55.2		
D-3 MED-LOW	1064	M	116	0.73	8.00	14.5	19.6	01/18/73		56.4		
D-3 MED-LOW	1026	M	116	0.78	8.59	13.5	19.2	01/18/73		56.4		

* INDICATES AGE IN MONTHS SINCE BIRTH, ALL OTHER AGES ARE IN MONTHS SINCE EXPOSURE

DOSE-EFFECT STUDIES WITH INHALED PU-238 OXIDE IN BEAGLES

DOSE GROUP	DOG NUMBER	SEX	INITIAL ALVEOLAR DEPOSITION NCI	NCI/G LUNG	NCI/ KG	INHALATION EXPOSURE WEIGHT (KG)	AGE* (MO)	DATE	DATE OF DEATH	MONTHS SINCE INHALATION 9/38/77	DEATH	COMMENTS ON DEAD DOGS
D-3 MED-LOW	1043	F	98	0.89	9.80	10.0	18.1	02/22/73		55.2		
D-3 MED-LOW	1031	F	76	0.92	10.13	7.5	19.1	02/22/73		55.2		
D-3 MED-LOW	1212	F	111	1.12	12.33	9.0	17.6	02/26/74		43.1		
D-4 MEDIUM	1176	M	129	0.87	9.56	13.5	16.6	11/06/73		46.8		
D-4 MEDIUM	1221	F	124	1.13	12.40	10.0	19.0	04/18/74		41.4		
D-4 MEDIUM	1195	M	22d	1.38	15.20	15.0	18.1	02/26/74		43.1		
D-4 MEDIUM	1032	M	162	1.40	15.43	10.5	16.3	11/30/72	12/08/72		0.3	SACRIFICED
D-4 MEDIUM	1053	F	148	1.42	15.58	9.5	17.9	02/22/73		55.2		
D-4 MEDIUM	997	M	203	1.60	17.65	11.5	19.6	01/18/73		56.4		
D-4 MEDIUM	991	F	194	1.76	19.40	10.0	18.8	12/19/72		57.4		
D-4 MEDIUM	1177	M	262	1.76	19.41	13.5	16.6	11/06/73		46.8		
D-4 MEDIUM	932	F	216	1.79	19.64	11.0	19.1	11/30/72	01/25/73		1.8	SACRIFICED
D-4 MEDIUM	1103	F	260	1.89	20.80	12.5	16.5	05/31/73		52.0		
D-4 MEDIUM	973	F	271	2.24	24.64	11.0	19.2	12/19/72		57.4		
D-4 MEDIUM	931	F	289	2.39	26.27	11.0	19.1	11/30/72	12/28/72		0.9	SACRIFICED
D-4 MEDIUM	1091	F	243	2.60	28.59	8.5	17.3	05/31/73		52.0		
D-4 MEDIUM	1114	M	430	2.70	29.66	14.5	16.4	05/31/73		52.0		
D-4 MEDIUM	1062	M	435	2.93	32.22	13.5	17.8	02/22/73		55.2		
D-4 MEDIUM	934	M	454	3.06	33.63	13.5	19.1	11/30/72	03/01/73		3.0	SACRIFICED
D-4 MEDIUM	1081	M	541	3.07	33.81	16.0	18.0	05/31/73		52.0		
D-4 MEDIUM	1030	F	340	3.25	35.79	9.5	19.1	02/22/73		55.2		
D-4 MEDIUM	952	F	365	3.49	38.42	9.5	19.2	32/19/72		57.4		
D-4 MEDIUM	1196	M	539	3.50	38.50	14.0	17.9	02/26/74		43.1		
D-4 MEDIUM	1166	M	673	4.08	44.87	15.0	17.3	11/06/73		46.8		
D-4 MEDIUM	1220	F	518	4.28	47.09	11.0	19.0	04/18/74		41.4		
D-4 MEDIUM	992	F	555	4.59	50.45	11.0	18.8	12/19/72		57.4		
D-4 MEDIUM	983	M	617	4.67	51.42	12.0	19.0	12/19/72		57.4		
D-5 MED-HI	1191	F	591	4.30	47.28	12.5	19.8	04/18/74	03/21/77		35.1	PNEUMONIA
D-5 MED-HI	1157	M	78d	4.71	51.85	13.5	17.7	11/06/73		46.8		
D-5 MED-HI	1035	F	571	5.46	60.11	9.5	18.2	02/22/73		55.2		
D-5 MED-HI	1192	F	754	6.23	68.55	11.0	18.1	02/26/74		43.1		
D-5 MED-HI	1140	M	1014	6.58	72.43	14.0	18.2	11/06/73		46.8		
D-5 MED-HI	1171	M	1269	6.79	74.65	17.0	18.1	05/31/73		52.0		
D-5 MED-HI	1173	M	1023	7.75	85.25	12.0	17.3	11/06/73		46.8		
D-5 MED-HI	1178	M	1125	8.52	93.75	12.0	16.6	11/06/73		46.8		

* INDICATES AGE IN MONTHS SINCE BIRTH, ALL OTHER AGES ARE IN MONTHS SINCE EXPOSURE

DOSE-EFFECT STUDIES WITH INHALED PU-238 OXIDE IN BEAGLES

DOSE GROUP	DOG NUMBER	SEX	INITIAL ALVEOLAR DEPOSITION NCI	NCI/G LUNG	NCI/ KG	INHALATION EXPOSURE WEIGHT (KG)	AGE* (MO)	DATE	DATE OF DEATH	MONTHS SINCE INHALATION 9/38/77	DEATH	COMMENTS ON DEAD DOGS
D-5 MED-HI	1047	M	900	8.61	94.74	9.5	18.1	02/22/73		55.2		
D-5 MED-HI	1109	F	1119	8.85	97.30	11.5	16.4	05/31/73		52.0		
D-5 MED-HI	1160	F	1344	9.77	107.52	12.5	17.3	11/06/73		46.8		
D-5 MED-HI	1211	M	1764	11.06	121.66	14.5	17.6	02/26/74		43.1		
D-5 MED-HI	1096	F	1476	12.20	134.18	11.0	16.6	05/31/73		52.0		
D-5 MED-HI	1218	F	1710	12.95	142.50	12.0	17.3	02/26/74		43.1		
D-5 MED-HI	1092	M	1848	13.44	147.84	12.5	17.3	05/31/73		52.0		
D-5 MED-HI	1027	M	2148	13.95	153.43	14.0	19.2	01/18/73		56.4		
D-5 MED-HI	1115	F	1885	14.90	163.91	11.5	16.1	05/31/73		52.0		
D-5 MED-HI	974	F	1718	15.62	171.80	10.0	20.2	01/18/73		56.4		
D-5 MED-HI	1079	M	2620	15.88	174.67	15.0	18.0	05/31/73		52.0		
D-5 MED-HI	1058	F	1907	16.51	181.62	10.5	17.8	02/22/73		55.2		
D-6 HIGH	1002	M	2907	1 . 8	207.64	14.0	19.6	01/18/73		56.4		
D-6 HIGH	1057	M	3116	20.98	230.81	13.5	17.9	02/22/73		55.2		
D-6 HIGH	1009	M	3630	26.40	290.40	12.5	19.6	01/18/73		56.4		
D-6 HIGH	1042	F	2959	28.32	311.47	9.5	18.1	02/22/73		55.2		
D-6 HIGH	994	F	3453	31.39	345.30	10.0	19.6	01/18/73	07/04/76		41.5	ADDISON'S DISEASE
D-6 HIGH	1006	F	3810	31.49	346.36	11.0	19.6	01/18/73		56.4		
D-6 HIGH	975	F	3968	36.07	396.80	10.0	20.2	01/18/73		56.4		
D-6 HIGH	1037	M	4854	44.13	485.40	10.0	18.2	02/22/73		55.2		
D-6 HIGH	1143	M	7691	53.78	591.62	13.0	18.2	11/06/73		46.8		
D-6 HIGH	1025	M	8479	57.10	628.07	13.5	19.2	01/18/73	03/17/77		49.9	LUNG TUMOR
D-6 HIGH	1064	M	9453	63.66	700.22	13.5	16.7	01/18/73	04/14/77		50.8	LUNG + BONE TUMOR
D-6 HIGH	1162	F	6959	70.29	773.22	9.0	17.3	11/06/73		46.8		
D-6 HIGH	1175	F	6201	75.16	826.80	7.5	16.6	11/06/73		46.8		

* INDICATES AGE IN MONTHS SINCE BIRTH, ALL OTHER AGES ARE IN MONTHS SINCE EXPOSURE

LOW LEVEL **PU-239** NITRATE INHALATION STUDIES

DOSE GROUP	DOG NUMBER	SEX	INITIAL ALVEOLAR DEPOSITION NCI	NCI/G LUNG	NCI/ KG	INHALATION EXPOSURE WEIGHT (KG)	AGE* (MO)	DATE	DATE OF DEATH	MONTHS SINCE INHALATION 9/30/77	DEATH	COMMENTS ON DEAD DOGS
CONTROL	1356	M	0	0.00	0.00					40.7*		
CONTROL	1365	M	0	0.00	0.00					40.6*		
CONTROL	1376	F	0	0.00	0.00					39.5*		
CONTROL	1388	M	0	0.00	0.00					39.3*		
CONTROL	1393	M	0	0.00	0.00					39.3*		
CONTROL	1405	M	0	0.00	0.00					38.9*		
CONTROL	1409	M	0	0.00	0.00					38.8*		
CONTROL	1418	M	0	0.00	0.00					38.5*		
CONTROL	1425	M	0	0.00	0.00					38.5*		
CONTROL	1450	F	0	0.00	0.00					38.3*		
CONTROL	1455	F	0	0.00	0.00					37.8*		
CONTROL	1483	F	0	0.00	0.00					36.9*		
CONTROL	1509	M	0	0.00	0.00					36.1*		
CONTROL	1516	F	0	0.00	0.00					35.8*		
CONTROL	1525	M	0	0.00	0.00					35.6'		
CONTROL	1526	M	0	0.00	0.00					35.6*		
CONTROL	1528	F	0	0.00	0.00					35.1*		
CONTROL	1543	M	0	0.00	0.00					34.9*		
CONTROL	1563	F	0	0.00	0.00					24.8*		
CONTROL	1572	F	0	0.00	0.00					24.7'		
CONTROL	1577	M	0	0.00	0.00					24.7'		
CONTROL	1584	F	0	0.00	0.00					24.6*		
CONTROL	1594	F	0	0.00	0.00					24.6'		
CONTROL	1608	M	0	0.00	0.00					24.3*		
VEHICLE	1361	M	0	0.00	0.00	15.5	21.0	02/13/76		19.5		
VEHICLE	1381	F	0	0.00	0.00	8.5	19.8	02/13/76		19.5		
VEHICLE	1392	M	0	0.00	0.00	13.0	22.0	04/22/76		17.3		
VEHICLE	1406	M	0	0.00	0.00	13.5	21.6	04/22/76		17.3		
VEHICLE	1412	F	0	0.00	0.00	9.0	19.0	02/13/76		19.5		
VEHICLE	1421	M	0	0.00	0.00	13.0	23.3	06/23/76		15.2		
VEHICLE	1457	F	0	0.00	0.00	12.0	20.6	04/22/76		17.3		
VEHICLE	1491	F	0	0.00	0.00	8.5	21.6	06/23/76		15.2		
VEHICLE	1504	F	0	0.00	0.00	10.0	20.9	06/23/76		15.2		
VEHICLE	1514	M	0	8.00	0.00	14.0	20.9	06/23/76		15.2		
VEHICLE	1524	M	0	0.00	0.00	12.0	21.5	07/27/76		14.1		

* INDICATES AGE IN MONTHS SINCE BIRTH, ALL OTHER AGES ARE IN MONTHS SINCE EXPOSURE

LOW LEVEL PU-239 NITRATE INHALATION STUDIES

DOSE GROUP	DOG NUMBER	SEX	INITIAL ALVEOLAR DEPOSITION NCI	NCI/G LUNG	NCI/ KG	INHALATION EXPOSURE WEIGHT (KG)	AGE* (MO)	DATE	DATE OF DEATH	MONTHS SINCE INHALATION 9/30/77	DEATH	COMMENTS ON DEAD DOGS
VEHICLE	1531	F	0	0.00	0.00	9.0	20.9	07/27/76		14.1		
VEHICLE	1542	M	0	0.00	0.00	12.0	20.8	07/27/76		14.1		
VEHICLE	1566	M	0	0.00	0.00	14.5	18.3	03/15/77		6.5		
VEHICLE	1578	M	0	0.00	0.00	10.5	18.2	03/15/77		6.5		
VEHICLE	1593	F	0	0.00	0.00	11.0	18.0	03/15/77		6.5		
VEHICLE	1601	F	0	0.00	0.00	8.5	18.0	03/15/77		6.5		
D-1 LOWEST	1351	M	0	0.00	0.00	11.0	17.2	10/16/75	11/13/75		0.9	SACRIFICED
D-1 LOWEST	1416	M	0	0.00	0.00	12.0	22.1	05/20/76		16.4		
D-1 LOWEST	1458	F	0	0.00	0.00	10.5	21.5	05/20/76		16.4		
D-1 LOWEST	1489	F	0	0.00	0.00	8.5	20.5	05/20/76		16.4		
D-1 LOWEST	1501	M	0	0.00	0.00	12.5	20.4	05/20/76		16.4		
D-1 LOWEST	1515	M	0	0.00	0.00	13.5	19.8	05/20/76		16.4		
D-1 LOWEST	1573	M	0	0.00	0.00	11.5	19.4	04/19/77		5.4		
D-1 LOWEST	1581	M	0	0.00	0.00	16.5	19.3	04/19/77		5.4		
D-1 LOWEST	1596	M	0	0.00	0.00	14.0	19.2	04/19/77		5.4		
D-1 LOWEST	1600	F	1	0.01	0.11	11.0	19.2	04/19/77		5.4		
D-1 LOWEST	1603	M	2	0.01	0.12	14.0	19.2	04/19/77		5.4		
D-1 LOWEST	1339	F	2	0.02	0.22	9.0	17.5	10/16/75	11/13/75		0.9	SACRIFICED
D-1 LOWEST	1519	M	2	0.02	0.18	12.5	19.5	05/20/76		16.4		
D-1 LOWEST	1570	F	2	0.02	0.17	10.5	19.4	04/19/77		5.4		
D-1 LOWEST	1465	F	4	0.03	0.33	12.5	21.0	05/20/76		16.4		
D-1 LOWEST	1470	F	3	0.03	0.29	10.5	21.0	05/20/76		16.4		
D-1 LOWEST	1507	M	4	0.03	0.32	14.0	19.8	05/20/76		16.4		
D-1 LOWEST	1592	F	4	0.03	0.29	13.3	19.2	04/19/77		5.4		
D-1 LOWEST	1607	M	5	0.03	0.35	13.0	19.0	04/19/77		5.4		
D-1 LOWEST	1335	M	5	0.04	0.42	11.5	18.0	10/16/75	11/13/75		0.9	SACRIFICED
D-1 LOWEST	1487	F	6	0.04	0.46	13.0	20.5	05/20/76		16.4		
D-1 LOWEST	1583	F	4	0.04	0.40	9.5	19.2	04/19/77		5.4		
D-1 LOWEST	1565	F	8	0.06	0.67	11.5	19.4	04/19/77		5.4		
D-2 LOW	1513	M	0	0.00	0.00	11.5	19.8	05/20/76		16.4		
D-2 LOW	1520	M	1	0.01	0.12	10.5	19.5	05/20/76		16.4		
D-2 LOW	1415	M	2	0.02	0.20	11.5	22.2	05/20/76		16.4		
D-2 LOW	1575	M	3	0.02	0.19	14.0	19.4	04/19/77		5.4		
D-2 LOW	1466	F	5	0.03	0.37	14.0	21.0	05/20/76		16.4		
D-2 LOW	1606	F	5	0.04	0.42	12.5	19.0	04/19/77		5.4		

* INDICATES AGE IN MONTHS SINCE BIRTH, ALL OTHER AGES ARE IN MONTHS SINCE EXPOSURE

LOW LEVEL PU-239 NITRATE INHALATION STUDIES

DOSE GROUP	DOG NUMBER	SEX	INITIAL ALVEOLAR DEPOSITION NCI	NCI/G LUNG	NCI/ KG	INHALATION EXPOSURE WEIGHT (KG)	AGE* (MO)	DATE	DATE OF DEATH	MONTHS SINCE INHALATION 9/30/77	DEATH	COMMENTS ON DEAD DOGS
D-2 LOW	1579	M	8	0.05	0.59	14.0	19.3	04/19/77		5.4		
U-2 LON	1590	F	6	0.05	0.51	12.0	19.2	04/19/77		5.4		
D-2 LOW	1585	F	8	0.06	0.68	12.0	19.2	04/19/77		5.4		
D-2 LON	1580	F	9	0.07	0.82	11.0	19.3	04/19/77		5.4		
D-2 LOW	1591	M	11	0.07	0.76	15.0	19.2	04/19/77		5.4		
D-2 LOW	1417	M	11	0.08	0.89	12.0	22.1	05/20/76		16.4		
D-2 LOW	1423	M	10	0.08	0.87	11.0	22.1	05/20/76		16.4		
D-2 LOW	1567	M	10	0.08	0.83	12.0	19.4	04/19/77		5.4		
D-2 LOW	1472	F	10	0.09	1.01	10.0	21.0	05/20/76		16.4		
D-2 LOW	1503	F	9	0.09	0.97	9.0	19.8	05/20/76		16.4		
D-2 LOW	1602	M	15	0.09	1.03	14.5	19.2	04/19/77		5.4		
D-2 LON	1484	F	11	0.10	1.08	10.0	20.5	05/20/76		16.4		
D-2 LOW	1599	F	13	0.13	1.39	9.0	19.2	04/19/77		5.4		
D-2 LOW	1490	F	16	0.15	1.65	9.5	20.5	05/20/76		16.4		
D-3 MED-LOW	1336	M	21	0.14	1.52	13.5	18.0	10/16/75	11/13/75		0.9	SACRIFICED
D-3 MED-LOW	1341	F	19	0.16	1.78	10.5	17.2	10/16/75	11/13/75		0.9	SACRIFICED
D-3 MED-LOW	1605	F	22	0.17	1.89	11.5	17.8	03/15/77		6.5		
0-3 MED-LOW	1386	M	34	0.21	2.36	14.5	22.0	04/20/76		17.3		
D-3 MED-LOW	1389	M	27	0.23	2.54	10.5	21.9	04/20/76	05/04/76		0.5	SACRIFICED
D-3 MED-LOW	1413	F	29	0.24	2.68	11.0	18.2	01/20/76		20.3		
U-3 MED-LOW	1445	F	34	0.24	2.68	13.0	21.0	04/20/76	05/05/76		0.5	SACRIFICED
D-3 MED-LOW	1568	M	46	0.29	3.17	14.5	18.3	03/15/77		6.5		
D-3 MED-LOW	1390	M	43	0.30	3.29	13.0	21.9	04/20/76	05/04/76		0.5	SACRIFICED
D-3 MED-LOW	1391	M	54	0.30	3.26	16.5	21.9	04/20/76		17.3		
D-3 MED-LOW	1587	M	53	0.31	3.40	15.5	18.1	03/15/77		6.5		
D-3 MED-LOW	1359	M	50	0.32	3.57	14.0	20.2	01/20/76	01/23/76		0.1	SACRIFICED
D-3 MED-LOW	1540	M	54	0.32	3.51	15.5	20.7	07/22/76		14.3		
D-3 NED-LOW	1589	F	41	0.34	3.75	11.0	18.0	03/15/77		6.5		
D-3 MED-LOW	1595	M	54	0.34	3.71	14.5	18.0	03/15/77		6.5		
D-3 MED-LOW	1588	M	50	0.36	3.98	12.5	18.1	03/15/77		6.5		
D-3 MED-LOW	1529	F	43	0.37	4.08	10.5	20.8	07/22/76	10/19/76		2.9	SACRIFICED
D-3 MED-LOW	1344	F	41	0.38	4.14	10.0	17.2	10/16/75	11/14/75		1.0	SACRIFICED
D-3 MED-LOW	1574	M	46	0.38	4.21	11.0	18.2	03/15/77		6.5		
D-3 MED-LOW	1375	F	50	0.40	4.35	11.5	19.1	01/20/76	01/23/76		0.1	SACRIFICED
D-3 MED-LOW	1564	F	40	0.40	4.44	9.0	18.3	03/15/77		6.5		

* INDICATES AGE IN SINCE BIRTH, ALL OTHER AGES ARE IN MONTHS SINCE EXPOSURE

LOW LEVEL PU-239 NITRATE INHALATION STUDIES

DOSE GROUP	DOG NUMBER	SEX	INITIAL ALVEOLAR DEPOSITION NCI	NCI/G LUNG	NCI/ KG	INHALATION EXPOSURE WEIGHT (KG)	AGE* (MOS)	SEX	DATE OF DEATH	MONTHS SINCE INHALATION 9/30/77	DEATH	COMMENTS ON DEAD DOGS
D-3 MED-LOW	1444	F	49	0.41	4.50	11.0	21.0	04/20/76		17.3		
D-3 MED-LOW	1439	F	53	0.42	4.61	11.5	21.0	04/20/76		17.3		
D-3 MED-LOW	1523	F	55	0.42	4.60	12.0	21.3	07/22/76		14.3		
D-3 MED-LOW	1539	M	65	0.45	4.99	13.0	20.7	07/22/76	10/20/76		3.0	SACRIFICED
D-3 MED-LOW	1380	M	63	0.46	5.06	12.5	19.1	01/20/76		20.3		
D-3 MED-LOW	1407	F	50	0.51	5.56	9.0	18.5	01/20/76	01/23/76		0.1	SACRIFICED
D-3 MED-LOW	1569	[illegible]	58	0.53	5.82	10.0	18.2	03/15/77		6.5		
D-3 MED-LOW	1576	M	70	0.53	5.86	12.0	18.2	03/15/77		6.5		
D-3 MED-LOW	1582	F	57	0.54	5.96	9.5	18.1	03/15/77		6.5		
D-3 MED-LOW	1571	F	68	0.57	6.22	11.0	18.2	03/15/77		6.5		
D-3 MED-LOW	[illegible]	F	68	0.62	6.81	10.0	21.1	04/20/76		[illegible]		
D-3 MED-LOW	1604	M	79	0.68	7.53	10.5	18.0	03/15/77		6.5		
D-3 MED-LOW	1522	F	78	0.71	7.78	10.0	21.3	07/22/76	10/18/76		2.9	SACRIFICED
D-3 MED-LOW	1363	M	85	0.74	8.09	10.5	20.2	01/20/76		20.3		
D-3 MED-LOW	1530	F	72	0.76	8.41	8.5	20.8	07/22/76		[illegible]		
D-3 MED-LOW	1456	F	61	0.79	8.68	7.0	20.5	04/20/76		17.3		
D-3 MED-LOW	1598	[illegible]	93	1.06	11.65	8.0	18.0	03/15/77		6.5		
D-3 MED-LOW	1422	F	99	1.12	12.35	8.0	18.1	01/20/76		20.3		
D-4 MEDIUM	1404	M	259	1.47	16.19	16.0	21.5	04/20/76		17.3		
D-4 MEDIUM	[illegible]	F	205	1.49	16.37	12.5	21.3	07/22/76		[illegible]		
D-4 MEDIUM	1379	M	[illegible]	1.74	19.16	14.5	19.1	01/20/76		20.3		
D-4 MEDIUM	1362	M	267	1.87	20.54	13.0	20.2	01/20/76		20.3		
D-4 MEDIUM	[illegible]	M	294	2.14	23.52	12.5	20.8	07/22/76		14.3		
D-4 MEDIUM	[illegible]	F	232	2.34	25.77	9.0	18.2	01/20/76		20.3		
D-4 MEDIUM	1385	M	370	2.40	26.45	14.0	19.0	01/20/76		20.3		
D-4 MEDIUM	1408	F	329	2.60	28.57	11.5	18.5	01/20/76		20.3		
D-4 MEDIUM	1428	F	[illegible]	3.13	34.47	11.0	21.1	04/20/76		[illegible]		
D-4 MEDIUM	[illegible]	F	344	[illegible]	34.41	10.0	20.7	07/22/76		14.3		
D-4 MEDIUM	1364	M	460	3.22	35.41	13.0	20.2	01/20/76		20.3		
D-4 MEDIUM	1446	F	354	3.22	35.40	10.0	21.0	04/20/76		[illegible]		
D-4 MEDIUM	1387	F	344	4.47	49.15	7.0	19.0	01/20/76		20.3		
D-5 MED-HI	1329	F	[illegible]	2.73	30.00	10.0	18.0	10/16/75	11/14/75		1.0	SACRIFICED
D-5 MED-HI	1346	M	662	4.46	49.05	13.5	17.2	10/16/75	11/14/75		1.0	SACRIFICED
D-5 MED-HI	[illegible]	[illegible]	695	7.02	77.18	9.0	17.2	10/16/75	11/14/75		1.0	SACRIFICED
D-5 MED-HI	1429	M	1376	9.62	105.85	13.0	23.2	06/23/76		15.2		

* INDICATES AGE IN MONTHS SINCE BIRTH, ALL OTHER AGES ARE IN MONTHS SINCE EXPOSURE

LOW LEVEL PU-239 NITRATE INHALATION STUDIES

DOSE GROUP	DOG NUMBER	SEX	INITIAL ALVEOLAR DEPOSITION NCI	NCI/G LUNG	NCI/KG	INHALATION EXPOSURE WEIGHT (KG)	AGE* (MO)	DATE	DATE OF DEATH	MONTHS SINCE INHALATION 9/38/77	DEATH	COMMENTS ON DEAD DOGS
D-5 MED-HI	1508	M	1709	10.71	117.86	14.5	20.9	06/23/76		15.2		
D-5 MED-HI	1512	M	2400	14.55	160.00	15.0	20.9	06/23/76		15.2		
D-5 MED-HI	1419	M	1559	14.92	164.11	9.5	23.3	06/23/76		15.2		
D-5 MED-HI	1498	F	2009	16.60	182.64	11.0	21.5	06/23/76		15.2		
D-5 MED-HI	1502	F	3007	20.25	222.74	13.5	20.9	06/23/76		15.2		
D-5 MED-HI	1485	F	2320	21.09	232.00	10.0	21.7	06/23/76		15.2		
D-5 MED-HI	1471	F	2532	21.92	241.14	10.5	22.1	06/23/76		15.2		
D-5 MED-HI	1492	F	2463	24.88	273.67	9.0	21.6	06/23/76		15.2		
D-5 MED-HI	1459	F	2645	26.72	293.89	9.0	22.6	06/23/76		15.2		
D-6 HIGH	1518	M	3537	29.23	321.55	11.0	20.6	06/23/76		15.2		
D-6 HIGH	1420	M	3840	30.36	333.91	11.5	23.3	06/23/76		15.2		
D-6 HIGH	1517	F	5185	49.62	545.79	9.5	20.6	06/23/76		15.2		
D-6 HIGH	1510	F	6968	55.08	605.91	11.5	20.9	06/23/76		15.2		
D-6 HIGH	1424	M	7438	67.62	743.80	10.0	23.2	06/23/76	08/31/77		14.3	RADIATION PNEUMONITIS

• INDICATES AGE IN MONTHS SINCE BIRTH, ALL OTHER AGES ARE IN MONTHS SINCE EXPOSURE

PDS>

PUBLICATIONS AND PRESENTATIONS

Reprints may be requested from the author at the address shown below[a], except for those articles marked with an asterisk (*), which are no longer available.

Allen, M. D., W. T. Kaune, and D. K. Craig. 1977. A method for vaporizing mixed oxide fast reactor fuels for animal inhalation studies. Health Phys. 32: 389-396.

*Andrew, F. D., R. L. Bernstine, D. D. Mahlum, and M. R. Sikov. 1977. Distribution of ^{239}Pu in the gravid baboon. Radiat. Res. 70: 637-638. (Abstract)

Andrew, F. D. and R. E. Staples. 1977. Prenatal toxicity of medroxyprogesterone acetate in rabbits, rats, and mice. Teratology 15: 25-32.

Andrew, F. D. 1976. Techniques for assessment of teratogenic effects: Developmental enzyme patterns. Environ. Health perspectives 18: 111-116.

Archer, B. G., T. B. Crawford, T. C. McGuire, and M. E. Frazier. 1977. RNA dependent DNA polymerase equine infectious anemia virus. J. Virol. 22: 16-22.

*Bair, W. J. 1977. Plutonium., pp. 344-347. In: McGraw-Hill Yearbook of Science and Technology, New York, NY.

*Bair, W. J. 1977. Current status of the hot particle issue (A review of relevant experimental and theoretical approaches), pp. 703-710. In: Proceedings of the IVth Int'l. Radiation Protection Association Meeting, Paris, France. IRPA, Paris, France.

Ballou, J. E., G. E. Dagle, K. E. McDonald, and R. L. Buschbom. 1977. Influence of inhaled Ca-DTPA on the long-term effects of inhaled Pu nitrate. Health Phys. 32: 479-487.

*Ballou, J. E. and R. A. Gies. 1976. The excretion and early disposition of inhaled transuranic nitrates in'rats. Health Phys. 31: 550. (Abstract)

Cohen, B. L. and H. Drucker. 1977. Regulation of exocellular protease in Neurospora crassa: Induction and repression under conditions of nitrogen starvation. Arch. Biochem. Biophys. 182: 601-613.

"Craig, D. K., J. F. Park, G. J. Powers, and D. L. Catt. 1977. The disposition of americium-241 oxide following inhalation by beagles. Radiat. Res. 70: 639. (Abstract)

*Dagle, G. E., K. E. McDonald, and J. E. Ballou. 1977. The morphology of lung tumors induced in rats with inhalation of plutonium nitrate. Lab. Invest. 36: 335. (Abstract)

Drucker, H. and R. E. Wildung, Eds. 1977. Biological Implications of Metals in the Environment, 682 p. (CONF-750929) NTIS, Springfield, VA.

*Hackett, P. L. and M. R. Sikov. 1977. Distribution and effects of lead in pregnant rats. Teratology 15: 30A. (Abstract)

Hadley, J. G., D. E. Gardner, D. L. Coffin, and D. B. Menzel. 1977. Enchanced binding of autologous red cells to the macrophage plasma membrane as a sensitive indicator of pollutant damage, pp. 66-77. In: Pulmonary Macrophage and Epithelial Cells (C. L. Sanders, R. P. Schneider, G. E. Dagle, and H. A. Ragan, Eds.) (CONF-760927) NTIS, Springfield, VA.

*Hadley, J. G. 1977. Membrane Receptors of the Alveolar Macrophage: Alterations by Environmental Contaminants. Ph.D. Thesis, Duke University, Durham, NC.

*Hadley, J. G., D. E. Gardner, D. L. Coffin, and D. B. Menzel. 1977. Effects of Cd and Ni on antibody-mediated rosette formation by rabbit alveolar macrophages. Toxicol. Appl. Pharmacol. 41: 152-153. (Abstract)

Hadley, J. G., D. E. Gardner, D. L. Coffin, and D. B. Menzel. 1977. Inhibition of antibody mediated rosette formation by alveolar macrophages: A sensitive assay for metal toxicity. J. Reticuloendothel. Soc. 22: 417-425.

*Hadley, J. G., D. E. Gardner, D. L. Coffin, and D. B. Menzel. 1977. Effects of ozone and nitrogen dioxide exposure of rabbits on the binding of autologous red cells to alveolar macrophages, pp. 505-512. In: Proc. Intl. Conf. on Photochemical Oxidant Pollution and Its Control Vol. I (B. Dimitriades, Ed.). EPA 600/3-77-001A. NTIS, Springfield, VA.

*Hadley, J. G., D. E. Gardner, D. L. Coffin, and D. B. Menzel. 1976. Effects of O_3 and NO_2 on the binding of autologous cells by alveolar macrophages. Pharmacologist 18: 244. (Abstract)

[a] Battelle, Pacific Northwest Laboratory, P.O. Box 999, Richland, Washington 99352

*Hanson, K. R. 1977. The use of glass capillary columns in routine gas chromatographic analysis of chemical compounds in physiological fluids, #ACSC-14C. In: Abstracts of Papers, 173rd ACS Meeting, American Chemical Society, Washington, D.C. (Abstract)

*Hjeresen, D. L. and R. D. Phillips. 1977. A behavioral response to high strength 60-Hz electric fields, p. 133. In: 1977 International USRI/USNC Symposium on the Biological Effects of Electromagnetic Waves. National Academy of Sciences, Washington, D.C. (Abstract)

*Hilton, D. [redacted], J. H. Chandon, and R. D. Phillips. 1977. ECG and heart rate response in rats exposed to 60-Hz electric fields, p. 131. In: 1977 International USRI/USNC Symposium on the Biological Effects of Electromagnetic Waves. National Academy of Sciences, Washington, D.C. (Abstract)

*Hungate, F. P., L. R. Bunnell, and W. F. Riemath. 1977. Progress on a portable blood irradiator for medical applications. Radiat. Res. 70: 663. (Abstract)

*Joshima, H., P. L. Hackett, and M. R. Sikov 1977. Effects of ^{239}Pu on hematopoiesis in prenatal rats. Radiat. Res. 70: 622. (Abstract)

*Kaune, W. T., J. R. Decker, R. D. Phillips, and D. L. Hjeresen. 1977. A system for the exposure of large numbers of small laboratory animals to vertical 60-Hz electric fieids, p. 20. In: 1977 International USRI/USNC Symposium on the Biological Effects of Electromagnetic Waves. National Academy of Sciences, Washington, D.C. (Abstract)

*Mahlum, D. D. 1977. Biological implications of magnetic fields from fusion reactors. Amer. Nucl. Soc. Transactions 26: 22. (Abstract)

*Mahlum, D. D. and M. D. Allen. 1977. Inhalation studies of condensation aerosols formed from PuO_2-UO_2 fuel and sodium vapor. Radiat. Res. 70: 638-639. (Abstract)

Moss, O. R., R. E. Filipy, W. C. Cannon, and D. K. Craig. 1977. SNS Source Term Evaluation Program, BNWL-2255, Battelle-Northwest, Richland, WA

*Pelroy, R. A. and P. E. Kolenbrander. 1977. The photoproduction of hydrogen from glucose by a glucose utilizing strain of Rhodopseudomonas sphaeriods, #I-137. In: Abstracts of the Annual Meeting of the American Society for Microbiology, ASM, Washington, D.C. (Abstract)

*Pelroy, R. A., H. Drucker, T. R. Garland, and R. E. Wildung. 1977. Multiple heavy metal resistance in several soil bacteria, #Q-38. In: Abstracts of the Annual Meeting of the American Society for Microbiology, ASM, Washington, D.C. (Abstract)

*Phillips, R. D., W. T. Kaune, J. R. Decker, and D. L. Hjeresen. 1977. Biological Effects of High Strength Electric Fields on Small Laboratory Animals, CONS/1830-1, Conservation Division, Energy Research and Development Administration, Washington, D.C.

*Phillips, R. D. and W. T. Kaune. 1977. Biological Effects of High Strength Electric Fields, CONS/1830-2, Conservation Division, Energy Research and Development Administration, Washington, D.C.

*Phillips, R. D., J. H. Chandon, L. Lang, and D. [redacted] Hilton. 1977. Biological effects of 60-Hz electric fields on growth and metabolic status of rats, p. 130. In: 1977 International USRI/USNC Symposium on the Biological Effects of Electromagnetic Waves. National Academy of Sciences, Washington, D.C. (Abstract)

Ragan, H. A. 1977. Body-iron stores and plutonium metabolism, pp. 570-577. In: Biological Implications of Metals in the Environment (H. Drucker and R. E. Wildung, Eds.). (CONF-750929) NTIS, Springfield, VA.

Ragan, H. A. 1977. Effects of iron deficiency on the absorption and distribution of lead and cadium in rats. J. Lab. Clin. Med. 90: 700-706.

*Ragan, H. A. 1977. Iron deficiency and pollutant metals. Blood 50: 97. (Abstract)

*Ragan, H. A., M. J. Pipes, W. T. Kaune, and R. D. Phillips. 1977. Hematologic and serum chemistry evaluations in rats exposed to 60-Hz electric fields, p. 126. In: 1977 International USRI/USNC Symposium on the Biological Effects of Electromagnetic Waves. National Academy of Sciences, Washington, D.C. (Abstract)

Robinson, A. V., T. R. Garland, G. S. Schneiderman, R. E. Wildung, and H. Drucker. 1977. Microbial transformation of a soluble organoplutonium complex, pp. 52-62. In: Biological Implications of Metals in the Environment (H. Drucker and R. E. Wildung, Eds.). (CONF-750929) NTIS, Springfield, VA.

Sanders, C. L., R. P. Schneider, G. E. Dagle, and H. A. Ragan, Eds. 1977. Pulmonary Macrophage and Epithelial Cells, 618 p. (CONF-760927) NTIS, Springfield, VA.

Sanders, C. L., R. R. Adee, K. Rhoads, and R. M. Madison. 1977. Life history of plutonium dioxide in the lung: From macrophage to carcinoma, pp. 451-462. In: Pulmonary Macrophage and Epithelial Cells (C. L. Sanders, R. P. Schneider, G. E. Dagle, and H. A. Ragan, Eds.) (CONF-760927) NTIS, Springfield, VA.

Sanders, C. L., G. E. Dagle, W. C. Cannon, G. J. Powers, and D. M. Meier. 1977. Inhalation carcinogenesis of high-fired $^{283}PuO_2$ in rats. Radiat. Res. 71: 528-546.

Sanders, C. L. 1977. Inhalation toxicity of $^{238}PuO_2$ and $^{239}PuO_2$ in Syrian golden hamsters. Radiat. Res. 70: 334-344.

*Sanders, C. L. 1976. Inhalation toxicology of $^{244}CmO_2$. Health Phys. 31: 536. (Abstract)

*Smith, V. H. 1977. Biological disposition of ^{237}Pu in the rat after intramuscular injection. Radiat. Res. 70: 635. (Abstract)

*Stuart, B. O., R. F. Palmer, R. E. Filipy, G. E. Dagle, and K. E. McDonald. 1977. Respiratory tract carcinogenesis in large and small experimental animals following daily inhalation of radon daughters and uranium ore dust, pp. 1337-1340. In: Proceedings of the IVth Int'l. Radiation Protection Association Meeting, Paris, France. IRPA, Paris, France.

Stuart, B. O. 1976. Deposition and clearance of inhaled particles. Environ. Health Perspectives 16: 41-53.

*Sullivan, M. F. and F. T. Cross. 1977. The role of target cells in the toxicity of ingested reactor core products. Radiat. Res. 70: 665. (Abstract)

*Thompson, R. C. 1977. The role of animal toxicity studies in the evaluation of human health risks from internally deposited transuranics, pp. 1335-1336. In: Proceedings of the IVth Int'l. Radiation Protection Association Meeting, Paris, France. IRPA, Paris, France.

*Tombropoulos, E. G., J. G. Hadley, J. M. Thomas, and D. K. Craig. 1977. Biochemical effects of inhaled $^{239}PuO_2$ on lung lipids. Health Phys. 32: 111-113.

*Wiemers, K. D. 1977. Sulfate ion analysis, # ACSC-11C. In: Abstracts of Papers, 173rd ACS Meeting, American Chemical Society, Washington, D.C. (Abstract)

*Wiley, W. R., R. G. Rupp, J. E. Morris, and L. S. Winn. 1977. Comparison of growth and S-100 synthesis by rat glial cell (C6) and sublines. Fed. Proc. 36: 2801. (Abstract)

Allen, M. D. Characterization of LMFBR fuel-sodium aerosols generated by laser vaporization. NRC Committee on LFMBR Aerosols, Silver Spring, MD, October.

Andrew, F. D., R. L. Bernstine, D. D. Mahlum, and M. R. Sikov. Distribution of ^{239}Pu in the gravid babbon. 25th Annual Radiation Research Society Meeting, San Juan, Puerto Rico, May.

Bair, W. J. Summary and future direction of radiation and multiple stresses. Annual American Industrial Hygiene Association Conference, New Orleans, LA, May.

Ballou, J. E. Studies with inhaled transuranic nitrates. Seminar, Biology Department, Battelle-Northwest, Richland, WA, May.

Ballou, J. E., G. E. Dagle, and K. E. McDonald. Latent effects of inhaled $Pu(NO_3)_4$ in rats. 22nd Annual Health Physics Society Meeting, Atlanta, GA, July.

Briant, J. K. and M. D. Allen. Investigation of possible fragmentation of chain-like aggregates in a round jet cascade impactor. 10th Aerosol Technology Meeting, Albuquerque, NM, September.

Craig, D. K., J. F. Park, G. J. Powers, and D. L. Catt. The disposition of americium-241 oxide following inhalation by beagles. 25th Annual Radiation Research Society Meeting, San Juan, Puerto Rico, May.

Craig, D. K., M. T. Karagianes, J. R. Decker, W. C. Cannon, and R. L. Buschbom. Initial deposition of inhaled PuO_2 aerosols in pigs. Annual American Industrial Hygiene Association Conference, New Orleans, LA, May.

Craig, D. K., J. F. Park, G. J. Powers, and D. L. Catt. The disposition of curium-244 oxide following inhalation by beagle dogs. 22nd Annual Health Physics Society Meeting, Atlanta, GA, July.

Craig, D. K. Deposition, translocation and effects of transuranic particles inhaled by experimental animals. Health and Safety Division, Oak Ridge National Laboratory, Oak Ridge, TN, September.

Craig, D. K., J. E. Ballou, G. E. Dagle, D. D. Mahlum, J. F. Park, C. L. Sanders, and B. O. Stuart. Deposition, translocation and effects of transuranic particles inhaled by experimental animals. Environmental Sciences Division Symposium of American Nuclear Society Winter Meeting, San Francisco, CA, November.

Dagle, J. E. Lung cancer in rats induced by cigarette smoke condensate. Seminar, Biology Department, Battelle-Northwest, Richland, WA, February.

Dagle, G. E., W. C. Cannon, H. A. Ragan, and C. R. Watson. Early effects of $^{239}Pu(NO_3)_4$ inhalation in dogs. 22nd Annual Health Physics Society Meeting, Atlanta, GA, July.

Dagle, G. E. Classification of lung tumors and non-neoplastic lesions of the lung in beagles. Canine Pathology Colloquium, Battelle Seattle Research Center, Seattle, WA, March.

Dagle, G. E., K. E. McDonald, and J. E. Ballou. The morphology of lung tumors induced in rats with inhalation of plutonium nitrate. 66th Annual Meeting of the International Academy of Pathology, Toronto, Ontario, Canada, March.

Dagle, G. E. Some aspects of cancer diagnosis in dogs. Richland Kennel Club, Richland, WA, November.

Dagle, G. E., G. M. Zwicker, and R. A. Renne. Morphological aspects of naturally occurring tumors of the central and peripheral nervous systems in the rat. American College of Veterinary Pathologist's Meeting, Toronto, Ontario, Canada, November.

Davis, D. Application of electron microprobe and scanning electron microscopy to bulk analysis of biological material. Seminar, Biology Department, Battelle-Northwest, Richland, WA, May.

Dionne, P. J., T. P. Harrington, D. L. Stevens, F. T. Cross, and G. E. Dagle. Modelling the early translocation of inhaled $^{239}Pu(NO_3)_4$ in dogs. 22nd Annual Health Physics Society Meeting, Atlanta, GA, July.

Frazier, M. E., R. N. Ushijima, and L. P. Mallavia. Retroviruses and radiation induced malignancies. Symposium - Persistant Viral Infections - Northwest Regional Meeting of the American Society for Microbiology, Pullman, WA, June.

Free, M. J., R. A. Jaffe, and R. A. Pelroy. Entry of circulating mutagens into the rete testis fluid of rats. 17th Hanford Biology Symposium, "Developmental Toxicology of Energy-Related Pollutants", Richland, WA, October.

Gandolfi, A. J., J. E. Lund, K. E. McDonald, and C. A. Shields. Pulmonary disposition and fibrogenic potential of oil shale dusts. Seminar, University of Cincinnati Medical School, Cincinnati, OH, July.

George, H. G. Library Services. Seminar, Biology Department, Battelle-Northwest, Richland, WA, November.

Hackett, P. L. and M. R. Sikov. Distribution and effects of lead in pregnant rats. Teratology Society Meeting, Reston, VA, May.

Hackett, P. L., J. O. Hess, and M. R. Sikov. Lead distribution and effects during development. 17th Hanford Biology Symposium, "Development Toxicity of Energy-Related Pollutants", Richland, WA, October.

Hadley, J. G. Some properties of alveolar macrophage receptors with special consideration to green macrophage with elephant trunks. Seminar, Biology Department, Battelle-Northwest, Richland, WA, January.

Hampton, J. C. The use of isotopes in biological research. Washington Association of College Biology Teachers Conference, Columbia Basin College, Pasco, WA, April.

Hanson, K. R. The use of glass capillary columns in routine gas chromatographic analysis of chemical compounds in physiological fluids. American Chemical Society's 18th Technician Symposium, New Orleans, LA, March.

Hilton, D. [redacted], J. H. Chandon, and R. D. Phillips. ECG and heart rate response in rats exposed to 60 Hz electric fields. URSI International Symposium on Biological Effects of Electromagnetic Waves, Airlie, VA, October.

Hjeresen, D. L. and R. D. Phillips. A behavioral response to high strength 60 Hz electric fields. URSI International Symposium on Biological Effects of Electromagnetic Waves, Airlie, VA, October.

Horstman, V. G. Animals in Biomedical Research. Richland Kennel Club, Richland, WA, January; Association of Records Managers and Administrators, Richland, WA, November.

Horstman, V. G. Radiation Biology at Hanford. Seminar, Fred Hutchinson Cancer Research Center, Seattle, WA, March.

Hungate, F. P., L. R. Bunnell, and W. F. Riemath. Progress on a portable blood irradiator for medical applications. 25th Annual Radiation Research Society Meeting, San Juan, Puerto Rico, May.

Hungate, F. P. Biological effects of radiation. 26th Annual Meeting of the Civil Defense Council, Long Beach, CA, October.

Joshima, H., P. L. Hackett, and M. R. Sikov. Effects of ^{239}Pu on hematopoiesis in prenatal rats. 25th Annual Radiation Research Society Meeting, San Juan, Puerto Rico, May.

Kaune, W. T., J. R. Decker, R. D. Phillips, and D. L. Hjeresen. A system for the exposure of large numbers of small laboratory animals to vertical 60-Hz electric fields. URSI International Symposium on Biological Effects of Electromagnetic Waves, Airlie, VA, October.

Mahlum, D. D. Environmental and health consequences and fusion energy. Seminar, Radiological Sciences, University of Washington, Seattle, WA, January; The Joint Center for Graduate Study, Richland, WA, January.

Mahlum, D. D. and M. D. Allen. Inhalation studies of condensation aerosols formed from PuO_2-UO_2 fuel and sodium vapor. 25th Annual Radiation Research Society Meeting, San Juan, Puerto Rico, May.

Mahlum, D. D. Biological implications of magnetic fields from fusion reactors. Annual Meeting of the American Nuclear Society, New York, NY, June.

Mahlum, D. D. Developmental toxicology of organic pollutants. 17th Hanford Biology Symposium, "Developmental Toxicology of Energy-Related Pollutants", Richland, WA, October.

Mahlum, D. D. Biomagnetic effects: A consideration in fusion reactor development. Department of Energy-sponsored Annual Health Protection Meeting, Las Vegas, NV, November.

Pelroy, R. A. Hydrogen production from glucose by a photosynthetic bacterium. Seminar, Biology Department, Battelle-Northwest, Richland, WA, March.

Pelroy, R. A. and P. E. Kolenbrander. The photoproduction of hydrogen from glucose by a glucose utilizing strain of Rhodopseudomonas sphaeriodes. American Society of Microbiology, Chicago, IL, May; Northwest Regional Meeting of the American Chemical Society, Portland State University, Portland, OR, June.

Pelroy, R. A. Use of Ames test in evaluation of shale oil fractions. US-Soviet Workshop on Health Effects of Shale Oil Development, Denver, CO, May.

Phelps, D. W. Determination of nicotine and cotinite in physiological fluids by capillary column gas chromatography. Seminar, Continental Oil Company, Ponca City, OK, October.

Phillips, R. D., J. H. Chandon, L. L. Lang, and D. L. Hilton. Biological effects of 60 Hz electric fields on growth and metabolic status of rats. URSI International Symposium on Biological Effects of Electromagnetic Waves, Airlie, VA, October.

Ragan, H. A., J. F. Park, R. J. Olson, and R. Buschbom. Selective lymphopenia induced in beagles following inhalation of $^{239}PuO_2$. Workshop on "Use of Beagle Models for Biomedical Research", Radiobiology Laboratory, University of California, Davis, CA, May.

Ragan, H. A. Effects of iron deficiency on the absorption of pollutant metals. American Industrial Hygiene Association Conference, New Orleans, LA, May.

Ragan, H. A., M. J. Pipes, W. T. Kaune, and R. D. Phillips. Hematologic and serum chemistry evaluations in rats exposed to 60 Hz electric fields. URSI International Symposium on Biological Effects of Electromagnetic Waves, Airlie, VA, October.

Sanders, C. L. Inhaled transuranics in rodents. Seminar, Radiological Sciences, Joint Center for Graduate Study, Richland, WA, March.

Sanders, C. L. Cocarcinogenesis of inhaled plutonium dioxide and beryllium oxide. American Industrial Hygiene Association Conference, New Orleans, LA, May.

Sanders, C. L. Hazards of cigarette smoke. U.S. Naval Reserve, Pasco, WA, May.

Sikov, M. R., G. M. Zwicker, J. O. Hess, and D. D. Mahlum. Late effects of perinatally injected ^{239}Pu. 17th Hanford Biology Symposium, "Developmental Toxicology of Energy-Related Pollutants", Richland, WA, October.

Smith, V. H. Biological disposition of ^{237}Pu in the rat after intramuscular injection. 25th Annual Radiation Research Society Meeting, San Juan, Puerto Rico, May.

Stuart, B. O. Experimental studies of inhaled radon daughters. Workshop on Dosimetry for Radon Daughters, Oak Ridge National Laboratory, Oak Ridge, TN, April.

Stuart, B. O., R. F. Palmer, G. E. Dagle, and K. E. McDonald. Respiratory tract carcinogenesis in large and small experimental animals following daily inhalation of radon daughters and uranium ore dust. Fourth Congress of the International Radiation Protection Association, Paris, France, April.

Stuart, B. O., R. F. Palmer, R. E. Filipy, G. E. Dagle, and K. E. McDonald. Pulmonary disease induced in experimental animals by interactions of radon daughters, uranium ore dust and diesel engine exhaust. American Industrial Hygiene Association Conference, New Orleans, LA, May.

Stuart, B. O. Experimental studies of inhaled radon daughters. Workshop on Environmental Development Planning, Washington, D.C., July.

Sullivan, M. F. and F. T. Cross. The role of target cells in the toxicity of ingested reactor core products. 25th Annual Radiation Research Society Meeting, San Juan, Puerto Rico, May.

Thompson, R. C. Health effects from nuclear fuel cycle pollutants. Seminar, Energy Systems Department, Battelle-Northwest, Richland, WA, April.

Thompson, R. C. The role of animal toxicity studies in the evaluation of human health risks from internally deposited transuranics. Fourth Congress of the International Radiation Protection Association, Paris, France, April.

Thompson, R. C. Radiation Biology. NORCUS College Faculty and Students, Battelle-Northwest Richland, WA July.

Thompson, R. C. Forthcoming ICRP and NCRP action on internal exposure limits. Seminar, Biology Department, Battelle-Northwest, Richland, WA, December.

Wehner, A. P. and B. O. Stuart. Inhalation studies with Syrian golden hamsters. Symposium, "Syrian Hamster in Toxicology and Carcinogenesis Research", Boston, MA, November.

Wiemers, K. Sulfate ion analysis. American Chemical Society's 18th Technician Symposium, New Orleans, LA, March.

Wiley, W. R., R. G. Rupp, J. E. Morris, and L. S. Winn. Comparison of growth and S-100 synthesis by rat glial cell (C6) and subcell lines. 61st FASEB Annual Meeting, Chicago, IL, April.

Willard, D. H. and J. E. Ballou. The disposition of ^{85}Kr in the rat. 22nd Annual Health Physics Society Meeting, Atlanta, GA, July.

Zwicker, G. M. and G. E. Dagle. Spontaneous Tyzzer's disease in guinea pigs. 28th Annual Session of the American Association for Laboratory Animal Science, Anaheim, CA, October.

Zwicker, G. M. and S. M. Loscutoff. Preliminary report on developing the guinea pig as a model for correlating pulmonary function changes with pathology. American College of Veterinary Pathologist's Meeting, Toronto, Ontario, Canada, November.

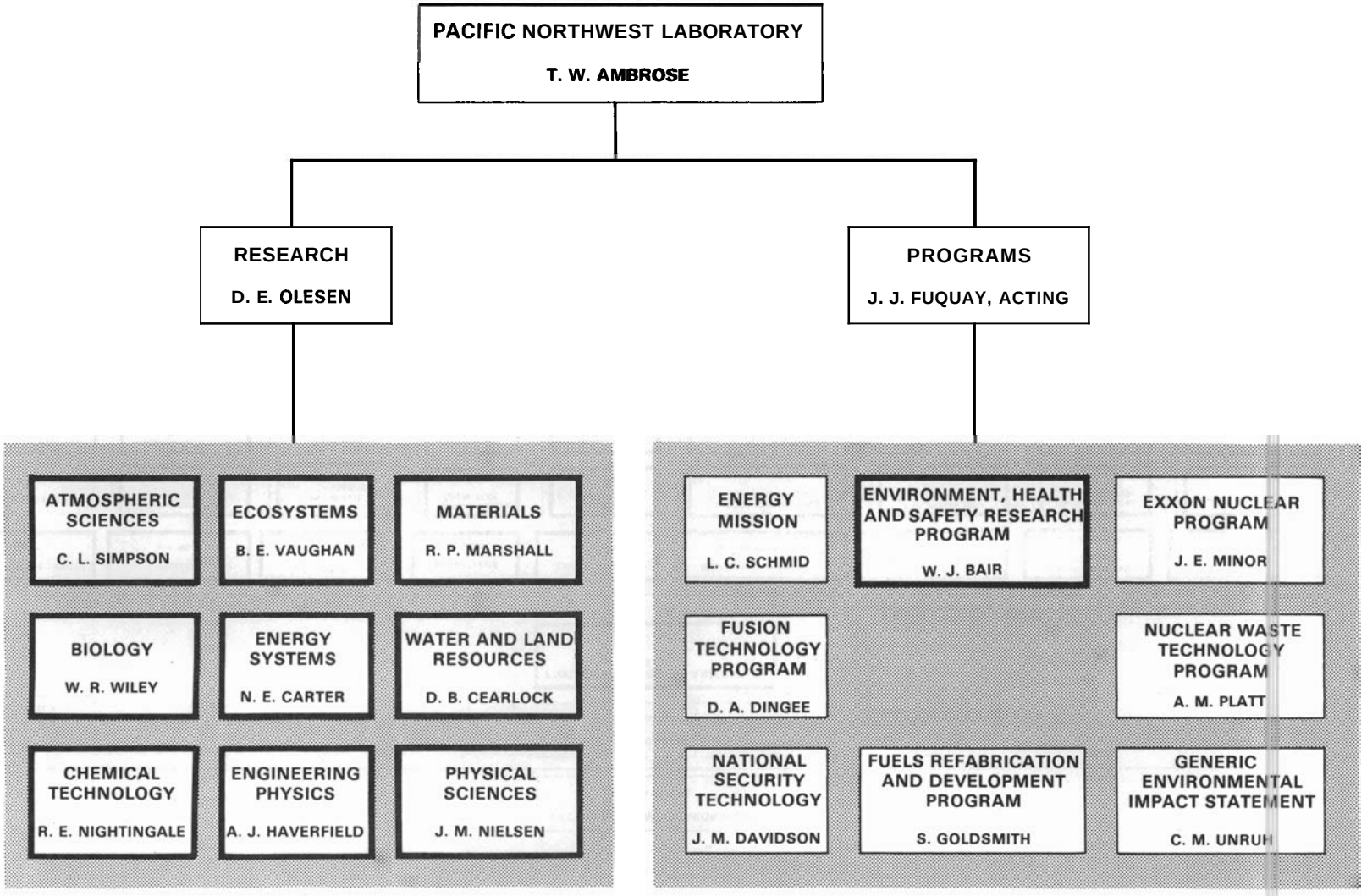

NOTE: HEAVY BLACK LINES DENOTE ORGANIZATIONAL COMPONENTS IN WHICH ENVIRONMENT, HEALTH, AND SAFETY RESEARCH IS BEING CONDUCTED.

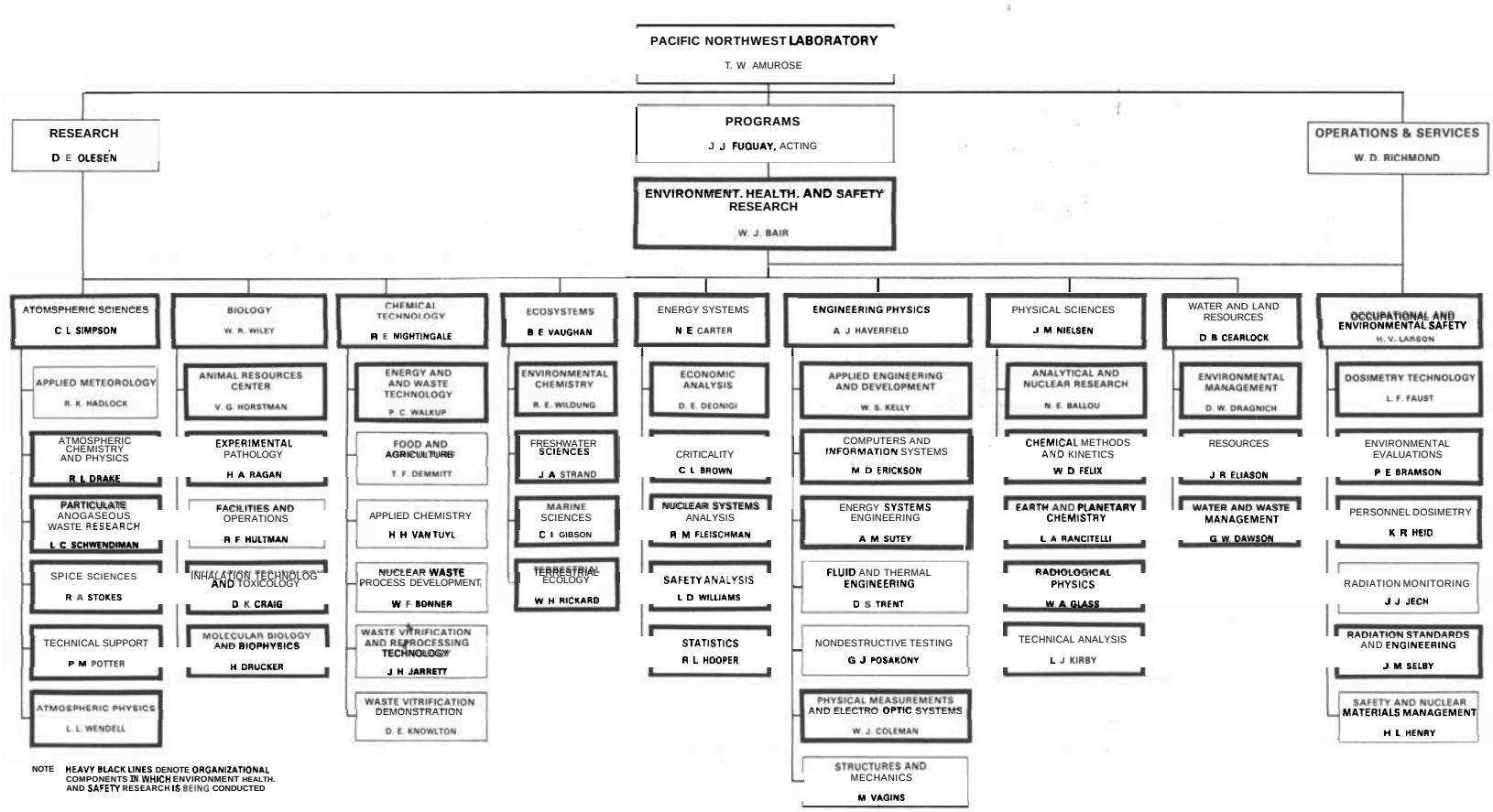

NOTE HEAVY BLACK LINES DENOTE ORGANIZATIONAL COMPONENTS IN WHICH ENVIRONMENT HEALTH. AND SAFETY RESEARCH IS BEING CONDUCTED

BIOLOGY DEPARTMENT
(7H20)

January 1, 1978

JF (Jim) Park, Associate Manager
+++D (David) Davis
°°°JA (Judie) Rising, Secretary
YOL (Dev) Felton, Editor/Writer
WHG (Harry) George, Librarian
#ZG (Zona) Wright, Clerk

WR (Bill) Wiley, Manager
MS (Marguerite) Stack, Secretary

#KS (Kathy) Mikols, Financial Specialist
WRD (Roger) Pollari, Financial Specialist
#RE (Ruth) Palmer, Clerk

°°°RF (Ray) Hultman, Quality Assurance Specialist

RC (Roy) Thompson, RT Program Coordinator
°°°JA (Judie) Rising, Secretary
. EM (Debra) Bessinger, Clerk

JE (Joanne) Olsen, Clerk

MF (Murlin) Gillis, Manager, Project Development

Facilities & Operations (7H20)

°°°RF (Ray) Hultman, Manager, Facilities
GG (Gertrude) Haggard, Clerk

RD (Russ) Tucker

NP (Nell) Couch, Receptionist
***KS (Kathleen) Flaherty, Receptionist
JL (Julie) Gurtisen, Receptionist
LR (Leila) Goldsmith, Clerk
***LL (LouAnn) Pratt, Clerk
***PR (Patricia) Saucier, Receptionist

Animal Resources Center (7H22)

YG (Glenn) Horstman, Manager
CA (Carol) Hanf, Secretary

MG (Gilbert) Bran
RF (Roy) Howard
SE (Stephen) Rove
VD (Val) Tyler
EL (Edward) Wierman

SM (Sharon) Baze
JA (Jan) Bergeson
MD (Mark) Brady
DR (Deborah) Bryant
RD (Ronald) Burdett
S (Stacey) Cochrane
VG (Victor) Dedmond
JC (John) Drewrey
GR (Gary) Ell
KL (Kathleen) Friday
DE (David) Friedrichs
MM (Myron) Hankins, Jr
DM (Dan) Harter
OL (Otis) Jackson
DD (Donald) Jenkins
TA (Troy) Johnson
RC (Robert) Joyce
TC (Thomas) Kinnas
JT (Judy) Kinsley
GL (Glen) Miller
WB (Wallace) Peterson
PD (Patrick) Pierce
KL (Kenneth) Scherbarth
RP (Robert) Schumacher
DC (Donald) Snyder
FL (Fred) Wallace
MA (Mary Ann) Whittle
CS (Connie) Williams

Molecular Biology & Biophysics (7H26)

H (Harvey) Drucker, Manager
RP (Richard) Schneider, Assoc. Mgr.
LM (Louise) Dilbeck, Secretary
*JE (Judith) Beck, Secretary

RR (Roy) Adee
++LE (Larry) Anderson
TK (Thomas) Andrews
HE (Marvin) Frazier
MP (Paul) Fujihara
AJ (Jay) Gandolfi
JG (John) Hadley
FP (Frank) Hungate
BJ (Bea) McClanahan
JE (James) Morris
LC (Louise) Neil
RA (Richard) Pelroy
AY (Alfred) Robinson
CL (Charles) Sanders
VH (Victor) Smith
MF (Maurice) Sullivan
LS (Laura) Winn

SI (Susanne) Baker
LM (Lucille) Butcher
AW (Allen) Conklin
JT (James) Cresto
RA (Ann) Gelman
LS (Linda) Gorham
TM (Tonia) Graham
***MJ (Marilyn) Hooper
***K (Kathleen) Rhoads
CA (Christine) Shields
SR (Stanley) Strankman
BB (Bonnie) Thompson
***IA (Ian) Watson
C (Clotis) White

Inhalation Technology & Toxicology (7H27)

DK (Douglas) Craig, Manager
MT (Manny) Karagianes, Assoc. Mgr.
JM (Judy) Christensen, Secretary
MG (Mona) Edwards, Secretary
BJ (Barbara) Cole, Secretary

MD (Michael) Allen
FD (Floyd) Andrew
JE (John) Ballou
JL (James) Beamer
EF (Edwin) Blanton
FG (Fred) Burton
WC (William) Cannon
DL (Dennis) Catt
JR (John) Decker
JC (John) Gaven
RA (Richard) Gies
PL (Patricia) Hackett
JP (John) Herring
JO (Joan) Hess
DL (Dennis) Hjeresen
RA (Richard) Jaffe
WT (William) Kaune
EG (Edward) Kuffel
**SM (Susan) Loscutoff
DD (Dennis) Mahlum
MC (Michael) Miller
OR (Owen) Moss
RF (Ray) Palmer
DW (Daniel) Phelps
RD (Richard) Phillips
GJ (Jerry) Powers
RE (Roger) Schirmer
MR (Melvin) Sikov
HE (Herbert) Stevens
BO (Bruce) Stuart
AP (Alfred) Wehner
DH (Donald) Willard

DH (Darlene) Akins
JS (Juanita) Barnett
JK (James) Briant
JH (James) Chandon
AJ (Jackie) Clary
MJ (Mary) Conger
HS (Henry) DeFord
***DR (DeVon) Doman
EA (Alair) Emory
BR (Benjamin) Garrity
XR (Kathleen) Hanson
LF (Linda) Hensley
DI (David) Hilton
GD (Gerald) Irwin
DL (Debora) Jeffs
BW (Bruce) Killand
LL (Lyn) Lang
***SE (Stanley) Leigh
LD (Larry) Montgomery
RL (Ramona) Music
LC (Chris) Oram
DA (Dale) Ostler
LR (Leonard) Peters
CR (Carl) Petty
***BL (Barbara) Philipp
KA (Kathleen) Poston
EJ (Ernest) Rossignol
LD (Lawrence) Sackmann
RL (Randi) Sheldon
W (Wilbur) Skinner
JD (Jean) Stearns
DA (Douglas) Teats
KC (K.C.) Upton
DL (Deborah) Walton
GL (Gary) Webb

Experimental Pathology (7H28)

HA (Harvey) Ragan, Manager
JF (Jeanette) Hunt, Secretary
JM (Judith) Proud, Secretary

GE (Gerald) Dagle
RE (Ronald) Filipy
MJ (Michael) Free
RM (Robin) Madison
KE (Keith) McDonald
RA (Roger) Renne
LG (Linda) Smith
GM (Gary) Zwicker

***M (MaryJo) Colton
***KH (Kathryn) Debban
KM (Karla) Dragoo
ET (Eugenia) Edmerson
SL (Sandra) English
VT (Victor) Faubert
RF (Robert) Flores
FS (Franna) Gerber
SL (Sherri) Krum
DM (Donna) Kugler
***KM (Karen) Lacy
JF (James) McShane
BG (Barbara) Moore
***ME (Michele) Moser
MC (Martha) Perkins
MJ (Marcia) Pipes
***JK (Judy) Sweeney
***CL (Carrie) Williams

Smoking Technicians

EM (Edward) Milliman
FM (Frances) Gordon
BD (Barbara) Holloway
AE (Alice) Marlin

DM (Deanna) Bowen
KT (Kreg) Brasel
VA (Vikki) Carter
LL (Laura) Fowlkes
DC (David) Oberg

LEGEND:
°°°Trainees, included in 7H00 total.
"""Dual assignment, included only once.
*Part-time employee, included in total
***Hourly employee, included in total.
#Assigned from another organization, not included in total.
++BI Postdoctoral Fellow, not included in total
YMP, not included in total.
+++ Univ. of Wash. Portdoctoral Fellow, not included in total.

Total Number of Exempt	= 75
Total Number of Non-Exempt	= 124
TOTAL	199

AUTHOR INDEX

DISTRIBUTION

No. of Copies

A. A. Churm, Director
Patent Division
DOE - Chicago Operations Office
9800 South Cass Avenue
Argonne, IL 60439

3 J. L. Liverman
Acting Assistant Secretary
Department of Energy
Office of the Assistant
Secretary for Environment
Washington, DC 20545

W. R. Albers
Department of Energy
Office of the Assistant
Secretary for Environment
Washington, DC 20545

R. W. Barber
Department of Energy
Office of the Assistant
Secretary for Environment
Washington, DC 20545

N. F. Barr
Department of Energy
Office of the Assistant
Secretary for Environment
Washington, DC 20545

M. A. Bell
Department of Energy
Office of the Assistant
Secretary for Environment
Washington, DC 20545

W. G. Belter
Department of Energy
Office of the Assistant
Secretary for Environment
Washington, DC 20545

J. W. Benson
Department of Energy
Office of the Assistant
Secretary for Environment
Washington, DC 20545

L. C. Brazley
Department of Energy
Office of the Assistant
Secretary for Environment
Washington, DC 20545

No. of Copies

W. A. Brobst
Department of Energy
Office of the Assistant
Secretary for Environment
Washington, DC 20545

A. L. Brooks
Department of Energy
Office of the Assistant
Secretary for Environment
Washington, DC 20545

W. W. Burr, Jr.
Department of Energy
Office of the Assistant
Secretary for Environment
Washington, DC 20545

4 C. E. Carter
Department of Energy
Office of the Assistant
Secretary for Environment
Washington, DC 20545

D. W. Cole
Department of Energy
Office of the Assistant
Secretary for Environment
Washington, DC 20545

J. A. Coleman
Departnient of Energy
Office of the Assistant
Secretary for Environment
Washington, DC 20545

R. A. Conaway
Department of Energy
Office of the Assistant
Secretary for Environment
Washington, DC 20545

R. D. Cooper
Department of Energy
Office of the Assistant
Secretary for Environment
Washington, DC 20545

L. J. Deal
Department of Energy
Office of the Assistant
Secretary for Environment
Washington, DC 20545

No. of Copies

G. P. Dix
Department of Energy
Office of the Assistant
Secretary for Environment
Washington, DC 20545

G. G. Duda
Department of Energy
Office of the Assistant
Secretary for Environment
Washington, DC 20545

C. W. Edington
Department of Energy
Office of the Assistant
Secretary for Environment
Washington, DC 20545

H. G. Fish
Department of Energy
Office of the Assistant
Secretary for Environment
Washington, DC 20545

R. E. Grossman
Department of Energy
Office of the Assistant
Secretary for Environment
Washington, DC 20545

G. Hagey
Department of Energy
Office of the Assistant
Secretary for Environment
Washingotn, DC 20545

J. H. Harley
Environmental Monitoring
Laboratory
376 Hudson St.
New York, NY 10014

E. B. Harvey
Departnient of Energy
Office of the Assistant
Secretary for Environment
Washington, DC 20545

H. Hollister
Department of Energy
Office of the Assistant
Secretary for Environment
Washington, DC 20545

No. of Copies

R. M. Jimeson
Department of Energy
Office of the Assistant
Secretary for Environment
Washington, DC 20545

R. L. Leith
Department of Energy
Office of the Assistant
Secretary for Environment
Washington, DC 20545

F. A. Leone
Department of Energy
Office of the Assistant
Secretary for Environment
Washington, DC 20545

W. J. Little, Jr.
Department of Energy
Office of the Assistant
Secretary for Environment
Washington, DC 20545

K. E. Lockridge
Department of Energy
Office of the Assistant
Secretary for Environment
Washington, DC 20545

V. M. Lott
Department of Energy
Office of the Assistant
Secretary for Environment
Washington, DC 20545

E. K. Loop
Department of Energy
Office of the Assistant
Secretary for Environment
Washington, DC 20545

J. N. Maddox
Department of Energy
Office of the Assistant
Secretary for Environment
Washington, DC 20545

J. R. Maher
Department of Energy
Office of the Assistant
Secretary for Environment
Washington, DC 20545

W. J. McCool
Department of Energy
Office of the Assistant
Secretary for Environment
Washington, DC 20545

No. of Copies

B. F. McCully
Department of Energy
Office of the Assistant
Secretary for Environment
Washington, DC 20545

J. L. Minthorn, Jr.
Department of Energy
Office of the Assistant
Secretary for Environment
Washington, DC 20545

D. Monti
Department of Energy
Office of the Assistant
Secretary for Environment
Washington, DC 20545

W. E. Mott
Department of Energy
Office of the Assistant
Secretary for Environment
Washington, DC 20545

D. E. Patterson
Department of Energy
Office of the Assistant
Secretary for Environment
Washington, DC 20545

W. H. Pennington
Department of Energy
Office of the Assistant
Secretary for Environment
Washington, DC 20545

R. Rabson
Department of Energy
Office of the Assistant
Secretary for Environment
Washington, DC 20545

R. W. Ramsey, Jr.
Department of Energy
Office of the Assistant
Secretary for Environment
Washington, DC 20545

D. M. Ross
Department of Energy
Office of the Assistant
Secretary for Environment
Washington, DC 20545

A. A. Schoen
Department of Energy
Office of the Assistant
Secretary for Environment
Washington, DC 20545

No. of Copies

M. Schulman
Department of Energy
Office of the Assistant
Secretary for Environment
Washington, DC 20545

D. E. Shaw
Department of Energy
Office of the Assistant
Secretary for Environment
Washington, DC 20545

G. Shippard
Department of Energy
Office of the Assistant
Secretary for Environment
Washington, DC 20545

R. D. Shull
Department of Energy
Office of the Assistant
Secretary for Environment
Washington DC, 20545

N. F. Simpson
Department of Energy
Office of the Assistant
Secretary for Environment
Washington DC, 20545

D. H. Slade
Department of Energy
Office of the Assistant
Secretary for Environment
Washington, DC 20545

D. Smith
Department of Energy
Office of the Assistant
Secretary for Environment
Washington, DC 20545

H. P. Smith
Department of Energy
Office of the Assistant
Secretary for Environment
Washington, DC 20545

J. Snyder
Department of Energy
Office of the Assistant
Secretary for Environment
Washington, DC 20545

G. E. Stapleton
Department of Energy
Office of the Assistant
Secretary for Environment
Washington, DC 20545

No. of Copies

J. B. Stronberg
Department of Energy
Office of the Assistant
Secretary for Environment
Washington, DC 20545

J. Swinebroad
Department of Energy
Office of the Assistant
Secretary for Environment
Washington, DC 20545

A. R. Vincent
Department of Energy
Office of the Assistant
Secretary for Environment
Washington, DC 20545

B. W. Wachholz
Department of Energy
Office of the Assistant
Secretary for Environment
Washington, DC 20545

H. R. Warson
Department of Energy
Office of the Assistant
Secretary for Environment
Washington, DC 20545

W. W. Weyzen
Department of Energy
Office of the Assistant
Secretary for Environment
Washington, DC 20545

J. C. Whitnah
Department of Energy
Office of the Assistant
Secretary for Environment
Washington, DC 20545

T. Williams
Department of Energy
Office of the Assistant
Secretary for Environment
Washington, DC 20545

R. W. Wood
Department of Energy
Office of the Assistant
Secretary for Environment
Washington, DC 20545

C. I. York
Department of Energy
Office of the Assistant
Secretary for Environment
Washington, DC 20545

No. of Copies

F. R. Zintz
Department of Energy
Office of the Assistant
Secretary for Environment
Washington, DC 20545

C. W. Fischer
Department of Energy
Office of Assistant Secretary
for Energy Information
Administration
Washington, DC 20545

Major General J. K. Bratton
Department of Energy
Office of the Assistant
Secretary for Defense
Programs
Washington, DC 20545

G. C. Facer
Department of Energy
Office of the Assistant
Secretary for Defense
Programs
Washington, DC 20545

Admiral H. G. Rickover
Department of Energy
Office of the Assistant
Secretary for Defense
Programs
Washington, DC 20545

A. D. Starbird
Department of Energy
Office of the Assistant
Secretary for Defense
Programs
Washington, DC 20545

C. B. Curtis
Department of Energy
Office of the Assistant
Secretary for Federal Energy
Regulatory Commission
Washington, DC 20545

W. E. Molloy
Department of Energy
Office of the Assistant
Secretary for Federal Energy
Regulatory Commission
Washington, DC 20545

H. P. Wald
Department of Energy
Office of the Assistant
Secretary for Federal Energy
Regulatory Commission
Washington, DC 20545

No. of Copies

D. Beattle
Department of Energy
Office of the Assistant
Secretary for Conservation
and Solar Applications
Washington, DC 20545

T. Noel
Department of Energy
Office of the Assistant
Secretary for Resource
Applications
Washington, DC 20545

J. Belding
Department of Energy
Office of the Assistant
Secretary for Energy
Technology
Washington, DC 20545

J. Bresee
Department of Energy
Office of the Assistant
Secretary for Energy
Technology
Washington, DC 20545

G. W. Cunningham
Department of Energy
Office of the Assistant
Secretary for Energy
Technology
Washington, DC 20545

T. J. Dobry
Department of Energy
Office of the Assistant
Secretary for Energy
Technology
Washington, DC 20545

H. Guthrie
Department of Energy
Office of the Assistant
Secretary for Energy
Technology
Washington, DC 20545

E. E. Kintner
Department of Energy
Office of the Assistant
Secretary for Energy
Technology
Washington, DC 20545

F. A. Koomanoff
Department of Energy
Office of the Assistant
Secretary for Energy
Technology
Washington, DC 20545

No. of Copies

C. Kuhlman
Department of Energy
Office of the Assistant Secretary for Energy Technology
Washington, DC 20545

R. Loose
Department of Energy
Office of the Assistant Secretary for Energy Technology
Washington, DC 20545

W. E. Lotz
Departnient of Energy
Office of the Assistant Secretary for Energy Technology
Washington, DC 20545

M. B. Neuworth
Department of Energy
Office of the Assistant Secretary for Energy Technology
Washington, DC 20545

F. F. Parry
Department of Energy
Office of the Assistant Secretary for Energy Technology
Washington, DC 20545

G. Perdirtz
Department of Energy
Office of the Assistant Secretary for Energy Technology
Washington, DC 20545

H. F. Soule
Department of Energy
Office of the Assistant Secretary for Energy Technology
Washington, DC 20545

R. D. Thorne
Department of Energy
Office of the Assistant Secretary for Energy Technology
Washington, DC 20545

P. C. White
Departnient of Energy
Office of the Assistant Secretary for Energy Technology
Washington, DC 20545

No. of Copies

E. Willis
Department of Energy
Office of the Assistant Secretary for Energy Technology
Washington, DC 20545

W. Bateman
Department of Energy
Office of the Assistant Secretary for Energy Research
Washington, DC 20545

3 J. M. Deutch
Department of Energy
Office of the Assistant Secretary for Energy Research
Washington, DC 20545

D. R. Israel
Departnient of Energy
Office of the Assistant Secretary for Energy Research
Washington, DC 20545

J. S. Kane
Department of Energy
Office of the Assistant Secretary for Energy Research
Washington, DC 20545

C. Jackson
DOE - San Francisco Operations Office
133 Broadway
Wells Fargo Building
Oakland, CA 94616

J. H. Spickard
DOE - Idaho Operations Commission
550 Second Street
Idaho Falls, ID 83401

D. M. Gardiner
DOE - Chicago Operations Office
9800 South Cass Avenue
Argonne, IL 60439

M. E. Gates
DOE - Nevada Operations Office
P.O. Box 14100
Las Vegas, NV 89114

No. of Copies

R. Ray
DOE - Nevada Operations Office
P.O. Box 14100
Las Vegas, NV 89114

P. B. Dunnaway
DOE - Nevada Operations Office
P.O. Box 14100
Las Vegas, NV 89114

J. R. Roeder
DOE - Albuquerque Operations Office
P.O. Box 5400
Albuquerque, NM 87115

E. W. Bean
Rocky Flats Area Office
DOE - Albuquerque Operations Office
P.O. Box 928
Golden, CO 80401

J. F. Stevens
Dayton Area Office
DOE - Albuquerque Operations Office
P.O. Box 66
Miamisburg, OH 45342

W. Reese
DOE - Savannah River Operations Office
P.O. Box A
Aiken, SC 29801

J. A. Lenhard
DOE - Oak Ridge Operations Office
P.O. Box E
Oak Ridge, TN 37830

J. S. Ball
Bartlesville Energy Research Center
Department of Energy
P.O. Box 1398
Bartlesville, OK 74003

G. H. Gronhovd
Grand Forks Energy Research Center
Department of Energy
Box 8213, University Station
Grand Forks, ND 58202

A. W. Decora
Laramie Energy Research Center
Department of Energy
P.O. Box 3395
University Station
Laramie, WY 83071

No. of Copies

R. D. Kerr
Laramie Energy Research Center
Department of Energy
P.O. Box 3395
University Station
Laramie, WY 83071

A. A. Pitrolo
Morgantown Energy Research Center
Department of Energy
P.O. Box 880
Morgantown, WV 26505

I. Wender
Pittsburgh Energy Research Center
Department of Energy
4800 Forbes Avenue
Pittsburgh, PA 15213

B. M. Erickson
DOE - Schenectady Naval Reactors Office
P.O. Box 1069
Schenectady, NY 12301

2 T. J. Dobry
Department of Energy
Division of Nuclear Research and Application, Space Applications
Washington, DC 20545

198 DOE Technical Information Center

NRC Advisory Committee on Reactor Safeguards
Washington, DC 20555

W. Cool
Nuclear Regulatory Commission
Washington, DC 20545

R. Alexander
Nuclear Regulatory Commission
Washington, DC 20545

2 J. J. Davis
Assistant Director of Research
Nuclear Regulatory Commission
Washington, DC 20545

D. Smith
Environmental Protection Agency
Washington, DC 20460

No. of Copies

W. Mills
Environmental Protection Agency
Washington, DC 02460

J. W. McCaslin
INEL, Aerojet Nuclear
550 Second Street
Idaho Falls, ID 83401

R. C. Yoder
Rockwell International
P.O. Box 888
Golden, CO 80401

C. M. Patterson
E. I. DuPont de Nemours and Company
Savannah River Plant
Aiken, SC 29801

Technical Information Service
Room 773A
Savannah River Laboratory
E. I. DuPont de Neniours and Company
Aiken, SC 29801

C. L. Karl
National Lead Company of Ohio
P.O. Box 39158
Cincinnati, OH 45239

R. L. Kathren
Portland General Electric
621 S.W. Alder
Portland, OR 97205

V. P. Bond
Brookhaven National Laboratory
Upton, Long Island, NY 11973

C. B. Meinhold
Brookhaven National Laboratory
Upton, Long Island, NY 11973

Librarian
Research Library, Reference
Bookhaven National Laboratory
Upton, Long Island, NY 11973

C. R. Richmond
Oak Ridge National Laboratory
P.O. Box X
Oak Ridge, TN 37830

J. A. Auxier
Oak Ridge National Laboratory
P.O. Box X
Oak Ridge, TN 37830

No. of Copies

W. K. Sinclair
Argonne National Laboratory
9700 South Cass Avenue
Argonne, IL 60439

E. L. Alpen
Lawrence Berkeley Laboratory
University of California
Building 90, Room 2056
No. 1 Cyclotron Road
Berkeley, CA 94720

M. L. Mendelsohn
University of California
Lawrence Livermore Laboratory
P.O. Box 808
Livermore, CA 94550

Librarian
Lawrence Radiation Laboratory
University of California
Technical Information Dept., L-3
P.O. Box 808
Livermore, CA 94550

G. L. Voelz
University of California
Los Alamos Scientific Laboratory
P.O. Box 1663
Los Alamos, NM 87545

Librarian
Los Alamos Scientific Laboratory
P.O. Box 1663
Los Alamos, NM 87544

J. W. Healy
Los Alamos Scientific Laboratory
University of California
P.O. Box 1663
Los Alamos, NM 87545

Dr. Roger O. McClellan
Inhalation Toxicology Research Institute
Lovelace Foundation for Medical Education and Research
P.O. Box 5890
Albuquerque, NM 87115

K. A. Smith
Sandia Laboratories
P.O. Box 5800
Albuquerque, NM 87115

No. of Copies

J. E. Rasmussen
Battelle Human Affairs Research Centers
4000 N.E. 41st Street
P.O. Box 5395
Seattle, WA 98105

Librarian
Battelle Memorial Institute
Columbus Laboratories
505 King Avenue
Columbus, OH 53201

4 R. S. Paul
Battelle Memorial Institute
Columbus Laboratories
505 King Avenue
Columbus, OH 53201

F. G. Dawson
Battelle Memorial Institute,
505 King Avenue
Columbus, OH 53201

G. W. Duncan
Battelle
4000 NE 41st Street
Seattle, WA 98105

J. L. Hebert
Battelle
4000 NE 41st Street
Seattle, WA 98105

S. M. Nealey
4000 NE 41st Street
Seattle, WA 98105

B. D. Breitenstein
Hanford Environmental Health Foundation
Richland, WA 99352

P. A. Fuqua
Hanford Environmental Health Foundation
Richland, WA 99352

Librarian, Building 465
Atomic Energy Research Establishment
Harwell, Didcot
OXON OXII ORD, ENGLAND

H. Daw
Director, Division of Health, Safety and Waste Management
International Atomic Energy Agency
Vienna 1, Kaerntnerring 11,
AUSTRIA

No. of Copies

J. Z. Minczewski
International Atomic Energy Agency
Vienna 1, Kaerntenerring 11,
AUSTRIA

Director
Joint Center for Graduate Study
100 Sprout Road
Richland, WA 99352

David Rall, Director
NIEHS
P.O. Box 12233
Research Triangle Park,
NC 27709

D. Beirman
Chief, Document Service Branch
Central Intelligence Agency
Attn: CRS/DPSD/DSB/IAS/409779/DB
Washington, DC 20505

Council on Environmental Quality
72 Jackson Place, N.W.
Washington, DC 20006

Librarian
Centre d'Etudes Nucléaires de Saclay
P.O. Box 2, Saclay
Fig-sur-Yvette (S&O)
FRANCE

M. Rzekiecki
Commissariat à 1'Energie Atomique
Centre d'Etudes Nucléaires de Cadarache
BP n 13-St. Paul
Les Durance
FRANCE

Director
Commissariat à 1'Energie Atomique
Centre d'Etudes Nucléaires de Fontenay-aux-Roses (Seine)
FRANCE

Librarian
Commonwealth Scientific and Industrial Research Organization
314 Albert Street
P.O. Box 89
East Melbourne, Victoria
AUSTRALIA 3002

No. of Copies

Director
Commonwealth Scientific and Industrial Research Organization
Aspendal, Victoria,
AUSTRALIA

E. Wallauschek
ENEA (OECD) Health and Safety Office
38, Blvd. Suchet
Paris IVI,
FRANCE

Director
National Institute of Radiological Sciences
4-9-1, Anagawa
Chiba-shi
JAPAN

Librarian
Australian AEC
Riverina Laboratory
P.O. Box 226
Deniliquin
New South Wales
AUSTRALIA 2710

A. M. Marko
Director
Atomic Energy of Canada Ltd.
Biology and Health Physics Division
Chalk River Nuclear Laboratories
Chalk River, Ontario KOJ IJO
CANADA

F. D. Sowby
International Commission on Radiological Protection
Clifton Avenue
Sutton, Surrey
ENGLAND

W. R. Ney
Executive Director
National Council on Radiation Protection and Measurements
7910 Woodmont Avenue
Suite 1061
Washington, DC 20014

Leo Bustad, Dean
College of Veterinary Medicine
Washington State University
Pullman, WA 99163

G. W. Dolphin
National Radiological Protection Board
Harwell, Didcot
Oxfordshire OXI1 ORQ
ENGLAND

No. of Copies

ONSITE

8 DOE Richland Operations Office

P. F. X. Dunigan
J. L. Landon
W. Lei
H. E. Ransom
P. R. Rhodes
F. R. Standerfer
M. W. Tiernan
J. D. White

Rockwell Hanford Operations

V. A. Uresk

Douglas United Nuclear, Inc.

DUN File

3 Hanford Environmental Health

B. Breitenstein
P. A. Fuqua
W. D. Norwood

U.S. Testing

W. V. Baumgartner

523 Battelle-Northwest

R. R. Adee
M. D. Allen
T. W. Ambrose
L. E. Anderson
F. D. Andrews
T. K. Andrews
W. J. Bair (40)
J. E. Ballou
J. L. Beamer
E. F. Blanton
M. G. Brown
F. G. Burton
W. C. Cannon
N. E. Carter
A. Case
D. L. Catt
D. B. Cearlock

No. of Copies

J. P. Corley
D. K. Craig
G. E. Dagle
G. M. Dalen
J. R. Decker
D. A. Dingee
P. J. Dionne
H. Drucker
C. E. Elderkin
S. J. Farmer
D. Felton
R. E. Filipy
J. W. Finnigan
R. F. Foster
J. C. Fox
M. E. Frazier
M. J. Free
M. P. Fujihara
J. J. Fuquay
A. J. Gandolfi
J. C. Gaven
R. A. Gies
M. F. Gillis
W. A. Glass
P. L. Hackett
J. G. Hadley
A. J. Haverfield
R. Heid
J. P. Herring
J. O. Hess
D. L. Hessel
D. L. Hjeresen
V. G. Horstman
R. F. Howard
F. P. Hungate
R. A. Jaffe
M. T. Karagianes
W. T. Kaune
L. J. Kirby
E. G. Kuffel
H. V. Larson
S. M. Loscutoff
R. M. Madison
D. D. Mahlum
S. Marks
R. P. Marshall
B. J. McClanahan
K. E. McDonald
M. C. Miller
E. M. Milliman

No. of Copies

J. E. Morris
O. R. Moss
L. C. Neil
J. M. Nielsen
R. E. Nightingale
D. E. Olesen
R. F. Palmer
J. F. Park
H. M. Parker
R. A. Pelroy
R. W. Perkins
D. W. Phelps
R. D. Phillips
A. M. Platt
G. J. Powers
L. L. Rader
H. A. Ragan
R. A. Renne
W. D. Richmond
A. V. Robinson
W. C. Roesch
S. E. Rowe
C. L. Sanders
R. E. Schirmer
L. C. Schmid
R. P. Schneider
L. C. Schwendiman
M. R. Sikov
C. L. Simpson
L. G. Smith
V. H. Smith
H. E. Stevens
R. W. Stewart
B. O. Stuart
M. F. Sullivan
K. L. Swinth
W. L. Templeton
R. C. Thompson
V. D. Tyler
C. M. Unruh
B. E. Vaughan (7)
A. P. Wehner
E. L. Wierman
W. R. Wiley (350)
D. H. Willard
L. S. Winn
G. M. Zwicker
Biology Library (2)
Technical Information Files (5)
Technical Publications (4)

Battelle

March 16, 1978

To: Distribution

ERRATA

Please substitute the attached errata sheets in your copy of PNL-2500 Pt 1, Biomedical Sciences, Pacific Northwest Laboratory Annual Report for 1977 to the DOE Assistant Secretary for Environment, February 1978.

DISTRIBUTION

No. of Copies

A. A. Churm, Director
Patent Division
DOE - Chicago Operations Office
9800 South Cass Avenue
Argonne, IL 60439

3 J. L. Liverman
Acting Assistant Secretary
Department of Energy
Office of the Assistant
Secretary for Environment
Washington, DC 20545

W. R. Albers
Department of Energy
Office of the Assistant
Secretary for Environment
Washington, DC 20545

R. W. Barber
Department of Energy
Office of the Assistant
Secretary for Environment
Washington, DC 20545

N. F. Barr
Department of Energy
Office of the Assistant
Secretary for Environment
Washington, DC 20545

M. A. Bell
Department of Energy
Office of the Assistant
Secretary for Environment
Washington, DC 20545

W. G. Belter
Department of Energy
Office of the Assistant
Secretary for Environment
Washington, DC 20545

J. W. Benson
Department of Energy
Office of the Assistant
Secretary for Environment
Washington, DC 20545

L. C. Brazley
Department of Energy
Office of the Assistant
Secretary for Environment
Washington, DC 20545

No. of Copies

W. A. Brobst
Department of Energy
Office of the Assistant
Secretary for Environment
Washington, DC 20545

A. L. Brooks
Department of Energy
Office of the Assistant
Secretary for Environment
Washington, DC 20545

W. W. Burr, Jr.
Department of Energy
Office of the Assistant
Secretary for Environment
Washington, DC 20545

4 C. E. Carter
Department of Energy
Office of the Assistant
Secretary for Environment
Washington, DC 20545

D. W. Cole
Department of Energy
Office of the Assistant
Secretary for Environment
Washington, DC 20545

J. A. Coleman
Department of Energy
Office of the Assistant
Secretary for Environment
Washington, DC 20545

R. A. Conaway
Department of Energy
Office of the Assistant
Secretary for Environment
Washington, DC 20545

R. D. Cooper
Department of Energy
Office of the Assistant
Secretary for Environment
Washington, DC 20545

L. J. Deal
Department of Energy
Office of the Assistant
Secretary for Environment
Washington, DC 20545

No. of Copies

G. P. Dix
Department of Energy
Office of the Assistant
Secretary for Environment
Washington, DC 20545

G. G. Duda
Department of Energy
Office of the Assistant
Secretary for Environment
Washington, DC 20545

C. W. Edington
Department of Energy
Office of the Assistant
Secretary for Environment
Washington, DC 20545

H. G. Fish
Department of Energy
Office of the Assistant
Secretary for Environment
Washington, DC 20545

R. E. Grossman
Department of Energy
Office of the Assistant
Secretary for Environment
Washington, DC 20545

G. Hagey
Department of Energy
Office of the Assistant
Secretary for Environment
Washingotn, DC 20545

J. H. Harley
Environmental Monitoring
Laboratory
376 Hudson St.
New York, NY 10014

E. B. Harvey
Department of Energy
Office of the Assistant
Secretary for Environment
Washington, DC 20545

H. Hollister
Department of Energy
Office of the Assistant
Secretary for Environment
Washington, DC 20545

No. of Copies

R. M. Jimeson
Department of Energy
Office of the Assistant
Secretary for Environment
Washington, DC 20545

R. L. Leith
Department of Energy
Office of the Assistant
Secretary for Environment
Washington, DC 20545

F. A. Leone
Department of Energy
Office of the Assistant
Secretary for Environment
Washington, DC 20545

W. J. Little, Jr.
Department of Energy
Office of the Assistant
Secretary for Environment
Washington, DC 20545

K. E. Lockridge
Department of Energy
Office of the Assistant
Secretary for Environment
Washington, DC 20545

V. M. Lott
Department of Energy
Office of the Assistant
Secretary for Environment
Washington, DC 20545

E. K. Loop
Department of Energy
Office of the Assistant
Secretary for Environment
Washington, DC 20545

J. N. Maddox
Department of Energy
Office of the Assistant
Secretary for Environment
Washington, DC 20545

J. R. Maher
Department of Energy
Office of the Assistant
Secretary for Environment
Washington, DC 20545

W. J. McCool
Department of Energy
Office of the Assistant
Secretary for Environment
Washington, DC 20545

No. of Copies

B. F. McCully
Department of Energy
Office of the Assistant
Secretary for Environment
Washington, DC 20545

J. L. Minthorn, Jr.
Department of Energy
Office of the Assistant
Secretary for Environment
Washington, DC 20545

D. Monti
Department of Energy
Office of the Assistant
Secretary for Environment
Washington, DC 20545

W. E. Mott
Department of Energy
Office of the Assistant
Secretary for Environment
Washington, DC 20545

D. E. Patterson
Department of Energy
Office of the Assistant
Secretary for Environment
Washington, DC 20545

W. H. Pennington
Department of Energy
Office of the Assistant
Secretary for Environment
Washington, DC 20545

R. Rabson
Department of Energy
Office of the Assistant
Secretary for Environment
Washington, DC 20545

R. W. Ramsey, Jr.
Department of Energy
Office of the Assistant
Secretary for Environment
Washington, DC 20545

D. M. Ross
Department of Energy
Office of the Assistant
Secretary for Environment
Washington, DC 20545

A. A. Schoen
Department of Energy
Office of the Assistant
Secretary for Environment
Washington, DC 20545

No. of Copies

M. Schulman
Department of Energy
Office of the Assistant
Secretary for Environment
Washington, DC 20545

D. E. Shaw
Department of Energy
Office of the Assistant
Secretary for Environment
Washington, DC 20545

G. Shippard
Department of Energy
Office of the Assistant
Secretary for Environment
Washington, DC 20545

R. D. Shull
Department of Energy
Office of the Assistant
Secretary for Environment
Washington DC, 20545

N. F. Simpson
Department of Energy
Office of the Assistant
Secretary for Environment
Washington DC, 20545

D. H. Slade
Department of Energy
Office of the Assistant
Secretary for Environment
Washington, DC 20545

D. Smith
Department of Energy
Office of the Assistant
Secretary for Environment
Washington, DC 20545

H. P. Smith
Department of Energy
Office of the Assistant
Secretary for Environment
Washington, DC 20545

J. Snyder
Department of Energy
Office of the Assistant
Secretary for Environment
Washington, DC 20545

G. E. Stapleton
Department of Energy
Office of the Assistant
Secretary for Environment
Washington, DC 20545

No. of Copies

J. B. Stronberg
Department of Energy
Office of the Assistant
Secretary for Environment
Washington, DC 20545

J. Swinebroad
Department of Energy
Office of the Assistant
Secretary for Environment
Washington, DC 20545

A. R. Vincent
Department of Energy
Office of the Assistant
Secretary for Environnient
Washington, DC 20545

B. W. Wachholz
Department of Energy
Office of the Assistant
Secretary for Environment
Washington, DC 20545

H. R. Warson
Department of Energy
Office of the Assistant
Secretary for Environment
Washington, DC 20545

W. W. Weyzen
Department of Energy
Office of the Assistant
Secretary for Environment
Washington, DC 20545

J. C. Whitnah
Department of Energy
Office of the Assistant
Secretary for Environment
Washington, DC 20545

T. Williams
Department of Energy
Office of the Assistant
Secretary for Environment
Washington, DC 20545

R. W. Wood
Department of Energy
Office of the Assistant
Secretary for Environment
Washington, DC 20545

C. I. York
Department of Energy
Office of the Assistant
Secretary for Environment
Washington, DC 20545

No. of Copies

F. R. Zintz
Department of Energy
Office of the Assistant
Secretary for Environment
Washington, DC 20545

C. W. Fischer
Department of Energy
Office of Assistant Secretary
for Energy Information
Administration
Washington, DC 20545

Major General J. K. Bratton
Department of Energy
Office of the Assistant
Secretary for Defense
Programs
Washington, DC 20545

G. C. Facer
Department of Energy
Office of the Assistant
Secretary for Defense
Programs
Washington, DC 20545

Admiral H. G. Rickover
Department of Energy
Office of the Assistant
Secretary for Defense
Progranis
Washington, DC 20545

A. D. Starbird
Department of Energy
Office of the Assistant
Secretary for Defense
Programs
Washington, DC 20545

C. B. Curtis
Department of Energy
Office of the Assistant
Secretary for Federal Energy
Regulatory Commission
Washington, DC 20545

W. E. Molloy
Department of Energy
Office of the Assistant
Secretary for Federal Energy
Regulatory Commission
Washington, DC 20545

H. P. Wald
Department of Energy
Office of the Assistant
Secretary for Federal Energy
Regulatory Commission
Washington, DC 20545

No. of Copies

D. Beattle
Department of Energy
Office of the Assistant
Secretary for Conservation
and Solar Applications
Washington, DC 20545

T. Noel
Department of Energy
Office of the Assistant
Secretary for Resource
Applications
Washington, DC 20545

J. Belding
Department of Energy
Office of the Assistant
Secretary for Energy
Techno1ogy
Washington, DC 20545

J. Bresee
Department of Energy
Office of the Assistant
Secretary for Energy
Techno1ogy
Washington, DC 20545

G. W. Cunningham
Department of Energy
Office of the Assistant
Secretary for Energy
Techno1ogy
Washington, DC 20545

T. J. Dobry
Department of Energy
Office of the Assistant
Secretary for Energy
Techno1ogy
Washington, DC 20545

H. Guthrie
Department of Energy
Office of the Assistant
Secretary for Energy
Techno1ogy
Washington, DC 20545

E. E. Kintner
Department of Energy
Office of the Assistant
Secretary for Energy
Techno1ogy
Washington, DC 20545

F. A. Koomanoff
Department of Energy
Office of the Assistant
Secretary for Energy
Techno1ogy
Washington, DC 20545

No. of Copies

C. Kuhlnian
Department of Energy
Office of the Assistant Secretary for Energy Technology
Washington, DC 20545

R. Loose
Department of Energy
Office of the Assistant Secretary for Energy Technology
Washington, DC 20545

W. E. Lotz
Department of Energy
Office of the Assistant Secretary for Energy Technology
Washington, DC 20545

M. B. Neuworth
Department of Energy
Office of the Assistant Secretary for Energy Technology
Washington, DC 20545

F. F. Parry
Department of Energy
Office of the Assistant Secretary for Energy Technology
Washington, DC 20545

G. Perdirtz
Department of Energy
Office of the Assistant Secretary for Energy Technology
Washington, DC 20545

H. F. Soule
Department of Energy
Office of the Assistant Secretary for Energy Technology
Washington, DC 20545

R. D. Thorne
Department of Energy
Office of the Assistant Secretary for Energy Technology
Washington, DC 20545

P. C. White
Department of Energy
Office of the Assistant Secretary for Energy Technology
Washington, DC 20545

No. of Copies

E. Willis
Department of Energy
Office of the Assistant Secretary for Energy Technology
Washington, DC 20545

W. Bateman
Department of Energy
Office of the Assistant Secretary for Energy Research
Washington, DC 20545

3 J. M. Deutch
Department of Energy
Office of the Assistant Secretary for Energy Research
Washington, DC 20545

D. R. Israel
Department of Energy
Office of the Assistant Secretary for Energy Research
Washington, DC 20545

J. S. Kane
Department of Energy
Office of the Assistant Secretary for Energy Research
Washington, DC 20545

C. Jackson
DOE - San Francisco Operations Office
133 Broadway
Wells Fargo Building
Oakland, CA 94616

J. H. Spickard
DOE - Idaho Operations Commission
550 Second Street
Idaho Falls, ID 83401

D. M. Gardiner
DOE - Chicago Operations Office
9800 South Cass Avenue
Argonne, IL 60439

M. E. Gates
DOE - Nevada Operations Office
P.O. Box 14100
Las Vegas, NV 89114

No. of Copies

R. Ray
DOE - Nevada Operations Office
P.O. Box 14100
Las Vegas, NV 89114

P. B. Dunnaway
DOE - Nevada Operations Office
P.O. Box 14100
Las Vegas, NV 89114

J. R. Roeder
DOE - Albuquerque Operations Office
P.O. Box 5400
Albuquerque, NM 87115

E. W. Bean
Rocky Flats Area Office
DOE - Albuquerque Operations Office
P.O. Box 928
Golden, CO 80401

J. F. Stevens
Dayton Area Office
DOE - Albuquerque Operations Office
P.O. Box 66
Miamisburg, OH 45342

W. Reese
DOE - Savannah River Operations Office
P.O. Box A
Aiken, SC 29801

J. A. Lenhard
DOE - Oak Ridge Operations Office
P.O. Box E
Oak Ridge, TN 37830

J. S. Ball
Bartlesville Energy Research Center
Department of Energy
P.O. Box 1398
Bartlesville, OK 74003

G. H. Gronhovd
Grand Forks Energy Research Center
Department of Energy
Box 8213, University Station
Grand Forks, ND 58202

A. W. Decora
Laramie Energy Research Center
Department of Energy
P.O. Box 3395
University Station
Laramie, WY 83071

No. of Copies

R. D. Kerr
Laramie Energy Research Center
Department of Energy
P.O. Box 3395
University Station
Laramie, WY 83071

A. A. Pitrolo
Morgantown Energy Research Center
Department of Energy
P.O. Box 880
Morgantown, WV 26505

I. Wender
Pittsburgh Energy Research Center
Department of Energy
4800 Forbes Avenue
Pittsburgh, PA 15213

B. M. Erickson
DOE - Schenectady Naval Reactors Office
P.O. Box 1069
Schenectady, NY 12301

2 T. J. Dobry
Department of Energy
Division of Nuclear Research and Application, Space Applications
Washington, DC 20545

198 DOE Technical Inforniation Center

NRC Advisory Committee on Reactor Safeguards
Washington, DC 20555

W. Cool
Nuclear Regulatory Commission
Washington, DC 20545

R. Alexander
Nuclear Regulatory Commission
Washington, DC 20545

2 J. J. Davis
Assistant Director of Research
Nuclear Regulatory Commission
Washington, DC 20545

D. Sniith
Environmental Protection Agency
Washington, DC 20460

No. of Copies

W. Mills
Environmental Protection Agency
Washington, DC 02460

J. W. McCaslin
INEL, Aerojet Nuclear
550 Second Street
Idaho Falls, ID 83401

R. C. Yoder
Rockwell International
P.O. Box 888
Golden, CO 80401

C. M. Patterson
E. I. DuPont de Nemours and Company
Savannah River Plant
Aiken, SC 29801

Technical Information Service
Room 773A
Savannah River Laboratory
E. I. DuPont de Nemours and Company
Aiken, SC 29801

C. L. Karl
National Lead Company of Ohio
P.O. Box 39158
Cincinnati, OH 45239

R. L. Kathren
Portland General Electric
621 S.W. Alder
Portland, OR 97205

V. P. Bond
Brookhaven National Laboratory
Upton, Long Island, NY 11973

C. B. Meinhold
Brookhaven National Laboratory
Upton, Long Island, NY 11973

Librarian
Research Library, Reference
Bookhaven National Laboratory
Upton, Long Island, NY 11973

C. R. Richmond
Oak Ridge National Laboratory
P.O. Box X
Oak Ridge, TN 37830

J. A. Auxier
Oak Ridge National Laboratory
P.O. Box X
Oak Ridge, TN 37830

No. of Copies

W. K. Sinclair
Argonne National Laboratory
9700 South Cass Avenue
Argonne, IL 60439

E. L. Alpen
Lawrence Berkeley Laboratory
University of California
Building 90, Room 2056
No. 1 Cyclotron Road
Berkeley, CA 94720

M. L. Mendelsohn
University of California
Lawrence Livermore Laboratory
P.O. Box 808
Livermore, CA 94550

Librarian
Lawrence Radiation Laboratory
University of California
Technical Information Dept., L-3
P.O. Box 808
Livermore, CA 94550

G. L. Voelz
University of California
Los Alamos Scientific Laboratory
P.O. Box 1663
Los Alamos, NM 87545

Librarian
Los Alamos Scientific Laboratory
P.O. Box 1663
Los Alamos, NM 87544

J. W. Healy
Los Alamos Scientific Laboratory
University of California
P.O. Box 1663
Los Alanios, NM 87545

Dr. Roger O. McClellan
Inhalation Toxicology Research Institute
Lovelace Foundation for Medical Education and Research
P.O. Box 5890
Albuquerque, NM 87115

K. A. Sniith
Sandia Laboratories
P.O. Box 5800
Albuquerque, NM 87115

No. of Copies

J. E. Rasmussen
Battelle Human Affairs Research Centers
4000 N.E. 41st Street
P.O. Box 5395
Seattle, WA 98105

Librarian
Battelle Memorial Institute
Colunibus Laboratories
505 King Avenue
Columbus, OH 53201

4 R. S. Paul
Battelle Memorial Institute
Columbus Laboratories
505 King Avenue
Columbus, OH 53201

F. G. Dawson
Battelle Memorial Institute,
505 King Avenue
Columbus, OH 53201

G. W. Duncan
Battelle
4000 NE 41st Street
Seattle, WA 98105

J. L. Hebert
Battelle
4000 NE 41st Street
Seattle, WA 98105

S. M. Nealey
4000 NE 41st Street
Seattle, WA 98105

B. D. Breitenstein
Hanford Environmental Health Foundation
Richland, WA 99352

P. A. Fuqua
Hanford Environmental Health Foundation
Richland, WA 99352

Librarian, Building 465
Atomic Energy Research Establishment
Harwell, Didcot
OXON OXII ORD, ENGLAND

H. Daw
Director, Division of Health, Safety and Waste Management
International Atomic Energy Agency
Vienna 1, Kaerntnerring 11,
AUSTRIA

No. of Copies

J. Z. Minczewski
International Atomic Energy Agency
Vienna 1, Kaerntenerring 11,
AUSTRIA

Director
Joint Center for Graduate Study
100 Sprout Road
Richland, WA 99352

David Rall, Director
NIEHS
P.O. Box 12233
Research Triangle Park,
NC 27709

D. Beirman
Chief, Document Service Branch
Central Intelligence Agency
Attn: CRS/DPSD/DSB/IAS/409779/DB
Washington, DC 20505

Council on Environmental Quality
72 Jackson Place, N.W.
Washington, DC 20006

Librarian
Centre d'Etudes Nucléaires de Saclay
P.O. Box 2, Saclay
Fig-sur-Yvette (S&O)
FRANCE

M. Rzekiecki
Commissariat à 1'Energie Atomique
Centre d'Etudes Nucléaires de Cadarache
BP n 13-St. Paul
Les Durance
FRANCE

Director
Commissariat à l'Energie Atomique
Centre d'Etudes Nucléaires de Fontenay-aux-Roses (Seine)
FRANCE

Librarian
Commonwealth Scientific and Industrial Research Organization
314 Albert Street
P.O. Box 89
East Melbourne, Victoria
AUSTRALIA 3002

No. of Copies

Director
Commonwealth Scientific and Industrial Research Organization
Aspendal, Victoria,
AUSTRALIA

E. Wallauschek
ENEA (OECD) Health and Safety Office
38, Blvd. Suchet
Paris IVI,
FRANCE

Director
National Institute of Radiological Sciences
4-9-1, Anagawa
Chiba-shi
JAPAN

Librarian
Australian AEC
Riverina Laboratory
P.O. Box 226
Deniliquin
New South Wales
AUSTRALIA 2710

A. M. Marko
Director
Atomic Energy of Canada Ltd.
Biology and Health Physics Division
Chalk River Nuclear Laboratories
Chalk River, Ontario KOJ IJO
CANADA

F. D. Sowby
International Commission on Radiological Protection
Clifton Avenue
Sutton, Surrey
ENGLAND

W. R. Ney
Executive Director
National Council on Radiation Protection and Measurements
7910 Woodmont Avenue
Suite 1061
Washington, DC 20014

Leo Bustad, Dean
College of Veterinary Medicine
Washington State University
Pullman, WA 99163

G. W. Dolphin
National Radiological Protection Board
Harwell, Oidcot
Oxfordshire OXII ORQ
ENGLAND

No. of Copies

ONSITE

8 DOE Richland Operations Office

P. F. X. Dunigan
J. L. Landon
W. Lei
H. E. Ransom
P. R. Rhodes
F. R. Standerfer
M. W. Tiernan
J. D. White

Rockwell Hanford Operations

V. A. Uresk

Douglas United Nuclear, Inc.

DUN File

3 Hanford Environmental Health

B. Breitenstein
P. A. Fuqua
W. D. Norwood

U.S. Testing

W. V. Baumgartner

523 Battelle-Northwest

R. R. Adee
M. D. Allen
T. W. Ambrose
L. E. Anderson
F. D. Andrews
T. K. Andrews
W. J. Bair (40)
J. E. Ballou
J. L. Beamer
E. F. Blanton
M. G. Brown
F. G. Burton
W. C. Cannon
N. E. Carter
A. Case
D. L. Catt
D. B. Cearlock

No. of Copies

J. P. Corley
D. K. Craig
G. E. Dagle
G. M. Dalen
J. R. Decker
D. A. Dingee
P. J. Dionne
H. Drucker
C. E. Elderkin
S. J. Farmer
D. Felton
R. E. Filipy
J. W. Finnigan
R. F. Foster
J. C. Fox
M. E. Frazier
M. J. Free
M. P. Fujihara
J. J. Fuquay
A. J. Gandolfi
J. C. Gaven
R. A. Gies
M. F. Gillis
W. A. Glass
P. L. Hackett
J. G. Hadley
A. J. Haverfield
R. Heid
J. P. Herring
J. O. Hess
D. L. Hessel
D. L. Hjeresen
V. G. Horstman
R. F. Howard
F. P. Hungate
R. A. Jaffe
M. T. Karagianes
W. T. Kaune
L. J. Kirby
E. G. Kuffel
H. V. Larson
S. M. Loscutoff
R. M. Madison
D. D. Mahlum
S. Marks
R. P. Marshall
B. J. McClanahan
K. E. McDonald
M. C. Miller
E. M. Milliman

No. of Copies

J. E. Morris
O. R. Moss
L. C. Neil
J. M. Nielsen
R. E. Nightingale
D. E. Olesen
R. F. Palmer
J. F. Park
H. M. Parker
R. A. Pelroy
R. W. Perkins
D. W. Phelps
R. D. Phillips
A. M. Platt
G. J. Powers
L. L. Rader
H. A. Ragan
R. A. Renne
W. D. Richmond
A. V. Robinson
W. C. Roesch
S. E. Rowe
C. L. Sanders
R. E. Schirmer
L. C. Schmid
R. P. Schneider
L. C. Schwendiman
M. R. Sikov
C. L. Simpson
L. G. Smith
V. H. Smith
H. E. Stevens
R. W. Stewart
B. O. Stuart
M. F. Sullivan
K. L. Swinth
W. L. Templeton
R. C. Thompson
V. D. Tyler
C. M. Unruh
B. E. Vaughan (7)
A. P. Wehner
E. L. Wierman
W. R. Wiley (350)
D. H. Willard
L. S. Winn
G. M. Zwicker
Biology Library *(2)*
Technical Information Files (5)
Technical Publications (4)

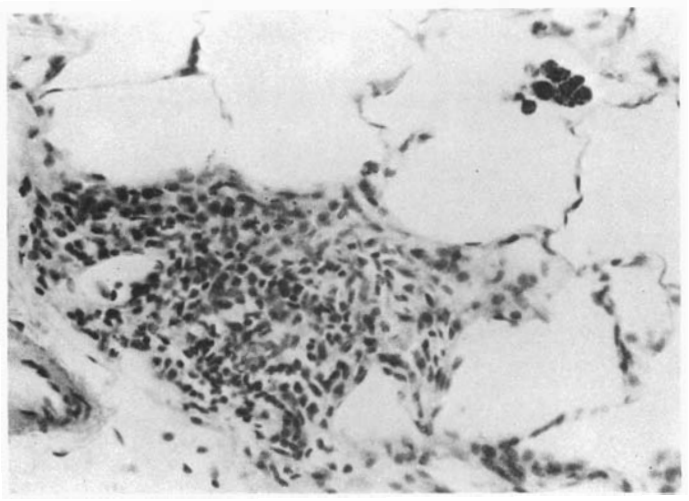

FIGURE 13. Focal Inflammation of Alveolar Epithelium in Lungs of a Rat that Received 8 Mo of Daily Exposures to Aerosols of 5 mg/m³ on Coal Mine Dust (H&E 320X)

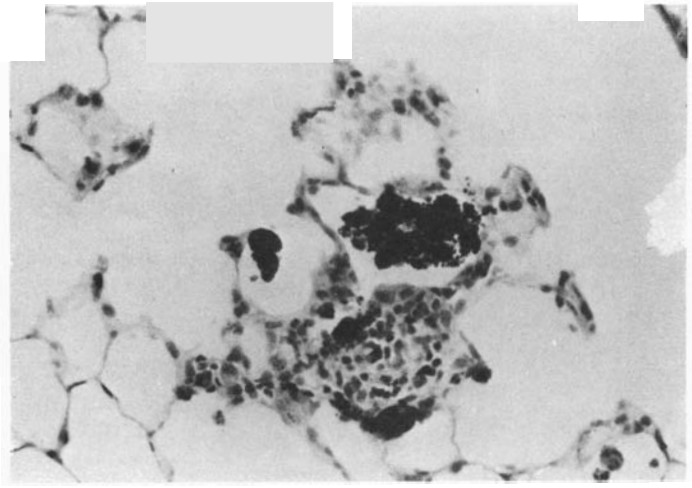

FIGURE 14. Inflammatory Reaction to Pigment in Lungs of a Rat that Received 8 Mo of Daily Exposures to Aerosols of 6 mg/m³ of Coal Mine Dust (H&E 320X)

- **Inhalation Hazard to Uranium Miners**

This project will determine the specific biological effects of daily exposures to known levels of pathogenic uranium mine air contaminants, using both large and small experimental animal models of human respiratory disease. Lung cancer and deaths by degenerative lung diseases have reached epidemic proportions among uranium miners, but the cause-effect relationships for these diseases are based on inadequate epidemiological data. This project will identify the agents or combinations of agents and their levels which are responsible for severe respiratory tract pathology, including respiratory epithelial carcinoma, pneumonconiosis, and emphysema. Determination of actual absorbed radiological and chemical doses of inhaled materials is essential to establish cause and effect relationships.

BIOLOGICAL EFFECTS OF INHALED CIGARETTE SMOKE IN BEAGLE DOGS

Investigators:

B. O. Stuart, R. F. Palmer, R. E. Filipy, and G. E. Dagle

Technical Assistance:

W. Skinner, C. Petty, K. C. Upton, and D. Teats

A group of twenty dogs has received up to 7 yr of daily cigarette smoking (10 cigarettes per day, 7 days per week), using realistic methods of oral inhalation and nose-plus-mouth exhalation. Three dogs that received 20 cigarettes per day over 9 mo developed respiratory tract lesions, including pleural thickening, alveolar septal fibrosis, vesicular emphysema, and chronic bronchitis, more rapidly than dogs receiving 10 cigarettes per day.

These experiments (Table 3.26) were initiated to examine cause and effect relationships in the development of respiratory tract pathology as a result of lifespan daily inhalation exposures of a large experimental animal to radon daughters with uranium ore dust and cigarette smoking, both combined and separately, under conditions that closely simulate conditions of human exposure in uranium mines. This report will concentrate on effects of chronic cigarette smoking alone.

Beagle dogs were trained to accept daily smoking of 10 cigarettes (Groups 2 and 3) or to receive identical daily periods of sham smoking of unlighted cigarettes (Controls, Groups 1 and 4). Fresh smoke was inhaled using masks specifically designed to simulate human patterns of cigarette smoking; i.e., oral smoke inhalation and nose plus mouth exhalation. These dogs were not anesthetized or tranquilized during smoke exposures, and received their repeated daily

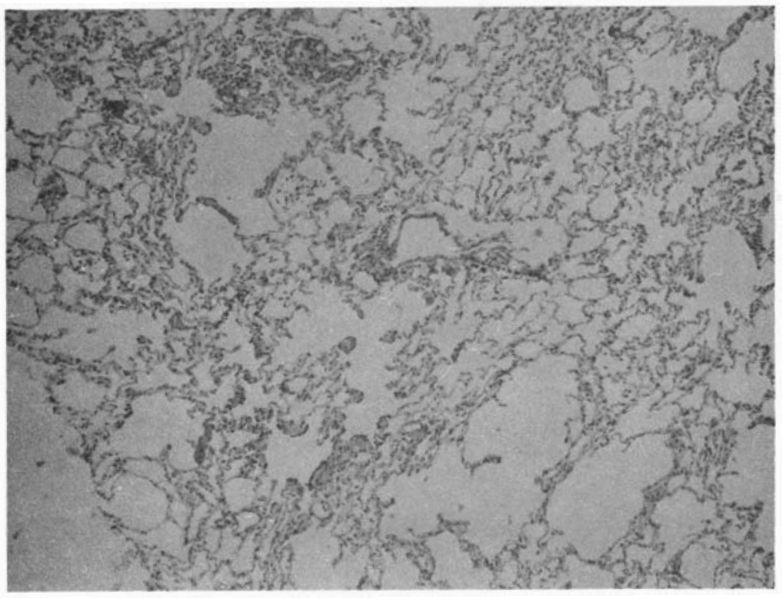

FIGURE 3.37. Vesicular Emphysema in a Section of the Same Lung Shown in Figure 3.35. (H&E 80X)

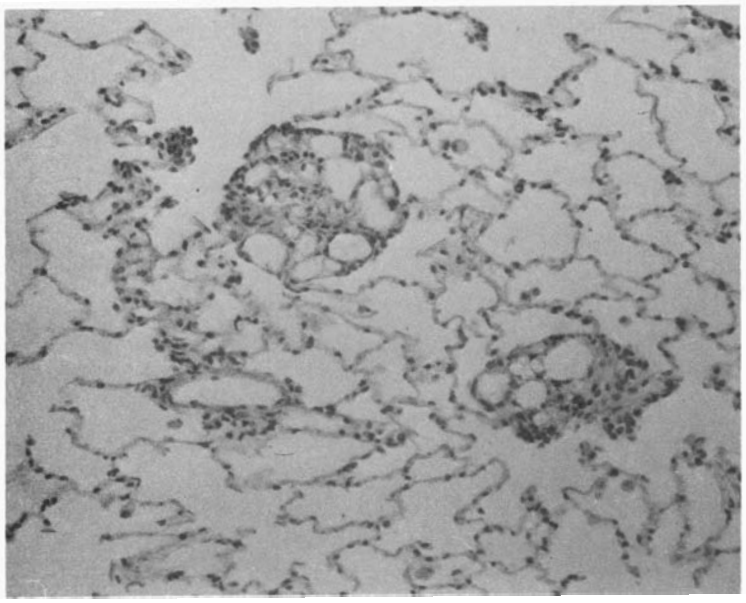

FIGURE 3.38. Focal Granulomata in a Lung Section from a Dog that had Smoked 20 Cigarettes per Day for 9 Months. (H&E 200X)

INHALED RADON DAUGHTERS AND URANIUM ORE DUST IN RODENTS

Investigators:

B. O. Stuart, R. F. Palmer, R. E. Filipy, and J. Gaven

Technical Assistance:

K. Mapstead

Male SPF rats are receiving daily inhalation exposures to radon daughters, with different levels of uranium ore dust. These studies will determine the dose rate dependence of pulmonary neoplastic or degenerative disease associated with inhaled radon daughters, and will define the possible physical, physiologic, or pathologic role of concomitantly inhaled aerosols of uranium ore dust.

Several studies are underway to determine the responsible agents (and their interactions) that cause respiratory tract carcinogenesis in uranium miners. These include studies described below, which exanine the influence of altered radiological dose rate and the physiologic or pathogenic role of uranium ore dust in neoplastic response.

Studies of altered carcinogenic and non-neoplastic response caused by inhaled radon daughters as a function of changing dose rate and total dose involve daily inhalation exposure of groups of male SPF Wistar rats to several concentrations (dose rates) and total doses (duration of exposures) of radon daughters. Epidemiological studies suggest that lung cancer in uranium miners is more prevalent following shorter, higher-level exposures, but this has not been shown in previous beagle dog studies. We have recently found that hamsters exposed to radon daughters at 900 WL[(a)] with dust for 15 mo at 30 hrjwk had a 1.0% incidence of pulmonary squamous carcinoma, but that rats receiving 900 WL with ore dust for 5 mo at 84 hr/wk showed 60% incidence of squamous carcinoma and adenocarcinoma (Table 3.27). Table 3.28 shows the protocol of current experiments, designed to test the hypothesis that shorter, more intense exposures to radon daughters with ore dust provide a significantly greater risk of developing lung cancer than do more protracted exposures (lower dose rate) accumulating the same total dose. If this hypothesis is disproved, and it is found that protracted expcsures are more carcinogenic, uranium miners who are presently exposed at lower dose rates under a fixed limit of total exposure dose will be at greater risk of developing lung cancer than were those early miners whose cases were used to derive the present limits for uranium miner exposure.

In addition to the markedly increased risk of lung cancer (6-fold greater than normal incidence for age-correlated cohorts) in uranium miners, recent epidemiological studies have shown a 5.3-fold increase in uranium miner deaths due to chronic respiratory insufficiency, including pneumoconiosis, pulmonary fibrosis, and emphysema. These findings may be related to concomitant inhalation exposure to silica-bearing uranium ore dust present in mine air.

We have observed massive fibrosis and bullous emphysema, as well as respiratory tract neoplasia, in beagle dogs after 2 to 5-1/2 yr of daily exposures to radon daughters with uranium ore, with and without concurrent cigarette smoking; and in hamsters and rats following chronic exposures to radon daughters with uranium ore dust.

(a) WL = Working Level: any combination of short-lived radon daughters per liter of air that will result in a total alpha decay of 1.3×10^5 MEV.

TABLE 3.27. Incidence of Lesions of Hamsters and Rats Following Exposure to Radon Daughters With and Without Uranium Ore Dust.

	Exposure Conditions	Results Following Exposures[a]		
Croup 1		Nasopharnyx	Trachea	Lung
34 Hamsters	Laboratory Air Controls	N	N	N
32 Rats		N	N	N
Croup 2				
34 Hamsters	375 WL Radon Daughters Alone 3800 WLM	34 Squamous Metaplasia	N	31 Slight Bronchiolization
		1 Squamous Carcinoma	5 Slight Hyperplasia	17 Slight Radiation Pneumonitis
32 Rats		32 Squamous Metaplasia	7 Squamous Metaplasia	32 Moderate Bronchiolization
		2 Squamous Carcinoma		16 Moderate Radiation Pneumonitis
				10 Adenomatosis
				2 Squamous Carcinoma
				1 Squamous Carcinoma and Bronchioloalveolar Carcinoma
Group 3				
34 Hamsters	900 WL Radon Daughters with Uranium Ore Dust (Carnotite, 15 mg/m³) 9200 WLM	14 Very Slight Squamous Metaplasia	N	32 Slight-Moderate Bronchiolization
				2 Extensive Fibrosis
				Adenomatosis
				Emphysema
32 Rats		26 Squamous Metaplasia	N	17 Squamous Carcinoma
				1 Adenocarcinoma
				1 Squamous Carcinoma and Adenocarcinoma.

[a] N = normal

TABLE 3.28. Comparison of Dose Rate Versus Total Dose in Animals Exposed to Radon Daughters.

Group	Number of Animals	Exposure Regimen	Total Exposures, WLM
1	48[a]	900 WL Radon Daughters 15 mg/m³[b]	320/640/2560
2	48	450 WL Radon Daughters 15 mg/m³	640
3	48	225 WL Radon Daughters 15 mg/m³	640
4	48	Controls	

[a] Forty-eight animals in each of the 320,640 and 2560 WLM groups. Six animals per group are sacrificed semiannually to assess developing pulmonary pathology, leaving 30 animals per group after 28 months, allowing a 0.96 probability of observing at least 3 neoplasms if the true incidence is 20% at 450 WL

[b] Concentration of uranium ore dust

We are testing the hypothesis that the presence of the ore dust may provide a physical or physiological interaction essential to pathogenesis by comparative carcinogenic studies using male SPF Wistar rats exposed to radon daughters with different levels of uranium ore dust. Our studies in uranium mines and using test chambers have shown that particle concentrations can be greatly reduced in the range of 10^6/cc to 10^5/cc without significantly altering the uncombined fraction (or attachment fraction) of radon daughters. This allows the study of the pathogenic role of the ore dust per se, without changing the physical behavior (hence deposition site) of the airborne radon daughters, as described in Table 3.29.

Pathology results from the first sacrifice schedule will be available in FY 1978.

TABLE 329. Role of Uranium Ore in Radon Daughters Carcinogenesis.

Group	Number of Animals	Exposure Regimen	Total Exposure, WLM
1	48[a]	900 WL Radon Daughter 15 mg/m³[b]	320/640/2560
2	48	900 WL Radon Daughter 3 mg/m³[c]	320/640/2560
3	48	Controls	

[a] Forty-eight animals in each of the 320, 640 and 2560 WLM groups. Six animals per group are sacrificed semiannually

[b] Concentration of uranium ore dust

[c] To determine the role of minimal ore dust levels while still maintaining very low fractions of unattached radon daughters, as found in present underground uranium mine operating conditions